AD NUMBER:	AD0113979
CLASSIFICATION CHANGES	
TO:	Unclassified
FROM:	Confidential
LIMITATION CHANGES	
TO:	Approved for public release; distribution is unlimited.
FROM:	Distribution authorized to U.S. Gov't. agencies only; Proprietary Information; 26 Aug 1955. Other requests shall be referred to the Army Chemcial Research and Develoment Center, Edgewood Arsenal, MD 21010
AUTHORITY	
	D/A, CRD ltr dtd 24 Aug 1981

AD NUMBER:	AD0113979
CLASSIFICATION CHANGES	
TO: Confidential	
FROM: Secret	
AUTHORITY	
31 Aug 1967, DoDD 5200.10, gp-3	

AD- 113979

SECURITY REMARKING REQUIREMENTS

DOD 5200.1-R, DEC 78

REVIEW ON 26 AUG 75

65,288

UNCLASSIFIED

AD 979

CLASSIFICATION CHANGED
TO: UNCLASSIFIED
FROM: CONFIDENTIAL
AUTHORITY:

Aug 81

UNCLASSIFIED

SECRET

U. S. ARMY
LOS ANGELES ORDNANCE DISTRICT

26 August 1955
Report No. 991
(Final)
Copy No. 24

FC

[redacted]

Brown Arrow—W. O. 1895—S—Report 991

FEASIBILITY AND DESIGN STUDY

WARHEADS FOR
THE ADVANCED BOMARC IM-99 ( )

Contract DA-04-495-ORD-617

SECRET

SECRET

26 August 1955

Report No. 991
(Final)

FEASIBILITY AND DESIGN STUDY

OF

WARHEADS FOR THE ADVANCED BOMARC IM-99( )

Contract DA-04-495-ORD-617

by

J. D. Bledsoe
R. V. Henry
D. R. Kennedy
W. L. Kincheloe
Jean Wylie

No. of Pages: 172

Approved by:

R. J. Mill
Chief, Armament Department

Period Covered:

21 December 1954 through 24 June 1955

NOTE 1: This document contains information affecting the national defense of the United States within the meaning of the Espionage Laws, Title 18, USC, Sections 793 and 794. The transmission or the revelation of its contents in any manner to an unauthorized person is prohibited by law.

NOTE 2: This document contains proprietary information of Aerojet-General Corporation and is not to be transmitted, reproduced, used, or disclosed to anyone without the permission of Aerojet-General Corporation; except that the Government has the right to reproduce, use and disclose for governmental purposes (including the right to give to foreign governments for their use as the national interest of the United States may demand) all or any part of this document as to which Aerojet-General Corporation is entitled to grant this right.

AEROJET-GENERAL CORPORATION

Azusa, California

SECRET

CONTENTS

CONTENTS (cont.)

CONTENTS (cont.)

CONTENTS (cont.)

CONTENTS (cont.)

CONTENTS (cont.)

CONTRACT FULFILLMENT STATEMENT

This final technical report completes the fulfillment of Contract DA-04-495-ORD-617.

ABSTRACT

The Bomarc weapon system is being developed for the defense of large areas against attacks by bombers and cruise-type missiles. The program has advanced to the point where the IM-99A, having a 300-lb warhead capacity is being developed from the prototype model, and the advanced Bomarc IM-99( ) interceptor, with a 600-lb warhead capacity, is in the preliminary design stage. This report is a feasibility and design study of warheads suitable primarily for the IM-99( ), although recommendations are also presented for the IM-99A.

A "frame-of-reference" section establishes the general background and assumptions necessary for the design and evaluation of the various warheads considered.

New preliminary designs are presented for the following warhead types: continuous rod, multiple-jet shaped charge, spin stabilized, rocket-propelled submissile (cluster type), and a guided, rocket-propelled submissile (cluster type). These are evaluated in comparison with each other, with fragmentation warheads, and with the T-44 cluster warhead (unstabilized, unpropelled, spigot-ejected submissiles).

Existing fuzing systems, such as the T-3010 and the T-3016 types, are compared with proposed infrared fuzing systems.

Recommended warhead-fuze combinations for both the IM-99( ) and the IM-99A interceptors are as follows:

The first recommendation is for a continuous-rod warhead with a modified T-3010 conical-skirt fuze. This combination is selected because of the high lethality associated with large root-mean-square guidance errors, the apparent reliability of the system, and the economy of production, after the warhead has been developed.

A multiple-jet, shaped-charge warhead with a modified T-3010 fuze system is recommended as second choice on the basis of lethality estimates, reliability, and economy of production.

It is believed that development time and costs would be lowest for the T-44 cluster type, since the background and experience gained by Aircraft Armaments, Incorporated, could be utilized.

ACKNOWLEDGMENTS

The cooperation and contributions of the following development groups is gratefully acknowledged: The Ballistic Research Laboratories at Aberdeen, Maryland, the IM-99 Weapon System Project Office and the Armament Laboratory at WADC, the Diamond Ordnance Fuze Laboratory at Washington, D.C., the New Mexico Institute of Mining and Technology at Socorro, New Mexico, the Boeing Airplane Company at Seattle, Washington, the Naval Ordnance Test Station, Inyokern, California, and the Davis-Monthan Air Force Base, Tucson, Arizona.

The following individuals of the Aerojet-General Corporation have also made important contributions to this study: F. H. Schuett, J. L. Johnson, P. W. Cramer, M. R. Gore, O. J. Demuth, and I. W. Snedden.

I. INTRODUCTION

The Bomarc weapon system is being developed for the defense of large areas against attacks by bombers and cruise-type missiles. The Bomarc program has advanced to the point where the IM-99A, with limited Service capabilities, is being developed from the experimental model configuration and has provisions for a 300-lb warhead. Warhead types currently under development for this interceptor include:

T-33 fragmentation warhead
T-44 cluster warhead
Multiple-jet shaped-charge warhead

The advanced Bomarc IM-99( ) interceptor is in the preliminary design and specification stage. This interceptor is the model planned for eventual production and Service use. The advanced IM-99( ) interceptor is expected to become operational during the period of 1960 to 1962. The time scale for the development of a suitable warhead for this interceptor is important because the configuration and design details must be frozen early enough to ensure compatibility with the interceptor. Since the Service life for the advanced IM-99( ) interceptor extends well beyond the 1962 date, the target aircraft against which it may be employed are mostly conjectural. In addition to high-performance manned bombers, potential targets will include cruise-type guided missiles. The obvious unavailability of information on actual target vulnerability precludes accurate or confident comparisons of warhead types, except in terms of present-day available aircraft targets. Hence, qualitative considerations are important, particularly where they relate to materials and/or structural configurations which might be expected in future targets.

A. OBJECTIVES

1. This feasibility and design study of warheads suitable for the advanced Bomarc IM-99( ) and for the interim tactical Bomarc IM-99A has been conducted under Army Ordnance Contract No. DA-04-495-ORD-617 in accordance with technical directives from the Ballistic Research Laboratories, Aberdeen Proving Ground. The basic objectives of this study program may be summarized as follows:

a. The establishment of a comparative framework involving technical and tactical considerations for the evaluation of armament systems for Bomarc interceptors, employing as much quantitative data as is available or may be justifiably presumed.

b. An investigation of the significant relationships between the design requirements of the interceptors and their components, and the requirements of an armement system, including fuze and warhead, to yield maximum lethality.

c. A study and analysis of the design mechanisms and the kinematics of achieving damage to aircraft targets, including the terminal ballistic effects of present, developmental, and new or unconventional types of armament systems.

d. The preparation of a summary of the feasibility and analysis study in the form of recommendations for the development of one or more armament systems which the evaluation studies show are the most promising.

2. The accomplishment of these objectives is modified by the interpretation of, and data in, a letter from the Ballistic Research Laboratories (Reference 1). This directive notes that the advanced Bomarc, IM-99( ), interceptor is an improved, higher-performance version of the IM-99A interceptor now being developed. This feasibility study, in accordance with the desire of the Air Force, is concerned primarily with the study and recommendations of armament systems which are optimal for the advanced Bomarc. The study is conducted in such terms, however, that recommendations of armament systems for the interim, or tactical, IM-99A Bomarc may be also made.

B. SCOPE

1. This feasibility and design study is concerned with the armament system, which includes the warhead, the fuze, and the safety and arming system (S and A). While the primary emphasis is on the warhead design and the effectiveness of the warhead and fuze against current and possible future targets, and the selection of a compatible fuzing system, the study is also concerned with the armament system's relation to, and integration with, the remainder of the Bomarc interceptor. Considerations affecting the warhead designs are functional and physical compatibility with the Bomarc interceptor, ground handling and support requirements, reliability, development requirements, availability and production potential, and cost. The following warhead types are considered in this investigation: fragmentation, external blast, cluster, shaped charge, and continuous rod.

2. These concepts are presented in the following sections:

ARMAMENT SYSTEM, FRAME OF REFERENCE — This section presents the overall philosophy of the study and shows most of the data and assumptions used.

WARHEAD DESIGN AND LETHALITY ESTIMATES — Preliminary designs for the continuous-rod and shaped-charge warheads, and lethality estimates for these as well as the cluster and fragmentation warheads are presented in this section.

WARHEAD FUZING-SYSTEM STUDIES — This section considers the effectiveness of the T-3010, T-3016, and infrared types of fuzing, and in addition discusses the effects of the terminal encounter-kinematics on the fuzing problems.

SUMMARY AND RECOMMENDATIONS — The conclusions of the study are presented in this section, and warhead types are recommended for the IM-99( ) and the IM-99A interceptors.

II. ARMAMENT SYSTEM, FRAME OF REFERENCE

A. INTRODUCTION

The following "frame of reference" discussion serves two purposes: first, to define the overall philosophy of the design study, and second, to show those data and assumptions regarding the interceptor and target characteristics which are required as input data for the design and feasibility study. The objectives of this study may be itemized as follows:

1. Development of the design principles for the warhead, which shall reflect the operational and tactical requirements of the Bomarc weapon system, as well as physical and functional compatibility with the interceptor.

2. Establishment of the warhead lethality requirements, including the criteria for kill.

3. Discussion of the capabilities of both the interceptor and the expected aircraft targets.

B. DESIGN PRINCIPLES

1. The design of the IM-99( ) interceptor warhead should consider the following factors:

a. Optimization of kill probability for all expected tactical situations.

b. The capability of functioning under peripheral or extremely difficult conditions.

c. Continuing growth or improvement potential.

d. Functional independence of the armament system from the guidance system and other components of the interceptor.

2. The limited number of expected encounters against an enemy using nuclear weapons diminishes the reliability of elaborate statistical methods of evaluation. Therefore, the design of the armament system must indicate success under those conditions normally considered as a statistical minority.

3. No feature of the design should be so limited or established that continuing advances in the state of the art will cause obsolescence and require complete redesign of the entire system in order to improve performance.

4. Functional compatibility is desirable, and is dependent on the following aspects of the weapons system:

Airframe performance
Target seeker performance
Interceptor and target tracking capability
Interceptor command control capability

5. The tactical considerations determine the spatial distribution of attack directions and miss distances, and thereby contribute to the evaluation of the effectiveness of the warhead. Optimum warheads for all-around, tail-only, or head-on-only directions of approaching the target may be considerably different. Furthermore, the direction of approach may greatly affect the design and performance of the required fuze. The scope of the present study does not permit a detailed tactical analysis. Therefore, it is assumed that the warhead shall be designed for attacking the target from any direction.

C. WARHEAD LETHALITY ESTIMATES

1. The USAF directive to OCO to conduct this study specified that the warhead for the advanced Bomarc IM-99( ) interceptor is to have a K-kill probability of between 0.5 and 0.9, assuming a normal distribution of miss distances with a dispersion of σ_G = 60 ft in any one dimension normal to the trajectory.

2. Since the earliest anticipated operational date for the IM-99( ) is 1960, it is reasonable to exclude from the likely targets all hostile aircraft types which may be presumed obsolescent by this time or shortly thereafter. By that time, the employment of such aircraft as the B-29 and the B-50, with their low speeds and limited ceilings, for intercontinental attacks is improbable. While aircraft of these slow types cannot be entirely omitted from consideration, the emphasis should be placed upon high-speed targets which may be considered likely, either from available intelligence data or on the basis of American development planning. In other words, the warhead for the IM-99( ) should be designed for best effectiveness in achieving K-kills of known or anticipated aircraft types which may be in service after 1960. However, the absence of quantitative lethality estimates on advanced targets precludes complete adherence to this approach. Nevertheless, the capability of a warhead to successfully attack advanced structural designs and materials will be stressed in the subsequent evaluation.

3. The criteria for evaluation of a K-kill has been the subject of considerable controversy. Reference 19 defines a "K-kill" as "Immediate kill of the aircraft, but not KK.* Sometimes defined as 'the aircraft falls or goes out of control within thirty seconds.'" It is universally agreed that the infliction of structural damage is a kill when the damage is so severe that the aircraft breaks up, or that sufficient wing or tail surface is removed so that control of the aircraft is irrevocably lost. The following factors that have the possibility of producing a K-kill have been excluded from the present evaluation as a result of the conference of 17 January 1955 at BRL:

*KK — Immediate disintegration of the aircraft (e.g., the kill required to stop a Kamikaze-type attack)

a. The loss of all engines without specifically assessing associated structural damage. This might be assumed sufficient to constitute a K-kill; however, the 17 January conference imposed the requirement that a simultaneous structural kill be obtained. Therefore, engine K-kills are considered only from a "bonus" viewpoint.

b. The effective loss of the flight crew by killing or incapacitation. As directed by the 17 January conference, this is also considered only from a "bonus" viewpoint.

c. Possible detonation of the target's payload.

D. INTERCEPTOR CAPABILITIES

1. The capabilities of the IM-99( ) affecting the warhead design are tentatively specified in Reference 2. A summary of the missile performance objectives for the IM-99A and the IM-99( ) is given in the following table:

Parameter	IM-99A Objectives	IM-99( ) Objectives
Missile range	125 nautical miles	250 nautical miles
Missile speed	Up to Mach 2.7	Up to Mach 2.7
Missile altitude	60,000 ft	80,000 ft
Target altitude	5000 to 60,000 ft	0 to 80,000 ft
Target speed	Up to Mach 1.3	Up to Mach 2.5
Target maneuverability	Up to 2.0 g lift	Up to 2.0 g lift

2. The AN/DPN-34 pulse-type radar seeker is being considered as one radar type for use in the IM-99A interceptor. With this radar, the presence of ground clutter may limit the acquisition range of the seeker to a value less than the missile altitude above the terrain. Errors in altitude determination and in range-gating may also limit the minimum altitude capability of the system. The pulse-type radar range-gating method may be refined in the future to reduce the minimum altitude limitation. Also, Doppler or continuous-wave types of radar, which are currently under development, may ultimately eliminate such a limitation by velocity discrimination. Since the terminal-phase navigation depends only upon the rate of angular rotation of the missile-to-target sight line, radar seekers of this type are satisfactory for homing. These advanced radar systems will be unable to furnish range information for fuzing.

3. The estimated root-mean-square miss-distance dispersions are 35 ft for a non-maneuvering target and 60 ft for an effectively maneuvering

target capable of 2 g maximum acceleration. The effect of electronic countermeasures which would increase the rms miss distance will be neglected in quantitative discussions in this study. However, the effectiveness of the warhead as the rms miss distance increases will be a primary parameter in the investigation of the performance of the armament system.

4. The angle of dive of the missile trajectory at the moment of interception of the target is influenced by the missile speed and the time of initiation of dive, the target speed and altitude, the missile dive doctrine used, and, to some extent, by the geographical framework in which the interception may take place. These variables, in different combinations, and with the assumption of a maneuvering target, result in random missile-to-target approach angles. It is considered reasonable to assume for the present that all approach angles in the upper hemisphere of the target are equally likely. Attacks from below are conceivable, but improbable. A typical plot of altitude and Mach number vs time for the terminal-dive phase is shown in Figure 1. This information may be converted into interceptor speed vs altitude, as shown in Figure 2. In view of the fact that the variables of the attack cannot be uniquely resolved, at least within the scope of this study, the following assumption is made: The Bomarc IM-99( ) missile can fly at any speed between 1000 ft/sec and 2500 ft/sec at any altitude from sea level to 80,000 ft, so long as the maximum flight angle of attack is not exceeded.

5. The angle of attack vs altitude for a 7-g maneuver is shown in Figure 3, based upon estimated data informally supplied by the Boeing Airplane Company. The flight angle of attack can vary from about 1.6 to 25°. This may have some effect on the fuzing and terminal kinematics of certain types of warheads, such as the cluster and shaped-charge types.

E. AIRCRAFT TARGET CAPABILITIES AND VULNERABILITY

1. The target speed, altitude, and maneuvering capabilities upon which the warhead for the IM-99( ) missile is based are shown in Figure 4.

2. Potential targets which should be considered include high-altitude, fast bombers with decoys, and also a range of smaller guided missiles such as the Snark-type missiles and other high-performance Navajo-type missiles to be subsequently developed.

3. The terminal-ballistic performance of the warhead for the advanced Bomarc is dependent upon the interaction of a subprojectile of some type with the target aircraft, since the interceptor guidance errors are sufficiently large so that the possibility of a collision is small. This generalized subprojectile may be a solid fragment, a continuous rod, or a small, unguided, cased and fuzed, high-explosive charge, possibly with its individual propulsion system.

4. Although vulnerability data are quite meager, even for American bombers which may become operational by 1960, and must be assumed for current hostile aircraft, as well as for both American and hostile aircraft to be used after 1960, certain principles are fundamental to the design of high-performance, high-speed aircraft. For example, the swept-wing design imposes high torque loads on the wing, which dictates the use of a thick-skin box structure. In order to conserve weight, a high-strength alloy must be used. Therefore, it is reasonable to assume that materials such as 7075-T aluminum in rather thick sections will be encountered for some time to come. It is also conceivable that other structural materials, possibly titanium, may come into common use in the period after 1960.

5. Accordingly, it is believed that the warhead evaluation should take into account the ability of a warhead type to attack successfully such structural designs and materials as may be expected for the period after 1960. However, it is not always possible to present such an evaluation statistically by assigning a value of kill probability.

F. SPECIFICATION OF DESIGN REQUIREMENTS

1. Physical and general functional compatibility of the advanced warhead and the Service model of the IM-99( ) are assured if the following overall design requirements and limitations are adopted:

a. The maximum weight allowable for the IM-99( ) warhead assembly, including the fuze computer, arming and safetying devices, and booster and auxiliary separators shall not exceed 600 lb. This limitation is in accordance with the preliminary design specifications of the IM-99( ) project group of the Boeing Airplane Company, as approved by the BRL and the USAF. For the IM-99A, the maximum weight shall not exceed 300 lb.

b. The maximum diameter of a unit warhead assembly shall be less than 35 in. by the minimum amount required to provide clearance for the aircraft structure through the warhead compartment. It is planned to formulate the preliminary design studies on the basis of a 30-in. maximum diameter of the warhead assembly, thus providing a 2.5-in. annular space for structural clearance and attachments.

c. The maximum length of a unit warhead assembly shall not exceed 35 in. This maximum length is based upon estimated size data for an alternative warhead which may be provided for certain interceptors. The Boeing Airplane Company considers it desirable to reduce this maximum length to 30 in. for the IM-99( ) if possible. For the IM-99A, the maximum length shall not exceed 17 in.*

*Information as of June 1955. It is possible that the space allowed for the warhead in the IM-99A may change as the design progresses.

d. Variable input data for determination of the warhead firing instant in the fuze computer shall be limited to, but not necessarily employ, the following:

(1) The instantaneous altitude of the Bomarc, with an error of not more than about 5000 or 6000 ft.

(2) The instantaneous airspeed of the Bomarc, with an error of not more than 5 to 10%. (This may be provided in terms of an expected average speed for a measured altitude.)

(3) Target-to-missile range closure rate, available for Bomarc seekers but with some susceptibility to electronic countermeasures.

(4) Target-to-missile range, available only from early seeker types with a high susceptibility to electronic countermeasures.

If the target speed and altitude are even approximately known, fuze computers utilizing these data preset into the computer at launching may be considered if, by bracketing these data into a small group of selectable computer channels, the effectiveness of fuzing increases significantly.

2. The warhead assembly, less fuze detector and computer devices, is considered to be a complete high-explosive subassembly for which the special safety rules for manufacturing, shipping, stowage, and handling of ordnance materiel are applicable.

3. For unit warhead assemblies, the warhead compartment of IM-99 interceptors capable of carrying the advanced warhead resulting from this study shall be assumed to have an access or loading hatch on one side of the aircraft sufficiently large to permit installation of the warhead assembly as a unit.

4. The arming and safetying provisions required for an acceptable advanced warhead are dependent upon the type of warhead which is selected. Compliance with all pertinent requirements of Army Ordnance shall be mandatory.

5. The warheads considered for the Bomarc IM-99( ) and IM-99A shall be designed for installation between the tank and electronics compartments. Warheads requiring jettisoning or removal of the electronics compartment are specifically excluded.

6. Warheads involving circumferential bias of fragment or cluster patterns shall not be considered. This type of warhead requires biasing of the main seeker-autopilot system and would result in a net increase of the miss distance. The biased warhead would, in addition, impose limitations on the seeker-autopilot system capabilities.

III. WARHEAD DESIGN AND LETHALITY ESTIMATES

This section of the report presents methods of achieving damage, discusses the known warhead types which are considered applicable to the Bomarc, presents design proposals of specific warheads considered feasible for the IM-99( ) and the IM-99A, and finally, discusses the lethality estimates associated with each warhead considered.

A. METHODS OF ACHIEVING DAMAGE

Preliminary to a discussion of warhead designs, it is considered desirable to consider basic damage mechanisms. These mechanisms are as follows:

Fragmentation
External Blast
Internal Blast
Shaped Charge (including Misznay-Schardin)
Continuous Rod

1. Fragmentation

The fragmentation warhead produces many individual ballistic missiles which strike the target in a somewhat random pattern, achieving damage by three basic methods: First, individual perforations of the target skin or structure; second, a local deformation of target structure and material in the fragment path; and third, the impacts may be accompanied by brilliant flashes which have been described as the "vaporific" effect and which may be capable of igniting fuel or detonating a high-explosive payload. Target components particularly vulnerable to fragment damage include the fuel cells and fuel lines, the crew, the miscellaneous electronic gear, engine and engine accessories, and the aircraft payload. Of these, the fuel system is perhaps the most vulnerable to fragment kill, through the initiation of a fire, whereas the basic airframe is relatively invulnerable to destruction by fragment damage.

2. External Blast

A second method of destroying aircraft structures is the external-blast mechanism wherein relatively large quantities of high explosives are detonated in the proximity of the aircraft. External blasts create an overstressed condition, causing deformation and even breaking of target skin and structure. This phenomenon occurs over an area, rather than at a point (as in the case of a fragment impact). A secondary effect is the aerodynamic stress incurred as the blast wave passes the aircraft. This can be compared to flying through an extremely severe gust. Large fragmentation warheads are accompanied by external-blast effects which closely follow the fragment impacts and thus compound and increase the damage caused by the already perforated structure.

3. Internal Blast

Internal or mined blasts are those in which the high explosive is detonated within the target structure. Since the blast occurs in a confined volume, thereby increasing the ability to deform structure, significant damage can be obtained from comparatively small amounts of explosives as compared with the quantities generally required for comparable external-blast damage.

4. Shaped Charge (Including Misznay-Schardin)

The shaped-charge damage mechanism is characterized by a high concentration of high-speed fragment impacts resulting in severe damage to aircraft structure lying in its path. The localized damage is primarily a kinetic-energy transfer phenomenon, but because of the extremely high velocity of impact, the target material usually disintegrates and burns so that the damaged area is expanded by an apparent blast effect. The Misznay-Schardin type of warhead, as considered here, is a limiting form of the shaped charge and its damage effects are similar to those described.

5. Continuous Rod

The continuous rod damages the aircraft target primarily by cutting through the skin and structure. The entire airframe appears to be vulnerable to the cutting action of the continuous rod. Because of high impact velocity, components such as payload, fuel cells, etc. are quite vulnerable to continuous-rod impact; however, the basic airframe appears to be the largest single vulnerable component.

B. CONTINUOUS-ROD WARHEAD

1. General Discussion

a. The continuous-rod warhead, upon which research is being conducted at the New Mexico Institute of Mining and Technology under sponsorship of the Navy Bureau of Ordnance, offers considerable promise as a device for obtaining structural kills with a fragment-like warhead. Its effectiveness results from direct cutting of aircraft structures by an expanding steel rod moving at a velocity of several thousand feet per second relative to the target. The early testing against obsolete aircraft types has shown considerable promise, and is being supplemented with more recent data to permit the formulation of reliable quantitative estimates of lethality against modern and future aircraft types.

b. As a result of a recent survey (Spring 1955) of explosive-ordnance research, it has become apparent that the "cleanest" and surest structural damage results from the continuous-rod warhead, where such evidences of K-lethality as the almost complete severance of a fuselage or the complete chord-wise cutting of a section of B-47 wing skin (0.375-in. 7075-T6 aluminum alloy) have been observed. The continuous-rod system combines the best features of the cluster and shaped-charge types, in that the fuzing problem for the continuous-rod warhead is greatly simplified by the high ejection velocity, and the probability of hitting the target is essentially equivalent to that for an infinite number of sub-missiles ejected at high speed in a flat expanding circle.

c. Since the continuous-rod warhead concept has not been widely discussed in any but the most recent literature, the following description of the principle is presented:

(1) The continuous-rod warhead principle involves the high-speed ejection of a collapsed ring of welded steel rods in a rapidly expanding ring, in a manner than can probably be best likened to the stretching of a metallic expansion-type watch band. The outward expansion, however, is accomplished by means of high explosive, while forward motion is imparted by the motion of the primary missile. Prior to detonation, the warhead case is in the form of an annular shell of tightly packed, square rod segments, attached to each other in such a way as to permit expansion into a full circle (actually a many-sided polygon) or continuous-rod hoop with a maximum circumference approximately equal to that of the sum of the lengths of the individual segments. The continuous-rod principle employs low C/M ratios (in the range from 0.3 to 0.8), yielding initial velocities of radial expansion of about 4000 to 6000 ft/sec. Under the influence of the forward motion of the primary missile, the expanding rod describes a large-angle conical path permitting one or more parts of the ring to intercept the target structure.

(2) The rod segments comprising the head are usually square in cross section for efficient packing, and the rods are tightly nested about the periphery of the warhead in the form of two concentric shells of an equal number of rods each. The forward end of each rod segment in the outer ring is hinged by a weldment to the forward end of the rod segment lying just below it in the inner ring. The after end of each rod segment in the outer ring is welded to the inner row segment next adjacent to the one immediately below it, so that all rods are connected, thus describing a single continuous and endless path throughout the nest of rods.

(3) When the warhead explosive is detonated, the propelling action of the explosive gas products causes the nest of rods to first expand radially and then to flatten into a large multi-sided polygon. The welded end attachments first shear partly through, then twist as the rods orient themselves into the polygon. The successful design is that which will permit the shearing and twisting action in each rod segment to take place without breaking the continuity of the hoop until almost full diameter has been attained.

(4) After the full diameter is reached, which, depending on design efficiency, may be from 60 to 95% or more of theoretical maximum diameter, the hoop usually breaks up into segments approximately 10

ft long which continue to travel as submissiles in the original expanding cone. The potential killing power does not suddenly drop, however, but attenuates as the separation becomes greater and as the rod segments continue to decelerate. Strikes on an aircraft structure by segments of the hoop continue to be highly lethal, provided the segment is properly oriented in respect to the target under attack. Oblique attacks as high as 72° have demonstrated K-killing power on heavy aircraft skins. Strikes at higher obliquities still inflict damage which might result in K-kill loss of the aircraft if the strikes are made on air-loaded and stressed structures. In addition, the continuous rod is capable of readily exploding fuel and bomb payloads in target aircraft (Reference 38).

d. Current ordnance research activity at NMIMT has recently been extended (Spring 1955) to include an examination of several sizes and types of rod warheads other than that employed in the original 24-in. Talos warhead (Reference 39). Table I lists the sizes and certain performance characteristics, where available, of the various charges under current investigation. Some of the data have been computed on the basis of recent discussions with NMIMT personnel (Reference 54) and their assumptions regarding the warhead configurations. The data shown, however, are considered to be reasonably accurate and representative. For example, theoretical opening diameters are based on the total cumulative length of rods, less 3 in. per rod to allow for end attachments. As can be seen, the efficiency of the smaller, solid, centrally initiated designs is superior to that of the large, annular, Talos design because of the far simpler explosive initiation problems.

e. Tests of the continuous-rod warheads indicate that structural K-kills (defined very conservatively by NMIMT as being a 50% circumferential cut of a fuselage or a 75% cut of a wing surface) can be obtained up to angles of obliquity of 72°. However, examination of high-obliquity hits on surfaces using 2024-T or 7075-T6 aluminum indicate that this angular limit may be unduly conservative. In general, strikes on fuselages usually reveal severance of skin, longerons, and stringers on both sides of the fuselage. Strikes on wings result in skin severance, spar cap cutting or cracking, internal bulkhead separation, and "popping" of rivets or bolts over wide areas of surface. When 7075-T6 surfaces are struck, severe spalling and extensive cracking usually also result, terminating only when the crack reaches a rivet hole or a surface edge.

f. NMIMT research (Reference 54) to date indicates that, for continuous-rod warheads in the sizes and types considered here, the expected radial velocity of projection of the hoop should be greater than 4500 ft/sec, probably from 5000 to 6000 ft/sec. Deceleration has been estimated, on the basis of NMIMT tests, as averaging approximately 16 ft/sec per foot of travel for a 1/4-in. square rod having an initial velocity of 4000 to 4500 ft/sec at 4900 ft altitude. The estimated slowdown formula is

$$V = V_o e^{-.00348 x}$$

for 1/4 x 1/4-in. rods at 4900 ft altitude, where x is length of rod travel in feet.

g. The following summarizes in a general manner the design and performance details of the continuous-rod warhead as they appear at this time for the IM-99( ).

(1) Rod Size — The most effective rod cross section appears to be 1/4 in. square. Where severe weight or space limitations exist, 3/16-in. square wire can be effectively used although the velocity drop-off for distance traveled is more pronounced for the 3/16-in. square rod and the ability to cut tough targets is markedly poorer. Odd cross sections such as 1/4 x 3/16-in. and larger wire such as 5/16-in. square rod are feasible and have been successfully tested. However, the odd cross sections may lead to attachment troubles in edge-on orientations and in addition have not been sufficiently tested to warrant much consideration. The heavier cross sections (e.g., 5/16 in.) may over-kill and are hence wasteful of space and weight.

(2) Charge-to-Metal Ratio — The C/M ratio appears to be somewhat flexible, and successful results have been obtained by NMIMT with C/M ratios from 0.3 to 0.8. Initial velocities of rods are generally in accordance with the Gurney prediction, based on cylinders, with initial velocities in the region of 4000 to 6000 ft/sec being recorded in the NMIMT tests (see Table I). Some anomalous behavior has been noticed where low C/M ratios gave extraordinarily high initial velocities; however, these deviations can probably be traced to the small test sampling.

(3) Length-to-Diameter Ratio — Analysis of the limited firings conducted by NMIMT, and summarized in Table I, suggests that the L/D may be critical, and that the higher the ratio the more likelihood there is of achieving full opening before breakup. The theoretical hoop diameters in the calculations in Table II are computed on the basis of total effective rod length, less 3 in. per rod to account for end attachments. The ability of the expanding hoop to achieve full diameter before breakup depends largely on such factors as the strength or ability of the end attachments to withstand the twisting action accompanying the expansion and bending of the rods. It is considered also that the frequency of rod end attachments may be a factor in premature breakup, due to hinge failure and twisting of individual rods. For this reason, high L/D ratios are desirable to keep the number of attachments at a minimum for a given weight of warhead. Also, recent test results (Reference 54) reported by NMIMT indicate the superior performance of high L/D heads, although other factors, as yet undetermined, may have been responsible for the observed differences in performance. It may be noted in the design study tabulation (Table II) that degradation factors have been applied to the lower L/D-ratio designs. Assuming that L/D

ratios of less than 1 may lead to premature breakup of the rod ring, the following degradation-factor relation has been tentatively established:

$$D_e = nD_t$$

where D_e = expected maximum diameter of hoop at time of breakup

D_t = maximum theoretical diameter of hoops, which is equal to total length of rods less 3 in. per rod for attachment

n = degradation factor according to the following schedule:

L/D	n
≥ 1.0	0.9
0.91 - 1.0	0.8
0.81 - 0.90	0.7
≤ 0.8	0.6

These degradation factors are purely arbitrary and probably pessimistic, since recent NMIMT experience (Reference 54) suggests that any properly designed warhead should be able to achieve 90-95% of the full hoop diameter. This is, of course, subject to further developmental testing, and it is conceivable that the high factor indicated by NMIMT experience will hold true in the IM-99 designs.

2. Continuous-Rod-Warhead Configurations

a. A variety of possible configurations have been prepared which are based on variations in warhead length and diameter for both the 300-lb warhead for the IM-99A and the 600-lb warhead for the IM-99( ). The following basic criteria have been established for the continuous-rod-warhead design study:

(1) Length

The maximum possible length for the 600-lb IM-99( ) warhead has been set at 35 in. with a maximum preferable length of 30 in. The maximum length for the IM-99A warhead has been established at 17 in. (In June 1955, Boeing indicated that a 17-in. maximum could be made available for the IM-99A warhead.) Shorter versions are not considered since the L/D (length-diameter ratio) essentially rules out the use of shorter designs because of possibly severe hoop-diameter degradation.

(2) Diameter

A maximum diameter of 30 in. for either warhead was established with smaller diameters being explored to permit better L/D ratios.

(3) Weight

A maximum weight of 600 lb, including a 60-lb (10%) allowance for S and A devices and supporting structure, is established for the IM-99( ) design. The IM-99A warhead has a maximum weight of 300 lb, with 60-lb allowance for S and A and structure (same for either the 300- or 600-lb warhead).

(4) C/M Ratio

The charge-to-metal ratio should be in the range from 0.3 to 0.8.

(5) L/D Ratio

The length-to-diameter ratio should be as high as possible consistent with the permitted envelopes, wire cross sections, and desired hoop diameter.

(6) Hoop Diameter

The full, unbroken-hoop diameter should be no greater than approximately twice the maximum expected miss of 3 σ (or 180 ft). Excessive hoop diameter would be wasteful of weight and space and would probably result in a lower C/M ratio and a lower velocity than could otherwise be obtained.

b. Based upon these design assumptions, a matrix of some 60 possible design configurations has been prepared for the 300- and 600-lb warheads and is summarized in Table II. Of these designs, only a comparative few are considered worthy of further examination because of failure of the remaining configurations to meet one or more of these design criteria. In keeping with the informally expressed desire of Boeing to keep the length as short as possible, while at the same time maintaining as high an L/D ratio as can be accommodated, the best compromise 600-lb warheads appear to be those of the configurations summarized in the following table, in the order of decreasing acceptability:

Configuration	1	2	3	4	5	6
Overall length (in.)	30	30	25	35	35	35
Major dia (in.)	25	30	25	20	25	30
Overall weight[a] (lb)	598	600	540	580	600	600
Rod cross section (in./16)	4x4	4x4	3x4[b]	4x4	4x4	3x4[c]
C/M ratio	0.65	0.37	0.77	0.64	0.41	0.56
L/D ratio	1.20	1.00	1.00	1.75	1.40	1.17
Hoop dia (theoretical) (ft)	384	482	430	378	479	580
Hoop dia (expected) (ft)[d]	345	385	345	340	430	520
Weight of metal in hoop (lb)	328	394	272	312	382	347

a. Rods plus explosive plus 60 lb for miscellaneous structure.
b. Rods oriented to form a 1/2-in.-thick shell.
c. Rods oriented to form a 3/8-in.-thick shell.
d. Expected hoop dia is weighted percentage of theoretical dia, using assumed factor of 0.9 for L/D $\geq$1.0)

Configuration 1 appears to be the best compromise design, since it has reasonably high L/D and C/M ratios, which should result in good high-velocity hoop production, and a nominal 1/4-in. square rod, which experience has shown to be optimum (according to NMIMT). Configuration 4 would probably be still better for a warhead except that its length is at the upper limit of 35 in. Configuration 2 has been made the second choice because its L/D and C/M ratios are both lower than desirable. Configuration 3 may be a possible choice, although its odd rod cross section of 3/16 x 1/4 in., oriented on edge to form a 1/2-in.-thick wall may lead to attachment trouble, no tests having been conducted with rods in this position. It should be noted that none of the 3/16 or 5/16-in. square rods appear suitable for the 600-lb warhead design.

c. Because of the length limitation on the 300-lb warhead for the IM-99A, only variations in warhead diameter and rod cross section are considered as variables. Of the 12 combinations shown in Table II, four possible configurations have been selected and summarized below, again in the order of decreasing acceptability. It should be emphasized that none of these designs have as high an L/D ratio as is considered desirable for best performance in terms of fullness of hoop development before breakup.

Configuration	1A	2A	3A	4A
Overall length (in.)	17	17	17	17
Major dia (in.)	30	25	20	25
Overall weight (lb)	300	300	298	300
Rod cross section (in./16)	3x3	3x3	3x4	3x4*
C/M ratio	0.37	0.79	0.68	0.34
L/D ratio	0.57	0.68	0.85	0.68
Hoop dia, theoretical (ft)	312	258	203	258
Hoop dia, expected (ft)**	187	155	142	155
Weight of metal in hoop (lb)	169	140	148	186

*Rods oriented to form 1/2-in.-thick shell.
**Degraded according to factors shown on p. 14.

The factors contributing to the choice of Configuration 1A are the fairly large hoop diameter expected and the use of uniform or square rods. The C/M and L/D ratios are both extremely low, although with proper development this warhead can probably be made to perform adequately. Configuration 2A, although having a much smaller hoop diameter, does have more satisfactory L/D and C/M ratios, and could conceivably perform better than Configuration 1A. Both 3A and 4A use 3/16 x 1/4-in. rods oriented in a double row to give a shell 1/2 in. thick. However, as previously stated, rod warheads have never been fabricated and tested using this particular orientation of 3/16 x 1/4-in. rods, and hinging trouble may be encountered in end attachments, although NMIMT (Reference 54) indicates that this may not necessarily be the case if other design factors are optimized. Configuration 3A does not compare favorably with 1A or 2A from the standpoint of hoop diameter, but it does have the most satisfactory C/M and L/D ratio combinations of all designs considered. If, as indicated by NMIMT personnel, the C/M and L/D ratios may not be critical, but are instead possibly quite flexible, then the logical choice will still be the design yielding the largest hoop of square rod, i.e., Configuration 1A. It is noteworthy that none of the 1/4-in. square or 5/16-in. square rods appear to be usable in the IM-99A 300-lb warhead.

d. The design study tabulation (Table II) is representative only, and actual designs may depart from the nominal dimensions and weights shown. Two continuous-rod warhead configurations have been prepared, both of which have worked in tests with smaller warheads. The original design considered is shown in Figure 5 and is based on successful designs in smaller sizes (5- and 8-in. dia). Subsequent experience by NMIMT (Reference 54) indicates that a more successful approach is that shown in Figure 6, and the data for the best compromise designs for the IM-99( ) and IM-99A are shown in Figures 7 and 8, respectively. Although either design should produce rods having essentially equal radial velocities, there is evidence that the centrally initiated design shown in Figure 5 may bend and scab the centers of the rods and cause a localized stretch to occur which can become a point of failure. A centrally initiated design may also be difficult to load with cast explosives. A more promising approach is that illustrated in Figure 6, where end-center initiation is employed. This principle has been used successfully in a 13.5-in.-dia, 16-in.-long, NMIMT test warhead design having an 8.5-in.-dia central cavity, closed at the initiation end by a hemispherical dome.

e. The shock-wave buffer layer between the explosive and the rod shell is presently made of plaster of paris, although such materials as thick layers of cavity hot melt* have also been used with some success. The plaster layer is employed in the two designs illustrated because of the low melting point of hot melt, which precludes reliable and consistent cast explosive loading. It will be noted that the plaster buffer is thicker at the center of the head than at the ends, particularly in the centrally initiated design (Figure 5). This variation in thickness, which is a result of empirical development, is thought to attenuate the shock wave in such a manner as to reduce the bending of the rods. Future development should consider plastic materials such as epoxy resins etc. that will lend themselves to easier production.

f. Two alternative methods of rod end attachment are shown in the details of Figure 6. One is an arc-welding method employed with a high degree of success by NMIMT in their test warheads. The second is a projection, or spot-welding, method developed by the G. W. Galloway Company, Arcadia, California, in the construction of Talos warhead shells. The latter method is far more suitable for high production rates, but it requires the development of a satisfactory means of production weld inspection, since a high incidence of weld failures has occurred on some of the Talos heads.

g. It will be noted that a 1/2-in.-dia steel or copper tube is employed at the ends of the rod segments under the holding tab. These tubes act as shaped charges under the influence of the detonating explosive and sever the holding tabs at the time of rod projection.

h. The designs illustrated in Figures 6 and 5 incorporate a method of attachment of the warhead to the primary missile consisting of Marman-type clamps at each end. The aft clamp is a U- or V-channel type that restrains the warhead both radially and longitudinally, while the forward clamp provides only radial support. This arrangement will hold the warhead rigidly in the missile, while still accommodating longitudinal expansion or contraction and fabrication tolerances.

---

*Black Acid Proof Liner Paint, per JAN-P-450, Class 3.

i. Since the continuous-rod-warhead designs permit single-point initiation on the axis of the warhead, only a single S-and-A device is required. The most desirable location for such a unit is on the inside of the warhead, located on the forward face of the inner cavity bulkhead. Access can be through a hole and access door in the forward warhead-compartment bulkhead. It should not be necessary to install or remove the S-and-A device after the warhead is in the missile, although provision must be made for an electrical connection to the fuze. In all probability, S-and-A units currently being developed for the IM-99A can be used either as is, or with only a slight modification, with the continuous-rod warhead.

3. Continuous-Rod Lethality Estimates

a. The following discussion sets forth the basic assumptions, methods, and results used in estimating the lethality of the continuous-rod warhead:

(1) The cutting capability of rods determined by NMIMT and shown in Figure 9 (taken from Reference 38) is valid for both 3/16- and 1/4-in. square, continuous-rod segments.

(2) The aerodynamic-drag evaluation shown in Section IV, Fuzing Studies, is applicable to the continuous rod.

(3) A rod cut of 0.375-in. depth in aluminum target material is required for a K-kill (representing a tough stressed-wing skin or a spar cap in a box-type structure).

(4) Upon reaching maximum hoop diameter, the hoop breaks up into sections about 10 ft long.

(5) About 95% of the presented area of a modern high-performance bomber such as the B-47 is K-vulnerable to a continuous-rod cut.

(6) Since recent experiments at NMIMT have shown that high-obliquity impacts (above 72°) may be ineffective, the gross assumption is made that only 90% of the impacts will result in effective cuts.

b. In order to establish the impact velocity of the continuous rod upon the target, the method indicated in Figure 8, in paragraph IV,B,1,c, and particularly in Equations 10, 11, and 12 is used. The constants used in Section IV do not apply to this condition since they were evaluated considering the end view of the continuous-rod cylinder as it is ejected from the missile. In this section it is desired to determine the slowdown of a single rod section flying side-on rather than end-on; therefore, the weight, presented area, and drag coefficients assumed for Section IV do not apply here. A drag coefficient of 0.7 was found to closely approximate the experimental data from NMIMT (presented in paragraph 1,f, above) to a distance of about 300 ft. The presented area of the rod to the air stream is assumed to be the arithmetical mean between the flat and diagonal presented areas of the rod. For the 1/4-in. square rod, the presented area is calculated to be 0.302 sq in. per inch of rod, and for the 3/16-in. square rod, the presented area is 0.2265 sq in. per inch of rod. Ratios of presented area to weight are 0.1185 sq ft/lb for the 1/4-in. rod and 0.157 sq ft/lb for the 3/16-in. rod. Initial velocities of the rod have been determined as the vector sum of an assumed 5000-ft/sec radial ejection velocity and forward velocities (imparted by the primary missile) of 1000 and 2500 ft/sec. Initial velocities are 5100 ft/sec for a 1000-ft/sec missile and 5590 ft/sec for a 2500-ft/sec missile. Target velocities relative to the rod will vary with respect to the angle of approach. A stationary target is therefore assumed in order to allow for a mean impact velocity independent of the angle of approach.

c. Calculations of remaining velocity vs distance of travel along the rod trajectory were made for the initial conditions discussed above. The results of these calculations are shown in Figure 10, which indicate that the drag slowdown of the rod is severe at sea level but essentially negligible at 60,000 ft altitude. The velocities shown in Figure 10, multiplied by the square root of the cross section of the rod (in inches) were plotted against the depth of cut plot in Figure 9 to determine the expected depth of cut as a function of distance traveled. These distances were then converted to actual missile miss distances (in feet) and the results plotted in Figure 10, thus showing the expected cutting capability for continuous-rod warheads as a function of the primary, missile miss distance. From Figure 11, averaging the capabilities for the slow and fast missile, a distance of about 132 ft actual miss distance (at sea level) was established as the point where a 1/4-in. square rod can no longer penetrate 0.375-in. aluminum target material. It was similarly determined that the 3/16-in. square rod can no longer penetrate 0.375-in. target material at a miss distance of about 60 ft at sea level and about 165 ft at 30,000 ft. At 60,000 ft, slowdown is sufficiently negligible so that no such limitations exist for either the 1/4 or the 3/16 rod at miss distances of less than 300 ft.

d. In addition to the limitations of expected cutting ability, the continuous-rod also has the geometric limitation due to the previously described hoop breakup. After breakup, the length of rod which existed at the time of the breakup must be distributed around the circumference of an increasing circle, so that the gaps between the sections of rod will constantly increase. Therefore, the ratio of the desired length of rod (the circumference of the expanding circle) to the available length of rod (which was the circumference of the circle at breakup) can be expressed as R_m/R_2, where R_m is the radius of the circle at breakup and R_2 is any instantaneous post-breakup radius. These results, when multiplied by a factor to account for the assumed oblique-impact and vulnerable-area limiting factors

(0.90 and 0.95, respectively), indicate the limit due to expected rod breakup after reaching the maximum intended radius. (The maximum conditional-kill factor, 0.855, is determined by multiplying the 0.95 vulnerable-area factor by the 0.90 oblique-impact factor, discussed previously.)

e. These concepts are summarized in Figure 12 for the 600-lb IM-99( ) warhead and in Figure 13 for the 300-lb IM-99 A warhead. In these curves, a constant lethality or probability of a hit being a K-kill is assumed until either the limitation due to inability to cut target material or the geometric limitations due to rod breakup are reached.

f. The kill probability for a particular guidance dispersion, σ_G, is determined by the following approximation:

$$P_k = \sum_{i=1}^{n} \Delta P_h \, P_{hk}$$

where $$P_h = 1 - e^{-\frac{S^2}{2\sigma_G^2}}$$

P_h is the hit probability for the case considered, and may be defined as "the probability that an interceptor, having a guidance error of σ_G, will miss the target by a distance of less than S ft." It should be noted that P_{hk} includes, as the limit due to rod breakup after reaching maximum continuous-rod radius, the probability that a rod segment will hit the target. A small (point-size) target is assumed in this instance. An increment of 10 ft for ΔS is used to determine the values for ΔP_h. Maximum attainable values were calculated for the kill probability for the continuous-rod warhead, based on the foregoing method and assumptions, and assuming no fuzing error. These results are shown in Figure 14 for the IM-99( ) warhead using 1/4-in. square rod and in Figure 15 for the IM-99A warhead using 3/16-in. square rod.

4. Conclusions

The successful application of the continuous-rod-warhead principle to the Bomarc missile appears to be highly promising for the following reasons:

a. The conditional kill probability is high, in particular for the 600-lb IM-99( ) version which employs a 1/4-in. square rod. However, the smaller IM-99A 300-lb version, which employs a 3/16-in. square rod, has a short overall warhead length which may promote premature hoop breakup, plus severe slowdown at lower altitudes which will reduce the cutting ability of the rod.

b. The overall K-kill probability is high, and the characteristic damage produced by rod cutting (i.e., severance of structure) should cause loss of control of the target aircraft, which should be apparent to the interceptor's home radar. Hit-probability estimates indicate that a warhead producing a continuous hoop of 300-ft dia or more prior to breakup and ejected at radial velocities of about 5000 ft/sec can achieve an almost certain hit at almost any angle of attack and relative missile target velocity, up to a miss distance of about 150 ft. Fuze tolerances of about ± 0.0025 sec can be tolerated in this situation (see Section IV), and skewing of the primary missile due to angle of attack has a negligible effect.

c. The continuous-rod warhead, being characterized by high radial projection velocities as compared with the forward velocity of the missile, can be classified as an "equatorial" cone device, which can use modifications of existing cone-type fuzes such as the T-3010 (see Section IV).

d. The continuous-rod warhead is simple in design and can employ a single, already developed, safety-and-arming device which can be conveniently located within the internal cavity of the warhead.

e. Missile skin removal prior to warhead detonation does not appear necessary. However, any heavy external ducting or structural members should be removed to prevent rod-pattern disturbance.

f. The time required for development of the continuous rod should not be any greater than that required for other warhead types.

NOTE: It should be pointed out that these discussions and conclusions are based on NMIMT, experimentally demonstrated, test configurations. The publicized difficulties encountered by the Navy in the development of the continuous-rod warhead for Talos are not expected to arise with the proposed Bomarc warhead because of the differences in the way the warheads are designed and emplaced in the missile. The Talos has an annular design requiring the use of asymmetric initiation which has caused, among other things, difficulties in detonation-wave control with a resulting early breakup of the rod hoops. Such problems, being alien to the proposed Bomarc warhead design, should not be permitted to prejudice the consideration of this highly useful warhead type for the Bomarc missile.

C. SHAPED-CHARGE AND MISZNAY-SCHARDIN WARHEADS

The shaped charge and the closely related systems employing the Misznay-Schardin effect are promising mechanisms for the destruction of aircraft, especially if high-explosive payloads are vulnerable. These systems, however, require considerable research and development, since the terminal-ballistic effects, which have been exploited in other applications, such as antitank weapons, have been only meagerly investigated for use as antiaircraft armament. Both of these mechanisms, which may be generally classed as highly directional, hypervelocity, fragment-beam projectors, are based on the principle of projecting metallic fragments, either in random or controlled sizes, shapes, and patterns off the end of explosive charges rather than off the sides as in fragmenting warheads. Fundamentally, the conventional fragmentation warhead, the Misznay-Schardin, and the shaped charge are all interrelated, having in common a metal surface, an explosive filler, and a device for initiating detonation; the main differences being in the location and configuration of these principal components.

1. Misznay-Schardin Warhead Considerations

a. Explosive ordnance items utilizing the Misznay-Schardin effect may assume several forms. These usually consist of a segment of a thin-walled hollow sphere backed with high explosive. The segment, usually referred to as the "dish," may either be in one piece or be scribed to control fragmentation, or it may consist of discrete pre-cut fragments assembled in the form of a "dish" shape. The HE is usually initiated at the end opposite that in which the dish is located and along the warhead central axis. The shape of the fragmenting surface can vary from concave, for concentrated beams, to concavo-convex, for a greater beam dispersion. It is possible to achieve maximum initial velocities of discrete fragments of about 15,000 ft/sec through suitable selection of an explosive charge-to-metal ratio (C/M). Proper design of the fragmenting surface and exercise of control over the detonation wave can provide good spatial control of the fragments. Almost uniform dispersion of hypervelocity fragments through cones up to 30° is not impossible to achieve. Deep, concave, spherically dished, solid-plate, Misznay-Schardin charges are also shaped charges, although they represent the lower regions of velocities for the latter.

b. Although considerable research work has been reported in the study of the Misznay-Schardin effect (chiefly by Pugh, Eichelberger, and others at Carnegie Institute of Technology), as far as is known, no full-scale or even model warhead employing this system has ever been fired at representative modern aircraft structures. This is a serious research and development gap, since it is quite possible that a satisfactory mechanism for the destruction of aircraft and missiles, particularly through the medium of payload detonation, may be within the capabilities of the Misznay-Schardin warhead system. It is believed that many of the aircraft damage effects observed in the experiments with wide-angled, shaped-charge liners at the Naval Ordnance Test Station, Inyokern, may also be representative of the Misznay-Schardin system. There is a probability, however, that the Misznay-Schardin type of warhead, which has an inherently wider spatial distribution of lower-initial-velocity fragments than does the highly directional shaped charge, would have a reduced effectiveness in terms of the damaging "vaporific" effect. Both systems do have a common requirement in that the warhead jet must point in the direction of the expected target intercept, since, like other efficiently designed conventional fragmenting warheads, the kill potential, except for the possible "bonus" blast effect, is nullified in the case of a near miss.

c. It has been established,* on the basis of a reasonably large number of test firings at NOTS, that fragment beam projection by means of one or more shaped charges results in spectacular structural damage to aircraft as a result of "vaporific" effects. This effect is an almost explosive combustion of the fragment particle and the local area of the target as a result of high-velocity impact (10,000 to 25,000 ft/sec). With the shaped charge, the continued buildup of explosive energy as the jet of particles or fragments strikes the target is capable of generating extensive structural damage, characterized by physical destruction of heavy members, removal of quantities of skin, incendiary effects on fuel, detonation of payload, etc. It is estimated that the vulnerable area of a modern high-performance bomber to attack by the large-caliber shaped charge (over 7.5 in. in diameter) is approximately 90% of the presented area, excluding from the K-kill vulnerable area such things as wing tips, single empennage surfaces, and the like. This conditional kill probability is applicable up to altitudes of approximately 30,000 ft and at standoff distances of 100 to 120 ft. There is evidence that at higher altitudes the lethality increases and can be achieved at much greater standoff distances.

d. When a single hit is involved, the conditional kill probability of 0.9 may appear to be optimistic for the shaped charge; however, in the case of multiple-jet shaped-charge warheads, more than one hit is expected, except for large miss distances. An additional consideration is that the large quantities of fuel carried aboard modern turbojet bombers may render these aircraft unusually vulnerable to the shaped charge from both explosive ignition of the fuel and structural airframe damage from hydraulic ram effect.

2. Shaped-Charge Considerations

The shaped charge as used for antiaircraft applications can vary from shallow dished types to deep conical shapes similar to those developed specifically for use in antitank weapons. Initial fragment velocities for

*These comments are based on published and unpublished NOTS data for the period 1950-1953 and on recent conversations with NOTS personnel engaged in this work (see References 31 and 32).

centrally initiated, Service-type, shaped charges as high as 31,000 ft/sec have been measured when thin, deep, conical liners using lightweight materials are used. This velocity represents an upper practical limit in mechanical projection velocity for systems in general Service use.

3. Damage Mechanisms

The highly directional shaped-charge jet consists of a stream or jet of fragments of finite but increasing length, with a decreasing velocity gradient from the leading end of the jet because of the effectively lower instantaneous C/M ratio existing as the explosive or detonation wave sweeps down the liner from apex to base. These successive groups of hypervelocity, high-energy fragments probably contribute to the target destruction capability of long-standoff shaped-charge jets by means of the phenomenon of "vaporifics." With regard to this phenomenon, early investigations of problems associated with hypervelocity fragments (Reference 57) indicated that above certain threshold values of mass and velocity, fragment strikes on aluminum-alloy plate were accompanied by a brilliant flash of light, and the impact area appeared to be damaged in a different manner than had occurred in the case of lower-velocity fragments and bullets. The area around the impact holes in aluminum plate was "petalled" backward rather than torn in the direction of fragment travel, and when two sheets of aluminum were spaced one behind the other, the second sheet suffered more damage than the first. Subsequent investigations at NOTS, Inyokern (Reference 33), led to the conclusion that "vaporifics" is, among other things, a result of the explosive combustion of extremely finely divided material which is produced by the impact of the rapidly moving fragment on the target skin. It is believed that the high rate of energy transfer at impact raises the energy level or temperature of the finely divided material to the point where rapid chemical combination with the surrounding atmosphere is possible. In most cases, aluminum "dust" explosions (Reference 58)* are obtained, although magnesium and even stainless steel exhibit "vaporific" effects. Both oxygen and nitrogen atmospheres have been found to promote "vaporific" phenomena, and increasing altitude, as mentioned above, seems to further increase them. Inert gases such as helium and engine-exhaust gas, however, almost completely suppress the effect. Current research work at NOTS supports an extended theory concerning the "vaporific" effect and suggests that the first material striking the target builds up within the target a small high-pressure volume of very hot higher-density products, and that as succeeding groups of fragments enter this region of high density, this "cloud" tends to act as an energy "trap" and absorb even more energy from the succeeding impacting particles. The region of high density and high energy

*Finely divided aluminum was detonated to produce so-called slow-burning-explosions which were noted to produce more extensive damage in enclosed targets than equivalent amounts of the more conventional high explosives.

rapidly expands until the target structure ruptures on the far side, as it would from the detonation of high explosives within the structure. Preliminary calculations by the NOTS group indicate that the energy delivered to targets by 7.5- to 8.5-in.-dia charges is equivalent to 4.3 to 5.5 lb of explosive.

4. Effects of Altitude on Shaped-Charge Jet Performance

Studies in the NOTS Controlled Atmosphere Laboratory with scaled-down charges (1.5-in. dia) under reduced pressures simulating altitudes up to 116,000 ft (Reference 31) indicated that above 40,000 ft (equivalent altitude) the reduced drag on the jet fragments permits both an increase in jet average velocity and a reduction in the radial dispersion (normally about 2-3 deg. total angle) of the fragments comprising the jet. The "vaporific" and mechanical damage observed on simulated aircraft target sections increased many fold at pressure altitudes above 40,000 ft and remained heavy even up to the highest altitudes studied. Since at high altitudes the finer-divided material comprising the jet is not eroded away and the larger fragments do not decelerate greatly, the average velocity and the mass of material arriving at the target are appreciably greater than at low altitudes. This leads to two basic assumptions concerning the performance of long-standoff shaped charges: (1) that the lethal range is increased perhaps many times at altitude, and (2) the target effects observed in open-air low-altitude firings (at 2000 ft altitude) are indicative of the least favorable conditions, and target damage at altitude can be expected to be appreciably more severe.

5. Shaped-Charge Liner

The liner diameter, cone angle, and materials are all important variables. Of these, the liner diameter appears to be the most critical, with liner material only slightly less important.

a. Current work at NOTS, Inyokern, with long-standoff shaped charges has included a comparison of terminal effects at a 60-ft standoff for shaped charges of various materials (including aluminum, magnesium, copper, steel, and zinc alloy) and of various diameters, on B-29 structural components (inner wing panels, bomb-bay section, after fuselage). These tests have substantiated conclusions drawn in earlier reports (e.g., Reference 32) that the size and material of the shaped-charge liner were critical and that for K-kill structural damage at 2000 ft altitude from a 60-ft standoff, the diameter should be more than 6 in. when used against aircraft of fighter size and more than 7.5 in. when used against aircraft of heavy-bomber size. These critical diameters are evidently a decreasing function of altitude as a consequence of "vaporifics" and an increasing function of standoff, which in the case of the Bomarc should be at least 180 ft for peripheral effectiveness. A further possibility which cannot at present be discounted, and about which little is known, is that the critical charge diameter may be dependent upon the target size and construction.

b. Optimum liner materials include aluminum, magnesium, and zinc in descending order, with the possibility that some such alloy as aluminum-magnesium-silicon may be superior to those investigated to date.

c. Of the cone angles investigated, a 120° angle (apex) appears to give the most consistently good results against aircraft structures.

d. Cones of smaller angles (80° and even 45°) have higher initial velocities, but break up into more finely divided material which at lower altitudes erodes rapidly in the airstream. Small-scale charges with 80° cones did not demonstrate the excellent terminal effects that have been observed for wider-angled (120°) designs in the altitude chamber. An experiment recently conducted at NOTS indicated that an equal-mass, wide-angled cone (with thickness increased to about twice normal) produced as much apparent damage to a B-29 fuselage section as did a deep-coned (45°) charge, but required a longer time, in terms of milliseconds, for target disintegration from time of initial jet impact.

e. At a 60-ft standoff, average velocities of 20,000 ft/sec or higher are consistently achieved with the largest light-metal coned charges. At low altitudes, however, deceleration due to the density of the air and erosion are so great that the mean velocity begins to drop off rapidly at ranges greater than 60 ft. NOTS 15-in. aluminum-lined charges, fired at 300-ft standoffs at an altitude of 2400 ft, averaged only 10,000 to 12,000 ft/sec in spite of their high initial velocities.

f. Liner thickness has been explored in a 120° conical aluminum configuration. Thicknesses up to 24% (thickness of wall expressed as a percentage of explosive diameter) have been investigated from the standpoint of both the character of damage produced on F6F fighter-aircraft wing structures and on the effective average velocity of the jet. It was determined that liner thicknesses between 6 and 10% produced the most structural damage in terms of area of target destroyed. Velocity of the jet dropped appreciably in liners thicker than 10%.

g. Based on work done to date, it appears that the best liner configurations are those employing aluminum alloy cones with a 120° apex angle and wall thicknesses of 6 to 10%, with the thicker liner being used where weight permits. The liner diameter should be approximately 8 in. to insure high kill potential against heavy targets. The charge-to-metal ratio should exceed 4 although detonation-wave shaping may reduce this ratio if properly applied.

6. <u>Problems Associated with Use of Shaped Charges in Bomarc</u>

a. Shaped-charge warheads used in the Bomarc would be located inside of the missile skin and would be fired laterally. The effect of high-velocity cross-wind firings on shaped charges has been only cursorily studied in some firings at NOTS (ca. 1948), where small 2-in.-dia, 45°-steel-cone, shaped charges were fired transversely from a sled moving at about 1300 ft/sec. As might be expected, the resulting jet fragments were dispersed in a wavelike pattern along the targets. "Vaporifics" were not investigated at the time of these tests; consequently, there is a continuing need for the study of the effects of high-velocity translation on the performance of shaped charges against aircraft. It is assumed, however, that the wide-angled cones described above would be superior to the deeper-angled cones, because the arrival time of all material at the target should be sufficiently short so that the jet will not be badly dispersed along the target.

b. The second potential problem, particularly for the shaped-charge system, is the possible adverse effect of the covering missile skin on the formation of the jet. It has long been the practice in the design of conventional shaped charges to avoid placing structure in the path of the jet, particularly in proximity to the open face of the liner. This rule has applied primarily to penetrating jets and weapons where there is a possibility of fuzes, windscreens, etc. being jammed into the cone at impact. However, it is thought that the warheads designed for the IM-99 interceptors would probably not be adversely affected by the 0.090-in. aluminum missile skin, since the "open faces" of the cones will be sufficiently far from the skin (minimum of 2.5 in.) to preclude disruption of the jet during the initial formation stages. Verification of this hypothesis requires experimental testing, although indications from past experiments are that little or no trouble should be encountered.

7. <u>Methods of Employing Shaped Charge in Bomarc System</u>

There are three possible approaches to the utilization of the shaped charge in an anti-aircraft missile: The first involves the pointing of a gimbal-mounted, large, single charge so that it tracks the target, or rather the expected target intercept point, and detonates at the point of nearest approach. The second involves the mounting of one or more rings of smaller charges normal to the axis and around the periphery of a cylindrical or ogival shell. The third possibility is the employment of helically oriented, wedge-shaped, fragment-beam projectors around the warhead cylinder to eliminate the gaps in the multiple-jet design.

a. Gimbal-Mounted, Single Shaped-Charge Projector

It is possible, as has been demonstrated several times against various representative targets (such as B-29s and F6Fs on the ground), to achieve structural K-kills and in many cases over-kills at standoffs as high as 300 ft from the point of warhead detonation, using a single, large, shaped charge with a 15-in.-dia aluminum liner. Since the single charge is comparatively large and requires accurate aiming, the most practical method would seem to be the gimbal mounting of the charge within the missile so that it can be accurately oriented and fired at the most opportune moment. To date, little has been accomplished on the design and development of gimbal-mounted target-tracking warheads because of the extremely difficult problems involved with such systems. A gimbal-mounted Misznay-Schardin system for the Wizard Project, using a 34-in.-dia, 500-lb warhead, is described in Reference 34. In that design study, the large flat disc was placed within a set of electrically powered gimbal rings. The electronic equipment associated with the system is complex, since the fire-control problem which the fuze must solve is particularly difficult, and the power demand at the time of actuation appears excessive. A more recent analysis of a gimbal system for shaped-charge warheads was conducted by the Ahrendt Instrument Company under a BuOrd contract in 1949-50. In this study, two major problems seemed to rule out the use of the gimbal system: the first, as mentioned above, was the excessive power demand, and the second was the inadequacy of radar angular guidance. Present power supplies, as exemplified by the lightweight propellant-gas-driven APU (auxiliary power unit), possibly can supply the energy required for operation of a gimbaled system; and lightweight high-strength materials, such as titanium alloys, can reduce the overall power requirements by lessening the inertial mass in the moving parts. The inadequacy of radar angular guidance and range for training the gimbaled head has been attributed to the rate of signal return, which is inadequate at close ranges and high closing rates, and also to the tendency of radar toward "glinting" or "looking" at randomly different parts of a complex aircraft target; a severe problem when close to large aircraft. It is possible to eliminate this restriction by employing an infrared fuze detector and computer, which however, would compromise to some extent the desired all-weather capability at low altitudes (below 30,000 ft). It is impossible to estimate a kill probability for this type of warhead without a detailed design of its control system. It has been noted in Reference 35, however, that a probability of destruction (P_k) of 0.75 might be attainable. This results almost entirely from the fuzing and control-system errors. If the fuzing and aiming limitations are for the moment assumed to be satisfactory, a gimbal-mounted warhead system for the advanced IM-99( ) Bomarc could conceivably be designed along the following general lines:

(1) The warhead proper could consist of a 10- to 15-in.-dia, wide-angled, thick metal liner backed by sufficient explosive to provide a C/M ratio of approximately 4, a low but satisfactory ratio for these diameters. The liner configuration can be in several forms. However, a successfully demonstrated design utilizes an aluminum alloy liner in the form of a cone of 120° included angle, with a thickness of 10% of the diameter. The warhead case would be designed in a hemispherical or ellipsoidal shape to conserve weight, and devices such as lightweight air-void wave shapers would be used within the explosive for increased efficiency. It is conceivable that an efficient warhead design would weigh approximately 100 to 150 lb, depending upon the liner diameter. The remaining 450 to 500 lb is available for the gimbal rings, gimbal-drive jet motors, power units, guidance and computing equipment, and warhead-training electronic equipment. The

electronic fire-control equipment and the associated servos will actually determine the final design of the warhead. If high accuracy of aim is maintained under conditions of intercept, then the charge can be designed as described above for maximum target lethality. However, aim is all-important with this type of shaped-charge warhead, since the jet is confined to about a 2.5° maximum spread, regardless of warhead size. At 60 ft the static impact area is hence only approximately 31 in. across, increasing to about 94 in. at a 180-ft standoff. The use of convex-shaped Misznay-Schardin charges would increase this spread considerably (e.g., 32.2 ft in diameter for a 30° spread at a 60-ft standoff), but the resulting target damage would be considerably less than the concentrated damage obtained with the shaped charge.

(2) The gimbal-ring assembly with the warhead mounted at its center might be packaged in a 20- and 22-in.-dia space, leaving ample space fore or aft of the gimbals for mounting electronic components. The fuze detector would of necessity be located in the missile nose at the tip of the radome, with the infrared sensing head located in the center of the nose. Since the I/R unit can be quite small (2.5 in. in diameter, 10.0 in. in maximum length) it could be located at the apex of the radome if the aberration effect is not too severe. For maximum efficiency, the warhead should be triggered when the least missile structure is in its path. This requires that the warhead "look" at its target at all times, and preferably fire just before the missile makes its nearest approach. Since, at nearest approach, the missile is either inside or abeam of the target, the warhead should fire at an angle with respect to the longitudinal missile axis of 60 to 120°, provided that the gimbal cage is centrally located in the warhead compartment. Locating the cage near either end of the compartment would shift the cone of efficient fire.

b. Multiple-Shaped-Charge Warheads

A second, and more readily achievable type of shaped-charge warhead system for the IM-99( ) is one employing multiple rows of radially projected, shaped charges or Misznay-Schardin, hypervelocity, fragment beams. Essentially this system involves the disposition of a number of shaped-charge cones about an annulus of high-explosive elements provided with a means of initiation that will cause the detonation front to approach each cone normally and as nearly simultaneously as possible. Detonation of the warhead results in the production of a high-energy, almost unidirectional stream of hypervelocity fragments from each of the cones in a plane nearly equatorial to the missile. The projection angle of the high-velocity (15,000-20,000 ft/sec) "equatorial" side spray from the shaped charges oriented at 90° with respect to the missile axis is almost independent of the initial projection velocity of the shaped-charge jet, and only slightly more dependent on the forward velocity of the primary missile. The following table lists the initial angles of departure of shaped-charge jets over the wide range of possible missile velocities and shaped-charge jet velocities, with reference to the longitudinal axis of the IM-99( ):

Case No.	Velocity of IM-99( ) V_m,ft/sec	Initial Velocity of Shaped-Charge Jet V_p,ft/sec	Angle of Departure with Respect to Missile Axis arctan V_m/V_p
1	1000	10,000	84° 17'
2	2500	10,000	75° 58'
3	1000	15,000	86° 11'
4	2500	15,000	80° 32'
5	1000	20,000	87° 8'
6	2500	20,000	82° 52'
7	1000	30,000	88° 5'
8	2500	30,000	85° 14'

Assuming that the individual useful fragments comprising any jet have a velocity gradient as great as 10,000 to 30,000 ft/sec (which is only remotely possible), the additional induced angular spread of the jet along the line of flight would be approximately 9° when the primary missile velocity V_m, is 2500 ft/sec (the worst condition) and only 4° when V_m is 1000 ft/sec. Since most shaped-charge liners used for antiaircraft applications are wide-angled, however, the velocity gradients will undoubtedly be much less, probably about 5000 ft/sec, or equivalent to an induced directional spread of about 1 or 2°. It can be seen that the concentration of the jet on the target will hence be comparatively tight, even when the relative velocities of the missile and target are high, as in a head-on attack.

(1) Warheads designed around multiples of shaped charges present certain problems that are unique to this type of ordnance. The major problem is that of charge initiation, particularly when the design calls for an annular arrangement of explosives and more than one row of cones. It has been determined in experiments with pairs of shaped charges placed in proximity to each other that the earlier-fired charge can adversely affect the adjacent charge to the extent of completely destroying its jet. This time lag between adjacent charges can be critical when the delay is only a fraction of a microsecond, since in an explosive, the detonation wave proceeds at about 1/3 in. per microsecond. Therefore, for optimum performance from a warhead using multiples of shaped charges, whether individually packaged or using a common explosive backing, it is considered imperative that the detonation wave approach each liner normal to its transverse axis and all liners as nearly simultaneously as possible. Multiple shaped-charge warheads having a common center (i.e., solid, hemispherical shape) have no unusual initiation problems. The generally annular arrangement is required for the IM-99A systems, which must provide both arming safety on the detonators and near-simultaneous initiation for as many points as there are cones in the head.

(2) Two methods for achieving near-simultaneous initiation have been successfully demonstrated with multiple shaped-charge warheads: one method using low-energy, high-quality electric detonators wired in series and fired by a discharge from a high-capacity condenser, and the other using accurately cut, equal lengths of Primacord, which are all initiated from a single detonator. In consideration of arming safety and least complexity, the latter system should probably be used in the IM-99 warheads, although the degree of simultaneity may not be as high as for the electrical system. Extreme care and some properly planned developmental testing will probably be required to insure that the Primacord system will function adequately. A single safety and arming device, possibly a modification of the device designed for the T-33, will serve as the safety barrier between the electrical detonator and the complex network of Primacord leads and required booster charges.

(3) Perhaps the most serious factor affecting the lethality of a multiple-jet shaped-charge warhead is the gap existing between adjacent jets. High probabilities of hit are favored by large numbers of jets so that the gap between the "spokes" is slight. However, weight and space limitations of the IM-99( ) warhead, plus the assumed need for at least 8-in.-dia individual liners greatly restrict the number of jets that can be produced from the warhead. While it is theoretically possible to accommodate 52 8-in.-dia liners in a cylindrical warhead shape 35 in. in diameter and 35 in. long, representing the IM-99( ), the attendant explosive weight and allied structure and initiation system to insure adequate performance would make such a warhead exceedingly heavy. Design studies show that it does not appear possible to package more than 30 8-in. liners in a 600-lb gross-weight package. With 30 discrete jets, all arranged to fire normal to the missile axis, the "spokes" will be at 12° intervals between jet center lines, or 12.5 ft apart at a 60-ft standoff and 37.4 ft apart at a 180-ft standoff. The natural spread of the individual jet, being approximately 2°, reduces the gap distance between adjacent areas of impact to 10.4 ft at 60 ft and 31.3 ft at 180 ft standoff.

(4) With the objective of attaining maximum efficiency in the multijet shaped-charge warheads for the IM-99( ) and IM-99A, and still remaining within the weight limitations of 600 and 300 lb, respectively, the designs shown in Figures 16 and 17 have been prepared. The following basic liner and explosive configurations were selected:

Cone material: Aluminum alloy; 2024-T, 2014, 356, or 4043 (Type apparently not critical)

Cone configuration: Wide-angled cone having 120° apex angle, straight-side, uniform wall thickness 6 to 10% of explosive diameter

Cone size: Minimum 8-in. dia for use against bomber-size targets

C/M ratio: 4 to 6 appears adequate (based on Misznay-Schardin studies by Carnegie Institute of Technology)

Explosive: Composition B, 60/40 RDX/TNT, unless newer explosives such as 75/25 Cyclotol or Octol became available in quantity

(5) Design studies have shown that it is impractical to attempt annular construction of either the advanced IM-99( ) or the interim IM-99A warhead using a common explosive backing, since even with maximum disposition of explosive immediately behind each cone, only about 2.5 in. of explosive can be accommodated along the cone axis because of weight limitations. A more efficient approach for the IM-99 warheads is the use of individual "projectors," as shown in Figure 18, each consisting of an 8-in.-dia, 120°, 0.5-in.-thick (6.25%) aluminum alloy cone; an ellipsoidal-shaped, thin, stainless steel case, containing about 13.5 lb of Composition B (for a C/M ratio of 6); and a booster cup and Primacord adapter. Each individual projector charge may be cast-loaded through a 1.7-in.-dia hole at the base. A 1/2-in.-long, 5/8-in.-dia tetryl booster is accommodated in the screw-on base closure, which also provides a firm attachment for the Primacord initiator lead. Thirty such projectors, ten for each of three rows, the rows staggered to give a spiral arrangement with 12° between cone center lines, are accommodated in the 600-lb IM-99( ) configuration (Figure 16), having a 30-in.-dia and an overall length of 30 in. A central cavity 14 in. in diameter is available for insertion of the Primacord network and the S-and-A device. The 300-lb IM-99A warhead accommodates 16 of these projectors in a 30-in.-dia, 17-in.-long assembly (Figure 17). In this warhead the individual charge projectors are nested closely together to keep the overall length to an absolute minimum, and are arranged so that the jet center lines are 22.5° apart.

(6) Initiation systems for the two warhead designs are similar. A Primacord network system emanating from a single-point source attached to the missile S-and-A unit is used in both assemblies. To assure the maximum probability of simultaneity, all Primacord booster paths are equal in length and precautions such as cutting all Primacord from a single spool to insure uniformity etc. are required. Each equal-length Primacord lead is attached to hubs surrounding a disc-shaped tetryl booster. The three-row design for the 600-lb warhead has two such hubs, each accepting 15 Primacord leads. Each hub is in turn connected by equal-length Primacord leads to a central booster initiated by the S-and-A device. All 16 Primacord leads on the 300-lb two-row head are attached directly to the central booster on the S-and-A device. The functioning time is dependent on the total length of any path (i.e., S-and-A booster, intermittent Primacord leads, hub booster, Primacord lead to projector, projector booster, and main projector charge).

The detonation impulse will proceed approximately at 0.312 in./microsec for Comp. B, 0.246 in./microsec for Primacord, and at 0.288 in./microsec for tetryl. The approximate functioning times of the explosive trains are hence 65 microsec and 80 microsec for the 300- and 600-lb designs, respectively. A variation in the assumed detonation rates of each component, even by ±1000 ft/sec, will then have a negligible effect on the total functioning time. For example, if all components are 1000 ft/sec faster than assumed, the 80 microsec would drop to only 77.2 microsec, and conversely, if values were all 1000 ft/sec slower, it would increase to only 84.4 microsec.

c. Helical-Wedge Shaped-Charge Projector

A third type of shaped-charge warhead system, which has not apparently been previously investigated, possibly offers the terminal ballistic advantages of the hypervelocity jet particles with a comparatively simple type of head without the limitation of the jet to a small number of lethal "spokes." This warhead design consists of a number of V-grooved, linear, shaped charges arranged along the missile longitudinal axis in a spiral, so as to eliminate all gaps in the fragment pattern. Although this explosive design probably cannot produce the dense local pattern or high initial velocities of the conical liners, the helical-wedge, or "screw-head," charge does promise many of the advantages of the multiple-charge system without the complex initiation problems or the extreme sensitivity to direction of approach of the detonation wave front. Actually, the "screw-head" is probably more of a "super" fragmentation head (very narrow fragment beam) than it is a shaped-charge or Misznay-Schardin system, although it is tentatively classed as a shaped charge because of its dependence on the shaped-charge mechanism for its functioning. Little experimental data on a warhead configuration of this type is available; however, limited studies on similar devices conducted by the Navy both at Dahlgren Proving Ground and at NOTS, Inyokern, and the more recent work at Aberdeen's Ballistic Research Laboratories, all suggest the technical feasibility of the "screw-head." Linear, shaped charges are no novelty, having been extensively used for years in demolition work and in explosive cutters, and more recently in ordnance in grooved-charge fragmentation heads. Experimental work has usually been concerned with radial or circumferential linear charges, such as the British "Diablo" (described briefly in Reference 35), which spread their material so widely as to be almost valueless. Recent experiments at Aberdeen, however, with longitudinal, linear, shaped charges have given promising results (References 55 and 56). The major improvement offered here is the slight spiraling of the V-grooves to eliminate gaps in the fragment pattern, at only a slight possible loss in effectiveness. The effect of linear spreading of the impact zone upon the vaporific effect necessary for target destruction is, of course, uncertain. In addition, the target speed can compound any effect. As a result, the assessment of the "screw-head" is sufficiently uncertain so that extensive consideration is not justified at this time, for application to warheads for the advanced or tactical Bomarc interceptors.

8. Shaped-Charge-Warhead Lethality Estimates

a. The basic assumptions used in determining the lethality estimates for the 30-projector shaped-charge warhead proposed for the IM-99( ) and the 16-projector warhead proposed for the IM-99A are as follows:

(1) 90% of the target presented area is K-vulnerable to an 8-in. shaped-charge projector, subject to the following altitude-range degradation.

(a) At sea level, the 8-in. shaped-charge projector is conservatively assumed lethal to a range of at least 60 ft.

(b) At 30,000 ft altitude, the 8-in. shaped-charge projector is conservatively assumed lethal to a range of at least 180 ft.

(c) At 60,000 ft altitude and above, the 8-in. shaped-charge projector is lethal to a range of at least 300 ft.

(2) The "average" target is assumed to have a dimension of 20 ft along an arc of the circle which lies in the plane defined by the shaped-charge jets. This assumption establishes a geometric limitation to the maximum lethality of the jets due to the "spoking" effect wherein at some large miss distance it would be possible for a finite target to fly unharmed between two adjacent jets.

b. The lethality estimates, based on the above assumptions, are presented in Figure 19, as a function of the actual miss distance for both the 30-projector IM-99( ) and the 16-projector IM-99A warheads.

c. Kill probabilities are determined by the same method as used in the evaluation of the continuous-rod warhead (see paragraph III,B,3,f). Based on a guidance error, σ_G of 60 ft, and assuming no fuzing error, the maximum attainable kill probabilities for the shaped-charge warheads are shown in Figure 20 for the IM-99( ) warhead and in Figure 21 for the IM-99A warhead. Since the IM-99A can accommodate only 300 lb of warhead, including support provisions, no more than 16 charges can be incorporated.

d. The multiple-jet, shaped-charge head, in addition to its jet effect, follows the fragment beams with a plane blast wave from the Comp. B filler, which, because of its multi-point initiation system, will probably have a greater blast effect than the usual equivalent-weight, point-initiated, external blast charge. The rapid following of the jet impact by the high over-pressure blast, at least at the smaller miss distances, should increase the resulting damage by extending the tearing of structure and by "gust-loading" the aircraft so that recovery of control becomes more difficult or impossible. The external-blast damage attributable to the high explosive is a "bonus" factor which has been explicitly excluded from the kill probability estimates.

D. CLUSTER, OR SUBMISSILE, WARHEADS

Cluster warheads eject a pattern of submissiles which may be categorized according to the characteristics of the submissiles as follows:

Unstabilized, unpropelled
Stabilized, unpropelled
Stabilized, propelled
Propelled and guided

The unstabilized, unpropelled submissiles include the "spigot-projected" block munitions, as typified by the Bomarc T-44 warhead being developed by the Aircraft Armaments Company, and the ball-shaped units in a propellant matrix or canister shot system under development by the Rheem Manufacturing Company. Stabilized unpropelled submissiles include drag-plate or fin-stabilization types. The stabilized, propelled submissiles include the fin-stabilized rocket, or a spin-stabilized rocket as typified by the Crossfire weapon proposed by the Aerojet-General Corporation. The most refined version of a submissile includes both propulsion and limited guidance in addition to stabilization.

1. Cluster Warheads Considered for IM-99( )

a. Unstabilized Blocks (Spigot-Projected, Omnidirectional Fuzes)

Each cluster unit as designed for the T-44 warhead contains 2.9 lb of HBX, has a cylindrical fuze well, a central cylindrical spigot adaptor well, and a thin aluminum box-like case with welded seams. The radial velocity of projection of each unit is about 100 to 400 ft/sec, which, considering the velocity of the primary missile, means that the angle of projection with respect to the missile flight path is small. For example, when launched 1500 ft from the target, from a missile traveling 2500 ft/sec, the ring of cluster units is about 180 ft in diameter by the time it reaches the target. Also, because of the box shape of the submissile with its attendant high drag, the launching missile is always ahead of the submissiles in flight and reaches the target area before the submissiles. This factor will, on the average, increase the miss distance between the target and the submissiles at low and intermediate altitudes. These effects are discussed more fully in the fuzing section of this report, wherein the effects of ejection velocity are considered. The primary disadvantages are the apparent difficulty of penetrating heavier targets to permit internal blast, as indicated in the Reference 25 tests, the requirements for omnidirectional fuzing of the blocks, and the difficulty of missile fuzing. There is also a moderate parasitic weight per unit. The principal advantages are the comparatively large number that can be carried (as many as 90, 5.0-lb units in a practical assembly) and the relatively large explosive charge (2.9 lb of HBX) per unit, which, when successfully detonated internally will cause K-kill damage to most targets. The problem of developing a reliable all-ways acting fuze with safety and arming, target sensitivity, and built-in self destruction is quite difficult.

The Reference 28 fuze-feasibility study includes tentative designs for an electromechanical fuze and consideration of a secondary, purely mechanical fuze to meet the submissile requirements. The properly designed submissile fuze should have the following characteristics:

(1) It should prevent submissile functioning if the warhead is accidentally fired on the ground prior to flight.

(2) It should partially arm during the 28-sec boost phase (acceleration up about 5 g only), unless arming is provided by the primary missile S and A.

(3) It should complete arming during the short but high acceleration (about 1400 g), submissile ejection phase.

(4) It should permit all-ways functioning regardless of the angle of impact or the strength or thickness of the target. It should also permit internal or in-surface bursts, depending on submissile case design or amount of high explosive carried.

(5) It should preferably provide for self-destruction after a suitable time interval.

(6) It should be completely contained, hermetically sealed, and have no external parts.

As can be seen, the omnidirectional fuze must meet stringent requirements, and attainment of satisfactory reliability and operability will be accordingly difficult. The force for initial partial arming is weak from the standpoint of the fuze-mechanism design, yet arming safety must be maintained. It is possible, of course, to have ground safety by mechanical or electrical interruption of the ejection system. Individual unit safety, however, cannot then be guaranteed. The fuze proposed in Reference 28 meets conditions (1), (3), (5), (6), and part of (4), but it does not provide ground safety or delay firing for internal bursts.

b. Stabilized Blocks (Spigot-Projected Unidirectional Fuzing, Drag-Stabilized)

The methods of achieving block submissile stability, as outlined in the Reference 27 feasibility study, would remove one of the major problems of the block cluster-warhead concept by simplifying the omnidirectional fuze-function requirement. Drag stabilization, however, would tend to appreciably increase the deceleration of the already poor aerodynamic shapes and to add to the kinematic fuzing problem, resulting in a serious degradation of the cluster warhead due to primary missile fuzing.

c. Fin-Stabilized Submissiles (Possibly Rocket-Propelled or Spigot-Ejected)

These submissile types are characterized by high length-to-diameter ratios and long, slender explosive charges. The advantages lie in simpler fuzing and greatly increased penetration abilities (Reference 29). The disadvantages include a low, radial velocity component common to all unpropelled submissiles with the consequent primary-missile fuzing degradation, and the requirement for deep penetration to get all the explosive inside the target structure — a fuzing delay problem.

d. Spin-Stabilized Submissiles (Crossfire-Type Cluster Warhead)

(1) The concept of a Crossfire-type weapon as developed by Aerojet, and outlined in Reference 9, has been applied to the IM-99( ) warhead. Figures 22 and 23 show typical configurations for such a warhead. Spin-stabilized submissiles should be given a high initial spin before they leave the launching missile to prevent instability arising as a result of the high initial angle of yaw with respect to the relative wind. This requires (a) that each submissile be launched from a rifled, closed-breech tube, and (b) that the submissile be either a gun-type projectile or a rocket projectile. It is believed that the optimum configuration for the IM-99( ) warhead is a spin-stabilized rocket having the highest warhead capacity possible and only sufficient propellant to achieve the necessary initial velocity and stability. Such features as a submerged delay fuze and "cookie-cutter" nose for yawed, high-obliquity penetration of heavy-skinned targets have been demonstrated in the 70-mm AEROFLAK (Reference 30), and are incorporated into the sub-missile design. The following table indicates the effect of caliber on high-explosive capacity and total number of rounds that could be accommodated in a typical IM-99( ) configuration (scaled from the 38-mm Crossfire configuration, Reference 9):

Round Diameter in.	Burned Wt of Round lb	Weight of HBX lb	Approximate No. of Rounds in Warhead
1.50	1.21	0.235	275
1.75	1.92	0.372	180
2.00	2.87	0.557	120
2.25	4.10	0.795	85
2.75	7.40	1.44	46

(2) An example of the projectile and of the launcher to be used in the Crossfire cluster-type warhead are shown in Figures 24 and 25 for the 38-mm (1.5-in.) size. The projectile is short (5 calibers) to insure cross-wind stability. Using the 1.5-in. submissile and allowing about 10% of the warhead weight for structure other than the launcher tubes,

approximately 275 submissiles could be packaged in a configuration similar to the one shown in Figure 22. A similar configuration for 119 submissiles of the 2.00-in. size, each containing 0.557 lb of HBX, is shown in Figure 23. These submissiles achieve a velocity of about 1250 ft/sec, which when projected in a forward cone and added vectorially to the velocity of the missile, produces a significant striking energy. It is possible, through the choice of launcher-tube angle and the variation of the initial velocity of the submissile (a characteristic of the motor design) to select the appropriate cone of dispersion considered most suitable for the primary missile fuze.

(3) To summarize, the principal advantages of spin-stabilized cluster units lie (a) in their improved and proven ability to penetrate heavy aircraft skins and detonate internally, (b) in their inherently simple, submissile fuze arming and functioning, and (c) in high velocity, added to that of the launching platform. The disadvantages of such a system are (a) the high parasitic weight for the weight of high explosive carried, (b) possible instability problems in supersonic cross-wind firing, and (c) the fuzing problems associated with submissile acceleration.

e. Guided, Propelled Submissiles

(1) Some consideration was given to the possibilities of using a small, infrared-guided, spin-stabilized aerial torpedo, as illustraed in Figure 26. Such a projectile would be fired from a low-pressure gun, such as that shown in Figure 27; and a group of 8 to 12 such submissiles with their launching guns might be packaged in a configuration such as that shown in Figure 28 for the IM-99( ). The projectile would have a short nose section mounting four control vanes and the infrared-seeker guidance equipment. The significant features of such a projectile are as follows:

(a) Yaw control of the projectile by parallel angular displacement of the commutated two (or four) vanes under command of the fuze-seeker computer, so that the course deflection is caused by precessing the projectile to develop aerodynamic body lift and a lateral component of thrust.

(b) The use of a short-burning, high-impulse propellant to obtain maximum controlled lateral displacement.

(c) The use of a high-scanning-rate search detector so that accurate angle and angular rate data are available for navigation.

(2) Design analysis proceeded to such a point that

(a) The projectile appears mechanically feasible to develop

(b) Aerodynamic control, with some modification of the vanes appears feasible

(c) A careful analysis of the avionic components required for the control system indicates that approximately four times as much space is required to package the electronic gear as is now available for the present configuration.

(3) The conclusion was reached, therefore, that the current state of the art and the expected developments during the development time scale for the IM-99( ) are such that the guided submissile does not appear feasible for application to the present program. Consequently no further evaluation was performed on this submissile.

2. Methods of Evaluation and Required Assumptions

a. All submissiles considered for cluster warheads to be used in the Bomarc armament system contain a charge of high explosive. Consequently, the mechanism of target damage is either internal or external blast, depending on whether the submissile penetrates the target skin before detonation, or detonates on contact with the surface of the target skin. Therefore, kill-probability methods and the necessary vulnerability assumptions are presented prior to a detailed discussion of the particular cluster warheads considered for Bomarc.

b. **The distribution of submissiles may be considered** as a forward-thrown projectile beam, since the cluster warheads to be considered have a comparatively low, submissile, radial ejection velocity (about 100 to 400 ft/sec), and must therefore be fired at a considerable standoff from the target to enable the ring of submissiles to reach optimum diameter.

c. The method for evaluating the effectiveness of such forward-thrown projectiles is outlined in a British report (Reference 22). In that analysis, it was assumed that the "fragments" are thrown forward in a cone, whose axis is the axis of the warhead, such that at any instant, they are distributed uniformly throughout a circle of radius R, which is a right section of that cone. The T-44-type cluster warhead fits this assumption quite well, since it is proposed that the 90 submissiles be ejected in more than one ring. Tumbling of the unstabilized blocks will cause them to be randomly distributed in a circle of radius equal to the radius of the outside ring.

d. The probability of a hit on an area $\bar{A}$ if it lies in the fragment zone is

$$1 - e^{-\frac{n\bar{A}}{\pi R^2}} \tag{1}$$

If the rms guidance error is σ_G, then the probability of the vulnerable area lying in the fragment zone is

$$1 - e^{-\frac{R^2}{2\sigma_G^2}} \tag{2}$$

Therefore, the overall hit probability becomes

$$P = \left[1 - e^{-\frac{(n\bar{A})}{(\pi R^2)}}\right]\left[1 - e^{-\frac{R^2}{2\sigma_G^2}}\right] \tag{3}$$

This equation may be applied directly if a constant radius of projectiles or submissiles is to be considered. The hit probability is maximum when

$$\frac{n\bar{A}}{R^2} = \frac{R^2}{2\sigma_G^2} \tag{4}$$

Therefore, the optimum radius of projectiles is

$$R_{(opt)} = \left[\frac{2\sigma_G^2 n\bar{A}}{\pi}\right]^{1/4} \tag{5}$$

or

$$\frac{R^2}{2\sigma_G^2} = \sqrt{\frac{n\bar{A}}{2\pi\sigma_G^2}} \tag{6}$$

and the maximum attainable hit probability becomes

$$P = \left[1 - e^{-\sqrt{\frac{\pi\bar{A}}{2\pi\sigma_G^2}}}\right]^2 \tag{7}$$

These last two equations are plotted versus the factor $n\bar{A}$ for various values of σ_G in Figures 29 and 30.

e. It may be noted that the use of $\bar{A}$ as the presented area of the target will yield calculations of hit probability on that presented area, whereas the use of vulnerable areas for A- or K-kills will result in calculation of such a kill on the target. If $R_{(opt)}$ is calculated using the presented area of the target, then the expected number of hits on this presented area may be shown as

$$N = \frac{n\bar{A}}{\pi R^2_{(opt)}} \tag{8}$$

The determination of the optimum radius, $R_{(opt)}$, will permit calculation of the kinematic relationships between standoff, cone angle, and radial ejection velocity of the submissiles or projectiles.

f. Vulnerable-area curves were obtained from Reference 12 for the B-47, and from Reference 11 for the Type 37 aircraft. Following are some of the more important factors which lead to the development of vulnerability concepts:

(1) The size and performance capability of the target, as reflected in the efficiency and/or redundancy of the structural layout.

(2) The altitude at which the attack is conducted in determining possible degradation of explosive effects.

(3) The fuzing of the submissile, with particular emphasis upon the increase in lethality of a successfully mined submissile relative to surface burst charges.

(4) The target penetration capability of the submissile as a combined effect of target skin thickness and type, impact obliquity, impact velocity, submissile case-to-charge weight ratio, and case design including fuze protection provisions.

The scope of available and reliable data on these effects is not large, particularly when modern and possible future targets are considered. Hence, assumptions are required when effectiveness studies are to be considered either quantitatively or comparatively to "optimize" a warhead design.

g. The evaluation of submissile lethality becomes more complicated when multiple hits are to be considered. Previous weapon evaluation studies, such as those summarized in References 5 through 9, have treated the multiple-hit case by assuming no damage accumulation, and by considering each projectile as if it were the only hit. In any optimization procedure these assumptions impart an obvious bias of unknown magnitude toward the higher warhead charge weights. While the extent of this bias is unknown, since extremely few multiple-hit tests have ever been conducted, it is considered likely that the effect on the calculated "optimum" charge or projectile may be appreciable. Some consideration has been given to this in the Reference 8 study by presenting effectiveness data, not only in terms of kill probability, but also in terms of the expected number of hits and the expected total weight of high explosive placed in the presented area of the target. The derivation of a valid theory for correctly evaluating the problem of multiple hits with high-explosive projectiles is not feasible at present because of the lack of experimental data.

h. Physical significance may be given to the vulnerable-area curves previously mentioned by a review of the results of extensive tests conducted at Davis-Monthan AFB, Arizona, during the spring of 1955. In these tests, B-29 aircraft sitting on the ground, were subjected to external, surface, and internal statically fired bursts from various quantities of a variety of high-explosives, both cased and uncased. Since the targets were stationary and only static charges were fired, no direct data were obtained on the effects of altitude or dynamic impact. The following conclusions, reached after inspection of the test aircraft, correlate generally with the vulnerable-area concepts presented in References 11 and 12.

(1) These tests support the theory that, to consistently produce structual kills on aircraft of the B-29 type with a single hit, the burst should be internal and of at least 1 lb of an explosive such as HBX or H-6. To obtain consistent K-kill assessments throughout the aircraft, including the large-volume fuselage structures and thin-skinned sections such as the empennage, more explosive is usually necessary (on the order of 2 or 3 lb). Single internal bursts of less than 1 lb can "kill" the aircraft if they detonate in critical regions such as the pilot compartment or in small tightly confined spaces such as wing-spar boxes. This emphasizes the fact that the area vulnerable to a small, fractional-pound charge is quite low compared to the area vulnerable to charges of 2 lb or more.

(2) External surface bursts of charges of 8 lb of H-6 were necessary to produce structural kills equivalent to those obtained from internally burst charges of 2 or 3 lb. An exception exists in the case of 8-lb charges strategically placed about the empennage section. Small external blasts (of 1 lb or less) in contact with the surface repeatedly failed to severely damage the aircraft structure unless the charge was critically placed. The threshold value for external-surface burst charges for accomplishing a required level of damage appears to range from 5 to 8 lb of an explosive such as H-6 or HBX. These tests would appear to agree with previous estimates (Reference 19) that three to five times as much explosive is required if static surface bursts are to compare with static internal detonations.

i. This last consideration leads to the comparison of internal and external bursts. An adequately thick and properly proportioned case of high-quality metal is required to penetrate heavy aircraft structures without premature destruction of all or part of the warhead by deflagration, or fuzing failure from deformation at target impact. When lightweight cases are employed, the fuze must provide for instantaneous high-order detonation of the high-explosive filler before a major fraction of the submissile deflagrates or breaks up. Some preliminary static firing tests, noted in Reference 10, suggest that a significant increase in charge weight is necessary when a surface burst is used to obtain the same damage level as given by a mined charge. Reference 8 notes the possibility of a dynamic effect with surface bursts, and thereby suggests a much smaller degradation factor. At the conference of 17 January 1955 at BRL, a factor of 1.5 was quoted for surface bursts. A factor of 2.0 is quoted in Reference 11. To bracket the possible range of this factor, it is assumed that the charge weight is increased 1.5 and 5.0 times to obtain surface-burst equivalent to internal-burst damage. The effect of the relative motion of the exploding projectile upon the damage inflicted on the target must also be assumed to modify the effectiveness indicated by static firings. This relative motion results in a dynamic yaw* effect which increases the stresses imposed on the submissile case.

3. Evaluation of Cluster-Type Warheads

a. The unstabilized-block submissiles of the T-44 type and the Crossfire, spin-stabilized, rocket-propelled submissiles remain as the most promising types to be considered for the IM-99( ) interceptor, after a careful consideration of the data discussed in paragraph III,D,1. Accordingly, a lethality analysis was made of these two types using the method and assumptions presented in paragraph III,D,2.

b. The T-44-type cluster warhead, because of the use of thin aluminum-skinned blocks, may be conservatively assumed to most often achieve damage by near-external or in-surface blast effect. It is consequently degraded, as discussed in the previous section, by dividing the weight of high explosive by the factors 1.5 and 5.0, in order to compare it directly with submissiles achieving their damage by internal blast.

c. Maximum attainable values of kill probability for the T-44 and 51-mm Crossfire warheads are computed for both the Type 37 and the B-47 targets for altitudes of 30,000 and 60,000 ft, for two typical missile-to-target aspects, and for a range of guidance errors from 20 to 150 ft, standard deviation. The results of these calculations for σ_G = 40, 60, and 80 ft are shown in Tables III, IV, and V.

---

*Dynamic yaw as used here is defined as the vector angle between the target and submissile velocities. As a result, the side loads imposed on the submissile while entering the target are considerably increased, particularly for a frontal or side impact.

d. If the Type 37 target is considered, the 51-mm Crossfire type provides a higher kill probability, at all values of guidance error, than does the modified T-44 cluster warhead if the latter is degraded by a factor of more than about 3.0. When the B-47 target is considered, the 51-mm Crossfire-type cluster is superior to the modified T-44 warhead for any given set of conditions, regardless of the degrading factor used.

e. A lethality comparison of the Crossfire-type cluster warheads, considering the Type 37 aircraft as a target, is shown in Figures 31 and 32. (The 540-lb weight shown in these figures has allowed 60 lb for structure.) Although the curves are quite flat, there is some advantage in maintaining a minimum of 0.5 lb of high explosive per round. From a practical standpoint, the selection of a slightly heavier charge than optimum is conservative if the vulnerability estimates should prove to be in error. Therefore, only the 51-mm-dia (2.00-in.) Crossfire submissile, with 0.557 lb of HBX, is compared with other types of cluster warheads.

f. Hit probabilities for a uniform distribution of 40, 90, 120, 180, and 300 submissiles were calculated, using presented target areas. The results are shown in Table VI. It should be noted that multiple hits may be expected with cluster-type warheads, assuming they are optimally fuzed.

g. It should be particularly noted that these calculations present the maximum possible performance which may be expected from the cluster-type warheads, assuming that the primary missile guidance is within the indicated errors, that there is no submissile slowdown, and that fuzing is optimum for the encounter. If the submissiles either lag behind the primary missile, as in the T-44-type warhead, or lead the primary missile, as in the Crossfire type, the miss distance of the primary missile is not that of the submissiles. The cluster centroid miss distance is then a function of the kinematics of the particular encounter. A discussion and evaluation of these errors is presented in the subsequent fuzing section.

h. The maximum attainable kill probabilities for the T-44 warhead, computed for a greater range of guidance errors than that shown in Tables II, III, and IV, are plotted in Figures 33 to 40.

i. It can be shown that a consideration of the primary missile fuzing will degrade these maximum attainable kill probabilities, particularly when the submissile either lags behind the primary missile as in the case of unpowered submissiles, or flies ahead of the primary missile as in the case of the rocket-propelled Crossfire-type submissile. This degradation effect is more serious at low altitudes. A discussion of this effect is presented in paragraph IV,B. An indication of the magnitude of fuzing degradation can be obtained from Figure 41, from an unpublished BRL Report (courtesy of Mr. Don Hall). It can be seen from these curves that, for a vertical dive approach, the inclusion of a 150-ft σ_F fuzing error will degrade the kill probabilities from 9 to 10%, at altitudes above 30,000 ft, depending on the number of submissiles and ejection velocities considered.

E. FRAGMENTATION AND EXTERNAL-BLAST WARHEADS

Fragmentation warheads considered here include only controlled-fragmentation systems producing generally cubical (or spherical) fragments, excluding special forms such as the continuous rod, the Misznay-Schardin, etc. which are discussed elsewhere.

1. Vulnerability

a. For fragments of the "conventional" type, the vulnerable components are usually limited to the fuel system, engines, and personnel. Criteria for establishing minimum fragment lethality may be readily determined without excessive uncertainty, except possibly in the case of fuel fires.

b. Since the IM-99( ) is designed for use against bombers such as the Type 37 and its successors, which can reach altitudes above 65,000 ft, where oxygen-rich cabin pressurization and pressure suits will be required, it may appear that fragmentation warheads would be particularly attractive from the standpoint of inducing "explosive decompression" of the crew compartment. In this case, the entire pressure cabin area may be subject to attack. The probability that a single fragment perforation will induce explosive decompression of the crew cabin depends upon the altitude pressure differential, the absolute altitude, and the susceptibility of the cabin wall to progressive cracking as a consequence of the fragment impact and the induced local stress concentration. If explosive decompression occurs, it is expected that an unprotected flight crew may be incapacitated within a few seconds at altitudes of 50,000 ft or higher. With unmanned targets, the complicated guidance equipment is assumed to be equally vulnerable to fragmentation.

c. Since some target components are sufficiently vulnerable to fragments, a more detailed examination of the fragmentation warhead for the IM-99 is warranted. The following discussion includes (1) the design of the 600-lb fragmentation warhead from the standpoint of optimum C/M ratio, (2) methods of obtaining fragmentation control, and (3) expected effectiveness.

2. Basic Design of 600-lb Fragmentation Warhead

It is assumed that the maximum damage effectiveness will be obtained from a warhead producing the greatest number of highly lethal individual fragments. Since it is impossible to have both great numbers of fragments and high weight and velocity of individual fragments in any given warhead envelope, there remains a weight relation between the explosive and the fragmentable metal where the highest effectiveness, expressed in overall fragment energy for a given amount of explosives, can be realized. It is then feasible to define an optimum design balance relating the explosive weight to the fragmentable-case weight (C/M) if the best design is defined as that for which the maximum kinetic energy is imparted to the greatest number of equal-mass fragments. This is not to be construed to be the maximum energy that can be imparted to any one fragment, where, of course, logic dictates that very high C/M ratios will be the rule.

a. The following assumptions are used:

(1) The Gurney empirical relation of initial velocity as a function of C/M is representative of fragmenting warhead designs which are generally cylindrical, with a length-to-diameter ratio greater than unity.

(2) The variation in fragment deceleration as a result of aerodynamic drag for equal-mass individual fragments over the velocity range considered here is neglected by assuming only high-altitude bursts.

(3) Of the 600 lb allowed for the warhead, 10% (or 60 lb) will be devoted to structure, leaving C + M = 540 lb.

b. In the curve shown in Figure 42, the initial velocity is plotted as a function of the C/M ratio, according to the empirical relation attributed to Gurney:

$$V_o = \sqrt{2E}\sqrt{\frac{C/M}{1 + C/2M}}$$

where $\sqrt{2E}$ is 8800 ft/sec for Comp. B high explosive.

c. Figure 43 shows the total mass of fragments plotted as a function of the C/M ratio, where C + M = 540 lb.

d. In Figure 44, the total kinetic energy available in controlled fragments is plotted as a function of C/M, based on the curves mentioned above and the relation for kinetic energy:

$$KE = \frac{M V^2}{2} \text{ or } \frac{W V^2}{2g} \text{ ft-lb}$$

Referring to Figure 44 for the 600-lb warhead, the maximum efficiency occurs at a C/M of about 1.5, where initial velocity is approximately 8200 ft/sec according to the Gurney relation, which is considered valid in this region of the C/M ratio.

e. At the optimum C/M ratio of 1.5, the 600-lb IM-99( ) fragmenting warhead would accommodate 216 lb of fragments, which, expressed as 120-grain cubes, constitutes some 12,600 individual fragments. If the warhead were designed to produce a uniform pattern of 30° width, and functioned perfectly at an actual miss distance of 60 ft, the target would receive 1.08 hits per sq ft or a hit every 0.924 sq ft.

3. Best Methods of Obtaining Fragmentation Control

a. Several systems capable of varying degrees of control have been developed for the creation of fragments in the desired size ranges. Methods for the production of fragments suitable for antiaircraft warhead use are discussed below in the approximate order of chronological development:

(1) Notched-Ring Fragmentation Control

This system, which probably first appeared in wire-wrapped bombs, consists of notching one side of a square wire at regular intervals so that, under the impulsive loading existing at the time of detonation, the wire rings will break at the notches. Variations of this method have appeared on the Navy's Sparrow and Terrier missiles, each using internally notched square wire arranged in discrete hoops or rings, stacks of which are furnace-brazed into ogival or barrel shapes. Certain other types of explosive ordnance use a continuous spiral of externally notched wire held together by a thin outer shell or other mechanical means. The primary difficulty with the notched-wire method lies in the preponderance of chaff, or small waste fragments, produced by the material in the vicinity of the notch. The furnace-brazed warheads further suffer from a tendency to create fragment clusters if the inter-ring braze is sufficiently strong to make the warhead a structurally integral shell.

(2) Grooved Explosive Charges

This system, which originated in the United Kingdom (Reference 13), was subsequently developed by the Aberdeen Proving Ground and more recently by the Naval Ordnance Test Station, Inyokern (Reference 14) in connection with the Zuni and Sidewinder programs. It consists of placing a thin preformed plastic (or rubber) liner inside a section of mild steel tubing. The "fragliner" has a regular pattern of identations in the form of staggered rows of simple cavities. This pattern grooves the surface of the explosive filler when the explosive is poured into the shell. This system works well on thinner-walled casings (maximum thickness of 1/4 in.) and produces a high percentage of explosively cut fragments of the approximate size and weight desired. The primary advantage of this system is low cost. However, the limitation of casing thickness and the occasional tendency for either "overcontrol" or "multiple fragments" are disadvantages for larger, maximum-efficiency systems.

(3) Cast-On Fragmentation Pattern

The warhead case is foundry-cast into a pattern which grooves either the inner or outer wall as desired. The pattern may be shell-molded for high producibility and accuracy, and the case can be founded in either steel or the better-grade cast irons such as nodular iron. Aerojet-General's experience with this system indicates that best performance can be obtained with an externally grooved, biased (45° to the longitudinal axis), deep-notched pattern. This system is suitable for readily producible, high-strength warheads, but it requires additional research and development. In particular, this system may also be subject to certain limitations on charge-to-metal ratio and thickness-to-radius ratio.

(4) Embodied-Mesh Fragmentation

A foundry method is used in which the matrix, either molten steel or iron, is poured over a specially coated steel-wire mesh having wires on center-to-center distances of the desired fragment size. This system works well in certain sizes, but it is apparently sensitive to the diameter of the warhead and possibly to the charge-to-metal ratio. Like the cast-on pattern method, this system has a high producibility and low cost, but must be tailored carefully for each application.

(5) Precut Fragments

The most successful approach to complete control of fragment size and shape is the pre-forming of the individual fragments, attaching them in some way about the explosive charge, and providing other structure to maintain warhead integrity. This pre-cut fragment method is currently used in the NIKE 1 warheads and is the basis of the earlier version of the T-33 warhead for the Bomarc IM-99. These two warheads both use structural shells of steel or aluminum between which the individual fragments are imbedded. The developers of both warheads have considered metal or plastic matrices to provide protection for the fragments from the shock-wave interaction that can cause spalling of the individual cubes. A more recent refinement of the precut-fragment concept has been developed by Aerojet-General for the 8-in.-dia, 150-lb warhead for the MX-2117 Bird Dog air-to-air missile, and for the 1100-lb T-45 fragmentation warhead for the NIKE B. These warheads probably represent the present state of the art in the refinement of controlled-fragmentation warheads, and provide, in addition to complete control of size and direction of fragments, a high structural strength for a minimum of parasitic weight. The cubical, low-carbon steel fragments are laid on an internal shell of epoxy resin reinforced with glass fibre. The resin is spread into the interstices between the fragments, and an outer shell (or an intermediate shell, with double walls) is laid up directly over the fragments. Epon (epoxy) resin-to-aluminum chemical bonds provide high end-attachment strength. Besides affording complete control with the least weight, the plastic layup also provides a built-in thermal barrier which reduces possibility of premature detonation from the high aerodynamic heating characteristic of supersonic missiles. The plastic lay-up, precut system has been evolved into a production technique for "laying up" many discrete cubes on each warhead (approximately 20,000 for the T-45, for example). Fragment sizes are usually such that steel wire may be procured in special mill runs, or parallelepipeds cut from standard wire sizes could be used.

b. To summarize, the current trend is toward the use of the highest-efficiency systems (plastic-precut) with increasing fragment sizes, since the increased cost is usually a secondary consideration when compared with the overall cost of the vehicle.

4. Effectiveness of Optimum Fragmentation Warheads as Designed for Bomarc

The following tabulation of the principal pertinent data has been prepared, based on computed kill probability as a function of warhead size, C/M ratio, associated blast, fragment size, etc., and all based on the B-29 airplane as the target. These kill probabilities are based upon perfect fuzing; that is, it is assumed that the fuze functions at the point of maximum lethality. As noted in Reference 4, however, these kill probabilities have to be reduced approximately one-fourth to one-third to account for effects of target variability on fuze functioning. In addition, these kill probabilities refer to A-damage, not K-damage, as required for the Bomarc, and in some cases they include an assumed bomb load.

a. The variation of the warhead shape and method of initiation are optimum in the estimates used in this table. In investigating the effects of charge-to-metal ratio, it has been found that an average C/M of 1.5 represents a sound design compromise.

Ref.	Warhead Wt (lb)	Frag. Wt (gr)	Alt. (ft)	A-Kill, P_k σ_G = 60 ft	2-min R-Kill, P_k σ_G = 60 ft	Remarks
15	600 (C/M = 1.5)	30	30,000	.533		30° fragment beam; 2-min kill - structural, blast, both pilots, or 3 or 4 engines
		60	30,000	.529		
		120	30,000	.471		
16 17	300 (C/M = 3)	132	35,000		.130	± 7.5° frag. beam; no bomb vulnerable
17	300 (C/M = 3)	132	35,000		.523	± 7.5° frag. beam; LC bomb vulnerable
17	300	132	35,000		.830	± 7.5° fragment beam; 2 4000-lb LC bombs vulnerable

b. If fuel vulnerability and bomb load are neglected, then these estimates based on B-29 vulnerability may be considered applicable to the Type 37 target.

c. The preceding table clearly reveals that while the most efficiently designed fragmentation warheads can have fairly high A-kill probabilities and even respectable K-kill probabilities, the conditions required to achieve this performance are incompatible with the advanced Bomarc requirements. To achieve the airframe structural damage required for a K-kill, the fragment concentration and velocity would have to be increased to a point impossible to obtain in fragmentation warheads. Special cases, where both the concentration and velocity might be increased to desired levels, are discussed in other sections under the Misznay-Schardin, shaped-charge, and continuous-rod systems. Hence, conventional fragmentation warheads for the advanced Bomarc appear incapable of meeting the minimum kill probability.

5. External-Blast Contribution

a. It has been concluded in Reference 20 (as a result of extensive static firings against stationary aircraft) that for large warheads (in excess of 50 lb), controlled-fragmentation warheads are better than external-blast types against large bombers. The Reference 18 analysis assessing the A-kill probability of an 1100-lb fragmentation warhead containing 600 lb of Comp. B, against a B-29 target at 30,000 ft altitude and at a σ_G of 60 ft, gives a 0.238 probability of A-kill for blast alone, as compared with an overall assessment of 0.770 for fragments and blast combined. This appears to be somewhat at variance with earlier results derived in References 20 and 21 (based on extrapolations of blast contour data obtained from static ground firings against lighter aircraft such as the A-20 and B-17) which predicted that, under the above conditions and assuming perfect fuzing, a 600-lb external-blast warhead should give an estimated P_k in excess of 0.75. It is considered that these earlier (1950) estimates are superseded by the work reported in Reference 18 and that this discussion indicates a correct ordering of fragmentation and external-blast warheads in A-kill capability. For the advanced Bomarc warheads, however, only K-kills are being considered.

b. An additional consideration relative to external-blast warheads as potential K-killing agents, particularly when used in conjunction with controlled fragmentation, is that all testing thus far has taken place under less than realistic conditions. The effects of relative target-missile motion, gust loading, etc. have not been sufficiently tested for modern high-performance airframes, and the mechanism of target-blast interaction is not well known. It is known, however, from the conduct of certain restricted experiments, that means exist for the enhancement of blast effect from cylindrical or annular-shaped warheads by the use of multi-point, nearly simultaneous initiation so that the time of detonation is reduced to a minimum. Since the impulse available is primarily a function of the mass and type of explosive used, regardless of disposition, the only means of increasing blast effect (for external-blast applications) is to increase the peak overpressure by accomplishing the production of detonation products in as short a time as possible. Of the current warhead designs, the annular and/or divided types, such as those used on the T-33 Bomarc and the Talos warheads, probably present the most difficult initiation and wave-control problems, from the standpoint not only of blast production, but also, because of the primary purpose of these warheads, the production of a continuous-rod or discrete fragments. The incorporation of multi-point initiation, using series-connected, low-energy, high-quality, electric detonators with a high-energy electrical source such as a pre-charged capacitor, would accelerate detonation time to increase blast effect, and at the same time, would probably resolve many of the fragment and rod directional-control and tumbling problems now being encountered. These improvements, however, may be expected to be reflected in bringing the effectiveness of these warheads up to predicted levels, rather than leading to large improvements in lethality.

c. To summarize the role of the external-blast warhead for the IM-99( ) application, it is believed that no matter how well this warhead is designed, the rapid falloff of blast effect as a function of miss distance, particularly at high altitude, rules out the conventional external-blast type of warhead as an aircraft structural kill agent for the 1960 era.

6. Conclusions

In reviewing the various fragmentation warheads for their ability to meet the criteria established for the optimum IM-99( ) advanced Bomarc, it is seen that no fragmentation type (excluding the special cases such as Misznay-Schardin or continuous-rod) can meet the requirements for a K-kill of the structure. Fragmentation warheads which cause numerous, discrete, and randomly located perforations of aircraft structure may kill an airplane, but probably not in 5 or 30 sec as required. It has been shown that even an "optimum" design which produces over 12,000 120-grain fragments over a comparatively narrow arc of 30° can produce at best only about 1 fragment per square foot at 60 ft from the point of burst. This calculated average frequency of 1 hit per square foot is of course quite optimistic, being dependent on perfect fuzing, perfect warhead design and functioning, complete elimination of fragment clusters, no loss of fragments to structure within the missile, instantaneous initiation, etc. When it is realized that, for a miss-distance dispersion of 60 ft, about 60% of the bursts will be at a greater range than 60 ft (up to 180 ft), it is evident that the resulting fragment spatial distribution and the accompanying effect of the blast from the 324-lb high-explosive charge is rapidly attenuated, thus reducing the probability of destroying the target far below acceptable values when peripheral conditions of attack are involved.

It is therefore concluded that fragmentation and external-blast warheads do not appear capable of developing sufficient K-damage lethality under the conditions and guidance errors specified for the Bomarc air-defense system. These warheads do, however, appear to have good A-damage capability if fuel vulnerability is assumed, as shown in Figures 45 and 46. High-altitude flight of the targets and the use of fuel inerting systems or nuclear power plants will eliminate most of this vulnerability, however, leaving only the crew and power plants as vulnerable elements.

IV. WARHEAD FUZING-SYSTEM STUDIES

A. GENERAL DISCUSSION

1. The basic requirement for a proximity fuzing system is that it be capable of detonating its associated warhead at that point along the missile trajectory for which the probability of killing a target is maximized. To accomplish this requirement, the fuzing system for the Bomarc antiaircraft guided missile must perform most of the basic functions of the fire-control system of an all-weather manned fighter, since the lethality of the missile warhead does not depend on contact fuzing. These fire-control functions include

a. Sensing the target's immediate presence

b. Computing the optimum firing time, based on exterior ballistic data of the warhead as modified by other inputs from the missile system

c. Generation of the firing impulse at the proper time.

These functions are examined for selected conditions indicative of the performance objectives of the guidance system for the IM-99( ) and IM-99A interceptors. As noted earlier in the frame-of-reference study, it is desirable that the fuzing and guidance systems be segregated insofar as practicable.

2. In a sense, the fuzing and warhead systems must compensate for inherent inaccuracies in the missile guidance or homing system which contribute to the target miss distance. Consequently, the fuzing system determines to a dominant degree the probability that the warhead will hit the target.

3. The principal parameters in the design of a proximity-fuze system for an antiaircraft guided missile such as Bomarc may be summarized as

a. Missile velocity and maneuver capabilities

b. Target velocity and maneuver capabilities

c. Changes in these over the operating altitude of the missile

d. Probable miss distances between Bomarc and target due to terminal guidance errors

e. Fragment or submissile velocity and dispersal patterns of the warhead

f. Variations in the approach angle between the Bomarc and its target due to tactical considerations.

With these basic design parameters established, the function of the fuzing system is the processing of sufficient and accurate information on the dynamic relationships of the terminal encounter between the missile and target rapidly enough to permit a solution of the fire-control problem and detonation of the warhead. In addition, for a gimbaled- or guided-warhead system, the fuzing system must also provide continuing guidance information for the warhead in addition to calculation of the time of detonation.

4. Two general types of fuzing, "collision fuzing" and "lead fuzing," may be distinguished. Collision fuzing assumes that some basic parameter such as lead angle or direction of fire is fixed. The function of the fuzing computer is the calculation of the fuzing time which will initiate detonation at the one instant when the preset condition is first satisfied. Lead fuzing, on the other hand, is based upon the continuous calculation of the proper lead angle. Hence, there is a time interval during which triggering may occur at any instant. Lead fuzing is more complicated that collision fuzing since a continuous knowledge of the dynamic or kinematic relationships between all of the moving masses is required to solve the fire-control problem.

5. In either case, the accuracy to which fuzing time must be calculated is a function of the armament system characteristics. The simplest fuze computer would be one of the collision type which would detonate an equatorial spray of fragments of such velocity that the target could be considered stationary for the length of time required for the fragments to reach it. Essentially, this type of computer need only determine a time of detonation on the basis of the measurement of fixed parameters. The fuze computer required for a gimbaled or guided warhead should be a lead fuze because of the necessity of supplying special guidance or steering information.

B. TERMINAL ENCOUNTER-KINEMATICS

The phrase "terminal encounter" is used here to designate that portion of the missile trajectory and target track during which fuzing of the warhead should occur for maximum kill probability. The kinematics of the terminal phase of any encounter exert a predominant influence on the overall effectiveness of the armament system, particularly for warheads having submissiles which are projected equatorially with a lateral velocity component appreciably less than about one-half the velocity of the primary missile.

The dual objectives of the terminal encounter-kinematics evaluation are (1) the determination of the possible limitations and effectiveness of computing and conical-scan types of fuzes when used with the equatorially fired submissile, and (2) the general delineation of design requirements for a suitable fuzing system for use with each basic type of warhead; considering realistic drag slow down of the submissiles.

1. Analysis of Terminal Encounter-Kinematics

a. The following analysis of the terminal encounter-kinematics is presented to provide a basis for typical performance data useful in the evaluation of the fuzing effectiveness or hit probability of high-speed interceptor missiles. Insofar as possible, the analysis is kept general; that is, it applies equally to any missile and any warhead which operates by ejecting submissiles, including continuous-rod and multiple shaped charges, in an equatorial belt. For analytical simplification, however, the encounter is assumed to be coplanar, or to take place in a plane defined by the instantaneous track of the target and the intercepting missile. Some additional assumptions are as follows:

(1) The target and interceptor are both traveling along straight lines during the time interval under study.

(2) The interceptor has no angle of attack, being aligned with its flight path.

(3) There is no variation in altitude effect during a given encounter.

(4) The target is a point target.

(5) The interceptor and the target have constant velocities.

Additional corollary assumptions are included and explained at appropriate places throughout the discussion. A comparison of the work and results presented herein with earlier discussions of the range error and slowdown effect in References 42 and 45 discloses general agreement, so that the results may be assumed to be typical.

b. Figure 47 represents a typical intercept case where the interceptor is approaching the target in a descending, head-on attack. In this case, the interceptor trajectory, line BC, is approaching the target track, line AJ, at an angle γ in such a manner that the nearest point of intercept will occur when the interceptor is at point E and the target at point D. The distance DE is the miss distance, called S in the derivations and calculations to follow. If, when the interceptor is at point B, and a distance AB = R_x from the target, the submissiles are ejected from the interceptor missile, then at the time of closest approach of the interceptor missile to the target (interceptor located at point E), the centroid of the submissile ring is located at point H (in an exaggerated case). The intersection of the plane of the submissile ring with the future target track is at point J. At some later time, the target having moved to point F and the centroid of the submissile ring having advanced to point G, the plane of the submissile ring will be intersected by the target itself. At this instant, the submissile ring may be designated by its intercepts, K and K', in the encounter plane. The distance FG is the true cluster or centroidal miss distance, designated y in the following discussion, while the radius of the submissile ring, KG, at the time of target intercept is called d.

c. Since unpropelled submissiles lag behind the interceptor missile after launching (Reference 41), the following analysis for the magnitude of the lag and its effect on the effective miss distance is undertaken to provide insight upon possible fuzing degradation for long-standoff warheads. A special case is described later wherein the submissiles are accelerated for a portion of their total flight time after launching (i.e., rocket-propelled submissiles). The notation employed is defined in the list of Symbols. The deceleration due to drag is given by

$$\frac{d^2x}{dt^2} = \frac{-F}{m} \qquad (9)$$

However

$$F = C_D \rho/2\, AV^2, \text{ and } m = \frac{W}{g}$$

and since $V = \frac{dx}{dt}$, the equation of motion for the submissile ring becomes

$$\frac{d^2x}{dt^2} = -\frac{C_D \rho A g \left(\frac{dx}{dt}\right)^2}{2W}$$

This differential equation is non-linear and must be solved numerically. One particular submissile and one altitude are assumed for each calculation, and hence a coefficient k may be defined

$$k = \frac{C_D \rho A g}{2W} \qquad (10)$$

which gives

$$\frac{d^2x}{dt^2} = -k \left(\frac{dx}{dt}\right)^2$$

This equation may be integrated to yield the following equations for the velocity and the distance traveled, respectively:

$$V_t = V_m e^{-ktV_m} \qquad (11)$$

$$x_t = \frac{1}{k} \ln (ktV_m + 1) \qquad (12)$$

During the same time interval, the spread of the submissiles is given by the relationship

$$d_t = x_t \frac{V_p}{V_m} \qquad (13)$$

To include target action and effect, consideration of Figure 48 and application of the rules of trigonometry gives the following relationships:

$$R_x = \frac{V_m t \sin \gamma + S \cos \gamma}{\sin \beta} \qquad (14)$$

where

$$\beta = \tan^{-1} \frac{V_m t \sin \gamma + S \cos \gamma}{(V_m \cos \gamma + V_T)\, t - S \sin \gamma} \qquad (15)$$

and

$$y = V_T \sin \gamma \left[\frac{V_m t - \frac{1}{k} \ln (ktV_m + 1)}{V_m e^{-ktV_m} + V_T \cos \gamma} \right] \pm S \qquad (16)$$

d. Figure 49 shows four possible coplanar encounters which are useful for the evaluation of these equations. By definition, the angle γ is measured in a clockwise direction so that $\cos \gamma$ is positive when γ is less than 90°, negative when γ exceeds 90°. When the miss occurs as shown in Figure 49a, above and behind a target during head-on approach, S is taken as positive. In like manner, it may be shown that S is positive when the approach is as shown in Figure 49c, a head-to-tail approach, missing below and behind the target. In the case illustrated in Figure 49b, head-on approach, missing below and ahead, or the case shown in Figure 49d, head-to-tail approach missing above and ahead, S should be taken as negative. The foregoing sign conventions apply to Equations 14, 15, and 16, where t has the special significance that it represents the time by which submissile ejection leads arrival of the interceptor at point E (Figure 47) on its trajectory, at which it is or would be nearest the target. This is to be distinguished from t (the time of flight after submissile launching) used in Equations 11 and 12, which permits the simultaneous evaluation of y_1, y_2, y_3, y_4, and d (Equation 13), and their tabulation with R_x to provide the summary of cases given in the tables comprising the appendix. These tables may be directly read to obtain the centroidal miss distance and submissile ring radius when the warhead is fired (submissiles are ejected) at any range, R_x, from the target. These determine the cases wherein the submissile misses the target, as shown in a later section. One simplifying assumption used in computing the tables in the appendix is the neglect of additional ring slowdown after the interceptor missile reaches its point of closest approach to the target (point E, Figure 47). After this time, the velocity of the submissile ring along the missile trajectory is assumed constant. Owing to the short time intervals involved in the encounter study, and the characteristic properties of the velocity-time relationship, this assumption does not introduce an additional error of significant magnitude.

e. For the case of powered submissiles, it is assumed that the rocket motor or other propulsive device operates for 0.2 sec after launching. To expedite the calculations, the value of k in Equations 11 and 12 was assigned an opposite algebraic sign for the first 0.2 sec. This assumption presupposes a thrust which varies with change of altitude. This practical error has no effect on the qualitative value of the calculations when they are used for comparisons, and represents a fair assumption for the forces employed, since no particular powered submissile is considered. A more "sophisticated" approach used in a few preliminary check calculations does not yield any significantly more useful results.

f. The total number of cases considered, for which results of calculations are presented in the appendix, are defined by appropriate combinations of the following conditions:

Z = 15K, 30K, 45K, and 60K ft

V_m = 1000, 1750, and 2500 ft/sec

V_T = 800 ft/sec, and also equal to V_m

$\gamma = 30^\circ, 45^\circ$, and 60°

V_P = 200 and 5000 ft/sec

The following are values of the important parameters used in the numerical calculations of submissile centroid miss distance.

C_D = 1.2 (clusters), 1.0 (continuous rod)*

W = 5 lb (clusters), 325 lb (continuous rod)*

A = 0.1 sq ft (cluster), 10 sq ft (continuous rod)*

*Values for the continuous rod are based on end-on presentation of rods to air-stream as opposed to side-on presentation considered in paragraph III, B,3,b.

ρ (Values of air density were taken from "Standard Atmosphere Tables and Data" prepared by the NACA.)

g (Variations of gravitational acceleration with altitude were obtained from standard gravimetric data.)

The time interval used for computing R_x, y, and d is 0.1 sec when V_P = 200 ft/sec, and 0.01 sec when V_P = 5000 ft/sec. In all cases, the miss distance S is assumed to be 60 ft.

2. Interpretation of Tables in Appendix

a. Each sheet of the tables summarizes computed miss-distance data for one type of warhead, at one altitude, for one interceptor missile velocity, for two target velocities (800 ft/sec and a velocity equal to the interceptor velocity), and for three approach angles. Since the spread of submissiles is independent of the approach angle (neglecting gravity), the radius of the submissile ring (d) is tabulated separately for each target velocity at the right border of each sheet. These values of d apply equally to any approach angle case tabulated in the body of the table. For any encounter described in Figure 49 the appropriate y column is selected. Then R_x, y, and d may be read. When y is greater than d, the target is in the plane of the submissile ring, but outside the submissile ring by a distance equal to the difference between y and d in feet. Conversely, when y is smaller than d, the target lies in the plane of the submissile ring but inside the ring by a distance equal to the difference between d and y in feet. It can be seen that two possible conditions occur:

(1) When $y \gg d$, the value of (y - d) in feet is sufficiently large so that no conceivable real target could be hit.

(2) When $y \ll d$, the submissile ring diameter may be so large as to completely surround a target without being able to hit it.

Of these two possibilities the second is unimportant for this study. The following example of reading the tables may be of assistance:

If the conditions to be evaluated are assumed to be

$$A = 15,000 \text{ ft}$$

$$V_m = 1000 \text{ ft/sec}$$

$$V_T = 1000 \text{ ft/sec}$$

$$\gamma = 45^\circ$$

$$V_P = 200 \text{ ft/sec}$$

If it is also assumed that the fuzing computer is designed to fire the warhead when the interceptor missile is 530 ft from the target and that the unpowered cluster-type warhead is being used, then by entering the appropriate tables in the appendix at R_x = 534 ft, the following data are obtained:

$$y_1 = 70.6 \text{ ft}$$

$$y_2 = -49.4 \text{ ft}$$

$$y_3 = 182.9 \text{ ft}$$

$$y_4 = 62.9 \text{ ft}$$

$$d = 55.0 \text{ ft}$$

Reference to Figure 49 permits isolation of the particular approach case and selection of the suitable y. In the example, if the head-on approach with "miss above" is assumed, then y_1, the centroidal miss distance, equals 70.6 ft. From a consideration of significance, then, the cluster elements, which are 55.0 ft (200 ft/sec ejection velocity) from the cluster centroid, miss the target center by 70.6 minus 55.0 or 15.6 ft. If the point target (target first sensed by fuze) had physical size, the adjustment of size and bias would be applied, indicating that a hit is feasible. If the approach had been such as described in Figure 49d, then y_3 would be the centroidal miss and the actual cluster miss would be 182.9 minus 55.0 or 127.9 ft. In this case, a total miss would be decided upon since there are no likely targets which might have such a size.

b. The results of some selected cases investigated are shown graphically as plots of y and d versus R_x in Figures 50 and 51. The cases, which differ only in altitude, have the following in common:

$$V_m = 2500 \text{ ft/sec}$$

$$V_T = 800 \text{ ft/sec}$$

$$\gamma = 60^\circ$$

Figure 50 shows the graphic presentation of tabular data for 30,000 ft, and Figure 51 shows the same data, to the same scale, for 60,000 ft. It may be seen from a study of Figure 50 that only two approaches - those resulting in misses y_2 and y_4, ahead of the target - can be typically expected to produce hits on the target at 30,000 ft altitude. Approaches resulting in misses y_1 and y_3 are complete misses unless the effective target radius is 33 ft for the y_1 case and 40 ft for the y_3 case. Figure 51 indicates, however, that hits can be expected from all approaches when the altitude of the encounter is increased to 60,000 ft.

c. All calculations for fuzing of the cluster-type warhead were carefully examined in a similar manner to determine a typical hit-possibility factor for the cluster hit probabilities as a result of submissile slowdown after ejection. These results, for a 200-ft/sec ejection speed and an 800-ft/sec target, indicate that the effect is quite altitude-sensitive:

Altitude ft	Total Cases Investigated	Cases Where Hit Is Possible	Hit Possibility Factor V_p = 200 ft/sec
15,000	48	28	0.583
30,000	72	47	0.653
45,000	72	63	0.875
60,000	48	42	0.875

At the comparatively low altitudes of 15,000 ft and lower, the cluster warhead can be in a position where a hit is possible in approximately 60% of its approaches as a result of submissile slowdown alone. At higher altitudes, 45,000 or 60,000 ft, where aerodynamic effect is reduced, the drag effect is decreased. At altitudes of 45,000 ft and higher, it is expected that the cluster-type warhead can effect a possible hit in 87.5% of its approaches. It may be noted, however, that the attack of targets faster than 800 ft/sec makes the slowdown effect become a critical factor at lower altitudes.

d. The kill probabilities shown in Figures 33 to 40 assume perfect fuzing and ignore the effects of terminal encounter-kinematics, and therefore represent the highest possible level of performance. Because of the low radial velocity of the submissiles, the T-44 type of warhead must be fired at a very considerable standoff, of about 500 to 1000 ft, to provide an optimum radius of submissiles. A range error in fuzing time, along the line of missile flight, has little effect on the subsequent radius of the submissile ring and consequently the lethality of the warhead. This fact is supported in References 22 and 43, and it may be shown from Figures 50 and 51 that a range error of fuzing of 40 ft will cause an error of less than 8 ft in the radius of the submissile ring at a standoff of about 500 ft. Air drag, however, has a very serious effect on the hit probability when submissiles of the configuration used in the T-44 type of warhead are considered, as shown in the following table, because of the increase in the effective miss distance:

Altitude ft	Missile Velocity ft/sec	Missile Travel ft	Submissile Lag ft	Submissile Remaining Velocity ft/sec
15,000	1750	875	167	1163
15,000	1750	1750	540	871
30,000	2500	1250	210	1751
30,000	2500	2500	694	1347
60,000	2500	1250	63	2257
60,000	2500	2500	236	2058

This effect is considered to be of much greater significance than has been generally assumed (References 22, 37, 41-45). When considered with the terminal kinematics of the missile-target encounter for which the miss distance of the primary missile is minimized, the submissile will miss even a realistically sized target in a significant percentage of the possible approach angles. It is further noted that this effect is quite altitude-sensitive, being much greater at low altitudes where dense air causes a greater drag and slowdown. At very high altitudes, well above 60,000 ft, the effect will become negligible. The preceding discussion was not intended to present a general solution, but to indicate the nature of the slowdown effect by solving for a series of approach angles and altitudes, for a specific miss distance of 60 ft between the primary missile and the target.

e. It can be shown that a similar problem exists if rocket-propelled submissiles are used in a narrow-cone, forward-thrown type of warhead. The only difference is that the submissiles now fly ahead of the primary missile instead of lagging behind it. This leads to the conclusion that the factor which should be minimized is the miss distance between the submissiles and the target, and that this will not necessarily be accomplished by reducing the guidance error of the primary missile to a minimum. This is a similar problem to that of the fighter interceptor launching rockets or firing bullets, and its proper solution requires a fire-control system to provide the function of both terminal guidance and fuzing. In other words, optimization of kill probability for the cluster-type warheads will require a fire-control system in the primary missile involving the basic elements of the complex E-4 to E-9 systems.

f. It has been suggested that increasing the radial ejection velocity to perhaps 400 ft/sec or more would improve effectiveness. The effect of radial ejection velocity on the cone angle is shown in the lower part of Figure 52. It can be seen from Figure 52 that even for a slow missile, the cone angle would not exceed about 22°, and would be about 8 to 15° for higher missile velocities. While this would no doubt improve the situation, it would represent only a minor improvement since the cone angle needs to be increased to about 45° or higher before this effect can be adequately eliminated or minimized. Such an increase would require radial ejection velocities of about 2500 ft/sec. The important conclusion to be drawn from this discussion is the change in the critical parameter in the fuzing of submissiles having a low versus a high radial ejection velocity. In the case of low radial ejection velocity, it has been shown that the effect of slowdown is important, whereas fuzing at an <u>exact</u> standoff distance is not important. However, with high-radial-ejection-velocity submissiles, such as the continuous rod and shaped charge, fuzing at the required standoff is critical, whereas the effect of slowdown on the hit probability is relatively unimportant.

g. To illustrate the effect of increased effective submissile velocity, and to provide additional examples of data extracted from the tables, values of centroidal miss distance, y, range to target, R_x, and submissile ring radius, d, are given below for the powered-cluster and continuous-rod warheads. In both cases, the basic conditions are as follows:

$$Z = 15{,}000 \text{ ft}$$

$$V_m = 1000 \text{ ft}$$

$$V_T = 1000 \text{ ft}$$

$$\gamma = 45^\circ$$

Powered Cluster		Continuous Rod	
R_x	534	R_x*	64.2
y_1	58.0	y_1	60.14
y_2	-62.0	y_2	-59.86
y_3	49.8	y_3	60.86
y_4	-70.2	y_4	-59.14
d	63.3	d	147.5

A major increase in the submissile ejection velocity to several thousand feet per second eliminates the slowdown effect almost completely. Small increases in this velocity to 400 or 600 ft/sec, however, bring only a relatively small increase in hit probability when faster targets are considered. This is illustrated in Figure 52.

h. The foregoing analysis of the fuzing of long-standoff warheads with relatively low ejection velocity for submissiles is obviously neither precise nor complete in analytical detail. However, the effect of slowdown is typical, especially at lower altitudes. Since the warheads for the Bomarc interceptors must, by specification, have a low-altitude capability, and since the necessary range data may not be available at any altitude for use in a T-3016-type computing fuze, a more detailed or precise analysis of the low-speed-cluster fuzing system is not believed justifiable within the scope of this study.

i. The foregoing theory may be extended for the fuzing of high-velocity submissiles which are equivalent to the continuous-rod and to multiple-jet shaped-charge warhead types. The terminal encounter-kinematics for these warheads is shown in Figure 53, which defines certain symbols used in the following discussion. Figure 53 shows an encounter

*It should be noted here that the range to target should vary inversely with the projection velocity and directly with the forward velocity of the submissile ring.

similar to the case illustrated in Figure 49a. Suitable geometrical and mathematical operations can evolve the terminal encounter-kinematics for any or all of the other encounters illustrated in Figure 49, and needless repetition would result from their presentation here. It is the purpose of this part of the discussion to derive and evaluate the "fuzing cone angle," ψ, required for the high-velocity warheads.

j. Reference to Figure 53 shows that when the primary missile is located at point B_F, and traveling along the track B_FC, with velocity V_m, the angle θ is the angle of projection of the submissile ring determined by the vector sum of V_P, the lateral projection velocity, and V_m, the missile velocity. When correlated with the target velocity, V_T, along track CT, the angle defines a second angle ψ, which is called the "fuzing angle." This fuzing angle is the angle between the track of the primary missile and the line connecting the missile and a target (T_F) measured at the instant of firing, and so oriented that a submissile traveling along path B_FT with velocity V_S ($= \vec{V}_P + \vec{V}_m$) will intercept the target at point T. Angles ϕ and ϵ of Figure 53 are convenient operators only, and have no significance for the encounter. By trigonometry it may be shown that the following relationships apply in the case illustrated in Figure 53:

$$\psi = \theta - \phi$$

$$\phi = \arcsin \frac{V_T \sin \epsilon}{V_C}$$

$$V_C^2 = V_S^2 + V_T^2 - 2V_S V_T \cos \epsilon$$

$$V_S^2 = V_m^2 + V_P^2$$

$$\epsilon = 180 - (e + \gamma)$$

For other approach angles, γ, and locations of the target, as illustrated in Figure 49, suitable operations give the full number of cases of equations which may be reduced to a general group. The selection of signs and equations given below will yield all possible cases of encounter:

$$V_C^2 = V_S^2 + V_T^2 - 2V_S V_T \cos \epsilon \quad \text{(Figures 49a and 49c)}$$

$$V_C^2 = V_S^2 + V_T^2 + 2V_S V_T \cos \epsilon \quad \text{(Figures 49b and 49d)}$$

$$\epsilon = 180 - (\theta + \gamma) \quad \text{(Figures 49a and 49c)}$$

$$\epsilon = \theta - \gamma \quad \text{(Figures 49b and 49d)}$$

Appropriate values may be chosen for all velocities involved. Three angles of approach, γ, are postulated, and four altitudes are chosen - all corresponding to previous work in this section - for the calculation of a limited number of cases of encounters. Results of these calculations are given in Table IV of the appendix and on the graphs of Figures 54 and 55 for the cases illustrated in Figures 49a and 49b. The angle ψ of the tables applies to encounters illustrated in Figure 49a, and the angle ψ_1 refers to the cases shown in Figure 49b. The curves in Figure 56 show the extreme variations in optimum skirt angle due to changes in target velocity and approach angle, assuming the skirt angle, ψ, can be continuously corrected for missile velocity variation.

3. Design Requirements for Fuze

From a careful consideration of all the data derived in the preceding paragraphs and a consideration of physical, or "real," targets, the requirements for a fuze design may be stated as follows:

$$\sigma_{\tau} = 0.0025 \text{ sec}$$

$$\sigma_G = 60 \text{ ft}$$

where σ_{τ} is the tolerance for fuzing time and σ_G is the rms miss distance postulated for the Bomarc IM-99( ) interceptor.

C. METHODS OF FUZING

1. Fuze Systems Utilizing Guidance Information

a. Various parameters which determine the kinematic relationship between the missile and target in inertial space are found in the terminal guidance system of the Bomarc. In the AN/DPN-34 pulse-type radar, target range and angular position relative to the missile axis are available. A computer utilizing this information, and other parameters such as missile velocity, warhead fragment velocity, missile angle of attack, and altitude correction, could establish a lead fuzing time for the warhead based on the predicted location of the target at some later time.

b. This type of fuze computer requires a settling time which forces fuzing information to be taken at ranges of several thousand feet in view of the anticipated closing velocities of 4000 ft/sec. At these ranges, information would be reasonably accurate, if available from the type of radar used, but bearing information would not. Because of these limitations, this type of fuze computer would not provide accurate proximity fuzing for the Bomarc.

c. A simplified version of the fuze predictor-computer would require range information only. Instead of using several range and bearing readings over a time interval, this computer (the T-3016 type) would only measure two fixed points of target range and from these predict a warhead release time. The accuracy of the T-3016 fuze computer depends on the availablity and accuracy of range measurements. This fuze computer could obtain its range measurements before the radar range information has begun to deteriorate. Such a system functions best with low-radial-velocity submissiles which require a long standoff from the target when the submissiles are ejected. From information available at present and from a study of the characteristics of the fragmentation, cluster, shaped-charge, and continuous-rod warheads, it appears that effective fuzing using the T-3016-type of fuze computer requires a high degree of range and mechanization accuracy.

d. In a pulse-Doppler terminal guidance system, fuzing could be based on the characteristic behavior of the Doppler frequency in the vicinity of target interception. The Doppler frequency measured by a missile intercepting a target is $\frac{V_T \pm V_m}{\lambda}$ $(1 + \cos \phi)$, where V_T is the velocity of the target, V_m is the velocity of the missile, λ is the velocity of light, and ϕ is the instantaneous look angle of the target with respect to the missile line of flight. With a head-on or tail-chase attack and the range to the target long compared with the miss distance, $\phi \approx 0$ and the Doppler frequency becomes $\frac{2(V_T + V_m)}{\lambda}$. At the point of minimum miss distance, ϕ is 90° and the Doppler frequency becomes $\frac{V_T \pm V_m}{\lambda}$, one-half its original value. Using a high radial ejection velocity, as with the continuous rod or shaped charge, and allowing time for warhead detonation and dispersal by fuzing at some fixed frequency ratio before the Doppler frequency has dropped to one-half of its original value, a very accurate fuze system could possibly be developed. However, the limitations of this fuzing system as applied to the Bomarc are evident. In any but a tail-chase or head-on attack, the change in Doppler frequency becomes a function of the approach angle, γ. For example, if the approach angle is 60°, a very likely tactical situation for the Bomarc, the original Doppler frequency is $\frac{V_T \pm V_m}{\lambda}$ (1.5). But the Doppler frequency at minimum miss distance is still $\frac{V_T \pm V_m}{\lambda}$. This means that if the fuzing point had been selected at $\frac{V_T \pm V_m}{\lambda}$, there would be a $\frac{.75 - .5}{.5}$ or 50% error in the fuzing frequency for this angle of approach; however, this would result in only a small change in fuzing point. In a proportional-navigation terminal guidance system, like that of the Bomarc, some method of measuring the target look angle from position pickoffs on the radar gimbal could be used to correct the selected detonation point. Further study along this line would be necessary to determine whether such a fuzing system would accurately detonate a warhead over any angle of approach between Bomarc and its target.

e. An infrared fuze computer developed for the Sparrow II missile (infrared version) is applicable for the warhead on the Bomarc. The basic equations for this computer are developed in Reference 46. An equation for the fuzing delay time, τ, based upon the implicit measurement of the ratio between minimum miss distance and relative velocity, $\frac{S}{V_C}$, was developed specifically for tactical situations in which the following assumptions were valid:

(1) Small angle of approach between missile and target, i.e., tail or head-on attack.

(2) Velocity of target considerably less than velocity of warhead.

(3) Missile tracker behaves dynamically as single time constant.

(4) Small component of target velocity normal to missile line of flight.

(5) Ratio between angular rate and angular acceleration could be approximated by finite differences and subsequent integration.

f. This fuze computer is designed to use information in the existing Sparrow III infrared tracking system and requires only one input parameter, the angular rate of target sight-line rotation. This fuzing principle is analogous to the change in the Doppler-frequency fuzing method previously noted. Assuming that the missile is attacking the target from head-on or by tail chase, the sight-line rotation rate at long range will be zero and will increase to a maximum rate at the minimum miss distance, just as, similarly, the Doppler frequency is constant at long range and drops to 50% of this value at the point of minimum miss distance.

g. The basic fuzing equation for the Sparrow III infrared missile derived from the missile-target geometry of Figure 48 is

$$\tau = K_{\phi} t_o \left[1 - K_{\phi} t_o \dot{\phi}_T \tan \Delta\right] - T_T$$

This equation does not require explicit measurement of miss distance, relative velocity, or range for its mechanization. The one explicit parameter required for this fuze computer is the sight-line rotation rate, which can be measured very accurately by optical trackers. In the application of a sight-line-rotation-rate type of fuzing system to a Bomarc warhead, it is found that equations of a more general nature than the original Sparrow fuzing equation are needed. Because of the possibility of Bomarc having an angle of attack up to 25°, this factor is found to be no longer negligible and the fuzing equation is modified accordingly. The new fuzing equation then becomes

$$\gamma = K_\phi t_o \left[1 - K_\phi t_o \phi_T \left(\frac{\frac{V_m}{V_P} + \sin\alpha}{\cos\alpha} \right) \right] - T_T$$

All other symbols are the same as in the simpler Sparrow III equation. Further efforts to generalize the original Sparrow fuzing equation to fit the Bomarc characteristics prove impractical, however. This is due to the following assumptions made for the Sparrow III which are not necessarily valid for the Bomarc:

Small angle of approach

Small component of target velocity normal to missile line of flight

Target velocity small compared to missile velocity

h. In addition, a study of the mechanization accuracy of this fuzing equation has been made. This study shows that, by very careful selection of electronic components, a fuzing accuracy of 5% can be obtained. Since overall fuzing times of 0.500 sec or more are anticipated for this fuzing system, this gives a fuzing error of 0.025 sec, or ten times larger than the allowable 0.0025-sec standard deviation required.

i. Another method of fuzing includes both the rate of sight-line rotation and target range information. It is thought that by using ranging information, if available, the fuzing accuracy of a sight-line rotation-rate fuzing system can be increased, if the resultant fuzing equation is not dominated by the range parameter. The resulting equation for the fuzing time of a system, using sight-line rotation rate plus range information, is as follows:

$$\gamma = \frac{R_x}{\dot{R}_x} \cdot \frac{1}{\left[1 - R\phi_s \dfrac{M_1 - M_2 M_3}{M_4 - M_5 M_3} \right]}$$

where

$$M_1 = \cos\phi_s$$

$$M_2 = \frac{\sin\phi_s}{\cos\alpha}$$

$$M_3 = \frac{V_m}{V_P} + \sin\alpha$$

$$M_4 = \sin\phi_s$$

$$M_5 = \frac{\cos\phi_s}{\cos\alpha}$$

It can be seen from these equations that all the important terminal-kinematic parameters are taken into account. The accuracy of the overall equation, however, is still dominated by the accuracy of the range information used. Furthermore, the mechanization of such a complex equation to any accuracy is not considered feasible, so that no further consideration of this fuzing method is deemed necessary.

2. Conical-Skirt Fuzing Systems

a. The principle of the conical-skirt type of fuze is based on the measurement of the time at which a target's presence has been detected by interception in one or more narrow conical skirts or conical, lobed radar beams originating from the missile. These devices provide no guidance information. Two types of conical-skirt fuzing systems are worthy of evaluation, radar and infrared.

b. The radar conical-skirt proximity fuze generally consists of slot antennas spaced around the circumference of the missile, resulting in a narrow-beam radiation pattern in any plane containing the longitudinal missile axis. The T-3010 fuzing system is a very simple and reliable device. The skirt angle can be set at some value less than 90° with respect to the missile longitudinal axis (measured from the missile nose), thus allowing time for the warhead to be detonated and its submissiles to intercept the target. Some limitation must be placed on the simplification of a fuze system to this extent, however. The use of a single skirt angle and a simple, fuzed time delay is based on the following assumptions:

(1) Missile velocity considerably greater than that of the target.

(2) Small approach angles between missile and target.

(3) Submissile velocity considerably greater than that of both target and missile.

c. With any of the radar trackers likely to be used on the Bomarc, at least approximate closing-velocity data are used in the T-3010 fuzing system to correct these limitations. With the conical-skirt angle and the closing velocity between the Bomarc and the target known at the instant the target enters the conical skirt, the closing velocity can then be resolved into components normal and parallel to the missile line of flight. These components are used to compute a variable delay time for detonating the warhead after the target is detected by the radar skirt. Even this type of fuzing system contains two basic assumptions: (1) that the miss distance is small enough to be ignored in view of the expected closing-velocity components, and (2) that the missile velocity is constant and small in relation to the submissile velocity. The first assumption is not serious if miss distances are not excessive and the target velocity is less than one-half the missile velocity. The second assumption concerns the submissiles as they leave the missile. Since the submissile velocity vector is the resultant of the missile velocity plus the radial submissile velocity, the angle and magnitude of the submissile velocity vector changes with the missile velocity if the radial submissile velocity and the missile velocity are of the same order of magnitude. Since the positioning of the radar skirt angle and the delay times inserted by the fuze computer are all based on a fixed submissile dispersal angle, serious errors would result in view of the variation of Bomarc velocity from 1000 to 2500 ft/sec. For example, using a continuous-rod warhead and with the radar skirt angle and fuze computer adjusted to a V_m of 2500 ft/sec and a radial submissile velocity of 5000 ft/sec, if the V_m dropped to 1000 ft/sec, the rod warhead would miss the centroid of a 1300 ft/sec target by 20 ft, at a range of 60 ft, neglecting all other fuzing errors. This limitation to the all-around accuracy of the T-3010 type of fuzing system could be removed if the radar skirt angle could be varied by a Mach senser. This, however, appears difficult because of the problems involved in mechanically changing the angle of the slot radiators in flight. An alternative approach involves using additional input data, such as altitude or missile speed, in the delay-time computer.

d. Two types of infrared conical skirts have been developed to the point where they could be used as fuze detectors, these being the sequential and convergent systems. Preliminary work on these two infrared fuzing systems was done by the General Tire and Rubber Company of California, results of which are covered in References 47 through 50.

e. A very serious problem must be considered in any type of infrared fuze detector, that is, false triggering due to targets such as the sun or the moon in the field of view. To overcome this problem, the sequential type of infrared conical skirt uses two reception beam patterns, such as those shown in Figure 57. By using the two conical skirts separated by an angle, the sight-line rotation rate can be used to discriminate against targets at long range from the missile. With this zone arrangement, the maximum time of transit between the two skirts by a target at 180 ft from the Bomarc missile is 18.6 ms. The sun transit time would be infinite for a missile flying a straight course, but under conditions of 10° missile oscillation at 3 cps, the sun transit time between the two zones would be 55.2 ms. By utilizing this information, the electronic circuits can be designed to accept only targets whose transit time is less than some preset time such as 25.0 ms.

f. Figure 58a shows the block diagram of an electronic circuit capable of providing discrimination against the sun or moon for the sequential conical skirt. Whenever a target or the sun, or both, enters the first conical skirt, a pulse is received from the first detector, which triggers a one-kick multivibrator. The multivibrator produces a positive square wave of approximately 25 ms duration, which is applied to the screen grid of a gating tube. If the pulse which triggers the multivibrator is produced by a target or a target and the sun, another pulse will be produced in channel 2 when the target enters the second conical skirt. This pulse is applied to the control grid of the gating tube and will cause it to conduct if the multivibrator pulse is still on the screen grid. The signal from the gating tube is then amplified and used to fire the fuzing thyratron. It is possible for this type of infrared conical skirt to be triggered by the sun being in the field of view of the second skirt at the same time as a target enters the field of view of the first skirt. Even though this is highly improbable due to the small field of view of the skirts, it would cause the warhead to be detonated a few milliseconds early, resulting in less chance of a definite kill. This condition could be alleviated by signal-level discrimination so that, if it is known that the sun is in the field of view of the second skirt, some fixed time delay for detonation could then be inserted after a target has entered the field of view of the first skirt. Further study along this line is necessary to ascertain the method of making such discrimination practicable.

g. The convergent or coincidence type of infrared conical skirt is based on the principle of an optical range finder. A diagram of such a system, as it might be applied to the Bomarc, is shown in Figure 59. This system employs two conical skirts arranged so that their beam patterns converge over a limited range. When a target is within the bounds of the shaded area in Figure 59, both skirt detectors are triggered, this being the necessary condition for detonating the warhead. The two skirts are located as far apart as dimensional limitations permit and are shielded so that any target at a range beyond S will transmit to the skirt detectors only a small fraction of its total emission and an object at still greater distances will be completely cut off. The value of S used can be determined by statistical evaluation of the miss distance between the Bomarc and the target due to terminal-guidance errors and of the warhead lethality radius. This type of conical skirt contains discrimination against the sun or moon. In addition, it provides discrimination in favor of a close target when the Bomarc is attacking a squadron formation. The block diagram of the electronic system necessary for the convergent or coincidence type of conical skirt is shown in Figure 58b. The mixer network produces enough signal to trigger the fuzing thyratron only when the target is in the field of view of both skirts. This system would also be triggered prematurely by the sun being in the field of view of the first conical skirt and a target in the field of view of the second conical skirt. This situation is much more probable for the convergent system than for the sequential system because of the wider skirt beam necessary to obtain the range discrimination. Another serious disadvantage of the convergent type of conical skirt is the base length necessary between the two beams. The unobstructed base length available on the Bomarc, from the tip of the radome to the fuze antenna compartment, is approximately 10 ft. If S is chosen as 180 ft, this causes the two beams to converge at an angle of less than 4°, imposing severe requirements on the shielding and alignment of the two beams. Furthermore, the problem of constructing an optical conical skirt around the missile body at the fuze antenna compartment to withstand the shock and vibration of the missile would be very difficult. In view of these limitations, only the sequential type of infrared conical skirt can be adapted to the characteristics of the Bomarc.

3. Comparison of Infrared and Radar Fuzes

a. A more detailed study of the fuzing accuracy of the sequential type of infrared conical skirt has been made to compare it with the accuracy of the radar conical skirt. In Figure 55 a plot of missile velocity vs optimum skirt angle is shown in a nose-on below or tail-on above attack situation, with the target velocity 800 ft/sec and the approach angle again 60°. The effect of altitude on the warhead velocity was also investigated in both of these typical situations. This study disclosed that the effect on the optimum skirt angle is negligible. The variation in optimum skirt angle over the missile velocity range is about 13 to 17°, however. These figures are based on a continuous-rod warhead with a velocity of 5000 ft/sec. Any warhead of a slower velocity would increase the variation in optimum skirt angle with missile velocity.

b. As noted previously, this same problem of variation in skirt angle with missile velocity is also inherent in the T-3010 radar conical skirt. In the sequential type of infrared conical-skirt system, however, it is possible to correct this condition very simply by varying the skirt angles as a function of input data. Figure 60 shows how such a sequential-type, infrared, conical-skirt fuzing system could be attached to the Bomarc radome. The two detector assemblies are mounted on a common rod which is moved fore and aft by a small d-c motor. This permits both skirt angles to be changed by approximately ±20° while changing the width of the skirt beams by only a very small amount. The excitation for the d-c motor is obtained from a simple position-servo system, with the reference input signal taken from a Mach indicator or from an altitude-mean-speed correlation function, and with the response position signal taken from a potentiometer driven by the translating gear. This produces a nearly optimum skirt angle for any missile velocity.

c. Figure 61 shows the results of a study of the fuzing errors for a sequential-type, infrared, conical skirt using the Mach corrector described above. For this study, the following assumptions were made:

(1) Under certain conditions, the Mach readings or the correlation function for an altimeter would be accurate only to ±20%.

(2) The skirt angle could be held only to ±5% of optimum by the servo system.

(3) The optics and the electronic circuits could only measure the location of the target to within 2°.

Delay time in electronics, fuzing relay, and warhead were lumped in the 2^{o} error also. The error curves in Figure 61 are based on a pessimistic tactical situation, that of a 30^{o} nose-approach angle with both target and missile velocity of 2500 ft/sec. It is evident that warhead miss distance due to the accumulative error is small at missile miss distances up to 120 ft. Approximate fuzing errors in seconds may be obtained from Figure 61 by dividing the warhead miss distance by the target velocity. For example, at a missile miss distance of 60 ft, the standard deviation of the cumulative fuzing error would not exceed approximately 2.5 ms, still within the allowable fuzing tolerance under the worst conditions.

D. CONCLUSIONS

1. The general conclusion to be drawn from the fuzing study of the Bomarc is that no very simple and reliable fuzing system can be made to meet all the requirements of the Bomarc missile. Due to the high closing velocities involved, very few terminal-kinematics parameters can be assumed to be constant or can be ignored. On the other hand, the overall fuzing accuracy is so important that only a relatively simple fuzing system can come within the fuzing tolerances required.

2. In consideration of these conflicting requirements, the following fuzing systems are recommended in the order of their value as proximity fuzes for continuous-rod and multiple-jet, shaped-charge warheads of the IM-99A and IM-99( ) Bomarc interceptors:

a. T-3010 Fuzing System - If the beam pattern of the radar can be held to within 2^{o} and with closing velocity information available from the pulse-Doppler radar to provide a variable time delay, the T-3010 should provide accurate proximity fuzing, provided that a high-velocity, unguided warhead such as the continuous rod or shaped charge is used. The only disadvantage of the T-3010 is that it does not correct the optimum skirt angle for changes in missile velocity. However, this does not appear to be too serious if the Bomarc is not required to attack very low-altitude targets. With a set or variable-range gate (assuming pulse-Doppler tracking radar), the T-3010 system can be made to fuze only on close-in targets when the Bomarc is attacking squadron formations. Because of the narrow beam width of the T-3010 fuze system, it would not be economically feasible to jam it with any countermeasure method now known.

b. Infrared Sequential Type, Conical Skirts - This type of fuzing system requires only very simple elements which can detect present multi-jet bombers at least 300 ft away. With the two zones, it provides discrimination against the sun or moon but cannot provide range or closing-velocity information. This must be supplied for the terminal guidance radar or through the command system. Missile velocity information can be used to correct the optimum skirt angle through translation of the simple optical elements. The infrared conical skirt has a possible slight advantage over the radar conical skirt with respect to countermeasures. Even though it is difficult to jam the radar conical skirt because of its narrow beam, it is even more difficult, if not impossible, to jam the infrared conical skirt because it is a passive detector. Further study appears necessary to fully determine the extent to which infrared conical skirts can be used to provide proximity fuzing for guided missiles.

c. T-3016 and Infrared Sight-Line-Rotation Fuze Systems - These two fuzing systems, as applied to the Bomarc, require the accurate measurement over a period of time of one or more parameters. The resolution of these parameter measurements is then used to determine a point of detonation, the same point which can be determined instantaneously by a conical-skirt fuze. Thus, the accuracy of the T-3016 or the infrared sight-line-rotation type of fuze system depends on more than one measurement of some parameters such as range, closing velocity, or sight-line rotation.

3. The primary accuracy of conical-skirt systems, however, depends on only one measurement of target position relative to the missile. This leads to the conclusion that only a conical-skirt type of fuze can provide fuzing accurate enough for the IM-99 Bomarc.

V. SUMMARY AND RECOMMENDATIONS

A. COMPARISON OF WARHEAD TYPES EVALUATED

The continuous-rod, the shaped-charge, and the T-44-type cluster warheads were given primary consideration for selection as the "optimum" warhead during this evaluation. Fragmentation and external-blast warhead types were dropped from active consideration after early analysis indicated that the K-kill potential of these types was definitely below the minimum standards required for the Bomarc interceptor. The guided, propelled submissile (cluster family) was dropped when it was realized that the present and the anticipated state of the art is not compatible with the development time scale required for the IM-99( ) warhead. The T-44 cluster was chosen over the Crossfire cluster for final evaluation and comparison because considerable development work has already been accomplished on this weapon, whereas the Crossfire round was, at the time, still subject to experimental determination of stability in extremely high cross-wind launchings.

1. Bases of Comparison

In the following paragraphs, the continuous-rod, shaped-charge, and T-44-type cluster warheads are compared on the following bases:

a. Estimated kill probability, including fuzing potential

b. Reliability of damage achievement

c. Reliability of warhead functioning

d. Problems associated with development and production.

2. Kill-Probability Comparisons

a. A comparison of the maximum attainable kill probabilities for the IM-99( ) is presented in Figure 62 for 30,000 ft altitude, and in Figure 63 for 60,000 ft altitude. Each of the curves for the T-44-type cluster warhead represents an average of the kill-probability curves for the two target approach angles considered in Figures 33 to 40 for the same target and altitude. Figures 62 and 63 show the T-44-type cluster to be superior to either the continuous rod or shaped charge at low guidance errors. However, beginning at rms guidance errors of about 30 to 40 ft and extending to 150 ft, the expected performance of the continuous-rod and shaped-charge warheads, with or without blast degradation, exceeds that of the T-44-type cluster. The expected lethality of the T-44 against a Type-37 target at a 1.5 blast degradation factor falls below the continuous-rod and shaped-charge estimates at a somewhat greater miss distance. The expected kill probability of the continuous-rod warhead falls off slowly with increasing guidance error, exceeding both other types at guidance errors greater than 50 to 70 ft at 30,000 ft altitude, and at guidance errors greater than 55 ft at 60,000 ft altitude. The kill probability for the 30-projector, shaped-charge warhead falls between that of the T-44-type cluster and that of the continuous rod at the larger guidance errors.

A similar comparison of the maximum attainable kill probabilities for the IM-99A is presented in Figure 64 for 30,000 ft altitude, and in Figure 65 for 60,000 ft altitude. The T-44-type cluster warhead is assumed to package 44 submissiles in the IM-99A installation. It is seen from Figures 64 and 65 that the lethality comparison follows exactly the trend established in the comparisons for the IM-99( ).

b. It should be noted that the preceding discussion has assumed perfect fuzing in all cases. A high degree of accuracy in standoff (range) is required for the continuous-rod and shaped-charge warheads; however this appears achievable by using the comparatively simple and reliable T-3010 conical skirt fuze, which requires no inputs from the seeker or guidance systems. However, the T-44-type cluster warhead has a much lower radial ejection velocity and hence must be fired at a greater standoff from the target than either the continuous-rod or shaped-charge warheads. Since the guidance system minimizes the miss distance between the interceptor and the target rather than the distance between the submissiles and the target, it has been shown (see Section IV,B, Terminal Encounter-Kinematics) that some combinations of approach angle and altitude exist for which it is impossible to achieve a collision between the ring of submissiles and the target. This is a result of aerodynamic drag causing the submissiles to lag behind the interceptor as it passes the target. An increase in radial ejection velocity will decrease the required standoff and improve this situation. However, a complicated fire-control system is the best method of providing accurate fuzing for such a submissile warhead. Assuming that such a fire-control system is not feasible for the IM-99( ) interceptor, the use of an alternative fuzing system will degrade the kill probabilities for the T-44-type warhead more than the use of the T-3010 fuzing system will degrade the kill probabilities for the continuous-rod and shaped-charge warheads. Therefore, it is the conclusion that, for realistic fuzing systems, the continuous-rod warhead will have the highest kill probability at guidance errors greater than 50 ft, followed in turn by the shaped-charge and T-44-type cluster warheads. At guidance errors of less than 50 ft, the warheads will be approximately equal in lethality, with the shaped charge showing a slight advantage.

3. Reliability of Damage Achievement

a. The clean, effective cut of structure provided by the continuous rod is a sure method of accomplishing the level of structural damage required by the provisions of this study to assess a K-kill. This effectiveness has been demonstrated by tests at NMIMT with both 1/4- and 3/16-in. square rods. The rod cuts through skin and structure to achieve its kill, and it therefore is not dependent on target size or configuration.

b. A shaped charge of the proper size and design can produce a spectacular and certain K-kill. However, the diameter and design of the shaped charge required to achieve this damage appears to be a function of target size and design. For example, tests show that an 8-in.-dia shaped charge is required to produce the same level of damage on a B-29 which can be produced by a 6-in.-dia charge on smaller targets.

c. The uncertainties associated with the evaluation of the T-44-type submissile can best be shown by citing the range of surface-blast degradation factors (1.5 to 5.0) required to accommodate the differences of professional opinion regarding this device. In addition, the evaluation of such a submissile always requires the use of a vulnerable-area concept which is dependent on the target size, structure, and configuration. It is, therefore, more difficult to predict the effectiveness of this device against possible future targets.

4. Reliability of Warhead Functioning

a. The continuous-rod warhead as proposed in this study can be assumed to function more reliably than any of the other types considered for the simple reason that it requires only one fuze (that of the primary missile), one S-and-A device, and only one detonator. The most important uncertainty for the continuous-rod warhead lies in the possible premature breaking of rod sections. Experience at NMIMT indicates that this problem can be solved by a proper development program for the warhead.

Such a program should include the development of an adequate method for the inspection of production weldments, as well as the development of an explosive-wave guide, tailored to the particular warhead design.

b. The multiple-jet shaped-charge warhead is somewhat less certain in its functioning, since a detonator or Primacord lead must be provided for each projector. In addition, a high degree of simultaneity of function of each of the several detonators or leads is required for successful performance of this warhead.

c. The T-44-type cluster warhead has the greatest number of components potentially capable of malfunctioning. In addition to the primary missile fuze, each submissile is provided with a separate ejection charge, including a primer and propellant charge and a separate omnidirectional fuze. Occasional malfunctions are known to exist in primers and propellant charges. Although a successful omnidirectional fuze has been developed, it is sufficiently complicated to warrant assessing a lower reliability factor for it than for a conventional unidirectional fuze. However, it should be noted that the failure of a single submissile does not appreciably degrade the performance of the entire warhead.

5. Problems Associated with Development and Production

a. The development of a successful continuous-rod warhead for the IM-99( ) requires a program of some magnitude, to determine the proper configuration of explosive and wave guides, to determine such design parameters as optimum C/M, L/D, etc., and to develop a reliable inspection method and nondestructive test procedure for production rod weldments. Once this development has been accomplished, production of the continuous-rod warhead should present no unusual problems. The materials employed are inexpensive and readily available, and production should be rapid and economical. It should be noted that fewer machining operations are involved in fabricating this warhead than either of the others considered here.

b. Based on available skill and background information, it is believed that less development time would be required to determine the optimum design parameters for a multi-jet shaped-charge warhead than would be required for the continuous rod. However, production is likely to be slower and more expensive, due to the precision required for components comprising the detonation system.

c. It can be assumed for the T-44-type cluster warhead that the experience of Aircraft Armaments, Inc., can be utilized. Since the cluster warhead as presently developed should be somewhat insensitive to minor changes in the IM-99 design and performance, the remaining development problems for such a warhead for the IM-99( ) should be negligible. However, the large number of individual components, the submissile fuze, ejector tubes, submissile cases, etc., which require detailed workmanship are such that this warhead is considered to pose the most difficult production problem of the three advanced warhead types considered here.

B. PRIMARY RECOMMENDATIONS

1. IM-99( ) Armament System

A continuous-rod warhead is recommended as optimum for the IM-99( ) interceptor in view of the foregoing considerations.

a. The primary recommended warhead design is shown in Figures 7 and 6. The total weight is 598 lb, including a 60-lb provision for support rings, duct cutters, and safety and arming device. The overall length of the required warhead compartment is 30 in. between clear bulkhead mold lines. The maximum diameter of the warhead assembly is 25 in. The welded rod elements are 1/4-in.-square mild steel bar. On firing, the expected diameter of the hoop at the start of hinge separation is 345 ft. After hinge breakup, the expanding rod segments will be approximately 8 to 12 ft long, and will lose lethality slowly only as a result of gapping. The 1/4-in.-square steel rod is recommended as a conservative size for the attack of the toughest targets. The warhead contains 213 lb of Composition B and 328 lb of steel in the rod ring. If explosive optical design techniques are used in the charge design, the initial radial velocity of rod projection may be expected to exceed 5000 ft/sec. The cavity of the warhead may be expected to yield a significant K-kill "bonus" through its directional blast action in disintegrating the Bomarc interceptor.

b. The safety-and-arming device employed with the recommended warhead is centrally located in the charge cavity. It can be inserted or removed through an access door in the forward support bulkhead. The device presently planned for use with the T-33 warhead can be used with a new booster, or a revised and simpler device may be developed.

c. The primary recommended fuze for the IM-99( ) armament system is the T-3010 fuze with the radar cone angle set at 64° with respect to the interceptor longitudinal center line, assuming a 5000-ft/sec initial rod velocity and a 2500-ft/sec interceptor velocity. The computer circuit used with this fuze to determine a variable time delay also will require modification to match the continuous-rod ballistics and target intercept relationships. It is recommended that the development of this modified delay computer include consideration of rough input data on interceptor altitude and true air speed in addition to an extrapolated range closure rate if improved target hit probability can be obtained, especially under conditions of peripheral attack. It is possible that approximate data on the target speed bracket might be advantageously preset into this computer at launching or in flight by the selection of a particular target speed band, such as high, intermediate, or low. The scope of the present study does not permit accomplishment of the detailed studies necessary to make specific conclusions and recommendations in this regard.

d. Installation of this primary recommended warhead in the advanced Bomarc may be accomplished in several ways. It is essential, however, that the warhead be a single assembly, since otherwise the functioning of the explosive may be seriously degraded. It is not expected that any interceptor skin need be removed or "peeled" prior to initiation of the main warhead charge. It will probably be necessary to explosively remove an external fuselage duct with its concentration of wiring and plumbing. If skin removal or duct removal proves necessary on the first firing trials, the mechanisms and techniques which have already been successfully demonstrated with developmental T-44 warheads may be directly adopted. The installations which are feasible are as follows:

(1) Four- or six-bolt separation of the fuselage nose so that it can be pulled forward. In this installation the warhead could be mounted either

(a) With the explosive web aft and with the main support from the forward face of a flat fuel-tank bulkhead, or

(b) With the explosive web forward and with the main support from the sides of a deep-drawn fuel-tank bulkhead projecting inside the charge cavity.

(2) Provision of a stress-skin access panel from one side or the bottom of the fuselage, so that the warhead assembly could slide or be hoisted into position for clamping.

The second installation listed under (1) above provides virtually no interchangeability for other warhead types and is hence not recommended despite obvious advantages in achieving a compact, lightweight airframe.

2. <u>IM-99A Armament System</u>

a. The armament system for the IM-99A Bomarc is limited arbitrarily to fit the maximum available length and weight provisions which can be tolerated in the latest version of the present airframes. All elements of the primary recommended armament system for this interim or tactical Bomarc are the same as those for the IM-99( ) advanced Bomarc except that the warhead is considerably smaller.

b. The IM-99A warhead assembly, based on the continuous-rod warhead concept, is shown in outline in Figure 8. Design details are similar to those shown in Figure 6. This warhead can be installed in a compartment which has a 17-in. clearance between clear bulkhead mold lines. The maximum diameter of the recommended design is 30 in. The smaller 3/16-in.-square mild steel rods are employed to attain a conservatively estimated maximum hoop diameter of 187 ft prior to hinge breakup. This diameter will probably increase to 280 ft if the latest performance data (from NMIMT) on hinging efficiency can be duplicated in this low length-to-diameter ratio. The warhead contains 63 lb of Composition B and 169 lb of steel in the rod ring. Despite the considerably smaller charge-to-metal ratio of this warhead, the expected initial radial velocity of the rod is about 5000 ft/sec, in accordance with NMIMT estimates.

C. SECONDARY RECOMMENDATIONS

1. It is recommended that an advanced, multiple-jet, shaped-charge warhead be developed and tested in a parallel, secondary program to the point where production tooling would be the next step.

2. In the IM-99( ) armament system, the multiple-jet warhead has 30 radially spaced charges with 8-in.-dia liners. The assembly is 30 in. long and approximately 30 in. in diameter, as shown in Figure 16. The detailed design of one of the charges is shown in Figure 18. The accessories for and installation of this warhead are similar to those for the continuous-rod warhead design shown in Figure 6. The T-3010 fuze can be used with this warhead. The cone angle, however, should be increased to 80 to 83° since the mean jet velocity varies from 10,000 to 20,000 ft/sec. The variable-delay-time computing circuit will also require minor modifications to account for the high jet velocity.

3. The alternative IM-99A armament system is a 16-jet version of the multiple-jet shaped-charge warhead, as shown in Figure 17. This warhead has a 30-in. dia and is 17 in. long, over all. The individual charge is the same as that for the larger warhead shown in Figure 18.

D. RECOMMENDATIONS FOR EXTENDED WORK ON CONTINUOUS-ROD WARHEAD DEVELOPMENT

To implement the primary recommendations of this feasibility design study with an orderly development of continuous-rod warheads for both the IM-99A and IM-99( ) missiles, the following developmental program is suggested. This recommended program entails two broad phases arranged chronologically to initially develop a system (both warhead and fuze) for the IM-99A on a high-priority basis, followed by the development of the warhead for the IM-99( ). The first phase would require the greatest effort, both in time and in manpower, to simultaneously develop the 300-lb, 3/16-in.-square-rod warhead, and to make studies of the associated fuzing requirements and computer design to assure "optimum" performance under all conditions of intercept and environment. It is estimated that the development of the warhead proper, including the delivery of a small number of prototype test units, can be accomplished within 9 months, and that the fuze studies should require the same time. Since most of the warhead design problems should be resolved in the first phase, and the fuzing work should be equally adaptable to both warheads, it is estimated that the second phase, the development of the 600-lb IM-99( ) continuous-rod warhead, could be accomplished in an additional 6 months, subsequent to the initial development of the smaller warhead under Phase I. These time schedules are dependent upon close technical coordination with the research group at NMIMT, and assume further that the development grou' will be working directly with the prime contractor and cognizant Government agencies. A bar chart of the target schedule is shown in Figure 66, indicating the suggested phasing of the work recommended.

1. Phase I - Design and Development of the 300-lb Continuous-Rod Warhead for the IM-99A, and Associated Fuzing Studies

a. Part A - Warhead Development

Based on (1) the initial suggested configuration discussed elsewhere in this report, (2) the current status of research at NMIMT, and (3) the technological status achieved by the present rod fabricator (the G. W. Galloway Company of Arcadia, California), a new design of a 300-lb-warhead test configuration should be prepared. Test warheads (120° sectors of the full cylinder) consisting of lengths of 3/8-in. square bars welded to simple end rings and otherwise conforming to the proposed dimensions and annular configuration of the eventual warhead should be fabricated, loaded, and tested. The 3/8-in.-square-rod test sections should be examined and checked by instruments for bending, scabbing, and other adverse effects; necessary modifications of design should be made, if warranted. Following these preliminary tests, test models using welded pairs of 3/16-in. square rods should be fired and subjected to similar examination. It is during these preliminary tests that such factors as the influence of C/M, L/D, the explosive disposition, shape of wave guides, and the like should be resolved. The construction of full cylinders using the continuous-rod nest should be undertaken next, and firings should be conducted against witness screens and target plates to determine functioning characteristics such as velocity, percentage of full diameter achieved before breakup, the performance when fired within a mockup warhead compartment, etc. Following successful testing of at least five complete warheads, a lot of 20 prototype warhead assemblies should be fabricated for delivery to the contracting agency or the missile contractor for their use. The time required to accomplish these steps in the program may be shortened appreciably if early success is encountered, which has sometimes been the case in recent NMIMT experience. Conversely, if unusual problems appear, as was the case in the TALOS development, it is conceivable that a longer effort may be required, although the inherent simplicity of the proposed IM-99 continuous-rod designs indicates that this probably would not be the case.

b. Part B - Fuzing Studies

Concurrently with the IM-99A warhead development, fuze studies should be undertaken along two lines, one to consist of "breadboard" and model studies to modify existing radar fuzing to make it compatible with the continuous-rod warhead, and the other to investigate the feasibility of developing an infrared fuze for the same purpose. The two lines of effort are suggested as desirable, since the former development should result in a quick solution suitable for interim application, while the latter could result in an advanced fuzing system optimized for the continuous-rod warhead.

The present T-3010 fuzing system should be examined with respect to the fuze-delay computations and settings and the required modifications of the computing circuit to provide for the alternative variable delay necessary to compensate for the variation in angle of projection of the rod hoop under the various conditions of environment (velocity and altitude) and intercept. Essentially, this would consist of incorporating instantaneous missile-velocity and altitude data into the computer-circuit input if available and desirable, and suitably converting this information into the variable time delay. For example, at low altitudes, the velocity of the IM-99( ) will be considerably less than at higher altitudes, and assuming that the IM-99( ) velocity is 1000 ft/sec and the radial projection velocity of the rod hoop is 5000 ft/sec, the angle of departure will be 78.5° with respect to the missile longitudinal axis. At high altitude, where the IM-99( ) can achieve 2500 ft/sec, the same rod would depart at an angle of only 64°. It can readily be seen that a fixed-cone fuze with a variable delay based only on extrapolated, range closure rates can conceivably result in a miss of the target if the angle of rod projection is not taken into consideration. Therefore, to insure "optimum" performance under peripheral conditions of attack, it is proposed that a "breadboard" and optical model laboratory investigation be undertaken during the Phase I warhead development to determine the desirability and practicability of modifying the T-3010 radar fuze as discussed above.

It is recommended that in addition to this study a similar "breadboard" and model feasibility study be conducted to evaluate infrared fuzing for this role. Since infrared fuzing is less susceptible to countermeasures and is capable of detecting either hot bodies or contrasting heat areas, a more refined fuzing, with respect to closure rate and specific target reference, is obtainable. With an infrared fuze, missile speed and altitude input data could be used to alter the cone or "look" angle, and the closure rate and/or missile speed data could set the variable time delay. This part of the fuze study should be conducted concurrently with the T-3010 modification study, so that developmental effort beyond these two investigations could be confined to the more promising system.

2. Phase II - Design and Development of 600-lb Continuous-Rod Warhead for the IM-99( )

Following the development of the 300-lb warhead under Phase I, an additional 6-month effort for the development of the larger 600-lb version, using 1/4-in. square rods, is proposed. Two factors make this warhead development practicable within the shorter development period: (a) The longer warhead is apparently more suitable for rapid transition to developmental hardware because of a more satisfactory L/D ratio, the use of 1/4-in. square rods, etc. (b) The data available from Phase I should be adaptable, at least in part, to this development. It is expected that single-bar and welded-pair firings would again be necessary prior to tests with full-scale rod designs, although indications are that the conversion can be comparatively rapid because of the simplicity of the design. Phase II should also culminate in the delivery of 20 units to the contracting agency or the missile contractor after qualification and applicable MIL-STD testing had been accomplished.

REFERENCES

1. Ballistic Research Laboratories, Letter ORDBG-BRL-W, APG S 160/8, to Aerojet-General Corp., dated 16 May 1955 (Secret)

2. Boeing Airplane Co., Document D-14808, "XF-99 Missile Data Affecting the Ordnance System Design," 9 April 1954 (Secret)

3. Boeing Airplane Co., Document D-16715, "Survey of Fragmentation Warhead Effectiveness," 22 March 1955 (Secret)

4. Ballistic Research Laboratories, Memo Report No. 776, "Efficiency of Assumed Fuzings for Bomarc Phase II Guided Missiles," March 1954 (Secret)

5. Ballistic Research Laboratories, Technical Note No. 807, "Methods for the Evaluation of Large Caliber H. E. Shell Fired from Fighter Aircraft on Pursuit and Offset Collision Courses," July 1953 (Secret)

6. Aerojet-General Corp., Report No. 767, Volumes I and II, "Design Feasibility Study 30-70mm Weapon Program," 2 Dec. 1953 (Conf.)

7. Aerojet-General Corp., Technical Memo No. 231B, "Preliminary Comparison of Forward-Firing Aircraft Rocket Weapons," Nov. 1954 (Secret)

8. Aerojet-General Corp., Report No. 889, Volumes I and II, Summary Report, "Feasibility Study for an Air-to-Air Quill-Type Missile," Jan. 1955 (Secret)

9. Aerojet-General Corp., Report No. 945, "Crossfire Aircraft Weapon," 29 March 1955 (Secret)

10. Ballistic Research Laboratories, Memo Report No. 747, "Damage to B-47 Aircraft by Internal Blast," Dec. 1953 (Secret)

11. Ballistic Research Laboratories, Technical Note No. 997, "Preliminary Estimation of the Internal Blast Vulnerability of the Type-37 Aircraft," April 1955 (Secret)

12. AA Lethality Committee, Paper No. 41, "Report of the Anglo-Canadian Lethality Mission to the USA," Nov.-Dec. 1953 (Secret)

13. Armament Research Establishment, Report 4/51, "Controlled Fragmentation of Metal Steel Castings by Means of Grooved Charges," April 1951 (Conf.)

14. Naval Ordnance Test Station, Rocket Quarterly, NAVORD Report No. 2085, Dec. 1953, pp. 1-8 (Conf.)

15. Ballistic Research Laboratories, Memo Report 739, "Optimum Warheads and Burst Points for Bomarc Phase II Guided Missiles," Nov. 1953 (Conf.)

REFERENCES (cont.)

16. Ballistic Research Laboratories, Technical Note 868, "Comparison of Designs of T-33 Bomarc Warheads for Use Against B-29 Type Aircraft," Feb. 1954 (Conf.)

17. Ballistic Research Laboratories, Memo Report 595, "Effectiveness of Bomarc 300-lb Warheads Against B-29 Type Bombers," Jan. 1952 (Conf.)

18. Ballistic Research Laboratories, Technical Note 979, "Kill Probability for the T-45 Fragmentation Warhead for NIKE B," Feb. 1955 (Secret)

19. Rand Corp., RM-1405, "The Terminal Vulnerability of Aircraft to Non-Nuclear Rounds," 3 Jan. 1955 (Secret)

20. Ballistic Research Laboratories, Memo Report 507, "Effectiveness of Warheads for Guided Missiles Used Against Aircraft," 20 March 1950 (Conf.)

21. Ballistic Research Laboratories, Report 741, "Damage to Aircraft by External Blast," 24 Oct. 1950 (Conf.)

22. Royal Aircraft Establishment, Technical Note No. G. W. 296, "Preliminary Discussion of Possible Future Antiaircraft Guided Weapon Warheads," Jan. 1954 (Secret)

23. Ballistic Research Laboratories, Memo Report 631, "Elementary Comparison of Antiaircraft Warhead Types," Nov. 1952 (Conf.)

24. Ballistic Research Laboratories, Memo Report 679, "Determination of the Optimum Charge Weight for a Cluster-Type Antiaircraft Warhead," June 1953 (Conf.)

25. Aircraft Armaments Inc., Report ER-173, "Design Study and Tests of Cluster Type Warhead for Bomarc Missile," Oct. 1953 (Conf.)

26. Aircraft Armaments Inc., Report No. ER-338, "Phase II Final Report, Cluster Warhead for NIKE I Missile," 25 May 1954 (Conf.)

27. Armour Research Foundation, Report ARD No. 1050, "Preliminary Design of a Cluster Warhead for the Bomarc Guided Missile," Nov. 1954 (Conf.)

28. Engineering Research Associates, Summary Report TAI-2703, "Feasibility Study of Bomarc Submissile Fuze," 28 Jan. 1954 (Conf.)

29. Aerojet-General Corp., Report No. L2827-2, "Ballistic Studies of Dart for Quill Missile," 9 May 1955 (Conf.)

30. Aerojet-General Corp., Report No. 871, "Terminal Ballistics Study AEROFLAK-K Rocket Warhead," 12 Oct. 1954 (Conf.)

REFERENCES (cont.)

31. Naval Ordnance Test Station, Technical Memo 1465, "Some Effects of Reduced Atmospheric Pressure on Hypervelocity Fragment Beams," May 1953 (Conf.)

32. Naval Ordnance Test Station, NAVORD Report No. 2018, "Studies of Damage to Aircraft Structure at Long Standoff," March 1953 (Conf.)

33. Naval Ordnance Test Station Technical Memo No. 411, "Effect of Single Hypervelocity Pellets Against Simulated Aircraft Sections," 19 April 1951 (Conf.)

34. University of Michigan, Report UMR PR-31, Project Wizard MX-794, Progress Report No. 31, 1 March - 1 June 1952 (Secret)

35. Royal Aircraft Establishment, Technical Memorandum No. G. W. 237 "A Review of Estimates of Guided Weapon Lethality," Dec. 1954 (Secret-Discreet)

36. Aerojet-General Corp., Letter PS-4610, Enclosure (1), "Proposal for Guided Warhead for the Destruction of Ballistic Missiles," 17 Jan. 1955 (Secret)

37. Boeing Airplane Co., Document D-14135, "Method to Evaluate Hit Probability of High Velocity Submissiles Launched from MX-1599 Warhead," 10 Feb. 1954 (Conf.)

38. New Mexico Institute of Mining and Technology, RDD Report T-821, "Rod Design," Feb. 1952 (Conf.)

39. New Mexico Institute of Mining and Technology, RDD Report T-9B, "Aircraft Damage Studies," June 1954 (Conf.)

40. New Mexico Institute of Mining and Technology, RDD Report T-907, "Aircraft Damage Studies," April 1953 (Conf.)

41. Ballistic Research Laboratories, Memo Report 630, "Preliminary Study of a Cone-Fuzed Cluster-Type Antiaircraft Warhead," Jan. 1953 (Conf.)

42. Ballistic Research Laboratories, Memo Report 800, "Single Shot Hit Probabilities for Bomarc Cluster Warheads," March 1954 (Conf.)

43. Ballistic Research Laboratories, Technical Note 808, "The Effect of Fuzing Errors on the Effectiveness of a Cluster-Type Antiaircraft Warhead," June 1953 (Conf.)

44. Boeing Airplane Co., Document D-14811, "Preliminary Study of Bomarc Fuze Problem," 23 Dec. 1953 (Conf.)

REFERENCES (cont.)

45. Diamond Ordnance Fuze Laboratory, Report TR-130, "Bomarc Cluster-Warhead Fuze - Effect of Combined Air-Drag and Range Error," 13 Dec. 1954 (Secret)

46. Aerojet-General Corp., Report No. 928, "Fuze Study for Sparrow III Missile with Infrared Guidance," 30 March 1955 (Secret)

47. General Tire and Rubber Co. of California, Report No. 2019, "First Progress Report - Model 23A," 8 Oct. 1948 (Secret)

48. General Tire and Rubber Co. of California, Report No. 2028, "Second Progress Report - Model 23A," 14 Jan. 1949 (Secret)

49. General Tire and Rubber Co. of California, Report No. 2031, "Third Progress Report - Model 23A," 4 Mar. 1949 (Secret)

50. General Tire and Rubber Co. of California, Report No. 2039, "Final Progress Report - Model 23A," 11 May 1949 (Secret)

51. Aerojet-General Corp., Report No. 939, "Optical Seeker for Missile Guidance," 18 March 1955 (Secret)

52. Aerojet-General Corp., Electronics and Guidance Division, TM-520:55-6-161, "A Preliminary Study of Target and Transmission Characteristics for Infrared Fuzing," 7 July 1955 (Conf.)

53. Jour. Appl. Phys., 23:2, "Fast Jets from Collapsing Cylinders," Dec. 1952, p. 1300

54. Discussion with Dr. C. B. Cassity and Mr. M. L. Kempton, of the New Mexico Institute of Mining and Technology, at Socorro, New Mexico, 9 May 1955 and 14 June 1955

55. Shaped Charge Journal, October 1954, "Flash Radiographic Study of the Effects of Initiation upon Jets from Linear Charges," L. Zernow, S. Kronman, G. Caudill

56. Rand Corp., Report S-34, "Proceedings of the Rand Symposium on High-Speed Impact," May 1955, pp. 67-130 (Secret)

57. New Mexico Institute of Mining and Technology, RDD Report 517, "Flash and Heat Effects Accompanying Perforation of Metal Targets by Fragment-Like Projectiles," J. Rinehart, et al., 3 Nov. 1947

58. NDRC Summary Technical Report, Div. 2 Vol. I, Chap. 2, pp. 93-95, "Effects of Impact and Explosion."

SYMBOLS

A = Effective area of submissile

C_D = Drag coefficient

d_t = Distance from submissile to centroid of submissile ring

F = Force (general)

g = Acceleration of gravity

k = Aerodynamic coefficient

K_ϕ = A constant determined by the selected tracker angular rate

m = Mass

P_{hk} = Probability that target suffers K-structural damage, given a hit

P_k = Probability that warhead functioning results in a K-kill of structure

P_n = Probability that the target is hit at least once

R_x = Range to target

$\dot{R}_x$ = Range rate

S = Shortest normal distance between primary missile and target

t = Time, or time interval

t_d = Time of detonation of warhead

t_m = Time computer stops operating

t_o = Time interval during which computer operates

T_T = Equivalent tracking-loop delay time

V = Velocity (general)

V_C = Closing velocity between primary missile and target

V_C' = Closing velocity between submissile and target

V_m = Primary missile velocity

SYMBOLS (cont.)

V_P = Submissile projection velocity normal to primary missile axis

V_S = Absolute submissile velocity

V_t = Instantaneous velocity of submissile at time, t, after firing

V_T = Target velocity

V_{TN} = Velocity of target normal to flight line of primary missile

V_{TP} = Velocity of target parallel to flight line of primary missile

W = Weight of submissile

X_t = Distance traveled in time, t

y = Distance from centroid of submissile ring to target in plane of ring

Z = Altitude above sea level (standard atmosphere)

α = Angle of attack of primary missile

β, ϵ, ϕ = Angles used as mathematical operators

γ = Angle of approach

Δ = The angle between any selected radial line emanating from a point target and the line of minimum distance between the missile flight path and the target

θ = Angle between flight path of submissiles and track of primary missile

λ = Velocity of light

ρ = Air density

σ_G = Standard deviation of guidance error normal to trajectory at point of nearest approach

σ_τ = Fuzing time tolerance

τ = Fuzing delay time

SYMBOLS (cont.)

ϕ_s = Sight-line angle relative to flight line of primary missile

$\dot{\phi}$ = Rate of change of sight-line angle

ϕ_T = Sight-line angle measured by tracker

ψ = Angle between primary missile flight line and line directly to target at t_d which will assure the submissiles striking the target

CONTINUOUS-ROD WARHEAD CONFIGURATIONS TESTED AT NMIMT

Diameter Type	Overall Length in.	Gross Weight lb	Rod Size in./16	Booster Position	C/M Ratio	L/D Ratio	Theoretical Dia ft	Attained Opening dia ft	Initial Velocity ft/sec	Theoretical Max Dia per lb of Head	Attained Dia per lb of Head
24 in. Annular	22.2	436	4 x 4	End at split line	0.45	0.94	240	120[3] 180 est	4500	0.550	0.413 est
13.5 Solid	18	210	4 x 4	End center or center of head	0.65	1.33	120	?	Exp 5000	0.572	—
13.5 Annular 8.4 in. Open Center	18	175	4 x 4	End center or center of head	0.30	1.33	120	?	Exp 5000	0.686	—
13.5 Solid	16	195 est	4 x 3	End center or center of head	Unknown	1.18	100	?	Exp 5000	0.513 est	—
13.5 Annular	16	135	4 x 3	End center or center of head	0.741	1.18	100	80[3]	5000	0.741	—
13.5 Annular	16	155	4 x 4	End center	0.508	1.18	—	—	—	—	—
12 Solid	22.2	210	4 x 4	End center or center of head	0.54	1.87	130	60[3]	5000	0.620	0.286[3]
8 Solid	14-15/16	60	3 x 3	End center or center of head	0.50	1.87	70	50[3]	5500	1.166	0.833[3]
5 Solid[1]	18-1/8	40	3 x 3	End center	0.46	3.62	45	45	6000	1.124	1.124
5 Solid	15-1/8	35	3 x 3	End center or center of head	0.46	3.02	45	Exp 45	Exp 5500	1.285	—
5 Solid[2]	19-5/8	40	3 x 3	End center	0.46	3.93	45	Exp 45	Exp 6000	1.124	—

1. Include 3 in. of non-continuous rod.
2. Include 4-7/8 in. of non-continuous rod.
3. No data at larger diameter.

Current as of 6-15-55

300 & 600 Pound Continuous Rod Design Study

Length (1)	Rod Size 1/16ths	DIAMETER 20 INCHES l/d	C/M (2)	M	D_t (3)	D_e (4)	W_t (5)	DIAMETER 25 INCHES l/d	C/M	M	D_t	D_e	W_t	DIAMETER 30 INCHES l/d	C/M	M	D_t	D_e	W_t
	3 x 3	.85	1.00	112	(8)	(8)	274	.68	.79	140	258	155	300	.57	.37	169	312	187	300 (6)
17	3 x 4	.85	.68	148	203	142	298 (7)	.68	.34	186	258	155	300 (7)	.57	.37	169	232	138	300
	4 x 4	.85	.68	148	151	106	298	.68	.34	186	191	115	300	.57	.09	224	232	138	300
	5 x 5	.85	.40	179	120	84	300	.68	.08	232	(8)	(8)	300	.57	(8)	(8)	(8)	(8)	(8)
	3 x 3	1.00	(8)					.80	(8)					.67	(8)				
	3 x 4	1.00	(8)					.80	(8)					.67	(8)				
20	4 x 4	1.00	(8)					.80	(8)					.67	(8)				
	4 x 5	1.00	(8)					.80	.76	273	190	133	540	.67	.69	318	229	137	580
	3 x 3	1.25	(8)					1.00	.97	205	(8)	(8)	465	.83	.81	247	(8)	(8)	510
	3 x 4	1.25	(8)					1.00	.77	272	430	345	540 (7)	.83	.64	315	522	365	580 (7)
25	4 x 4	1.25	(8)					1.00	.77	272	320	256	540	.83	.64	315	345	240	580
	5 x 5	1.25	1.00	243	(8)	(8)	540	1.00	.59	340	253	203	600	.83	.36	396	306	214	600
	3 x 3	1.50	1.01	197	(8)	(8)	457	1.20	.81	247	(8)	(8)	510	1.00	.70	297	623	500	580
	3 x 4	1.50	.85	260	(8)	(8)	540 (7)	1.20	.65	328	538	484	598 (7)	1.00	.70	297	482	385	580 (6)
30	4 x 4	1.50	.85	260	(8)	(8)	540	1.20	.65	328	384	345	598	1.00	.37	394	482	385	600
	5 x 5	1.50	.65	330	240	216	600	1.20	.32	409	315	284	600	1.00	.14	476	(8)	(8)	600
	3 x 3	1.75	.35	253	(8)	(8)	500	1.40	.70	288	645	580	550	1.17	.56	347	780	700	600
	3 x 4	1.75	.64	312	509	458	580 (7)	1.40	.41	382	645	580	600 (7)	1.17	.56	347	580	520	600 (6)
35	4 x 4	1.75	.64	312	378	340	580	1.40	.41	382	479	430	600	1.17	.17	460	(8)	(8)	600
	5 x 5	1.75	.39	390	295	265	600	1.40	(8)					1.17	(8)				

NOTES

(1) Lengths tabulated are over-all installed lengths. Effective rod length is 5 inches shorter than tabular value. 17 inch long warhead is longest possible in 300 lb. design. All other lengths all for 600 lb. design.

(2) C/M is ratio of explosive filler weight (C) to metal in the rods (M).

(3) D_t is the theoretical maximum diameter of the ring formed by the rods before breakup assuming 100% opening efficiency.

(4) D_e is the theoretical expected diameter of the ring formed by the rods before breakup. D_e is evaluated from the following relationship:

$D_e = nD_t$, where,

l/d	n
≥ 1.0	.9
.91 - 1.0	.8
.81 - .90	.7
≤ .8	.6

(5) W_t is total weight of warhead including rods, explosive, and a 60 lb. structural burden to account for mounting, safety and arming device, etc.

(6) Denotes 1/4 x 3/16 rods oriented to form a 3/8 inch thick shell.

(7) Denotes 1/4 x 3/16 rods oriented to form a 1/2 inch thick shell.

(8) Any warhead designated by this symbol, (8), in any column is unsatisfactory (either the c/m falls outside the range .3 - .8, or it is too heavy, or too light). Where the symbol, (8), is placed in the c/m column, simple examination will show that one of the faults mentioned must be present, and any consideration of the design will be omitted from this discussion.

TABLE III

MAXIMUM ATTAINABLE KILL PROBABILITY, σ_G = 40 FT, NO SLOWDOWN, PERFECT FUZING

Type 37 Target

	60,000 ft		30,000 ft	
	A = 45° E = 45°	A = 135° E = 45°	A = 45° E = 45°	A = 135° E = 45°
T-44 Design				
1.5 Factor	.930	.926	.960	.955
5.0 Factor	.815	.780	.888	.850
Crossfire 2.00-in. .557 lb HBX	.855	.838	.925	.910

B-47 Target

	60,000 ft*		30,000 ft	
	A = 0 E = 30°	A = 30° E = 45°	A = 0 E = 30°	A = 30° E = 45°
T-44 Design				
1.5 Factor	.780	.852	.800	.882
5.0 Factor	.765	.846	.765	.848
Crossfire 2.00-in.	.820	.890	.820	.895

*Average determined by using 0.65 of TNT equivalent for 30,000 ft. This assumption matches Type 37 data.

TABLE IV

MAXIMUM ATTAINABLE KILL PROBABILITY, σ_G = 60 FT, NO SLOWDOWN, PERFECT FUZING

Type 37 Target

	60,000 ft		30,000 ft	
	A = 45° E = 45°	A = 135° E = 45°	A = 45° E = 45°	A = 135° E = 45°
T-44 Design				
1.5 Factor	.810	.792	.875	.870
5.0 Factor	.622	.580	.730	.672
Crossfire 2.00-in. .557 lb HBX	.678	.660	.792	.770

B-47 Target*

	60,000 ft		30,000 ft	
	A = 0 E = 30°	A = 30° E = 45°	A = 0 E = 30°	A = 30° E = 45°
T-44 Design				
1.5 Factor	.580	.679	.605	.720
5.0 Factor	.567	.670	.567	.670
Crossfire 2.00-in.	.633	.735	.633	.738

*Average determined by using 0.65 of TNT equivalent for 30,000 ft. This assumption matches Type 37 data.

TABLE V

MAXIMUM ATTAINABLE KILL PROBABILITY, σ_G = 80 FT, NO SLOWDOWN, PERFECT FUZING

Type 37 Target

	60,000 ft		30,000 ft	
	A = 45° E = 45°	A = 135° E = 45°	A = 45° E = 45°	A = 135° E = 45°
T-44 Design				
1.5 Factor	.670	.652	.750	.745
5.0 Factor	.485	.447	.590	.530
Crossfire 2.00-in.	.538	.513	.655	.630

B-47 Target*

	60,000 ft		30,000 ft	
	A = 0 E = 30°	A = 30° E = 45°	A = 0 E = 30°	A = 30° E = 45°
T-44 Design				
1.5 Factor	.443	.535	.465	.580
5.0 Factor	.430	.527	.430	.528
Crossfire 2.00-in.	.493	.596	.493	.598

*Average determined by using 0.65 of TNT equivalent for 30,000 ft. This assumption matched Type 37 data.

TABLE VI

MAXIMUM ATTAINABLE PROBABILITY OF HITTING THE TARGET PRESENTED AREA
AND THE EXPECTED NUMBER OF HITS THEREON
FOR GENERALIZED CLUSTER WARHEADS, ASSUMING NO SLOWDOWN AND PERFECT FUZING

	No. of Submissiles	Hit Probability				Optimum Radius of Subprojectile Dispersion at Target				Expected No. of Hits			
		σ_G=40	60	80	100	σ_G=40	60	80	100	σ_G=40	60	80	100
T-37 Target A=45° E=45°	40	.955	.870	.742	.630	79	97	113	127	4.18	2.79	2.05	1.62
	90	.992	.962	.905	.838	98	120	141	156	6.10	4.13	2.98	2.41
	120	.995	.975	.935	.882	104	127	149	168	7.17	4.85	3.53	2.80
	180	.997	.987	.970	.937	116	141	168	185	8.76	5.89	4.20	3.43
	300	.999	.995	.992	.970	134	164	192	212	10.88	7.30	5.35	4.36
A=135° E=45°	40	.956	.871	.743	.631	80	98	114	128	4.17	2.80	2.07	1.63
	90	.993	.966	.908	.840	99	120	141	157	6.12	4.15	3.00	2.43
	120	.996	.976	.938	.884	106	128	151	170	7.11	4.88	3.53	2.78
	180	.997	.987	.970	.937	117	143	168	187	8.81	5.88	4.24	3.44
	300	.999	.995	.992	.970	135	165	192	213	10.96	7.36	5.40	4.41
B-47 Target A=0 E=30°	40	.830	.650	.508	.398	62	76	88	100	2.54	1.69	1.26	.98
	90	.948	.853	.712	.602	76	92	108	122	3.86	2.62	1.89	1.50
	120	.968	.900	.785	.680	82	100	117	131	4.38	2.97	2.17	1.72
	180	.990	.948	.860	.773	91	110	129	144	5.40	3.68	2.67	2.13
	300	.994	.973	.930	.874	104	127	148	165	6.82	4.60	3.34	2.69
A=30° E=45°	40	.870	.703	.562	.448	65	80	94	105	2.88	1.91	1.38	1.11
	90	.969	.900	.780	.675	80	98	115	129	4.30	2.84	2.09	1.66
	120	.980	.928	.822	.731	86	105	124	139	4.92	3.30	2.39	1.91
	180	.991	.960	.894	.820	96	117	137	154	5.94	3.99	2.92	2.31
	300	.997	.980	.948	.906	109	134	156	175	7.72	5.12	3.78	3.00

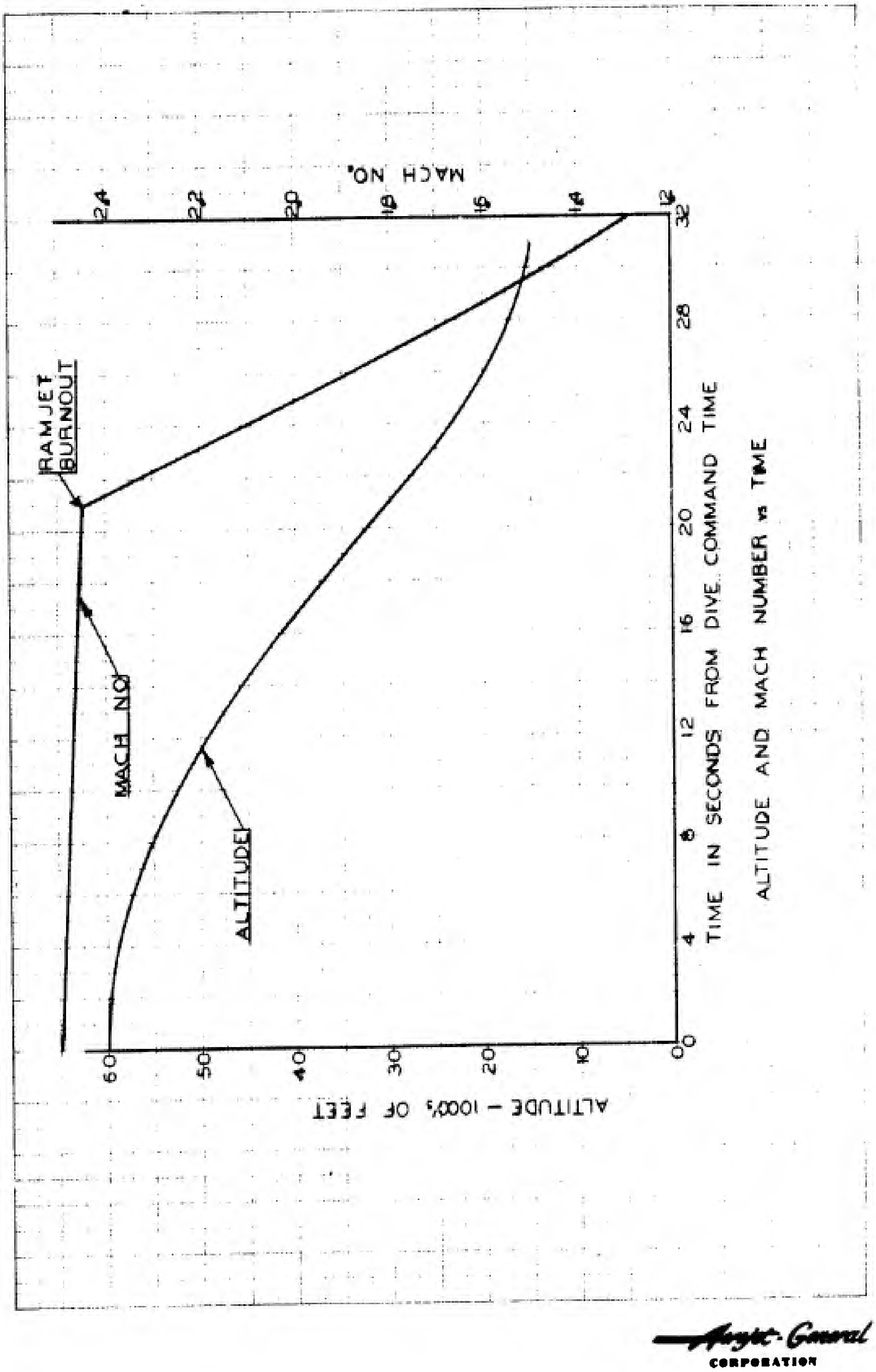

Aerojet-General CORPORATION

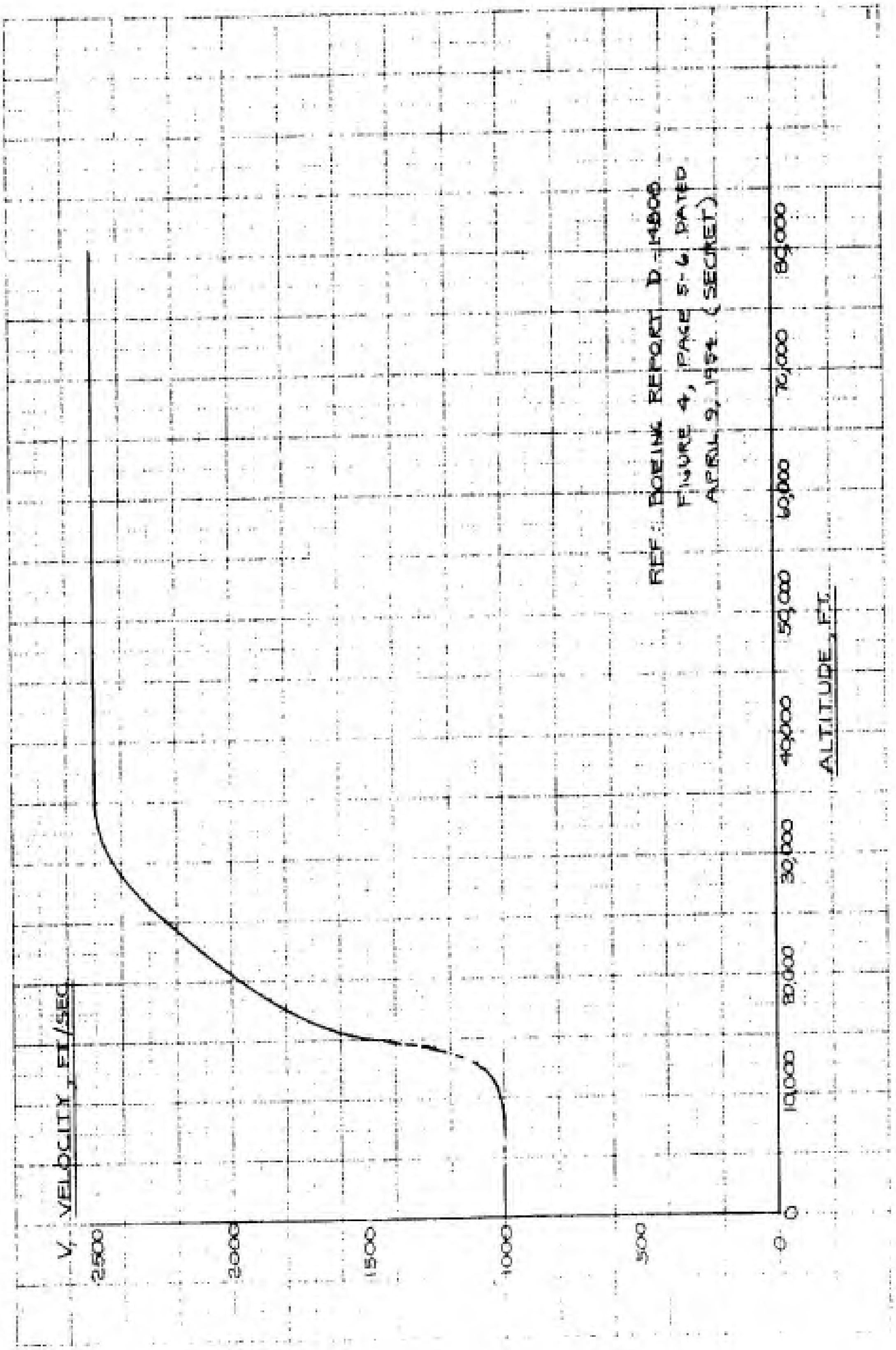

ESTIMATED TERMINAL DIVE VELOCITY FOR IM-99-( )

Aerojet-General CORPORATION

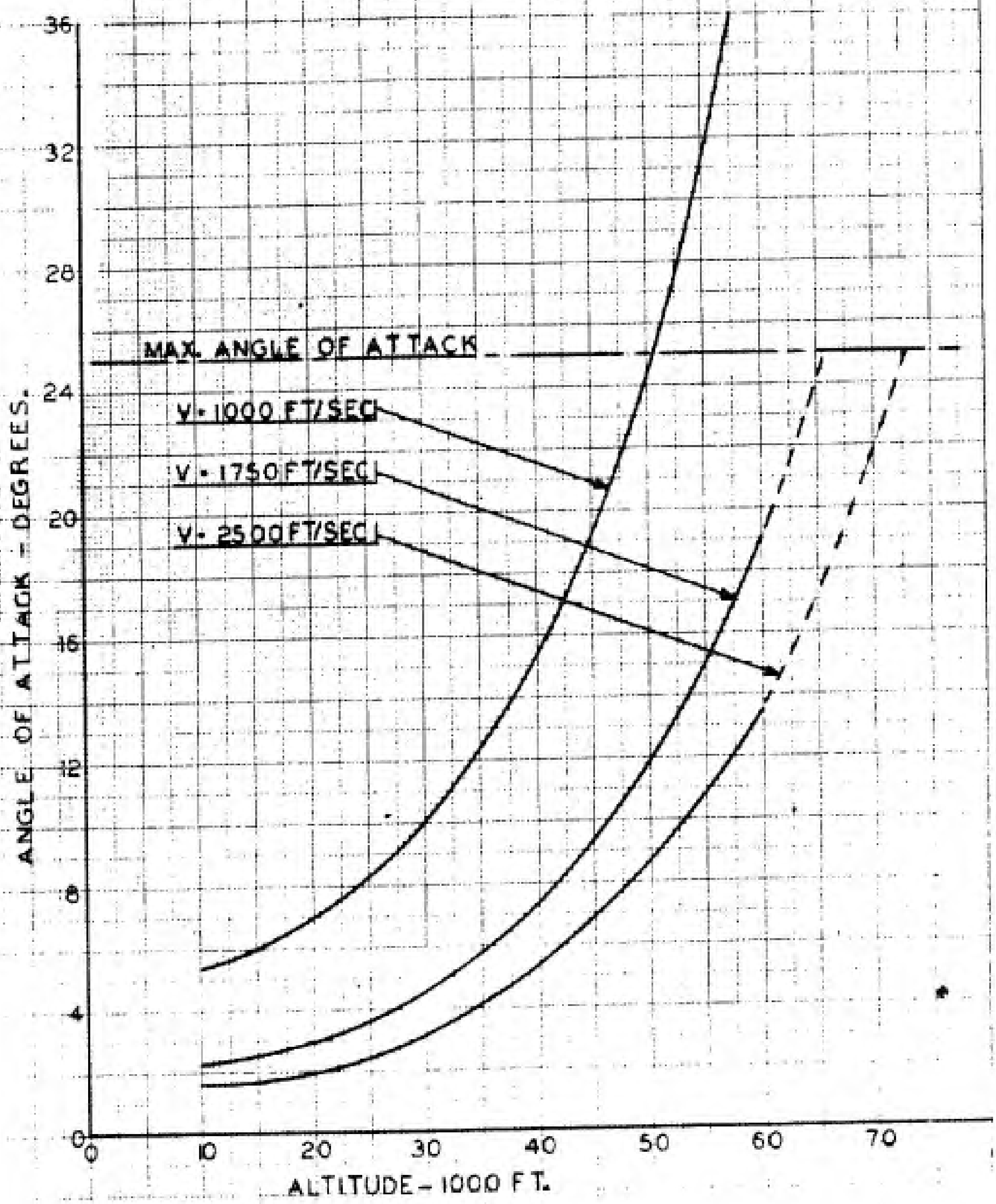

FLIGHT ANGLE OF ATTACK vs ALTITUDE FOR 7G MANEUVER

Convair-General CORPORATION

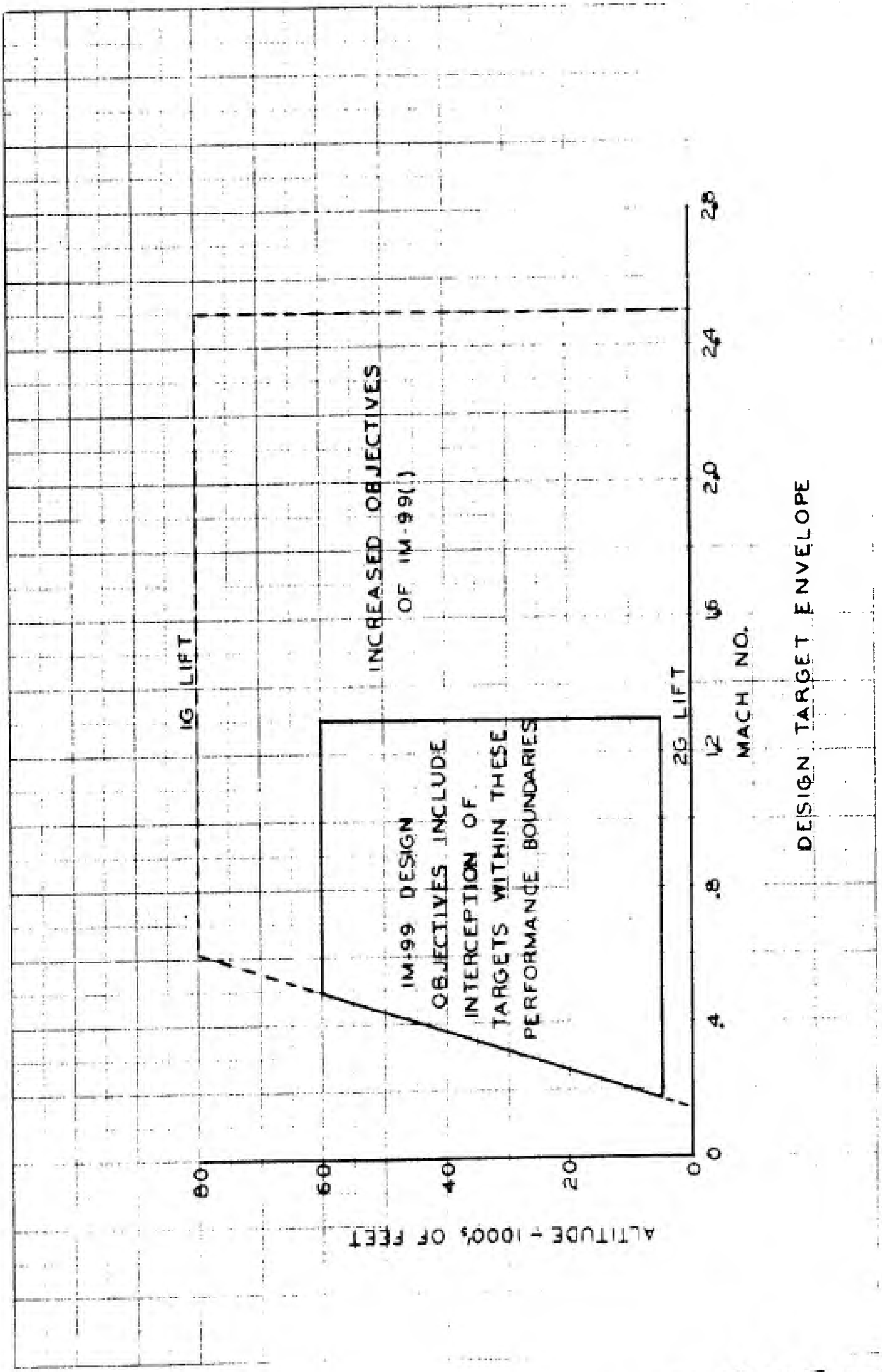

Aerojet-General CORPORATION

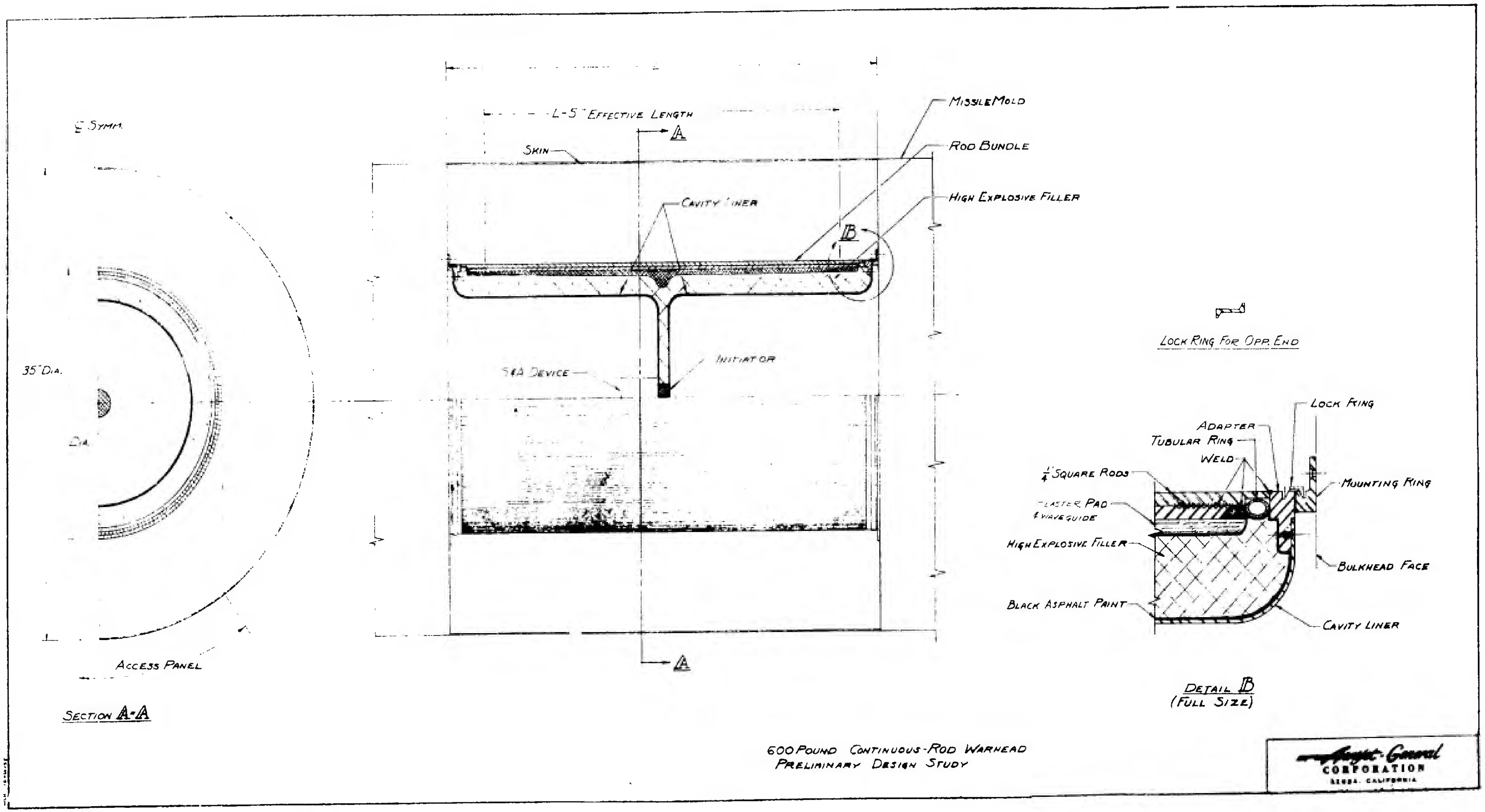
L-5" Effective Length
Skin
MissileMold
Rod Bundle
High Explosive Filler
Cavity Liner
Initiator
S&A Device
35" Dia.
Access Panel
Section A-A
Lock Ring For Opp. End
Lock Ring
Adapter
Tubular Ring
Weld
1/4" Square Rods
& Wave Guide
Mounting Ring
High Explosive Filler
Bulkhead Face
Black Asphalt Paint
Cavity Liner
Detail B
(Full Size)
600 Pound Continuous-Rod Warhead
Preliminary Design Study
Aerojet-General
Corporation

Figure 5

CONFIDENTIAL

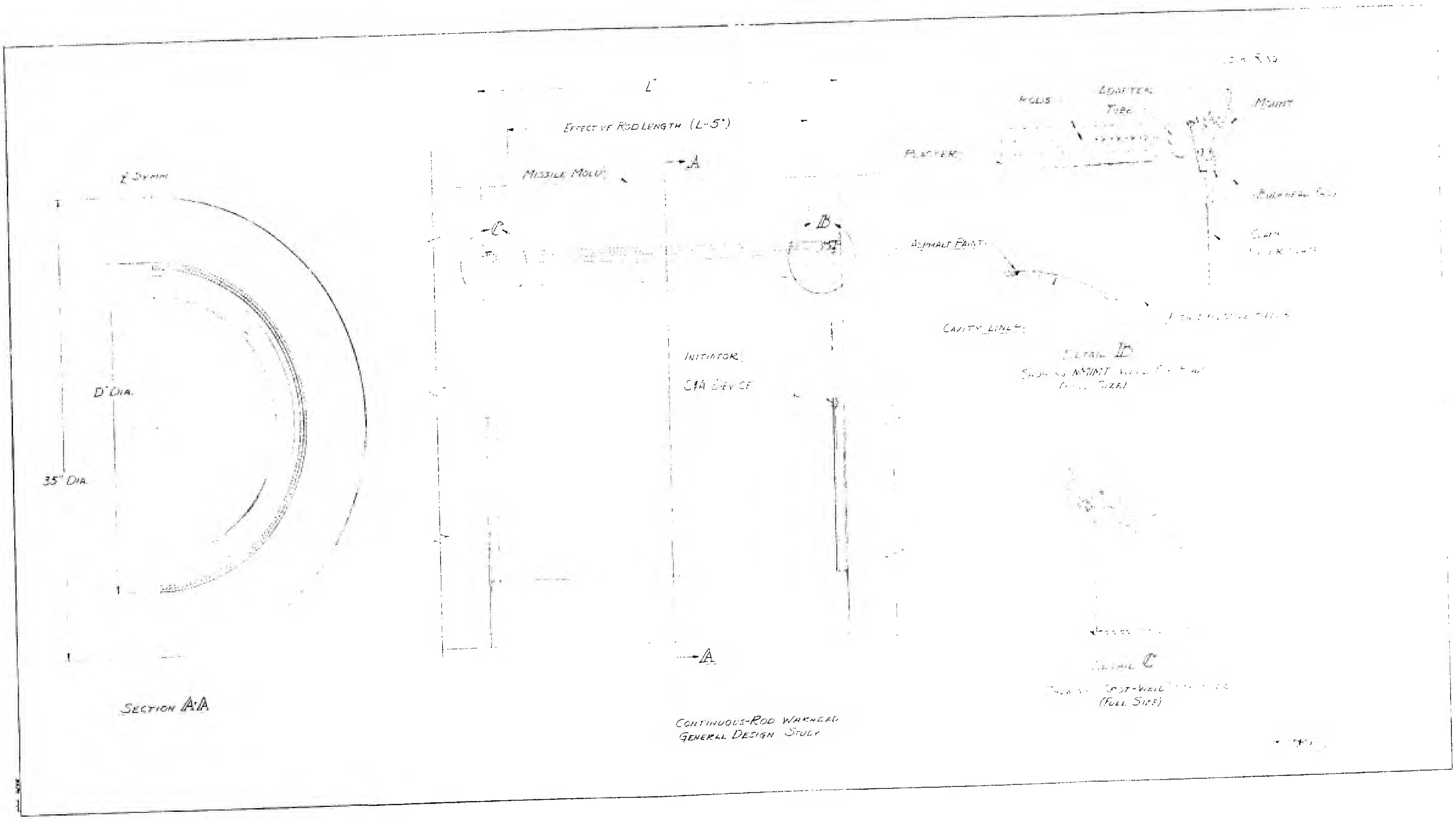

Figure 6

REPORT NO.________ PAGE________

Aerojet-General

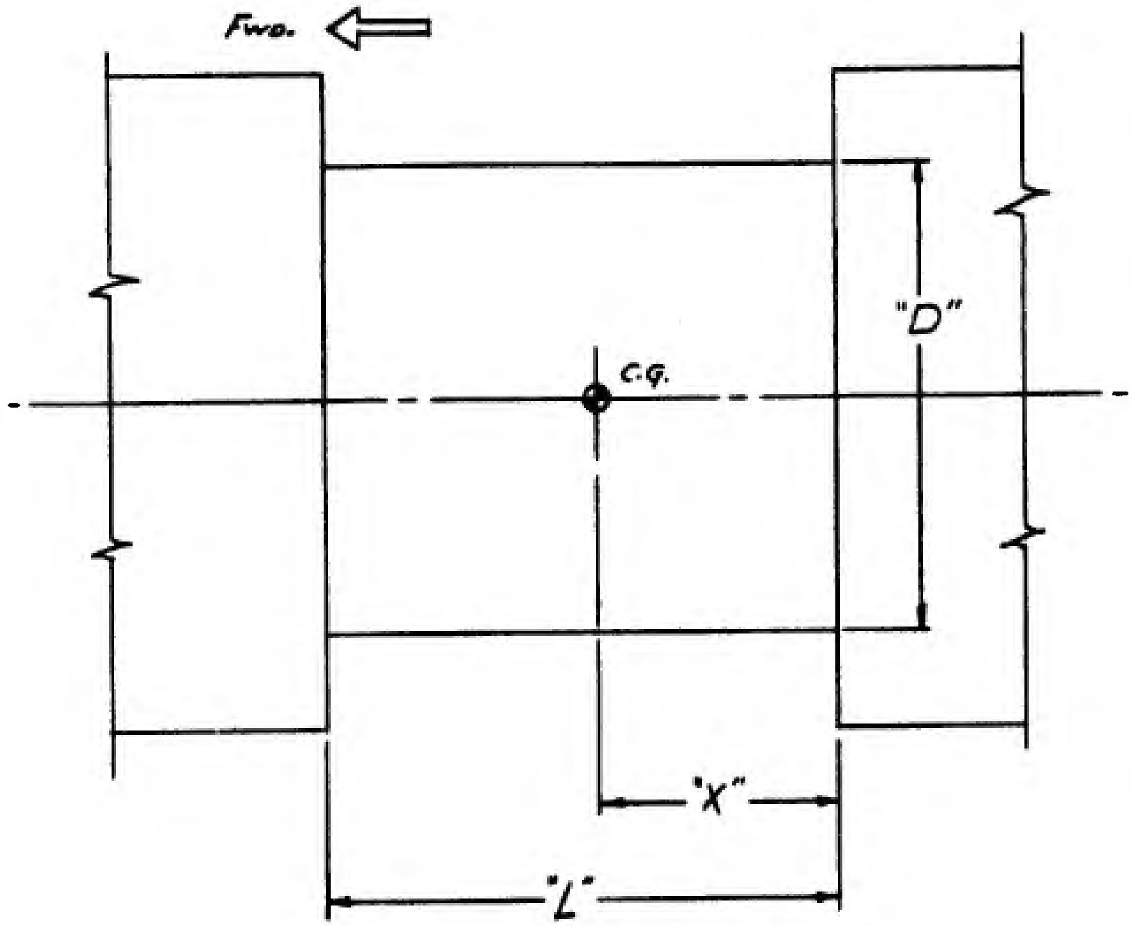

600 Pound Continuous Rod Warhead

Length "L"	30 Inches
Diameter "D"	25 Inches
C.G. Location "X" (Est.)	14 Inches
Metal In Rods	330 Pounds
C/M (Approx.)	.65
Structural Burden	60 Pounds
Rod Size	¼ x ¼ Inch

Theoretical Performance	
Max. Hoop Dia.	384 Ft.
Expected Hoop Dia. †	345 Ft.
Velocity of Rod	>4500 FPS

† Diameter which will probably occur before first break in hoop.

WLK 4/55

REPORT NO. PAGE
Aerojet-General

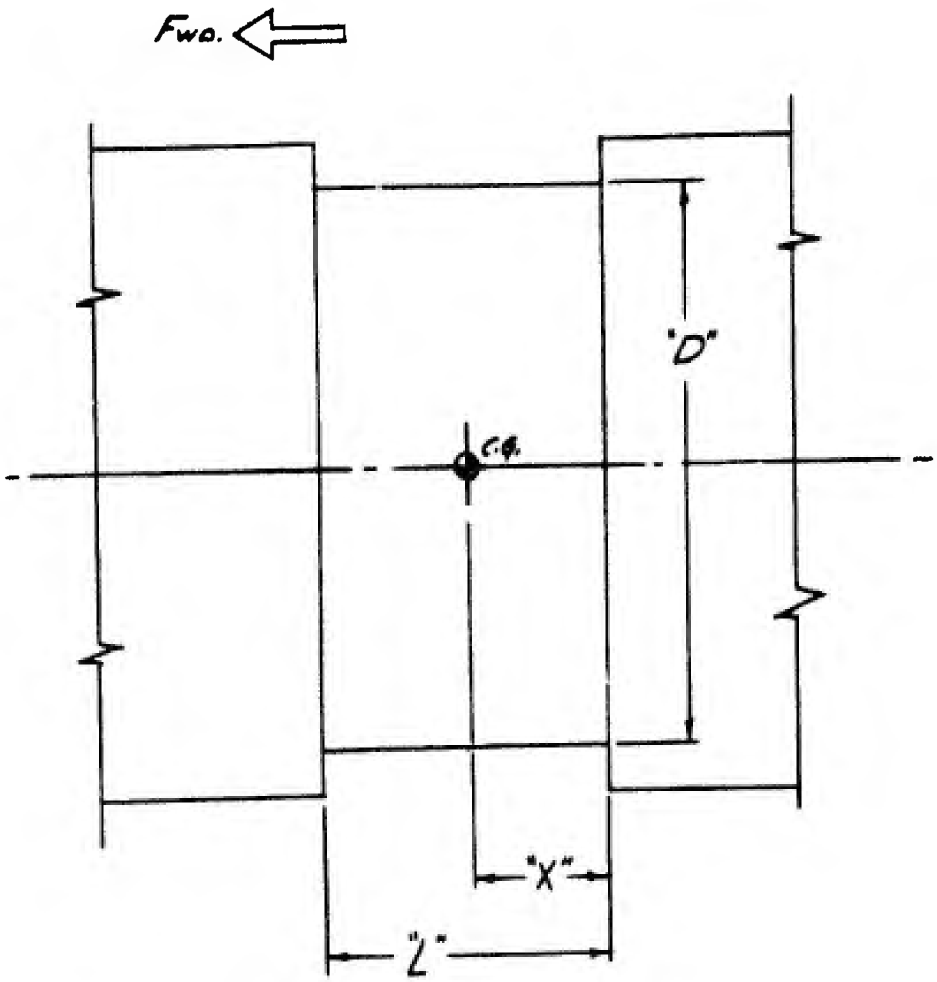

300 POUND CONTINUOUS ROD WARHEAD

LENGTH "L"	17 INCHES	THEORETICAL PERFORMANCE	
DIAMETER "D"	30 INCHES	MAX. HOOP DIA.	312 FT.
C.G. LOCATION "X" (EST.)	$8\frac{1}{4}$ INCHES	EXPECTED HOOP DIA.†	200 FT.
METAL IN RODS	170 POUNDS	VELOCITY OF ROD	>5000 FPS
C/M (APPROX.)	.4		
STRUCTURAL BURDEN	50 POUNDS		
ROD SIZE	3/16 x 3/16 INCH		

† DIAMETER WHICH WILL PROBABLY OCCUR BEFORE FIRST BREAK IN HOOP.

WMK 6/55

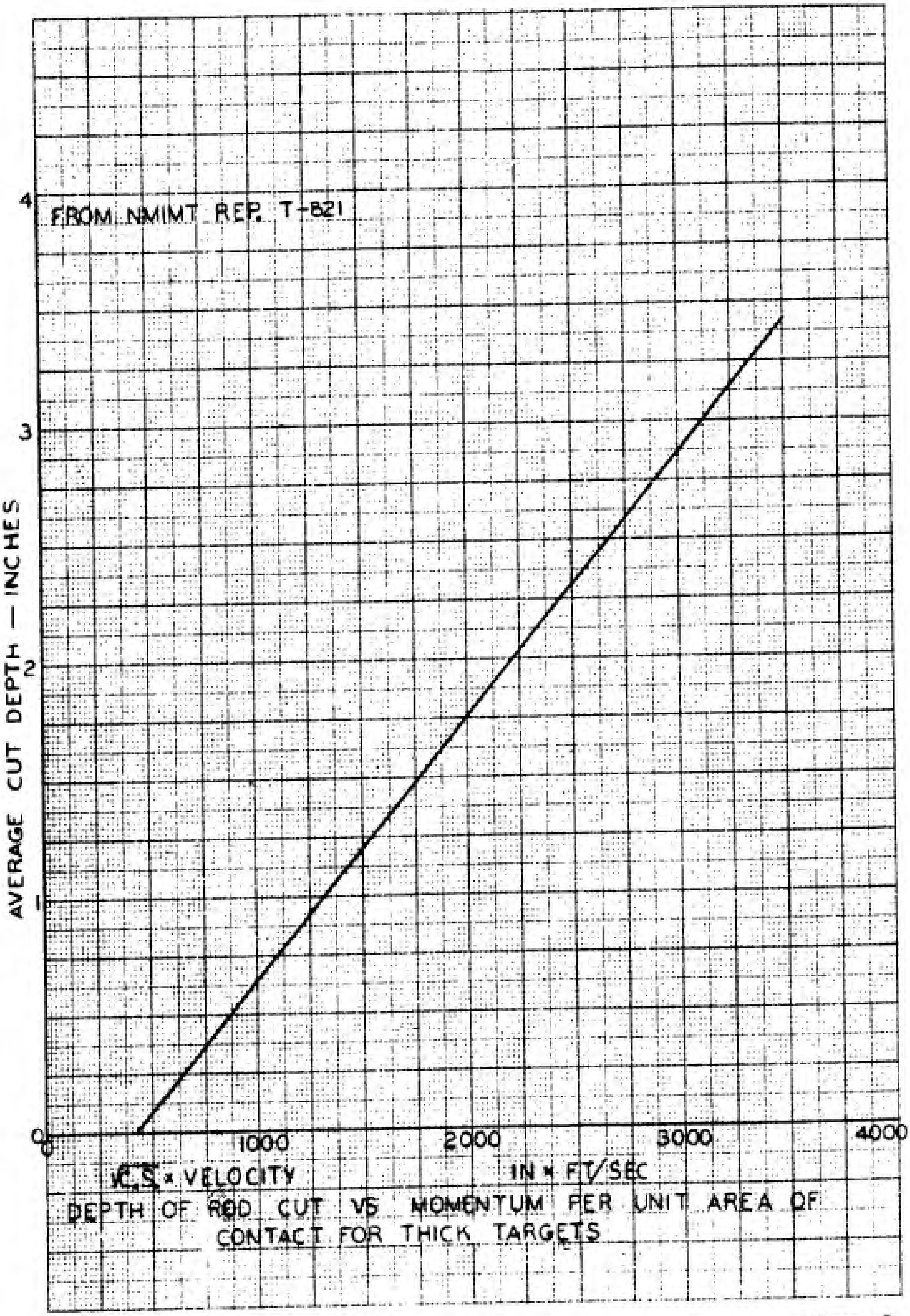
FROM NMIMT REP. T-821
AVERAGE CUT DEPTH — INCHES
4
3
2
1
0
0
1000
2000
3000
4000
K.S. × VELOCITY
IN × FT/SEC
DEPTH OF ROD CUT VS MOMENTUM PER UNIT AREA OF CONTACT FOR THICK TARGETS

Figure 9

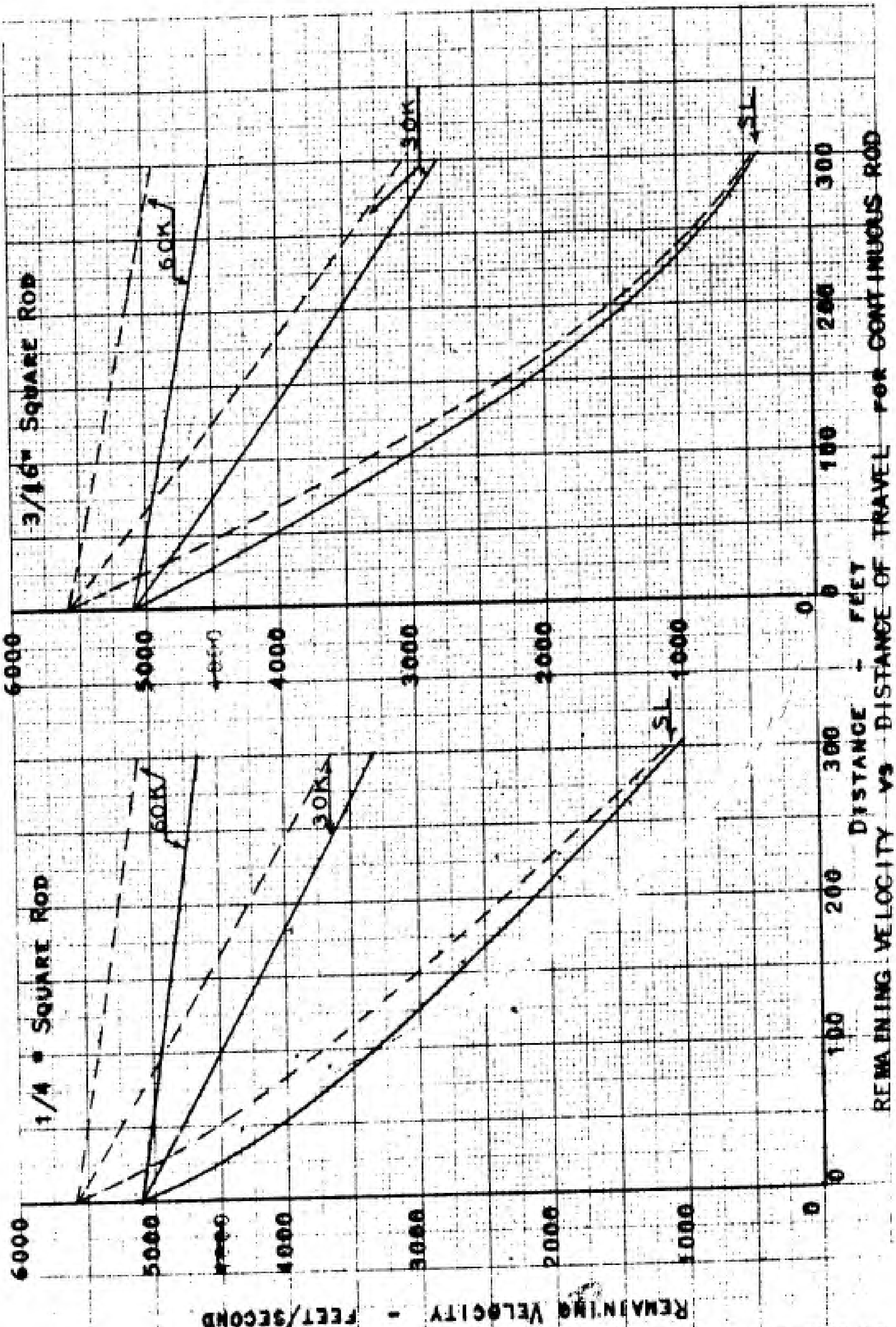
1/4" Square Rod
3/16" Square Rod
60K
30K
SL
6000
5000
4000
3000
2000
1000
0
100
200
300
Remaining Velocity - Feet/Second
Distance - Feet
Remaining Velocity vs Distance of Travel for Continuous Rod

Figure 10

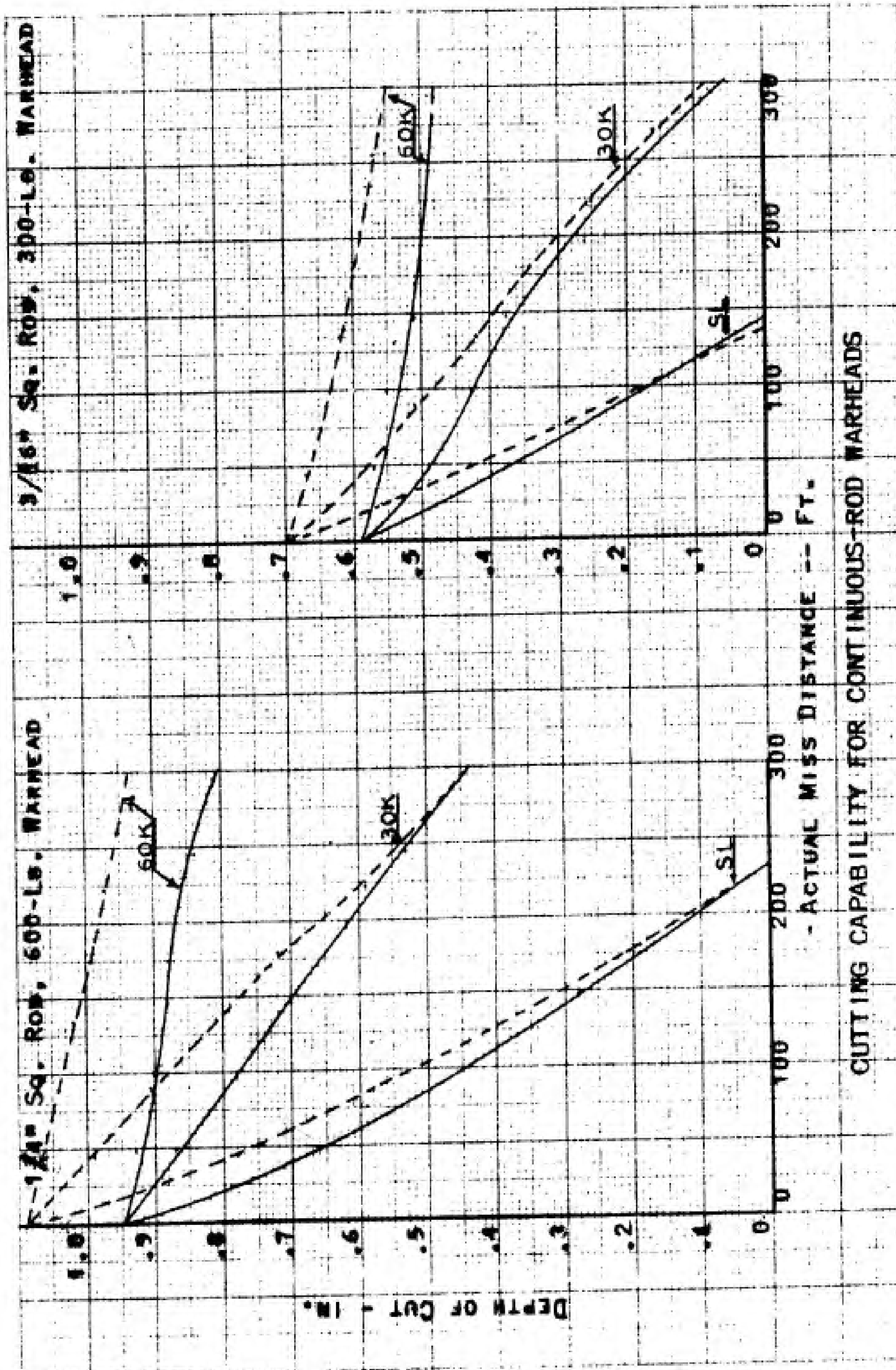

CUTTING CAPABILITY FOR CONTINUOUS-ROD WARHEADS

Figure 11

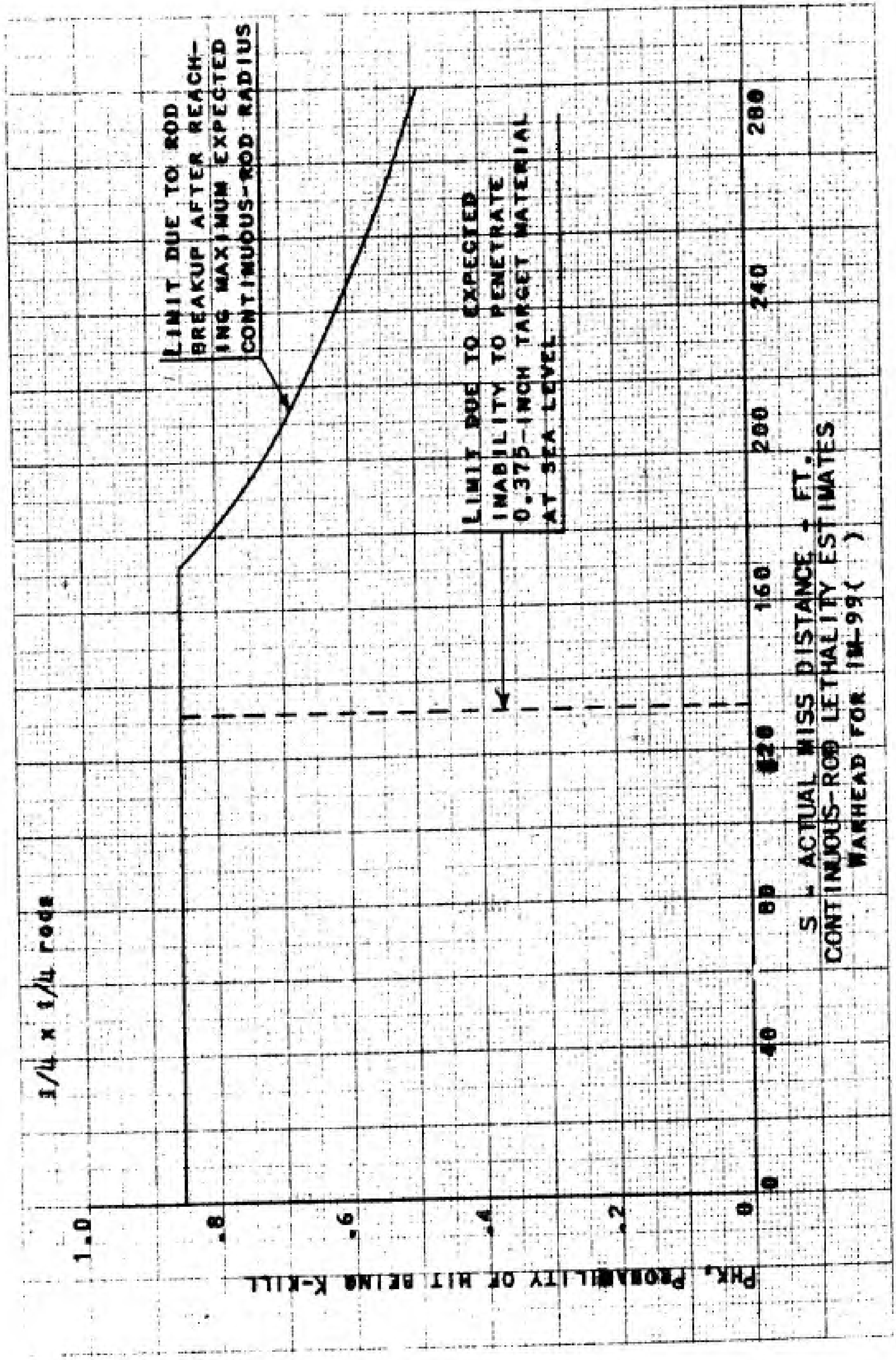

CONTINUOUS-ROD LETHALITY ESTIMATES
WARHEAD FOR IM-99( )

Figure 12

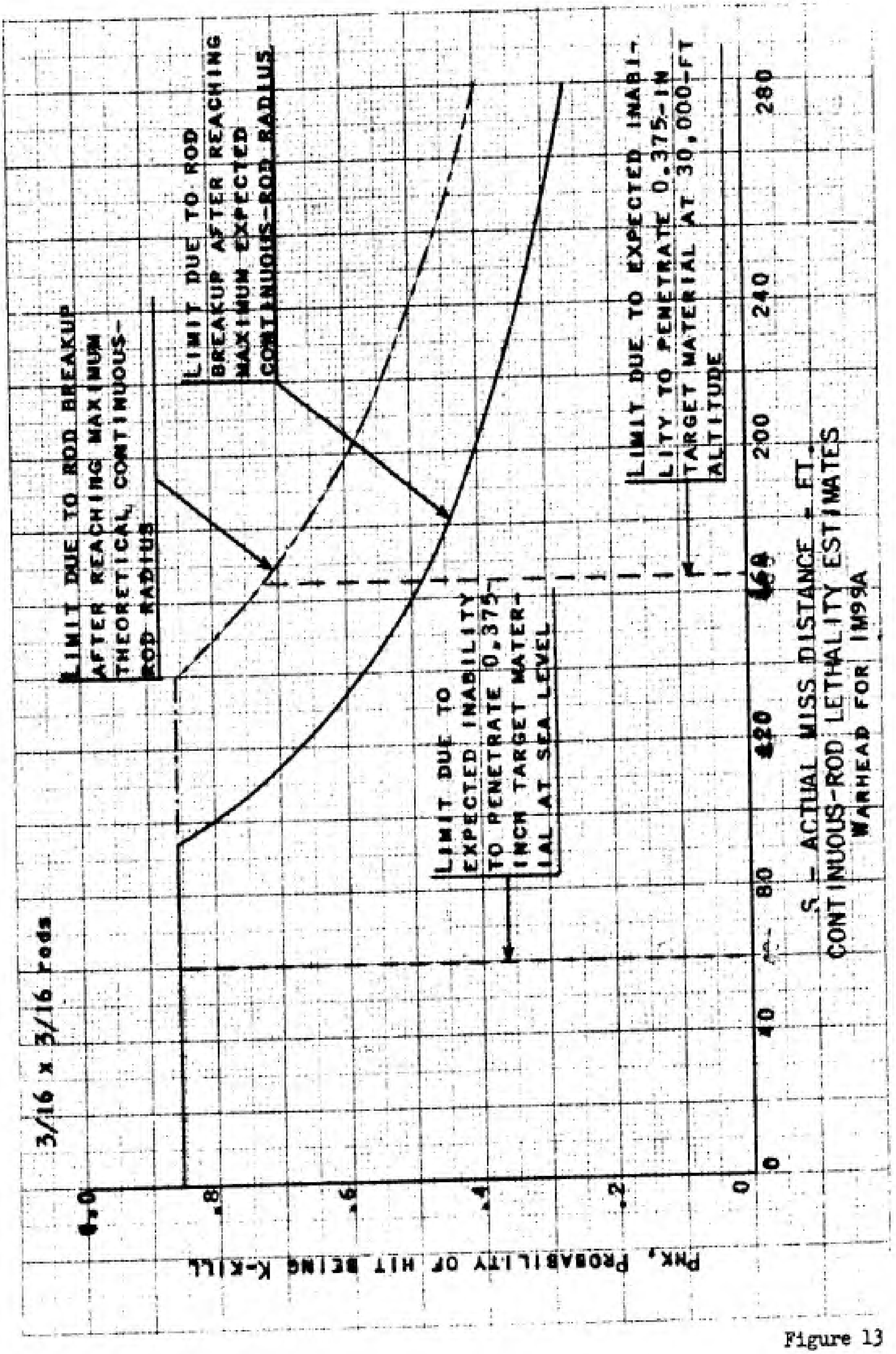
3/16 x 3/16 rods
LIMIT DUE TO ROD BREAKUP AFTER REACHING MAXIMUM THEORETICAL CONTINUOUS-ROD RADIUS
LIMIT DUE TO ROD BREAKUP AFTER REACHING MAXIMUM EXPECTED CONTINUOUS-ROD RADIUS
LIMIT DUE TO EXPECTED INABILITY TO PENETRATE 0.375-IN TARGET MATERIAL AT 30,000-FT ALTITUDE
LIMIT DUE TO EXPECTED INABILITY TO PENETRATE 0.375 INCH TARGET MATERIAL AT SEA LEVEL
PHK, PROBABILITY OF HIT BEING K-KILL
1.0
.8
.6
.4
.2
0
0
40
80
120
160
200
240
280
S - ACTUAL MISS DISTANCE - FT.
CONTINUOUS-ROD LETHALITY ESTIMATES
WARHEAD FOR IM99A

Figure 13

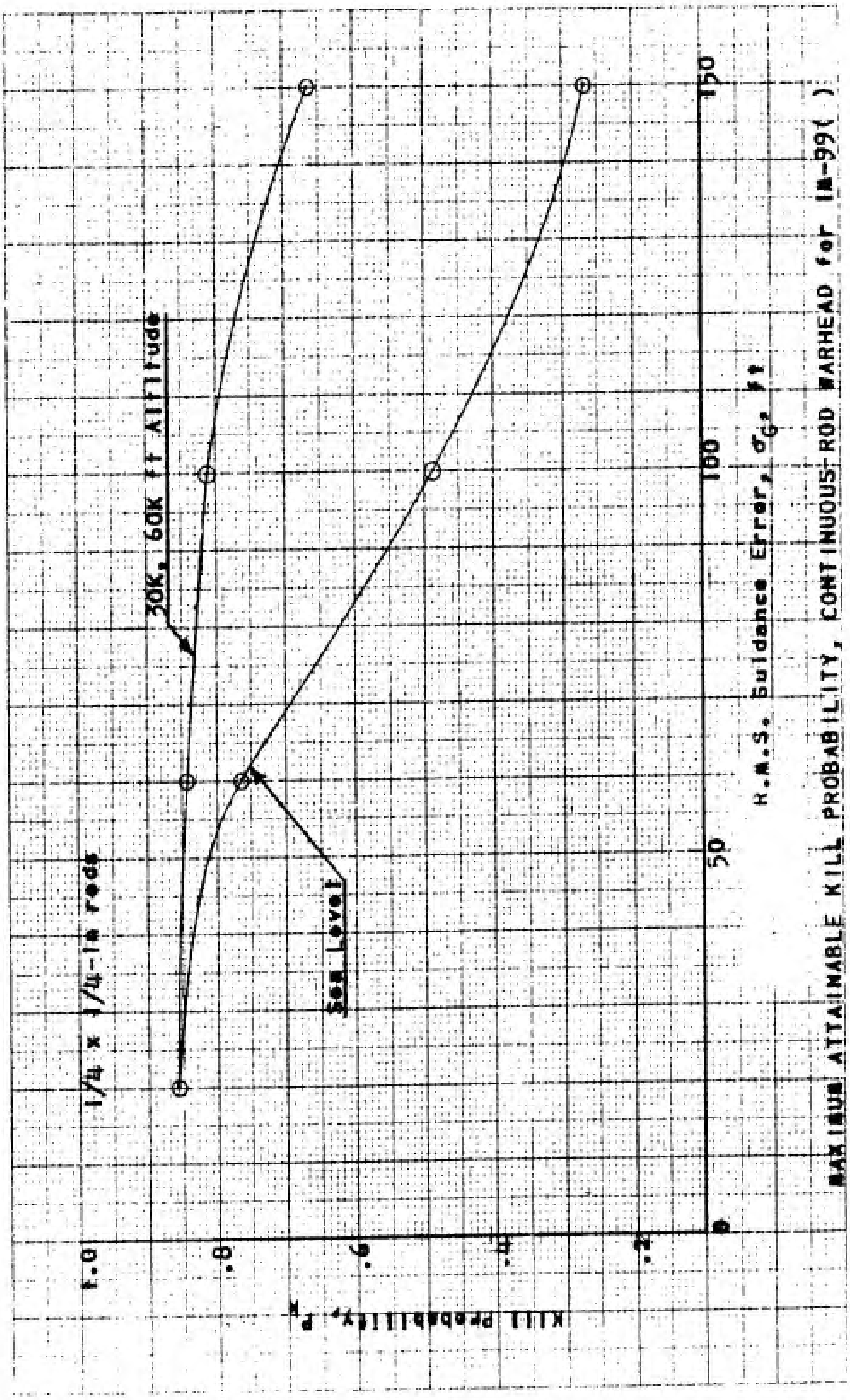
1/4 x 1/4-in rods
30K, 60K ft Altitude
Sea Level
1.0
.8
.6
.4
.2
0
50
100
150
Kill Probability, P_K
R.M.S. Guidance Error, σ_G, ft
MAXIMUM ATTAINABLE KILL PROBABILITY, CONTINUOUS-ROD WARHEAD for (R-99( )

Figure 14

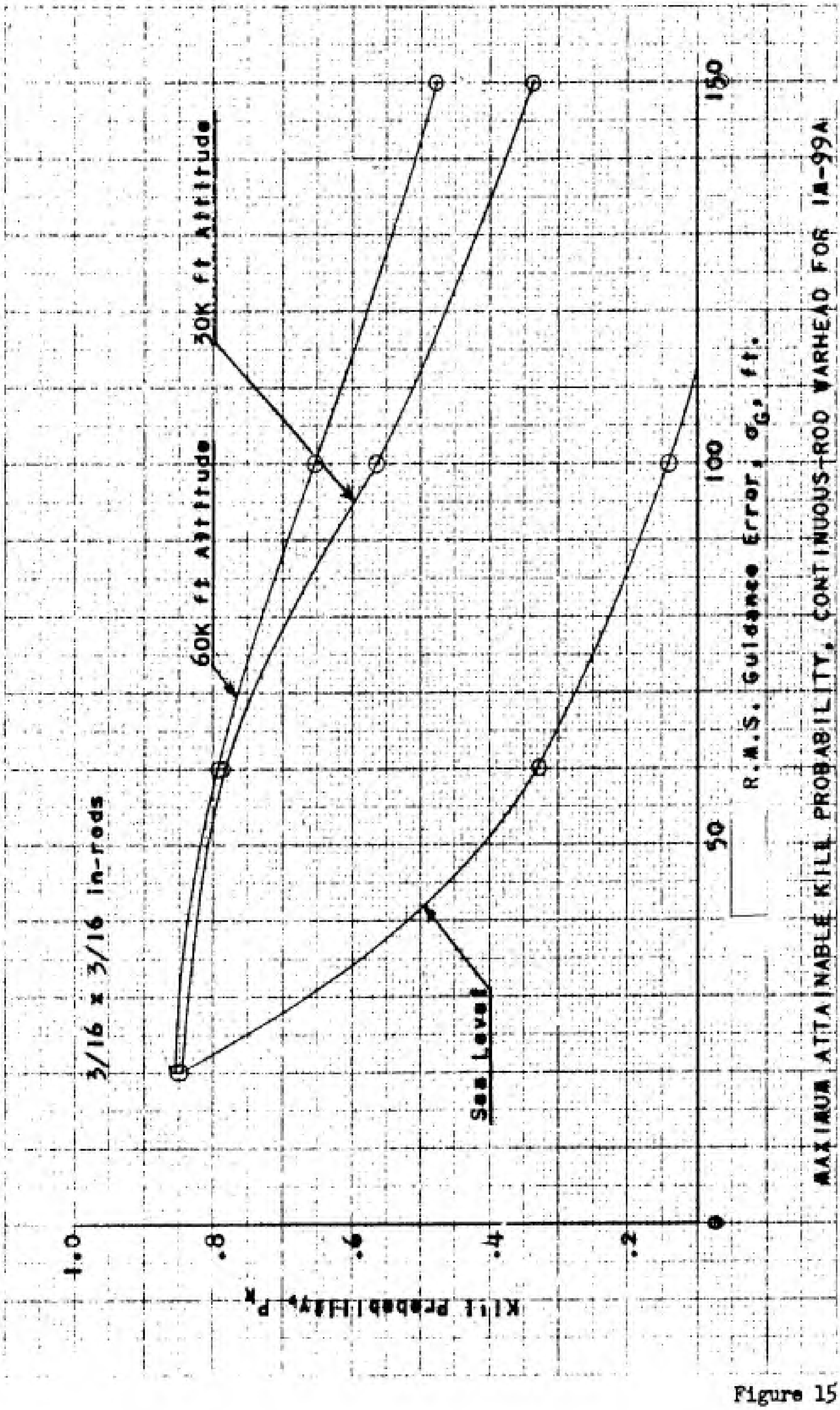
MAXIMUM ATTAINABLE KILL PROBABILITY, CONTINUOUS-ROD WARHEAD FOR IM-99A
R.M.S. Guidance Error, σ_G, ft.
Kill Probability, P_K
3/16 x 3/16 In-rods
30K ft Altitude
60K ft Altitude
Sea Level
0
50
100
150
.2
.4
.6
.8
1.0

Figure 15

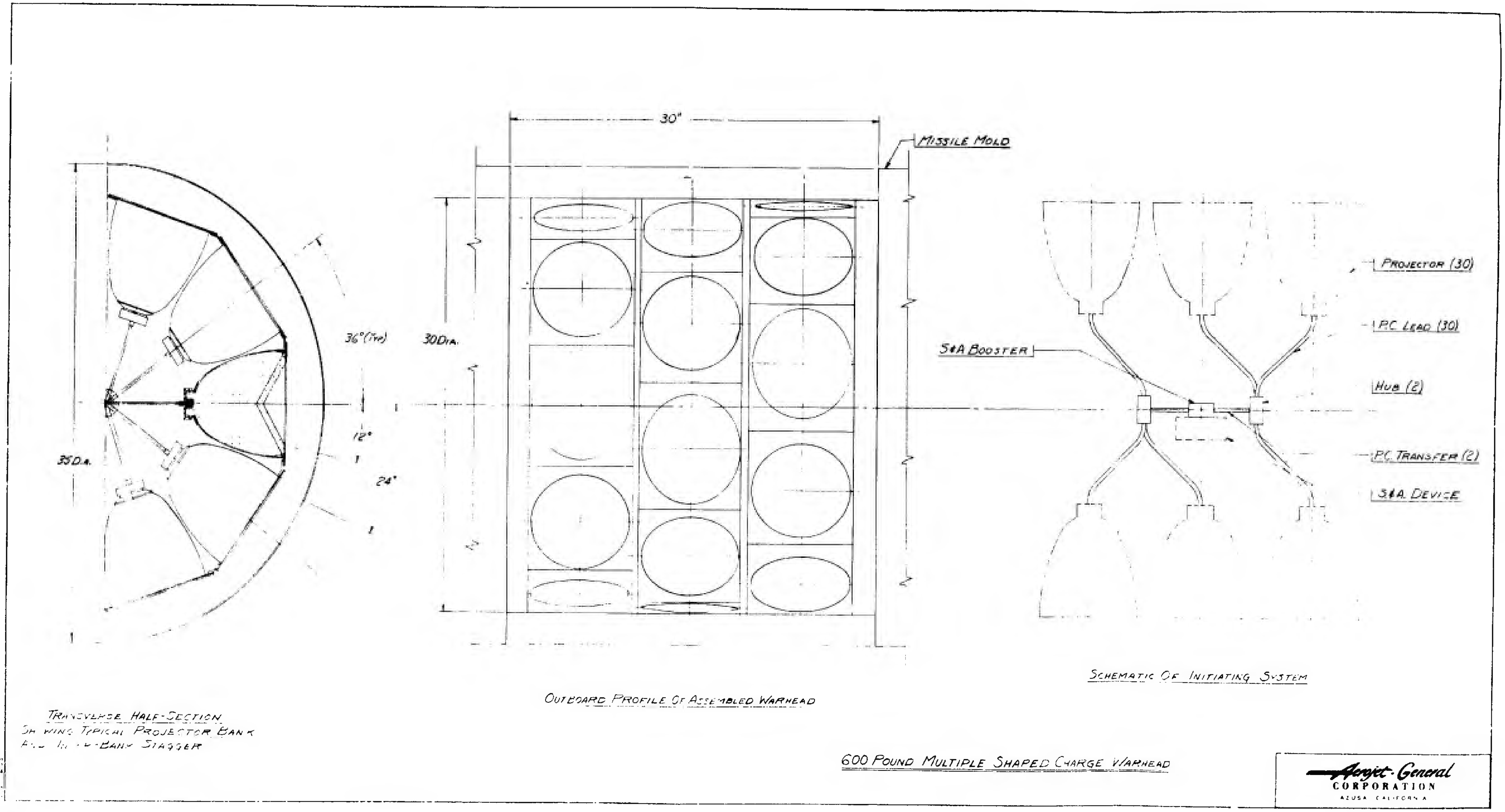
30"
MISSILE MOLD
36° (TYP)
30 DIA.
35 DIA.
12°
24°
PROJECTOR (30)
P.C. LEAD (30)
S&A BOOSTER
HUB (2)
P.C. TRANSFER (2)
S&A DEVICE
SCHEMATIC OF INITIATING SYSTEM
OUTBOARD PROFILE OF ASSEMBLED WARHEAD
TRANSVERSE HALF-SECTION
TYPICAL PROJECTOR BANK
STAGGER
600 POUND MULTIPLE SHAPED CHARGE WARHEAD
Aerojet-General
CORPORATION
AZUSA CALIFORNIA

Figure 16

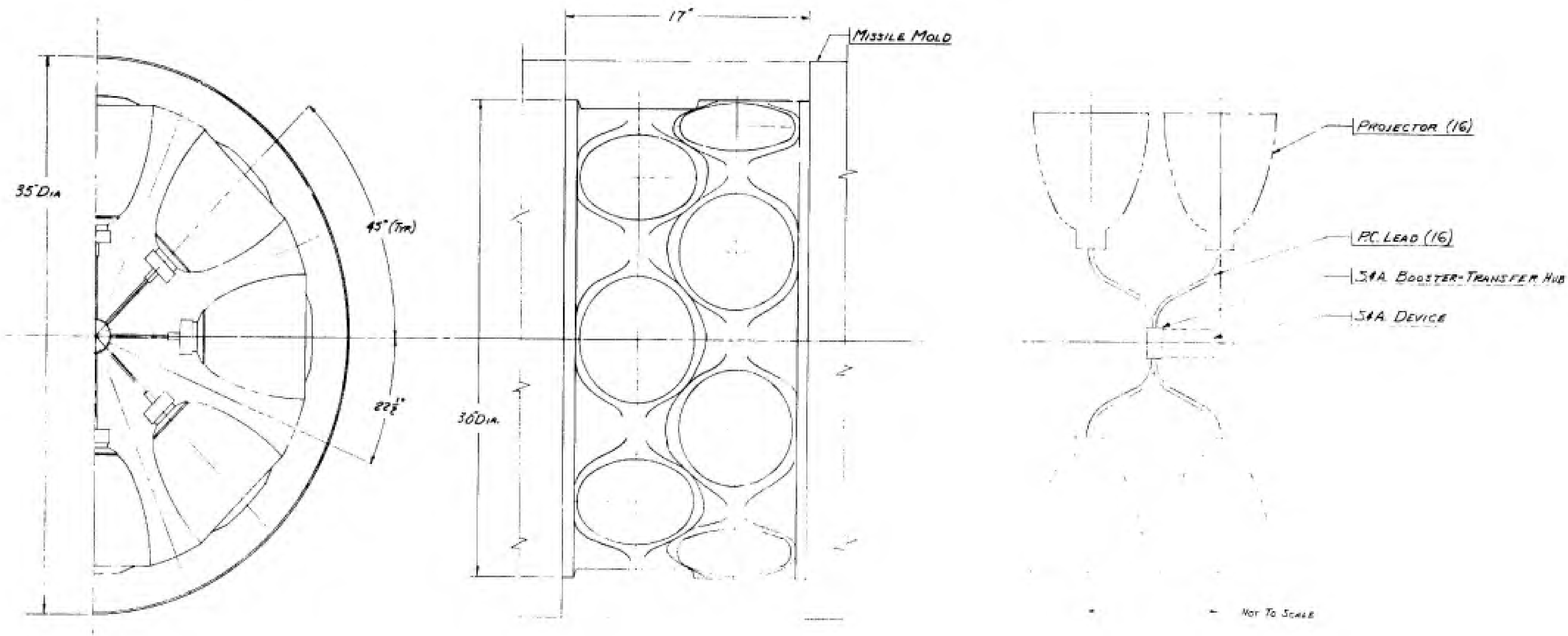

Transverse Half Section Showing Typical Tube Bank and Inter-Bank Stagger

Outboard Profile of Assembled Warhead

Schematic of Initiating System

300 Pound Multiple Shaped Charge Warhead

Aerojet-General Corporation
Azusa, California

Figure 17

REPORT NO. ______ PAGE ______

Aerojet-General

DETAILS

1. CLAMP NUT FOR P.C.
2. CLOSURE & P.C. GLAND
3. TETRYL PELLET
4. BOOSTER CUP
5. NECK
6. CASE
7. HIGH EXPLOSIVE FILLER
8. PLASTIC LUTING
9. RETAINING RINGS
10. CONICAL LINER

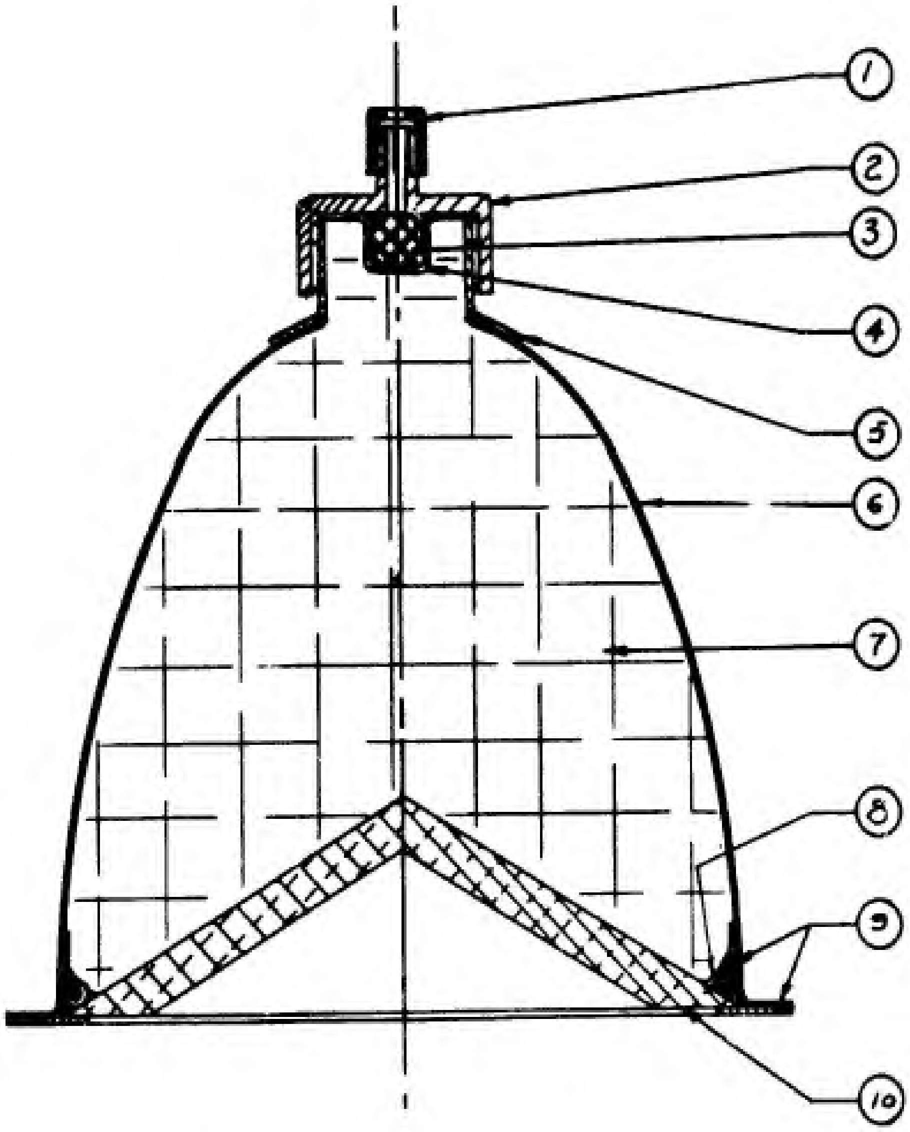

8 INCH DIAMETER SHAPED CHARGE PROJECTOR

WLK 4/8

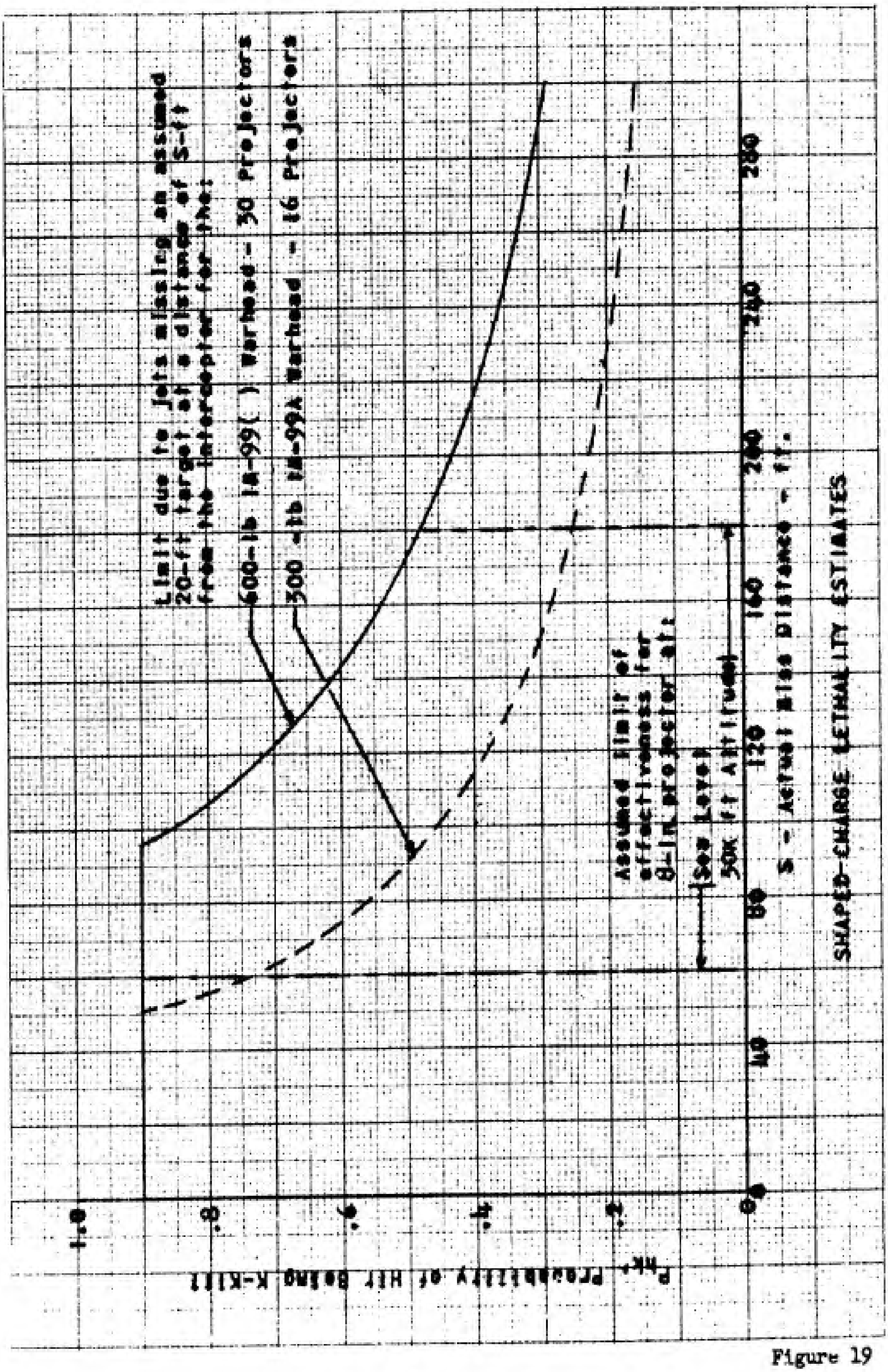
Limit due to Jets missing an assumed 20-ft target at a distance of S-ft from the interceptor
600-lb IM-99( ) Warhead - 30 Projectors
300-lb IM-99A Warhead - 16 Projectors
Assumed limit of effectiveness for 8-in projector at:
Sea Level
50K ft Altitude
S - Actual Miss Distance - ft.
SHAPED-CHARGE LETHALITY ESTIMATES
P_{hk}, Probability of Hit Being K-Kill
0
40
80
120
160
200
240
280
.2
.4
.6
.8
1.0

Figure 19

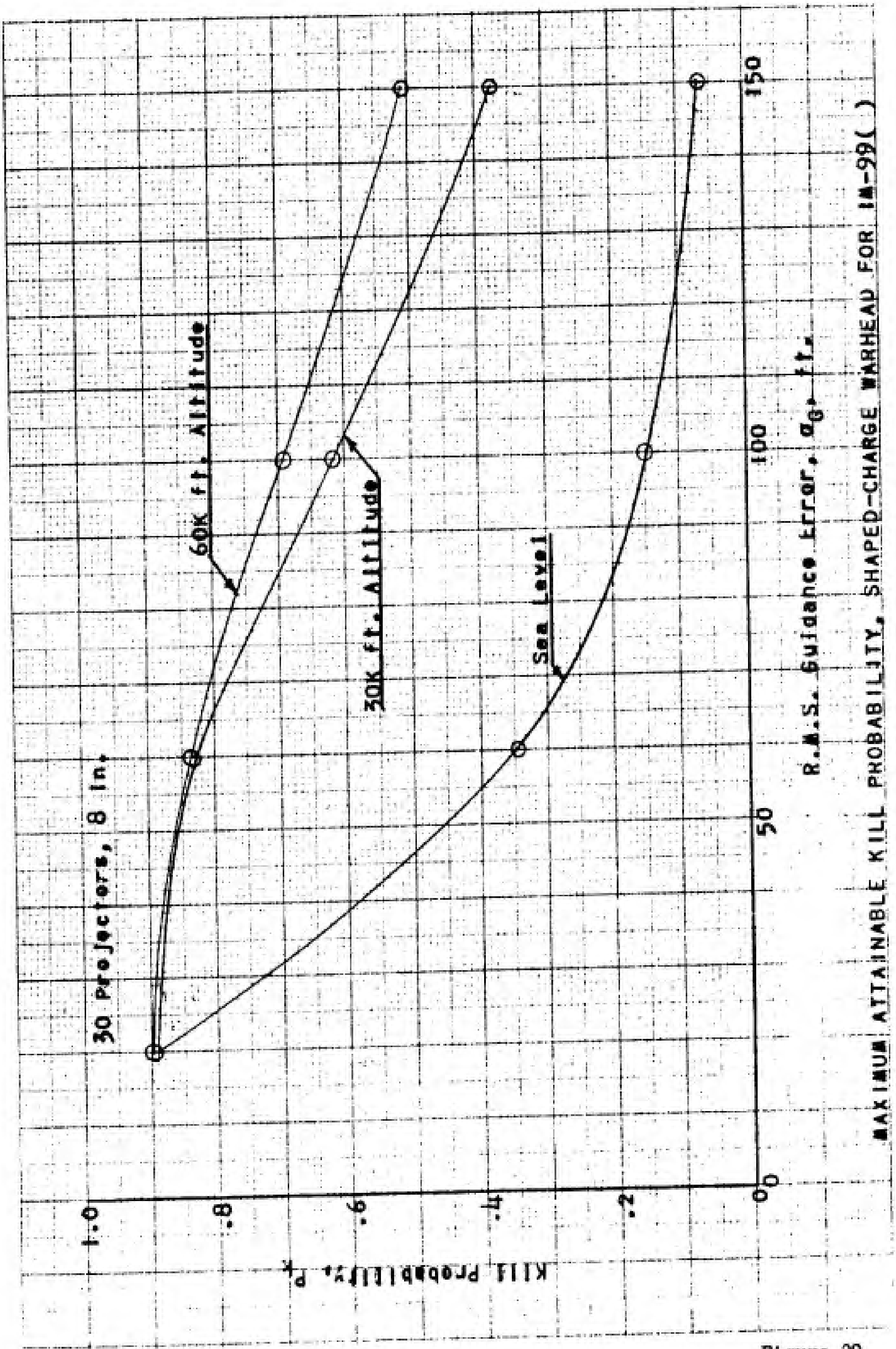

MAXIMUM ATTAINABLE KILL PROBABILITY, SHAPED-CHARGE WARHEAD FOR IM-99( )

Figure 20

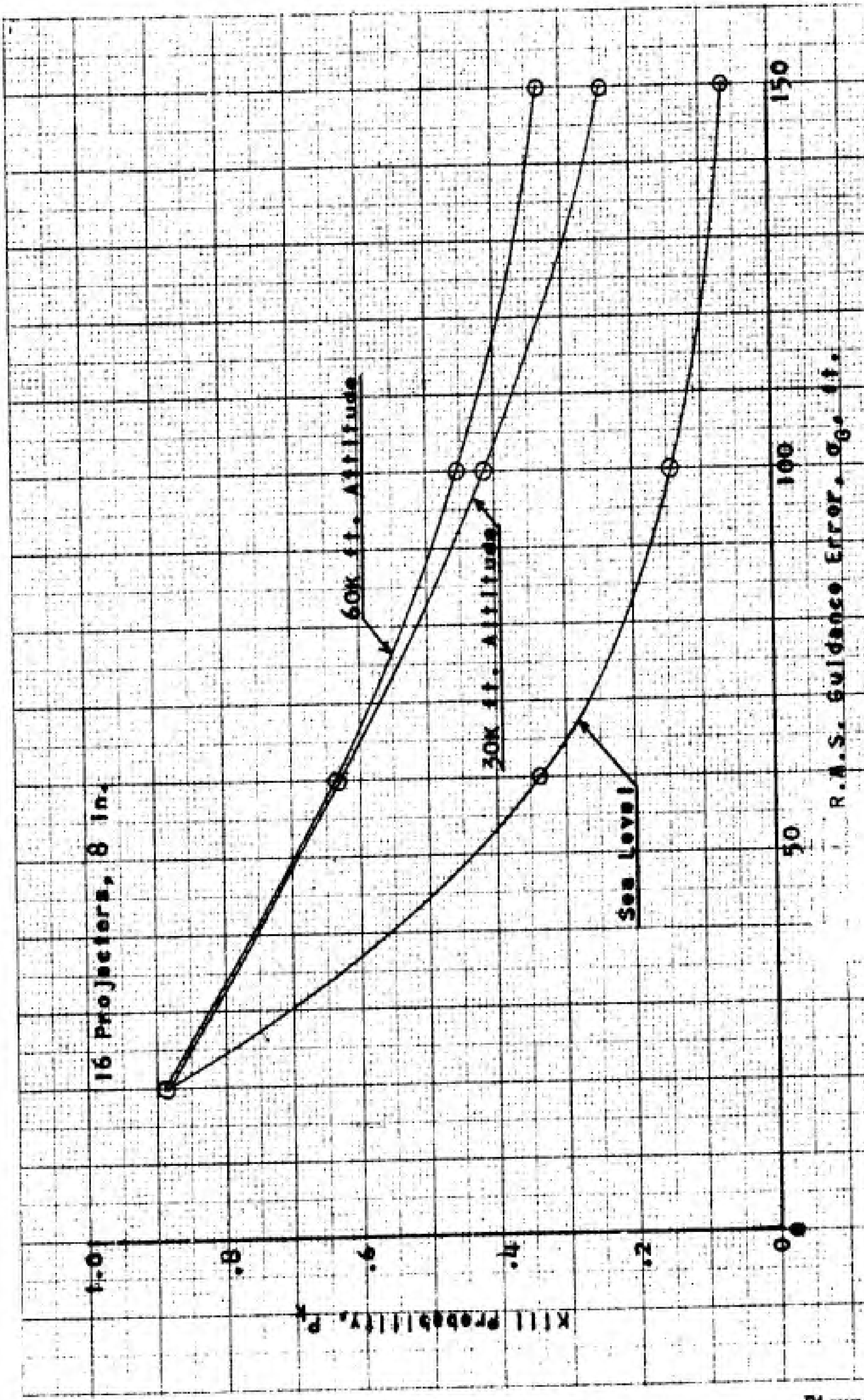

MAXIMUM ATTAINABLE KILL PROBABILITY, SHAPED-CHARGE WARHEAD FOR IA-99A

Figure 21

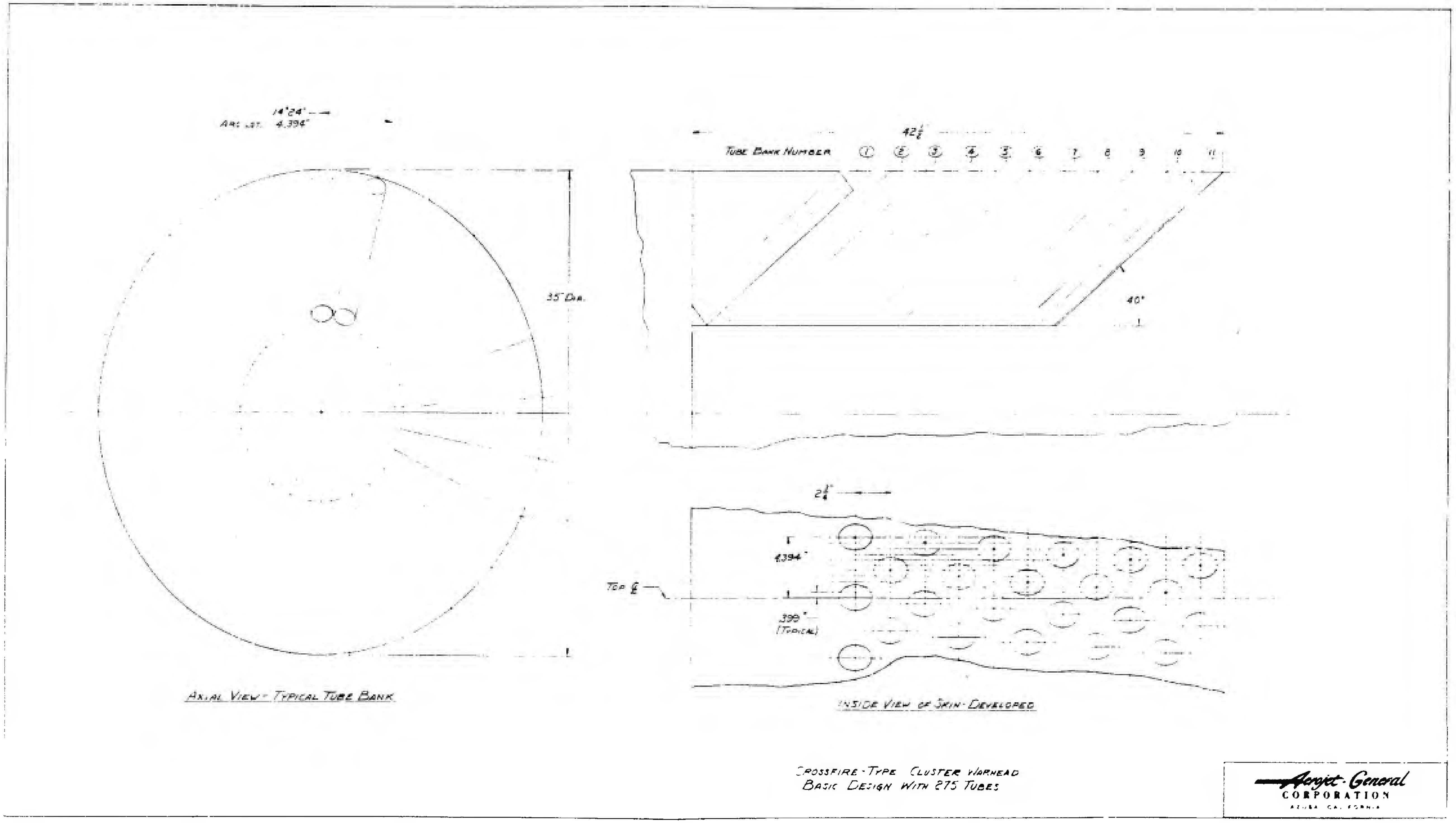
14°24'
ARC LGT. 4.394"
35" DIA.
AXIAL VIEW - TYPICAL TUBE BANK
42½
TUBE BANK NUMBER
1 2 3 4 5 6 7 8 9 10 11
40°
2¼"
4.394"
TOP ℄
.399"
(TYPICAL)
INSIDE VIEW OF SKIN - DEVELOPED
CROSSFIRE - TYPE CLUSTER WARHEAD
BASIC DESIGN WITH 275 TUBES
Aerojet-General
CORPORATION
AZUSA CALIFORNIA

Figure 22

CONFIDENTIAL

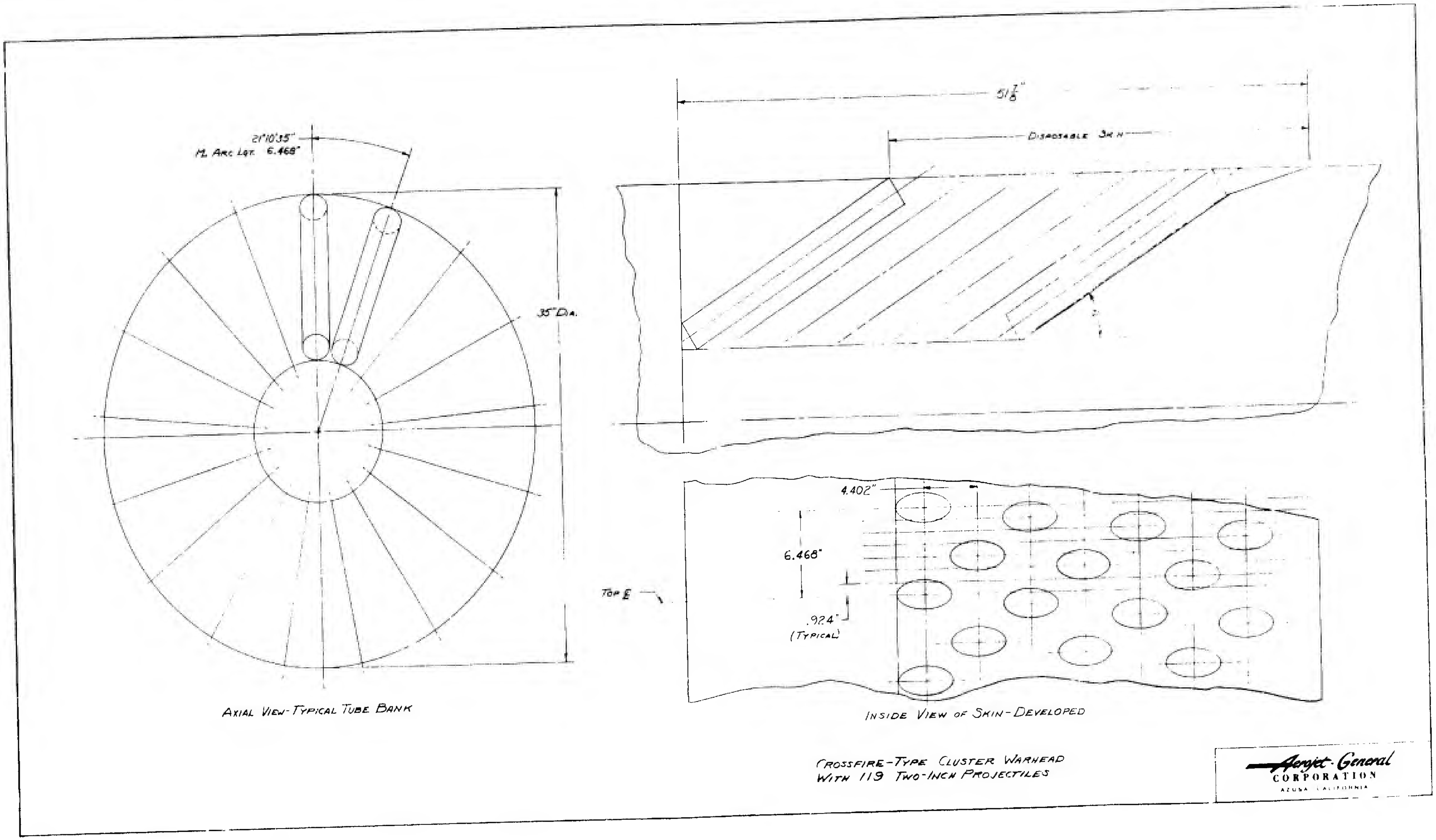

Figure 23

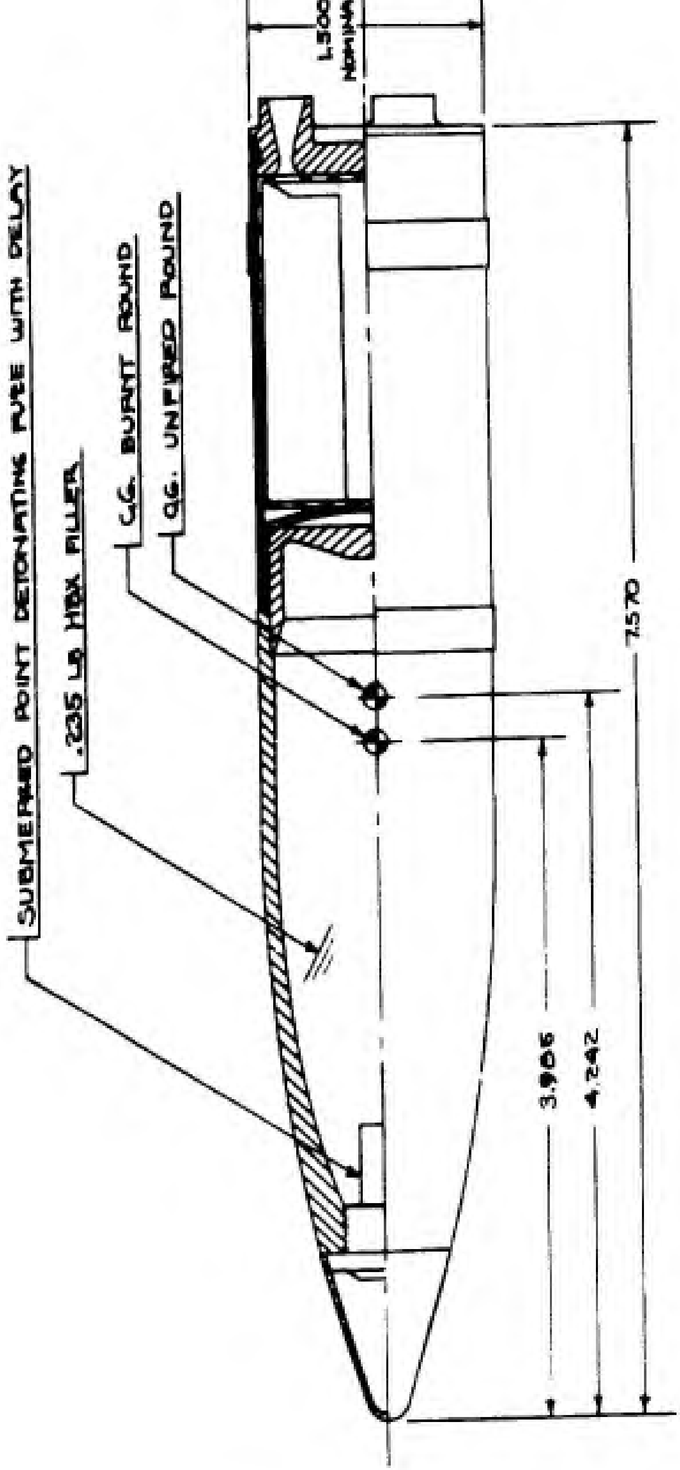

30 MM SSAR CROSSFIRE PROJECTILE

SCALE: FULL SIZE

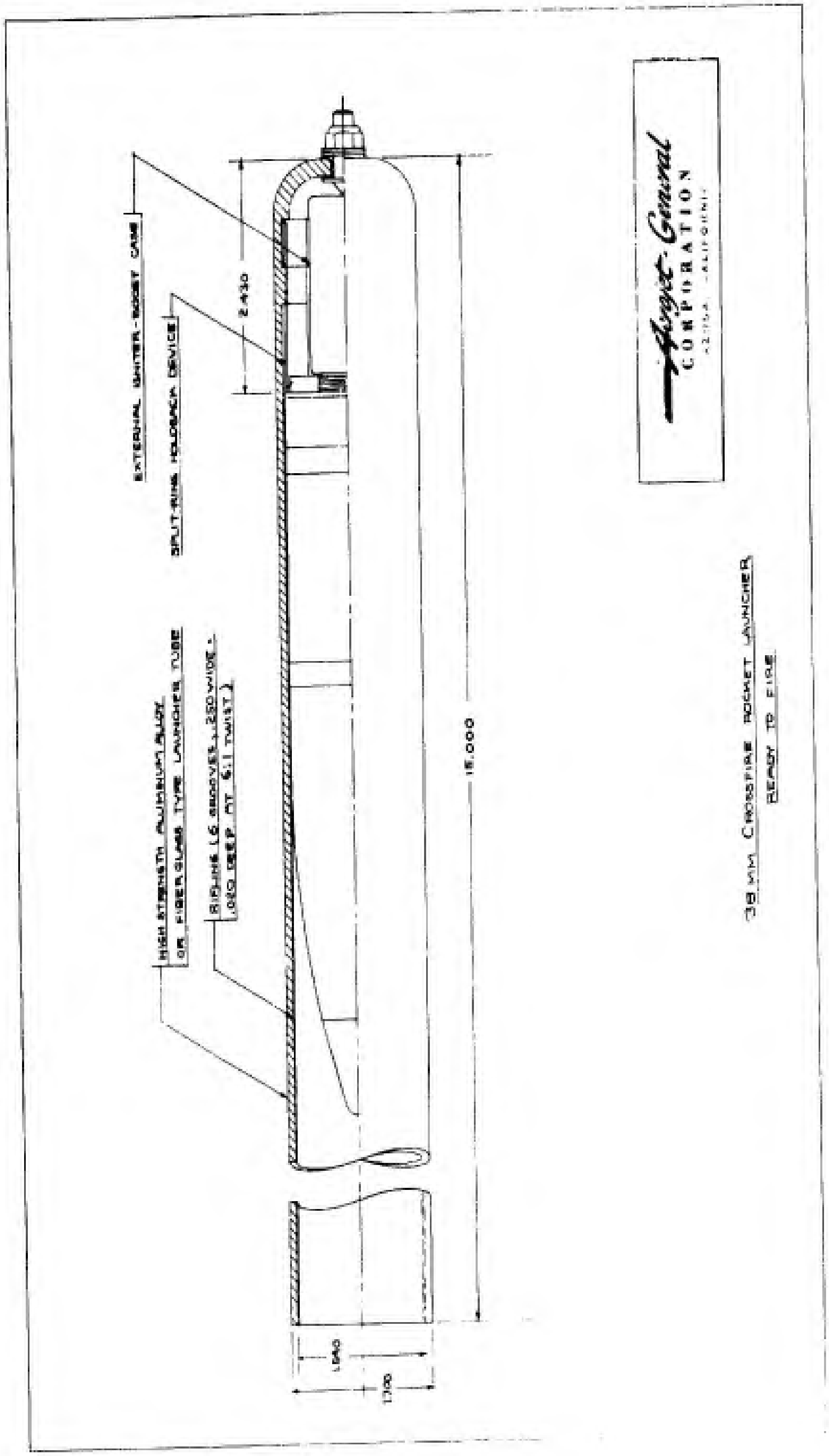
EXTERNAL IGNITER-BOOST CASE
SPLIT-RING HOLDBACK DEVICE
HIGH STRENGTH ALUMINUM ALLOY OR FIBERGLASS TYPE LAUNCHER TUBE
RIFLING (6 GROOVES, .250 WIDE x .020 DEEP AT 6:1 TWIST)
2.430
15.000
Aerojet-General CORPORATION
38 MM CROSSFIRE ROCKET LAUNCHER
READY TO FIRE

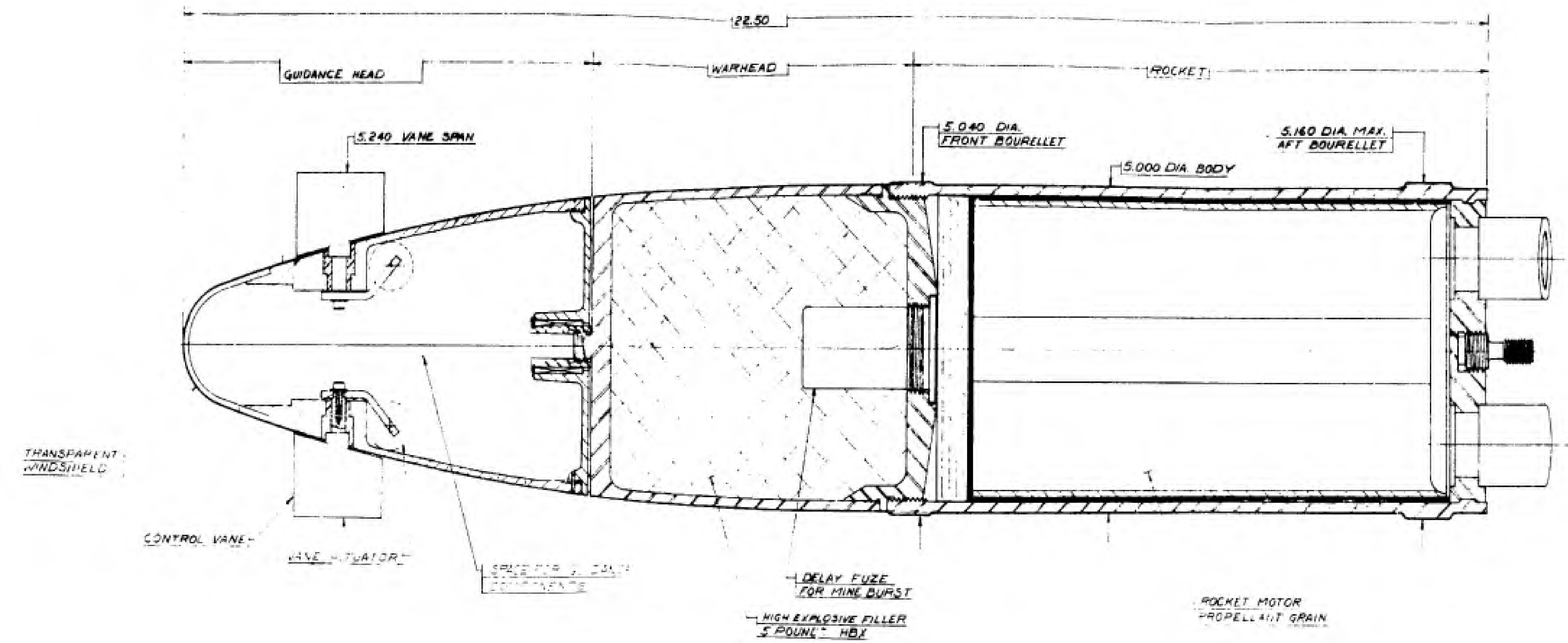

SPINNER PROJECTILE - AERIAL TORPEDO MK I

AEROJET – GENERAL CORPORATION AZUSA, CALIFORNIA

Figure 26

CONFIDENTIAL

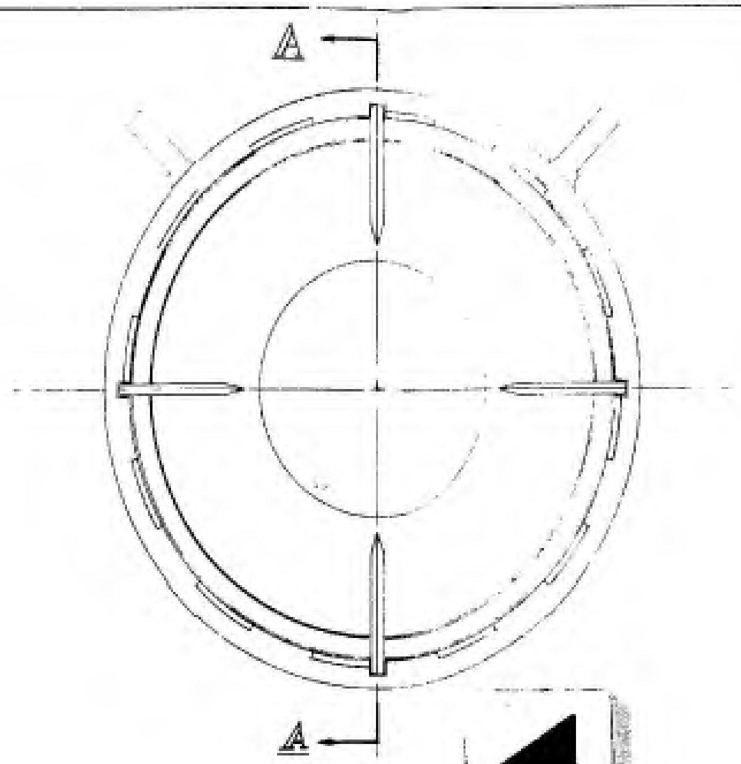

1

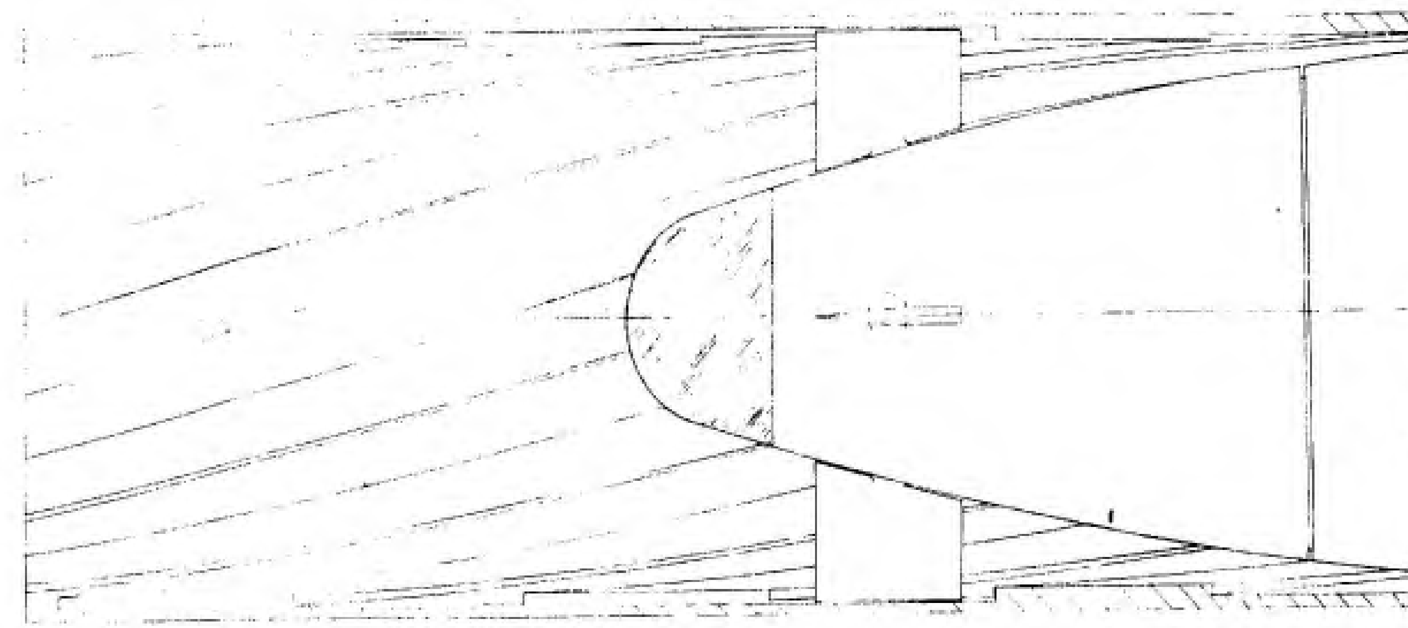

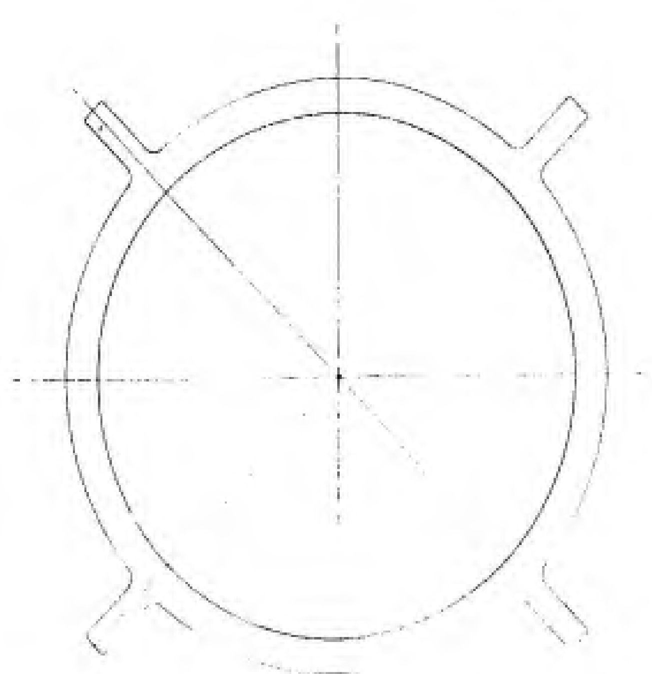

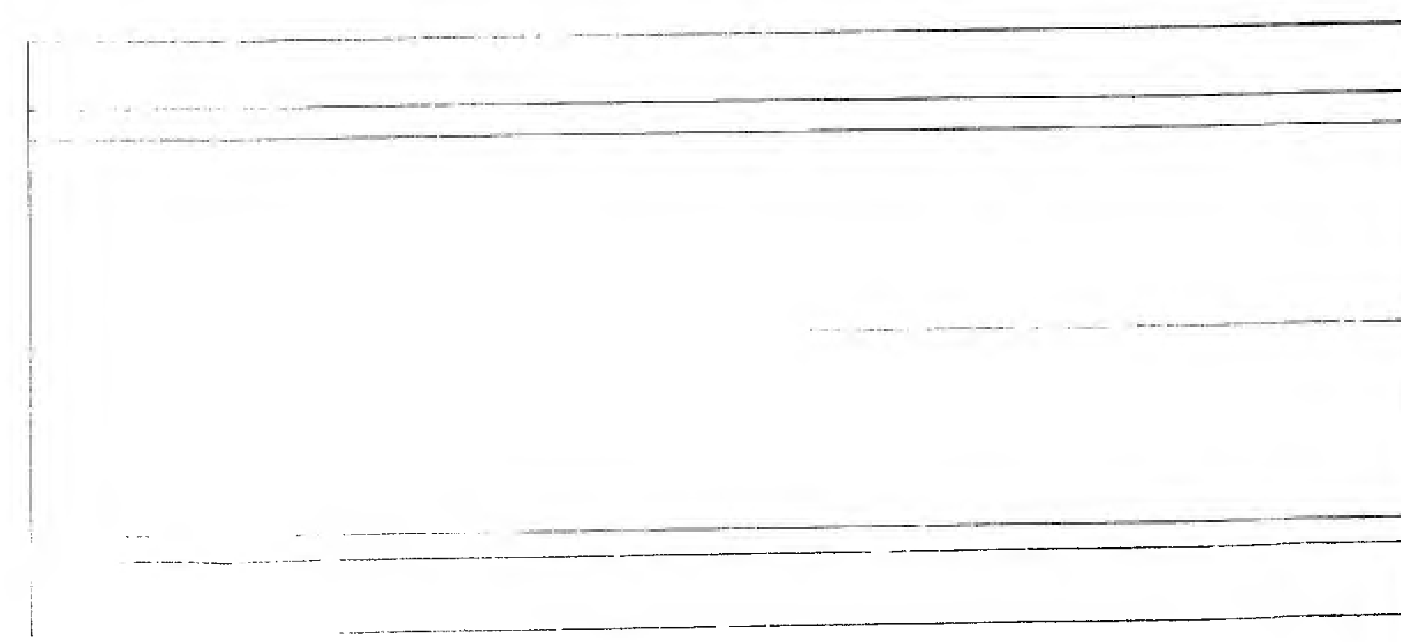

Basic Extrusion Shape (Shown Before Machining)

Launching Tube For SPAT

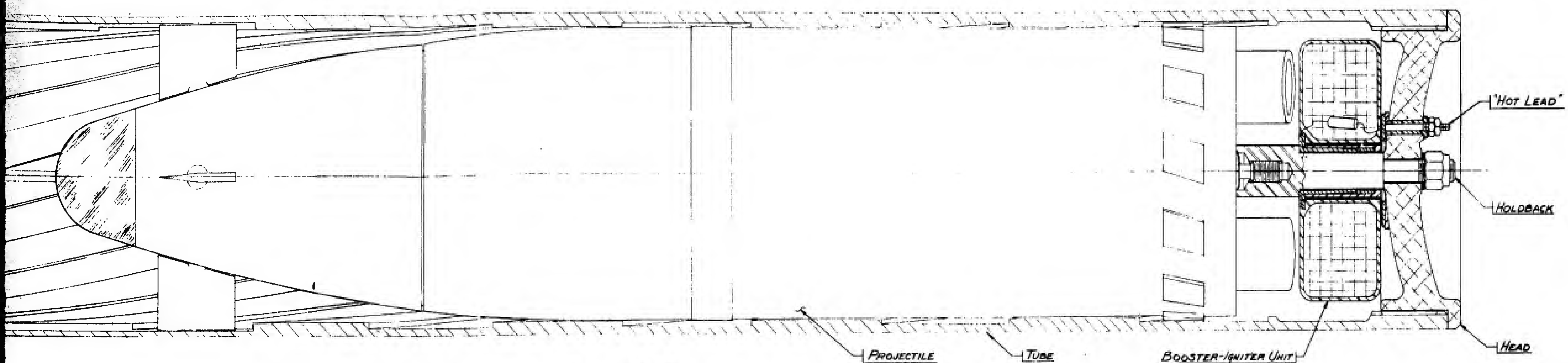

SECTION A-A

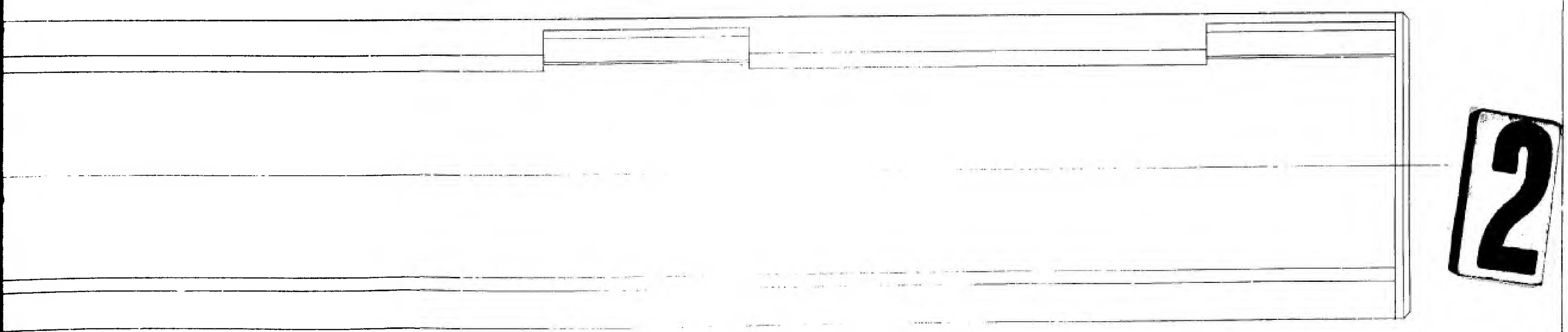

LAUNCHING TUBE FOR SPAT

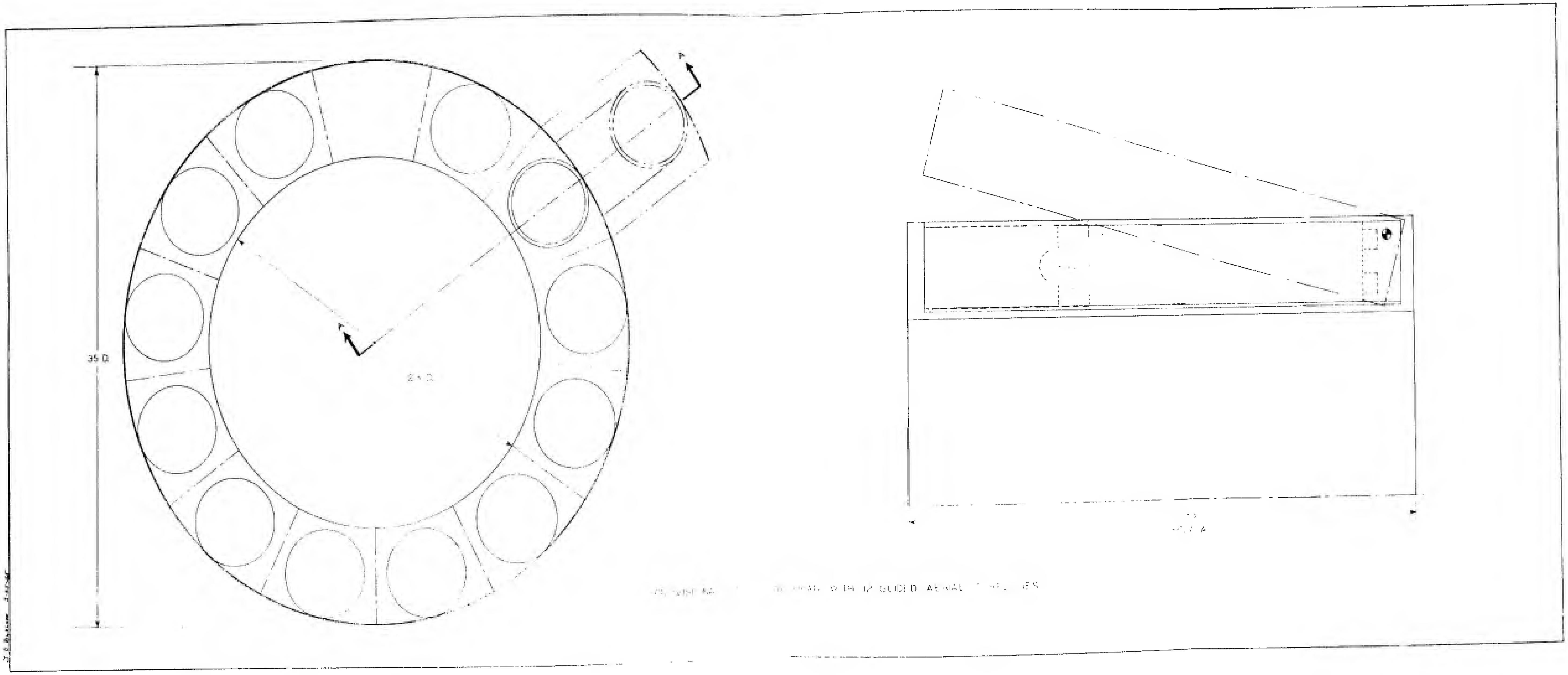

Figure 28

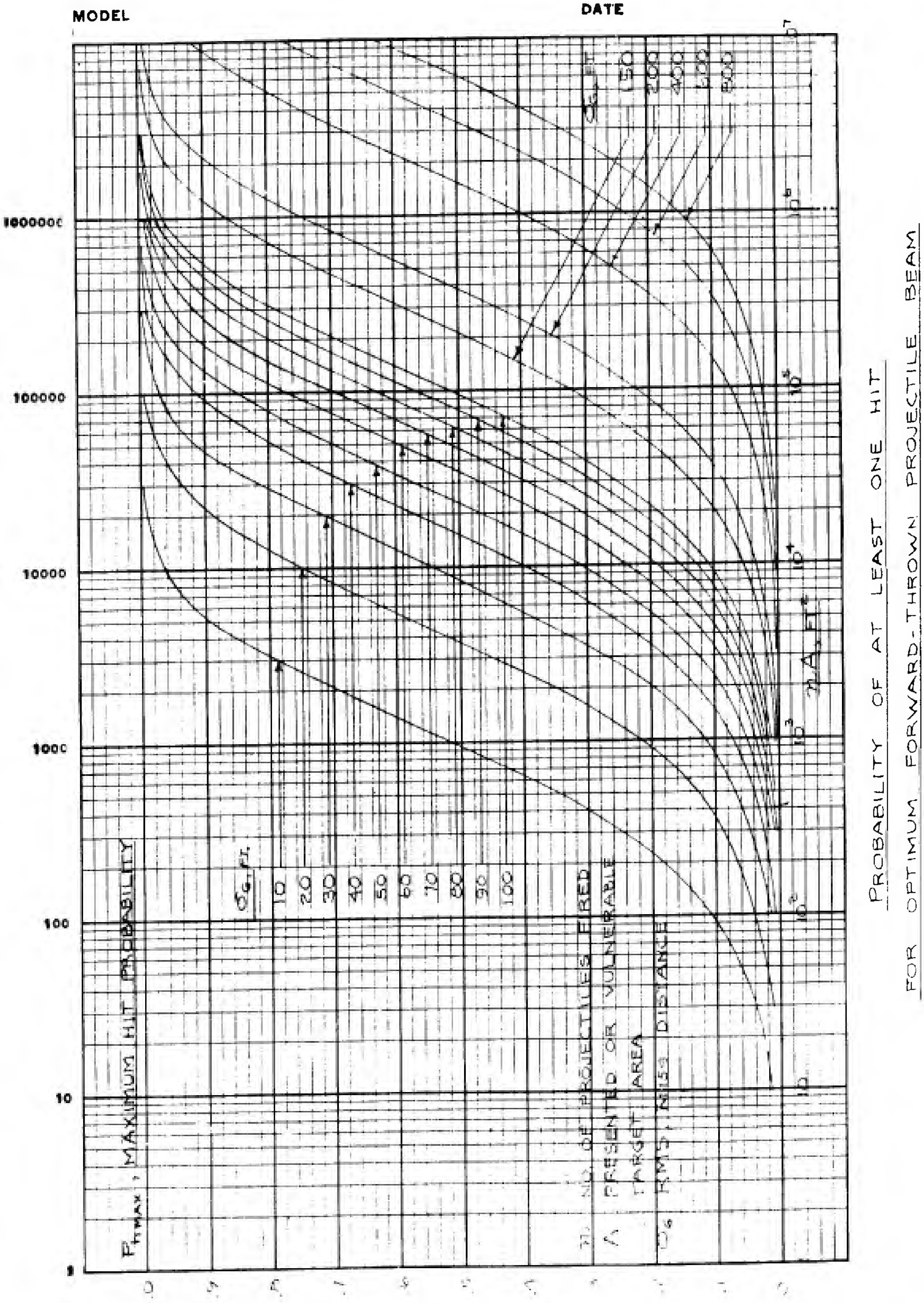
MODEL
DATE
1000000
100000
10000
1000
100
10
1
σ_G, FT.
10
20
30
40
50
60
70
80
90
100
σ_G FT
150
200
400
600
800
$P_{H_{MAX}}$, MAXIMUM HIT PROBABILITY
n NO. OF PROJECTILES FIRED
A PRESENTED OR VULNERABLE TARGET AREA
σ_G R.M.S. MISS DISTANCE
n A, FT²
10^7
10^6
10^5
10^4
10^3
10^2
10
PROBABILITY OF AT LEAST ONE HIT
FOR OPTIMUM FORWARD-THROWN PROJECTILE BEAM

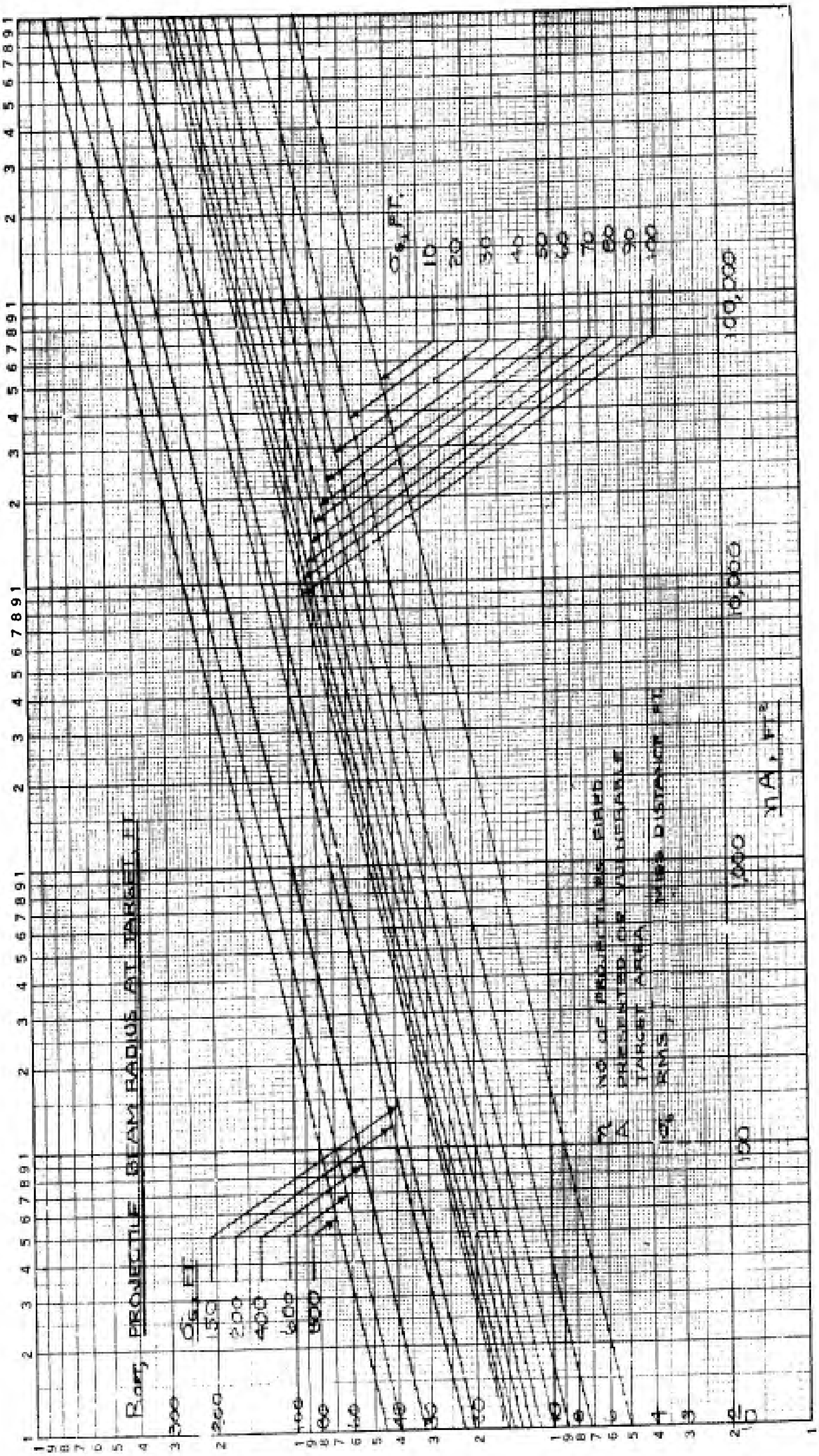

RADIUS OF UNIFORM-DENSITY PROJECTILE BEAM AT TARGET FOR OPTIMUM FORWARD-THROWN PROJECTILE BEAM

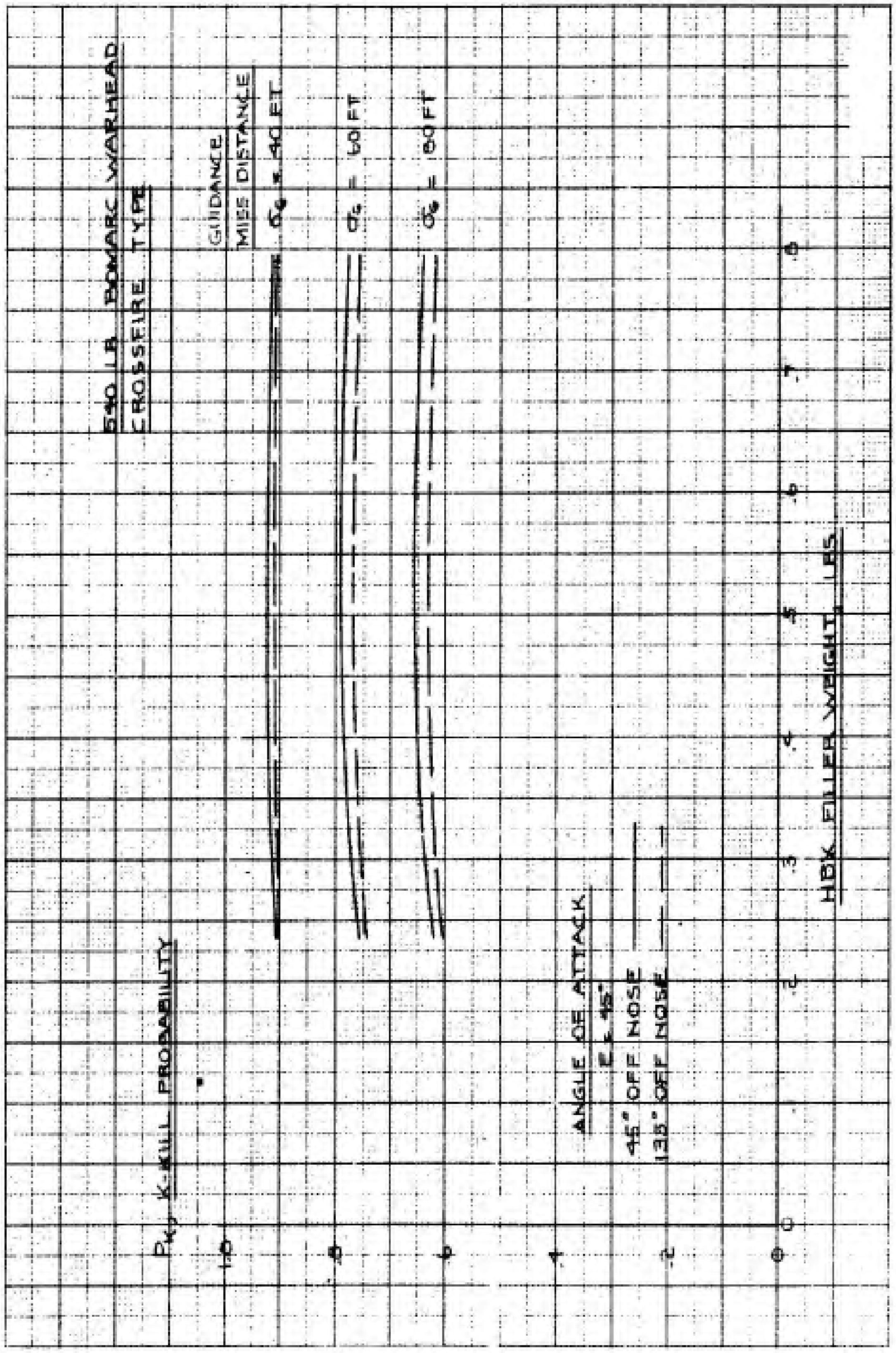

EFFECT OF CROSSFIRE ROUND HE LOADING ON MAXIMUM ATTAINABLE K-KILL PROBABILITY OF SOVIET TYPE 37 BOMBER AT 30,000 FT ALTITUDE

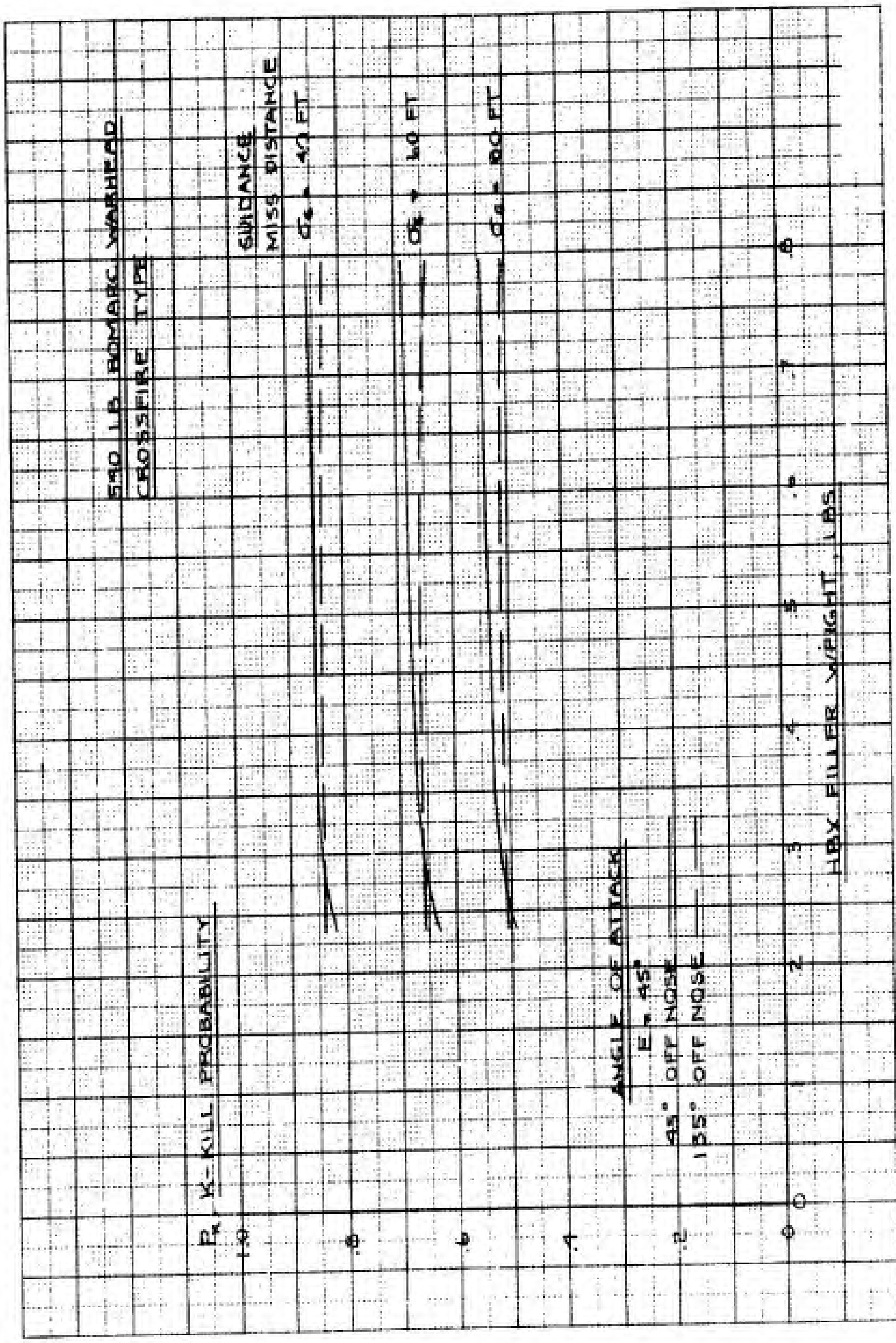

EFFECT OF CROSSFIRE ROUND HE LOADING ON MAXIMUM ATTAINABLE
K-KILL PROBABILITY ON SOVIET TYPE 37 BOMBER AT 60,000 FT. ALTITUDE

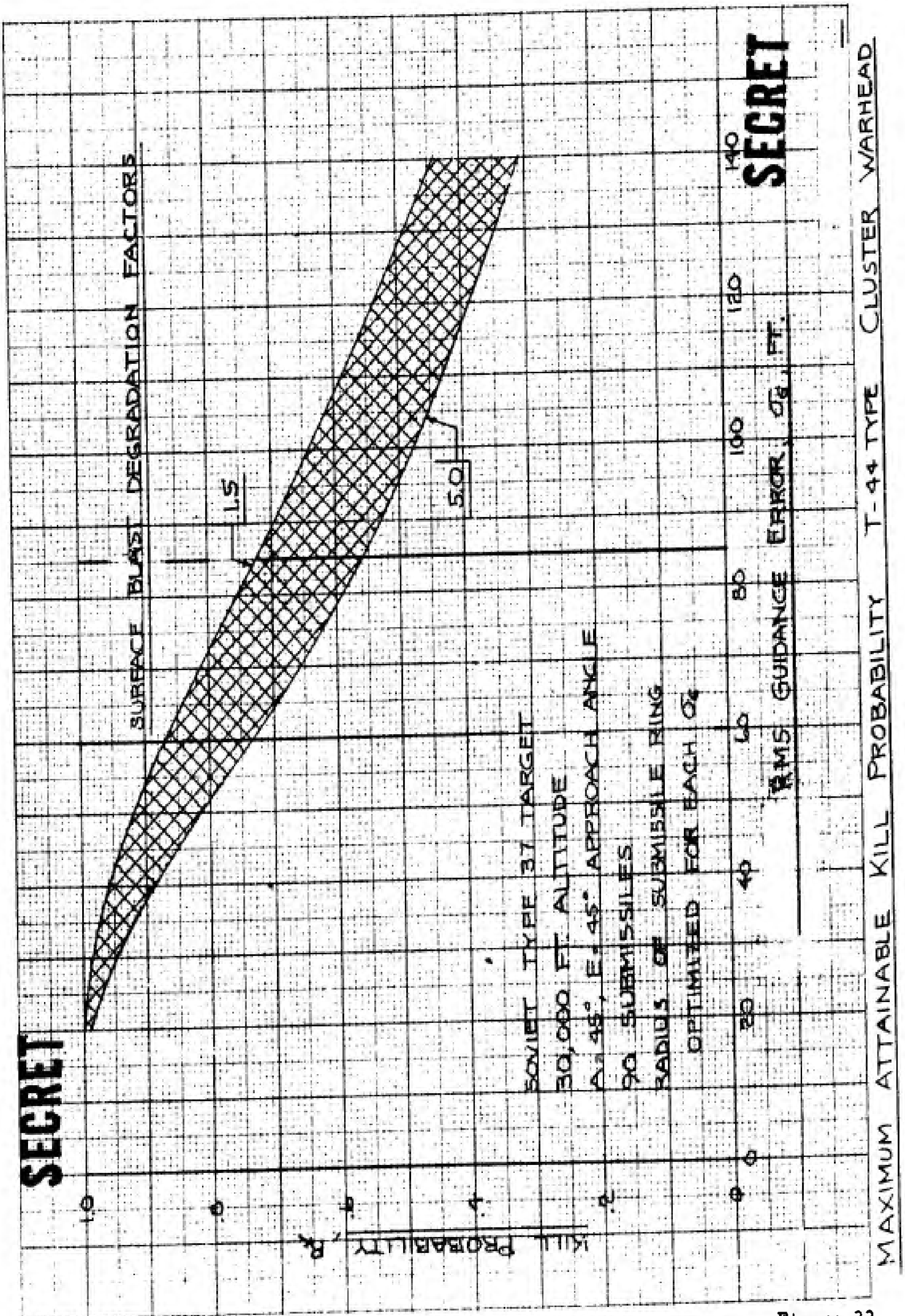
SECRET
MAXIMUM ATTAINABLE KILL PROBABILITY T-44 TYPE CLUSTER WARHEAD
SURFACE BLAST DEGRADATION FACTORS
1.5
5.0
SOVIET TYPE 37 TARGET
30,000 FT ALTITUDE
A = 45°, E = 45° APPROACH ANGLE
90 SUBMISSILES
RADIUS OF SUBMISSILE RING
OPTIMIZED FOR EACH σG
RMS GUIDANCE ERROR, σG, FT.
0
20
40
60
80
100
120
140
KILL PROBABILITY, PK
0
.2
.4
.6
.8
1.0
SECRET

Figure 33

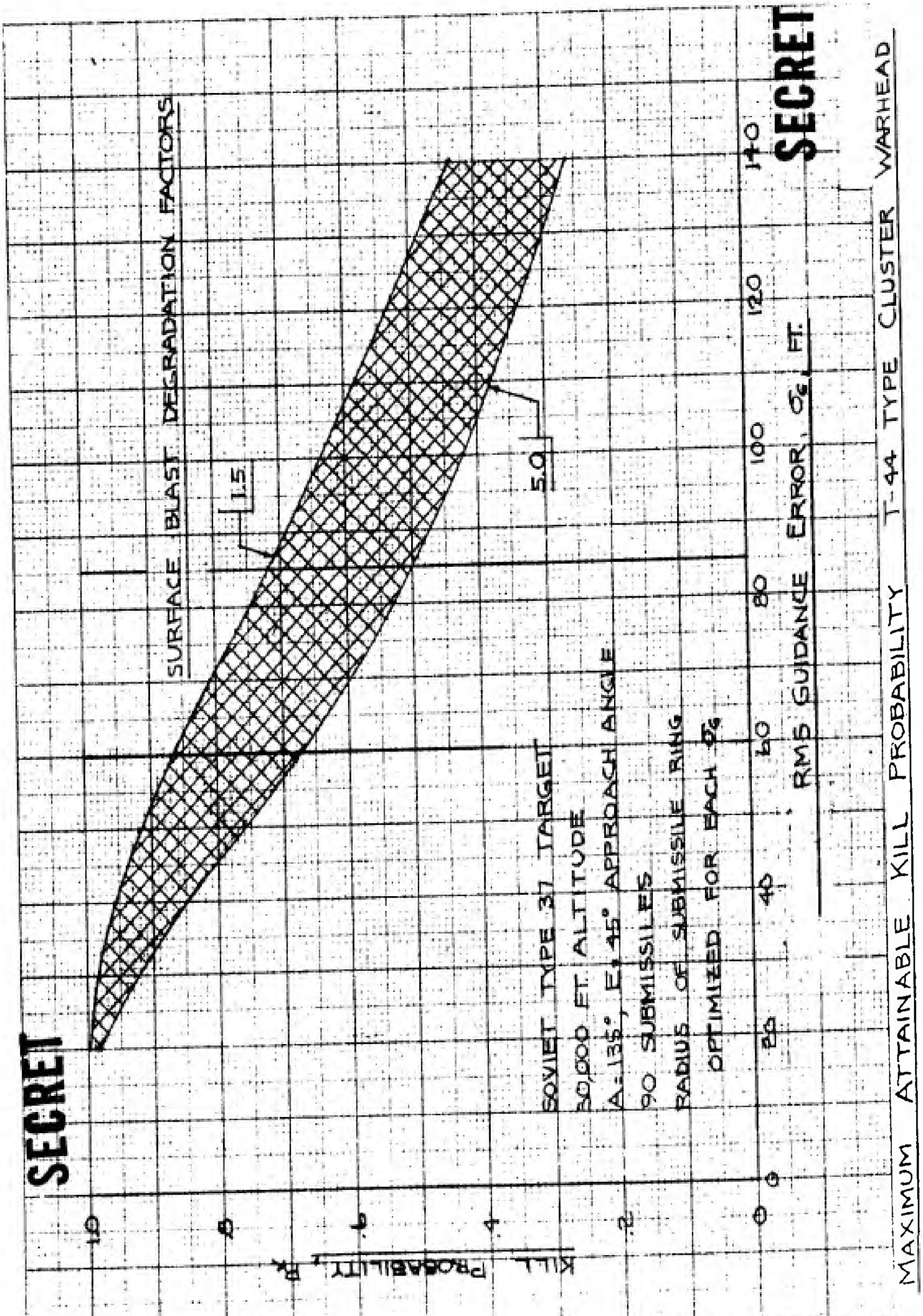
SECRET
SURFACE BLAST DEGRADATION FACTORS
1.5
5.0
SOVIET TYPE 37 TARGET
30,000 FT. ALTITUDE
A: 135°, E: 45° APPROACH ANGLE
90 SUBMISSILES
RADIUS OF SUBMISSILE RING
OPTIMIZED FOR EACH σG
KILL PROBABILITY, PK
1.0
.8
.6
.4
.2
0
0
20
40
60
80
100
120
140
RMS GUIDANCE ERROR, σG, FT.
MAXIMUM ATTAINABLE KILL PROBABILITY T-44 TYPE CLUSTER WARHEAD
SECRET

Figure 34

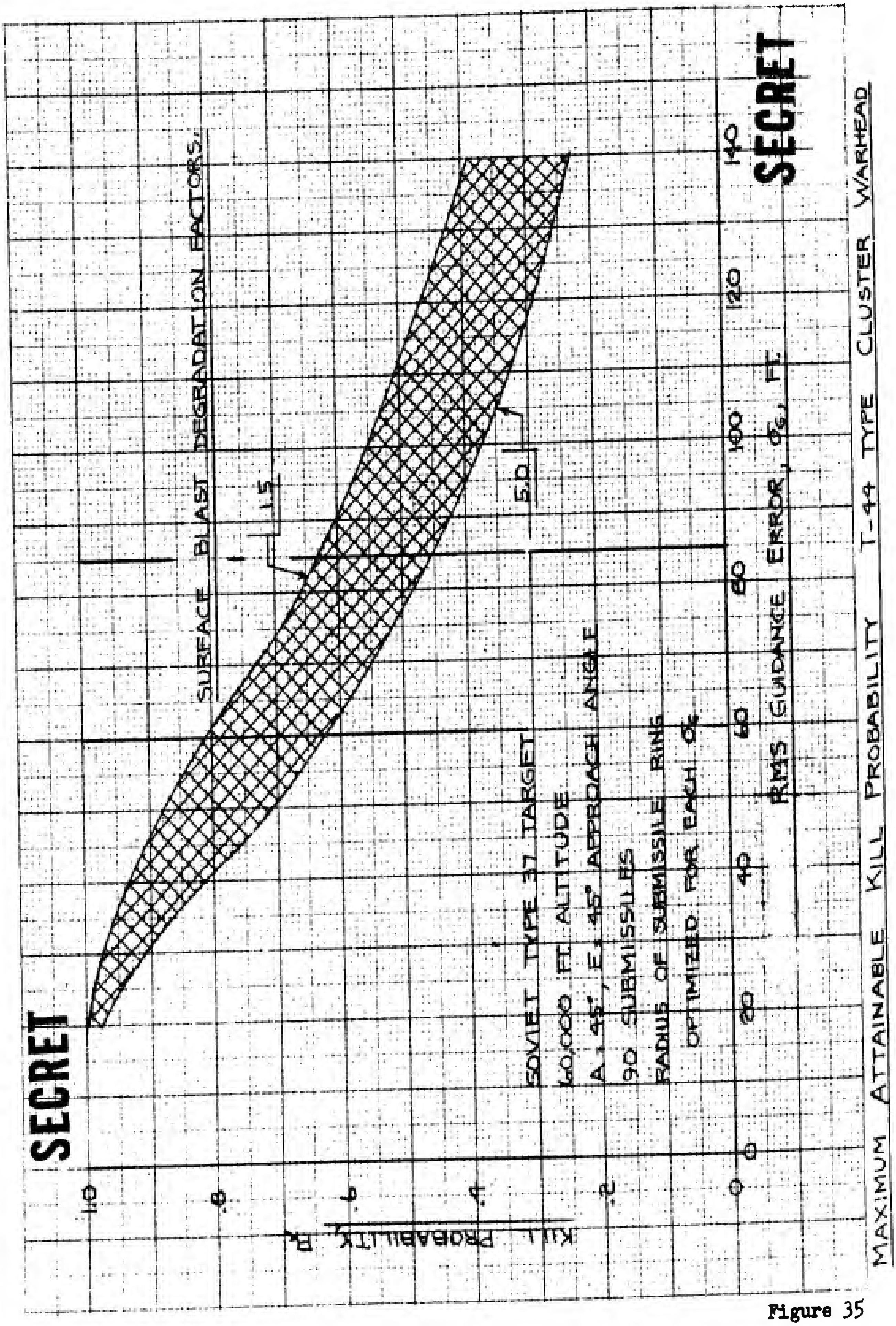
SECRET
MAXIMUM ATTAINABLE KILL PROBABILITY T-44 TYPE CLUSTER WARHEAD
SURFACE BLAST DEGRADATION FACTORS:
1.5
5.0
SOVIET TYPE 37 TARGET
60,000 FT. ALTITUDE
A: 45°, E: 45° APPROACH ANGLE
90 SUBMISSILES
RADIUS OF SUBMISSILE RING
OPTIMIZED FOR EACH σG
KILL PROBABILITY, PK
1.0
.8
.6
.4
.2
0
20
40
60
80
100
120
140
RMS GUIDANCE ERROR, σG, FT.
SECRET

Figure 35

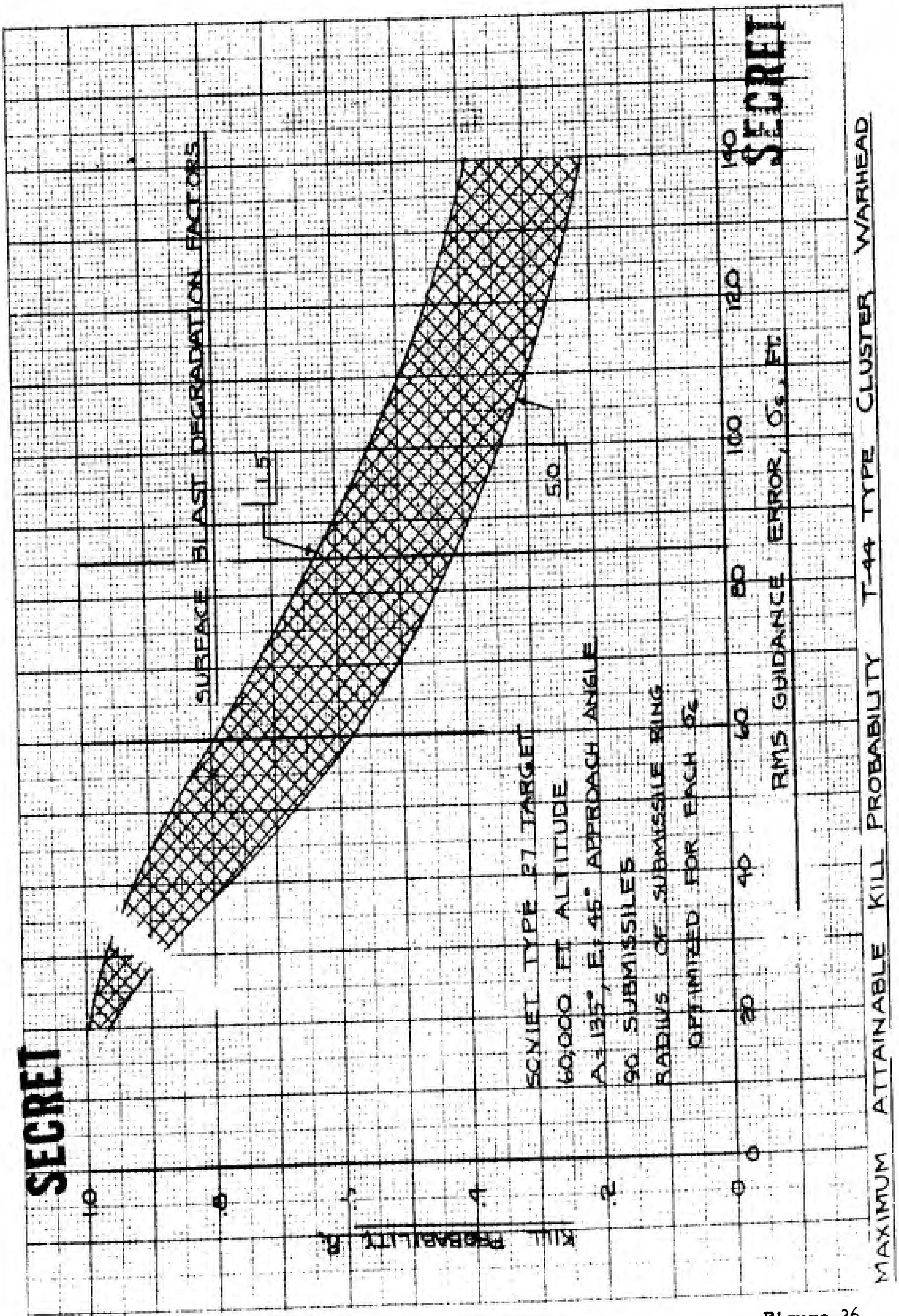
SECRET
SURFACE BLAST DEGRADATION FACTORS
1.5
5.0
SOVIET TYPE 27 TARGET
60,000 FT ALTITUDE
A=135°, E=45° APPROACH ANGLE
90 SUBMISSILES
RADIUS OF SUBMISSILE RING
OPTIMIZED FOR EACH σc
0
20
40
60
80
100
120
140
RMS GUIDANCE ERROR, σc, FT
1.0
.8
.6
.4
.2
0
KILL PROBABILITY
MAXIMUM ATTAINABLE KILL PROBABILITY T-44 TYPE CLUSTER WARHEAD
SECRET

Figure 36

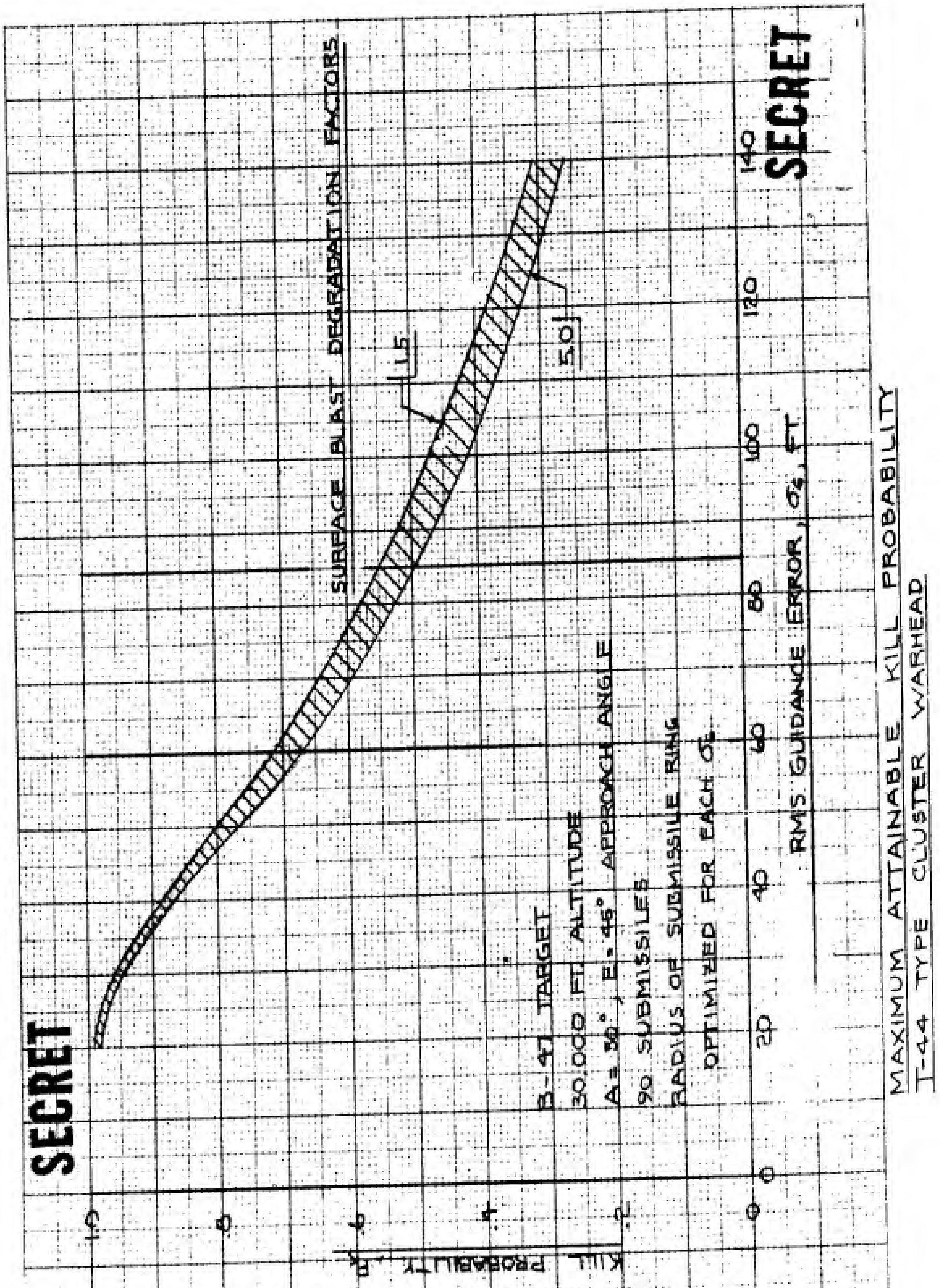
SECRET
SURFACE BLAST DEGRADATION FACTORS
1.5
5.0
B-47 TARGET
30,000 FT. ALTITUDE
A= 30°, E= 45° APPROACH ANGLE
90 SUBMISSILES
RADIUS OF SUBMISSILE RING
OPTIMIZED FOR EACH σ
RMS GUIDANCE ERROR, σ, FT
0
20
40
60
80
100
120
140
KILL PROBABILITY, P
0
.2
.4
.6
.8
1.0
MAXIMUM ATTAINABLE KILL PROBABILITY
T-44 TYPE CLUSTER WARHEAD
SECRET

Figure 37

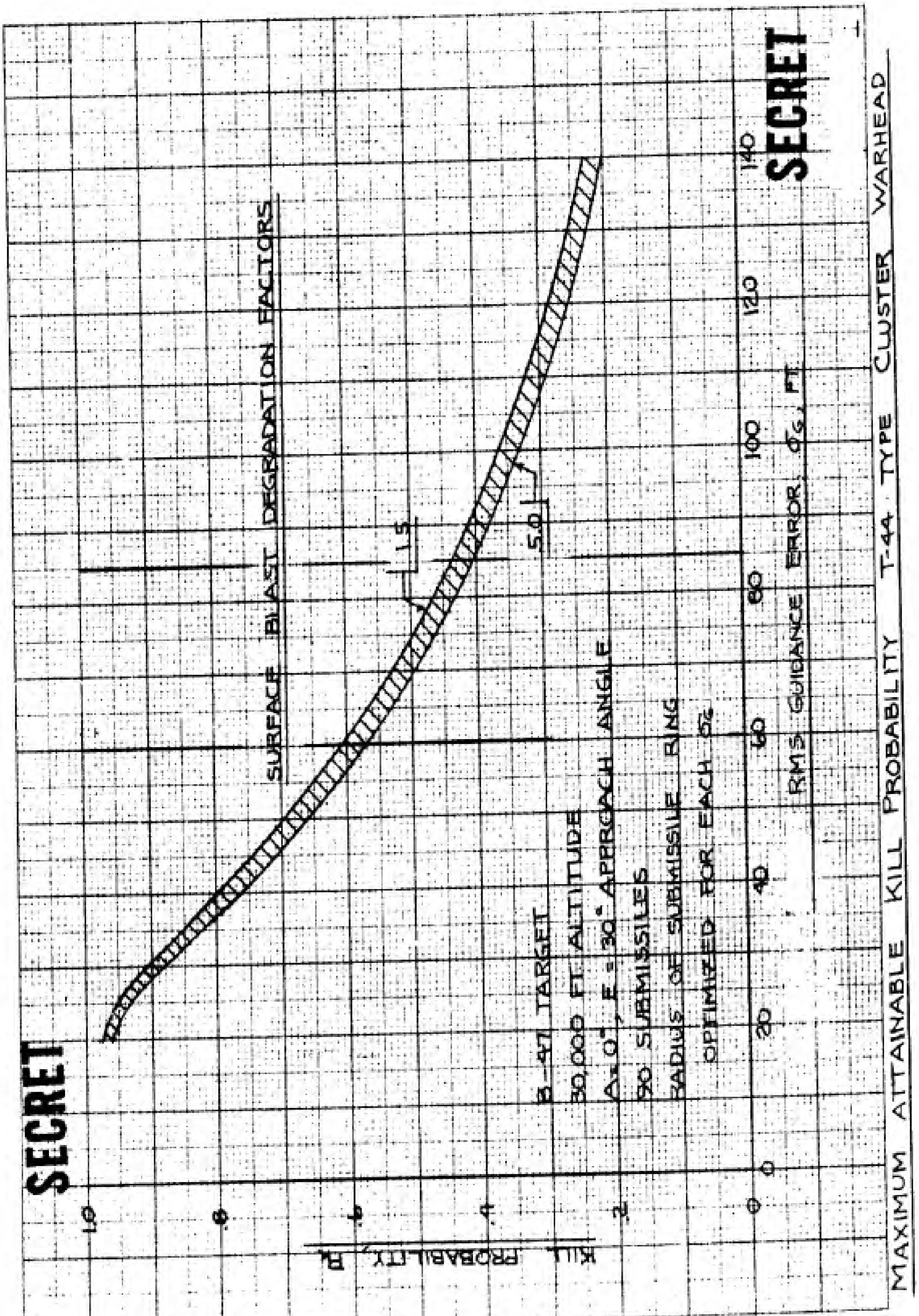
SECRET
MAXIMUM ATTAINABLE KILL PROBABILITY T-44 TYPE CLUSTER WARHEAD
SURFACE BLAST DEGRADATION FACTORS
1.5
5.0
B-47 TARGET
30,000 FT ALTITUDE
A = 0°, E = 30° APPROACH ANGLE
90 SUBMISSILES
RADIUS OF SUBMISSILE RING
OPTIMIZED FOR EACH σG
KILL PROBABILITY, PK
1.0
.8
.6
.4
.2
0
0
20
40
60
80
100
120
140
RMS GUIDANCE ERROR, σG, FT
SECRET

Figure 38

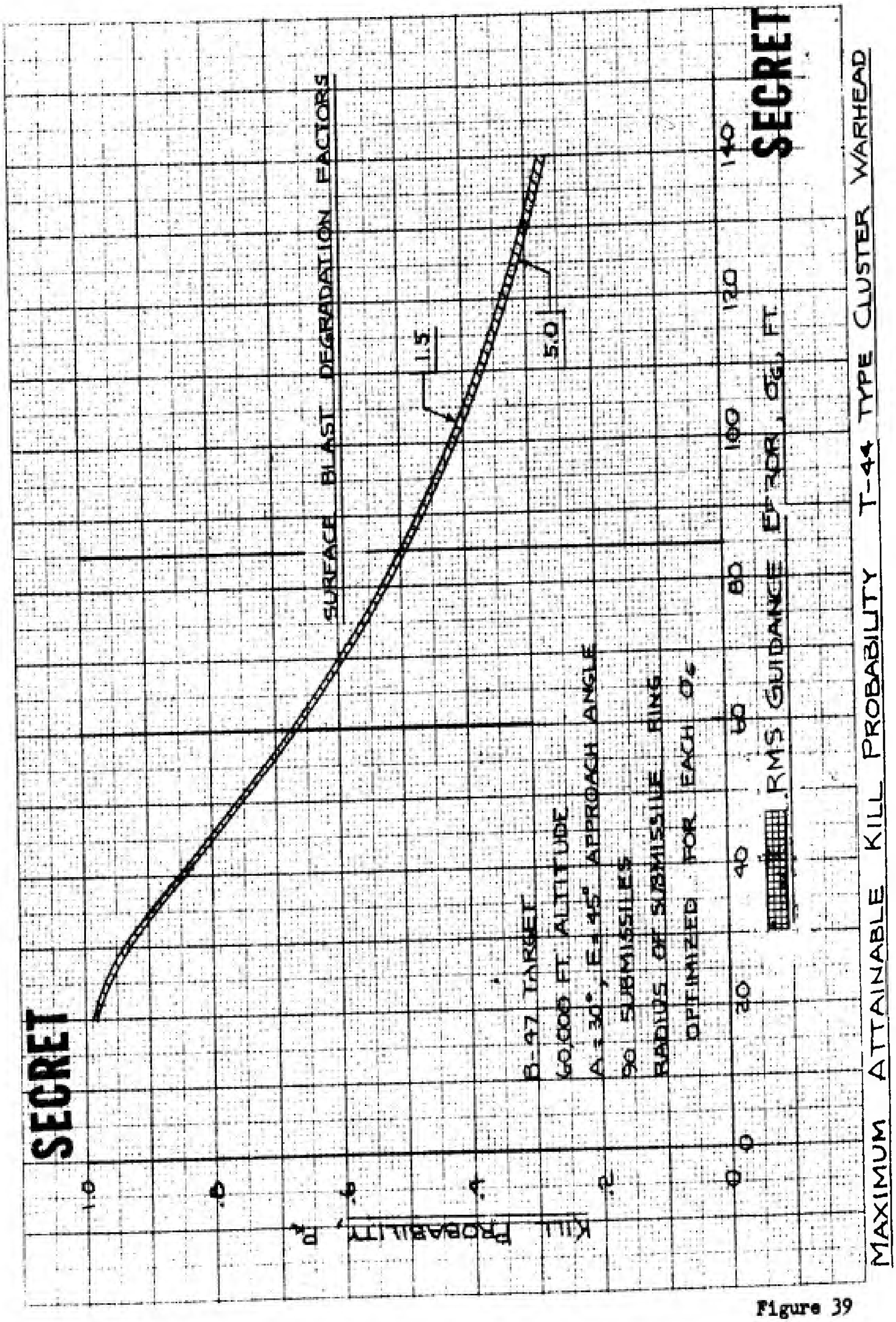
SECRET
SURFACE BLAST DEGRADATION FACTORS
1.5
5.0
B-47 TARGET
60,000 FT. ALTITUDE
A = 30°, E = 45° APPROACH ANGLE
90 SUBMISSILES
RADIUS OF SUBMISSILE RING
OPTIMIZED FOR EACH σG
0
20
40
60
80
100
120
140
RMS GUIDANCE ERROR, σG, FT.
0
.2
.4
.6
.8
1.0
KILL PROBABILITY, PK
SECRET
MAXIMUM ATTAINABLE KILL PROBABILITY T-44 TYPE CLUSTER WARHEAD

Figure 39

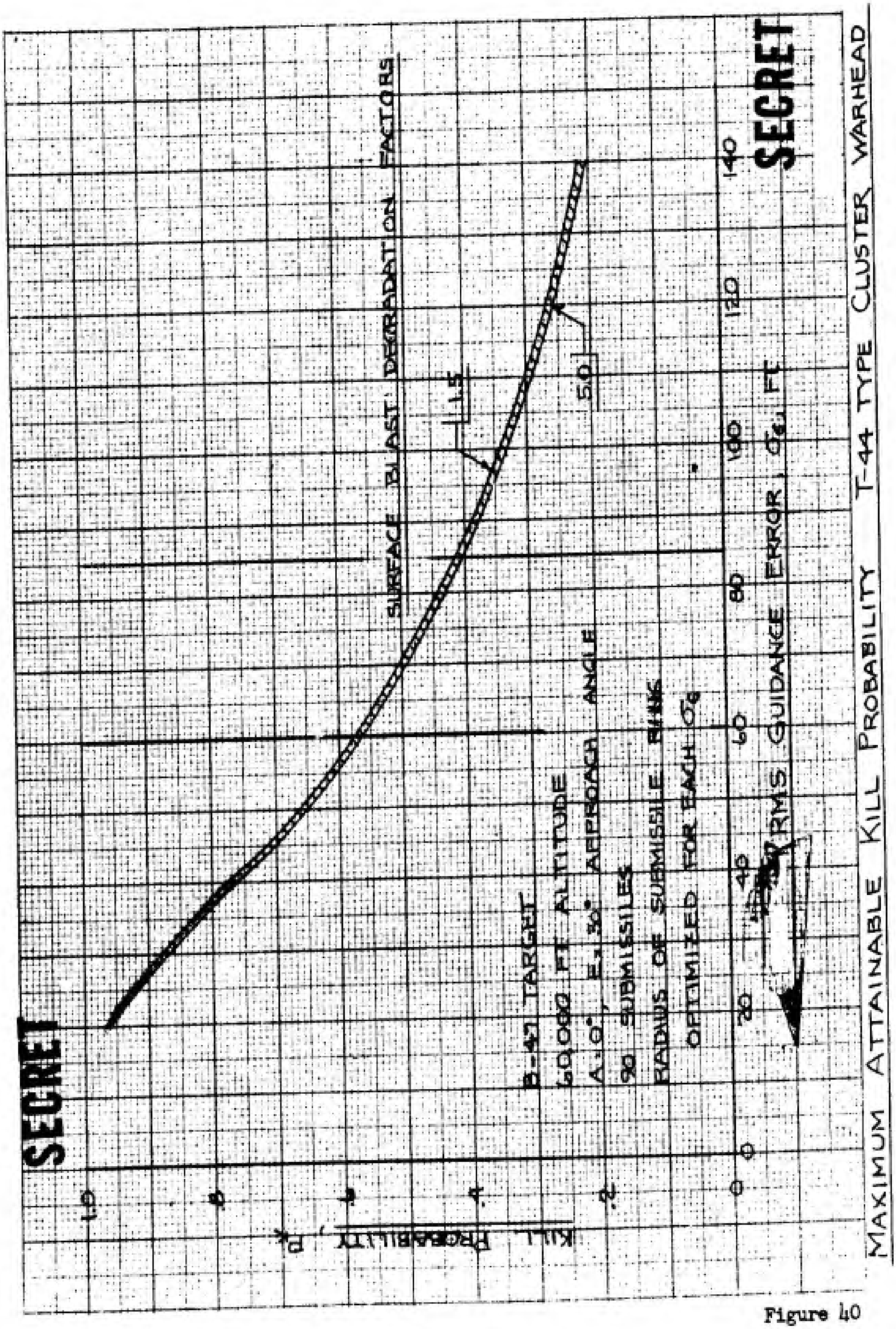
SECRET
SURFACE BLAST DEGRADATION FACTORS
1.15
5.0
B-47 TARGET
60,000 FT ALTITUDE
A:0°, E:30° APPROACH ANGLE
90 SUBMISSILES
RADIUS OF SUBMISSILE RING
OPTIMIZED FOR EACH σG
0
20
40
60
80
100
120
140
RMS GUIDANCE ERROR, σG, FT
1.0
.8
.6
.4
.2
0
KILL PROBABILITY, P*
MAXIMUM ATTAINABLE KILL PROBABILITY T-44 TYPE CLUSTER WARHEAD
SECRET

Figure 40

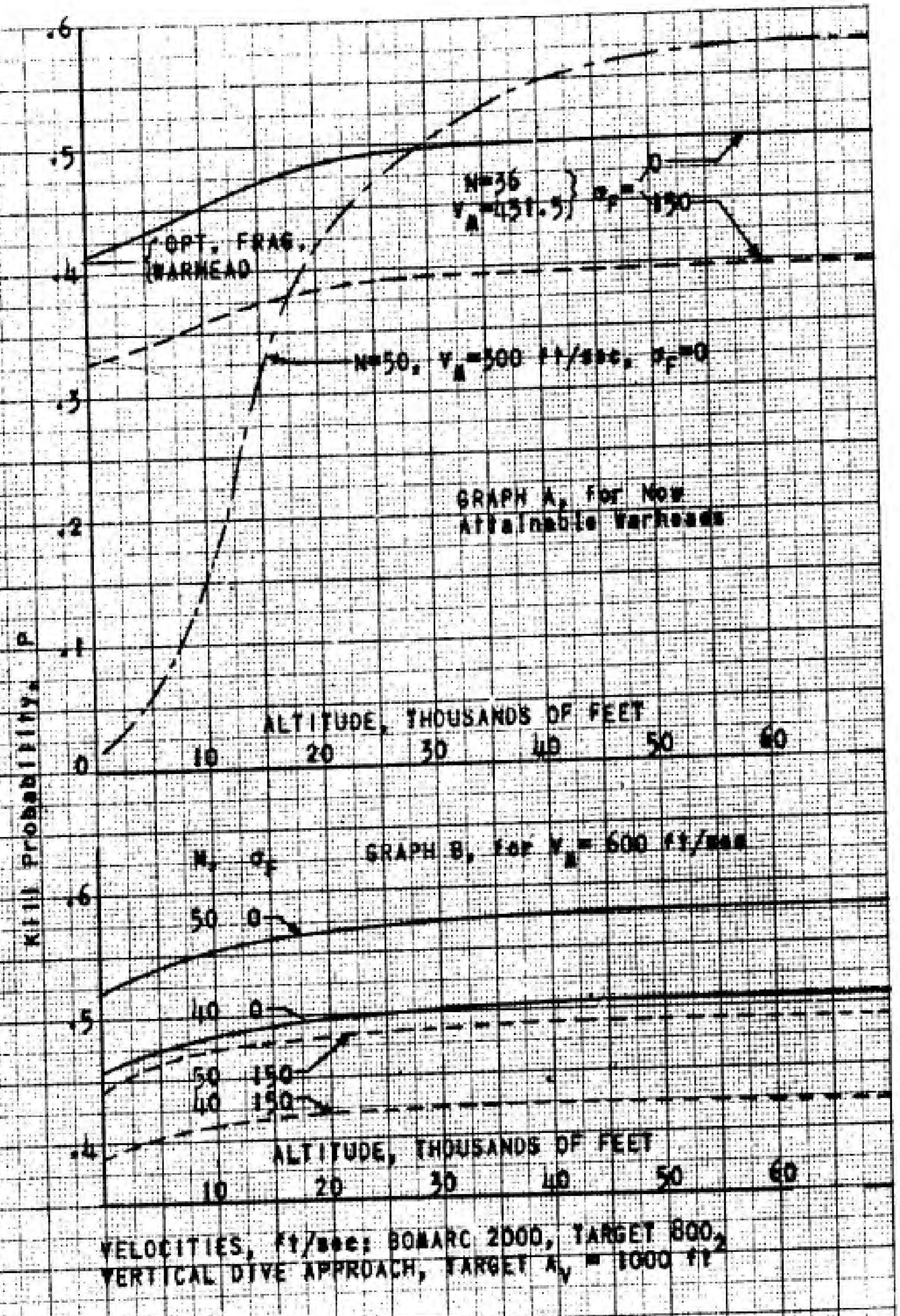

PROBABILITY THAT A CLUSTER WARHEAD KILLS A B-29 BOMBER AT DIFFERENT ALTITUDES, FOR STATED VELOCITIES

From BRL, unpublished report by Ed. Smith.

Figure 41

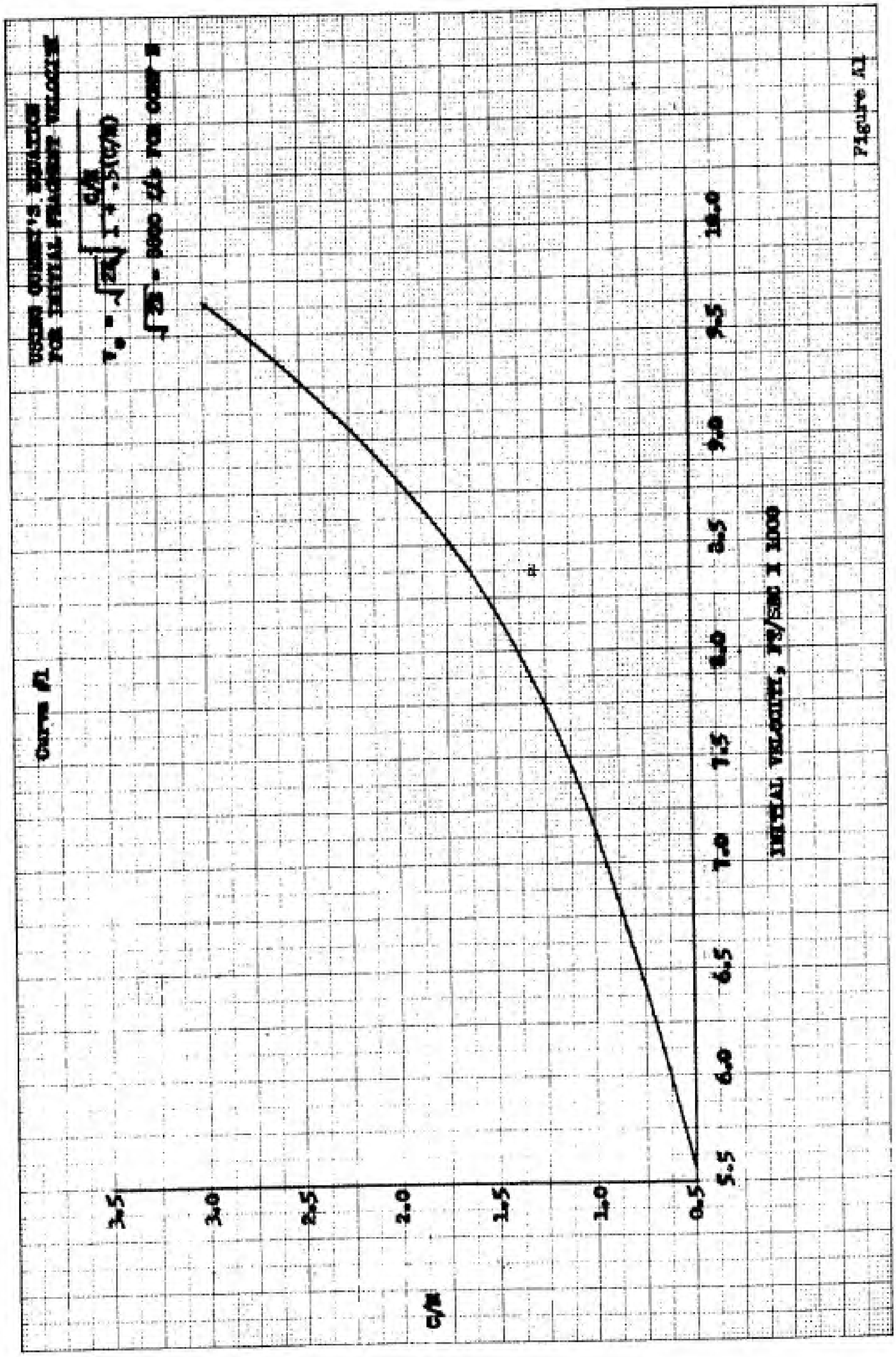
Figure 41
Curve #1
C/M
3.5
3.0
2.5
2.0
1.5
1.0
0.5
5.5
6.0
6.5
7.0
7.5
8.0
8.5
9.0
9.5
10.0
INITIAL VELOCITY, FT/SEC X 1000

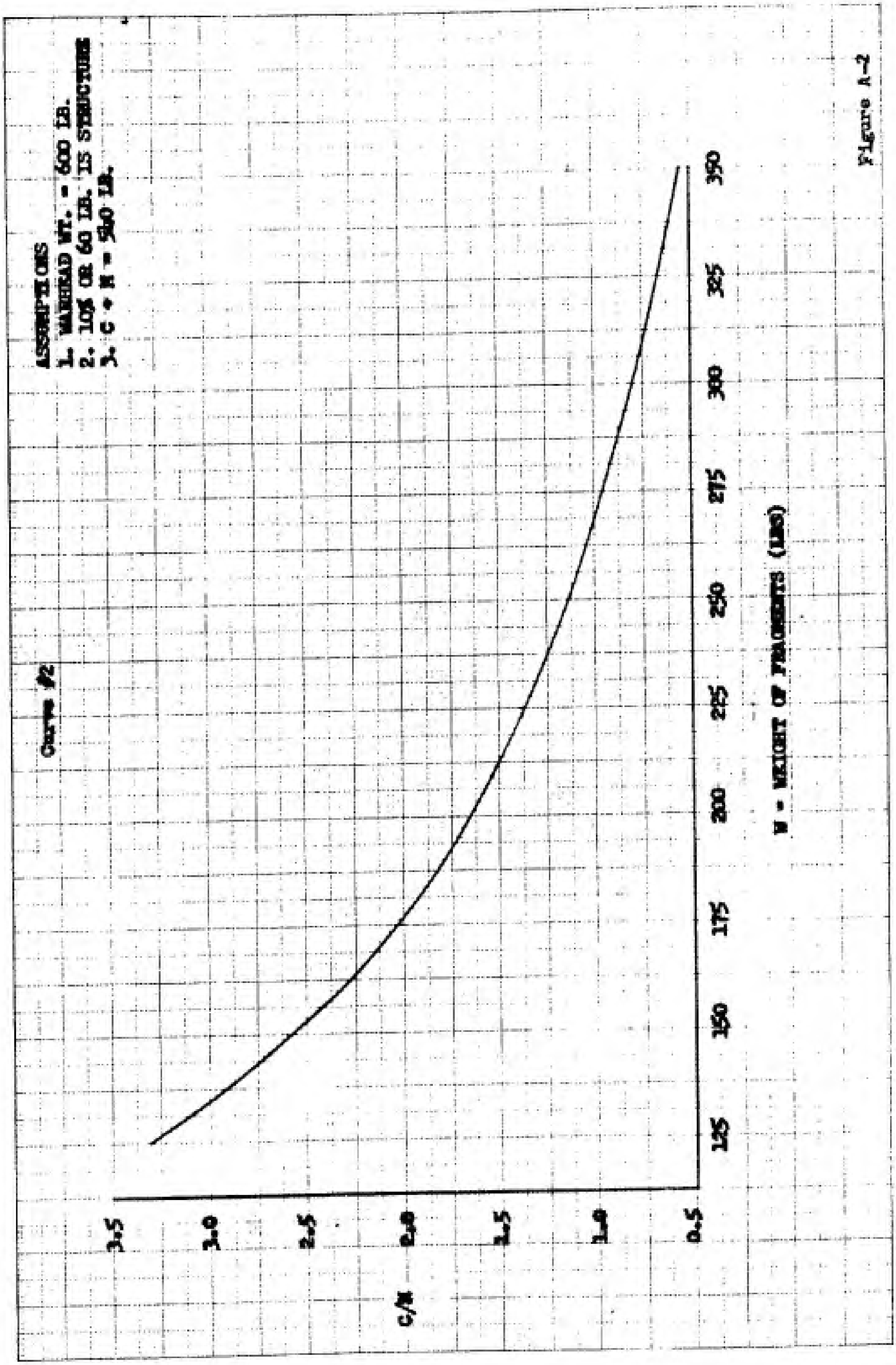
ASSUMPTIONS
1. WARHEAD WT. = 600 LB.
2. 10% OR 60 LB. IS STRUCTURE
3. C + M = 540 LB.
Curve #2
Figure A-2
W = WEIGHT OF FRAGMENTS (LBS)
125
150
175
200
225
250
275
300
325
350
C/M
3.5
3.0
2.5
2.0
1.5
1.0
0.5

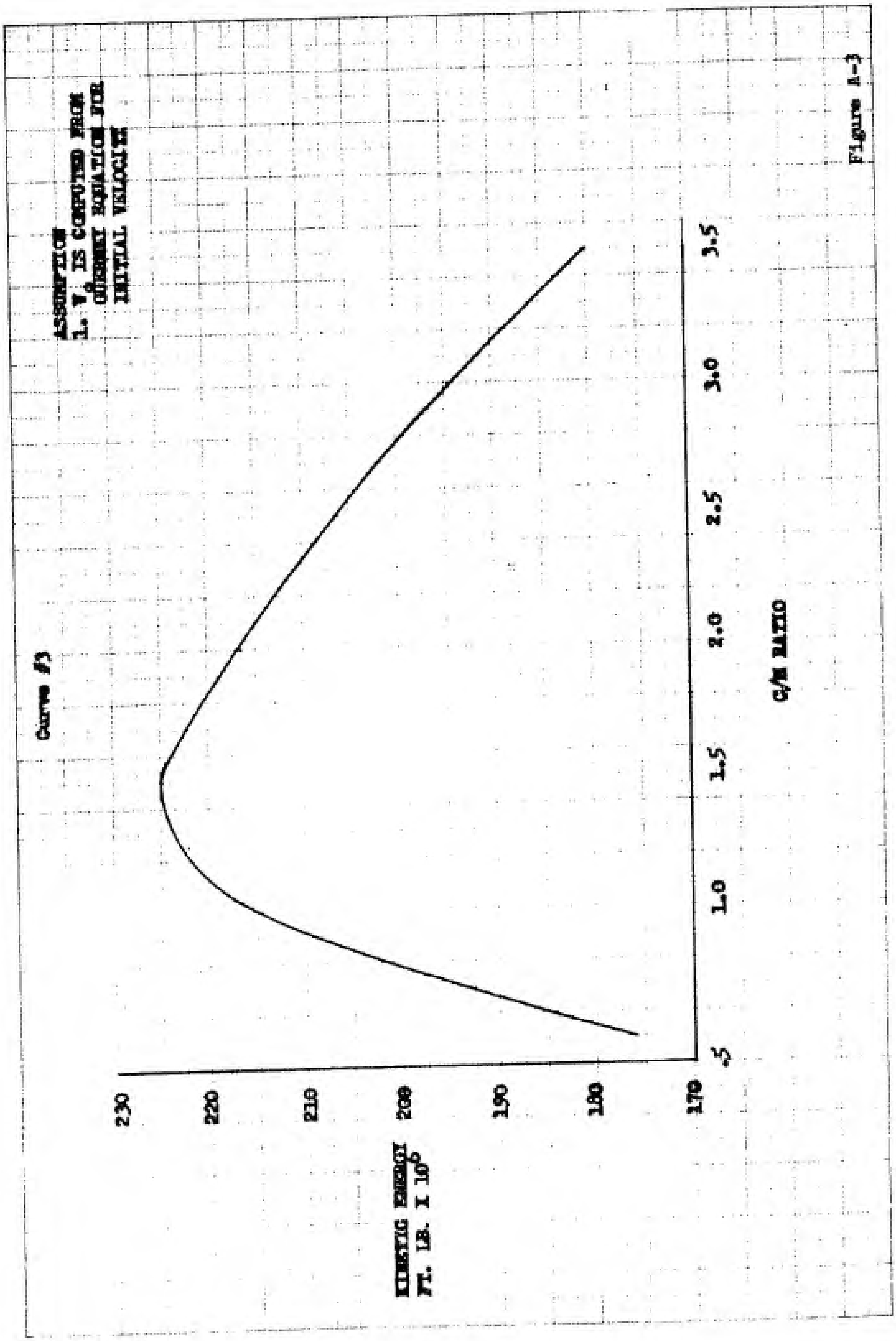
Figure A-3
ASSUMPTION
1. V IS COMPUTED FROM
GURNEY EQUATION FOR
INITIAL VELOCITY
Curve #3
KINETIC ENERGY
FT. LB. X 10^5
230
220
210
200
190
180
170
.5
1.0
1.5
2.0
2.5
3.0
3.5
C/M RATIO

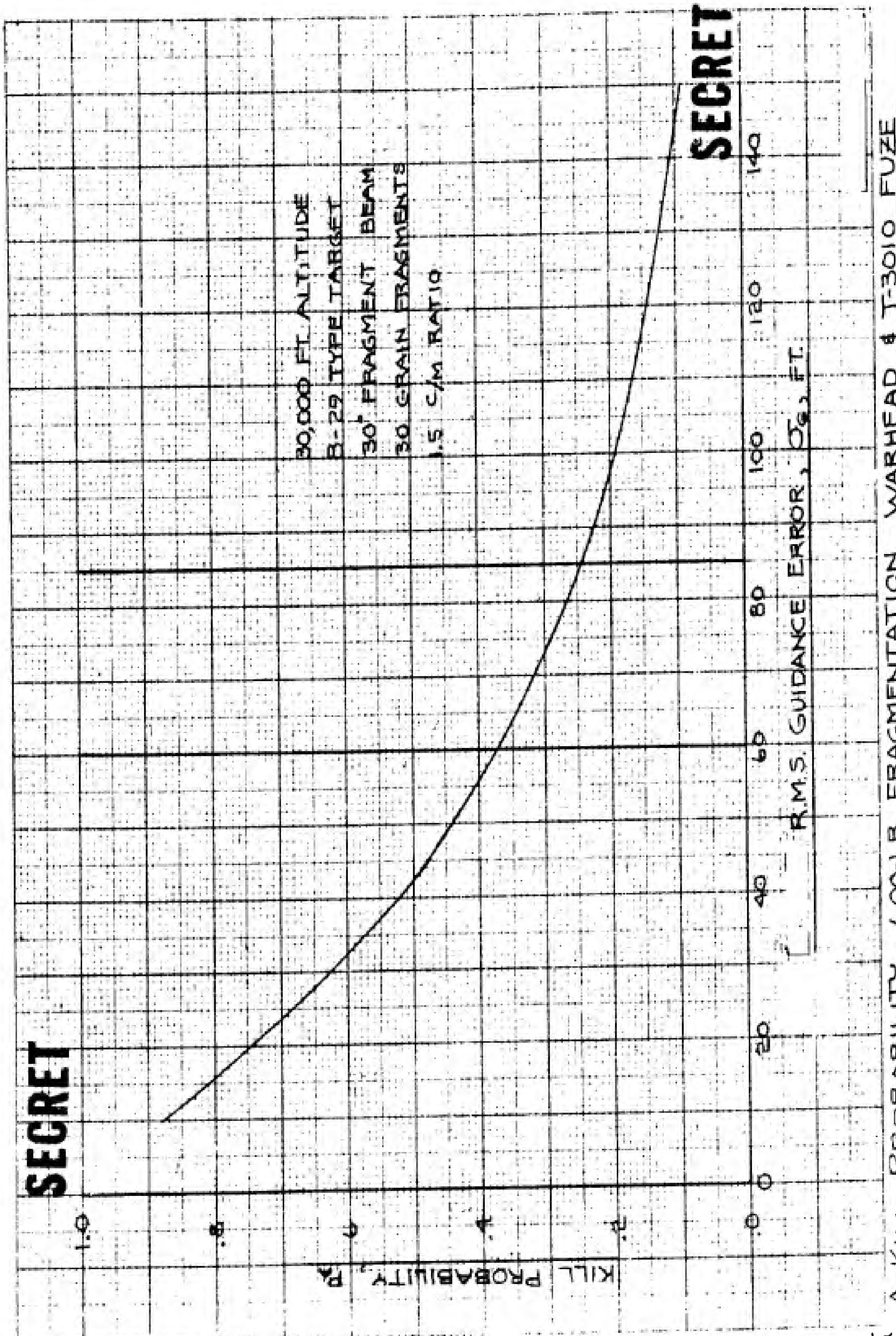
SECRET
30,000 FT ALTITUDE
B-29 TYPE TARGET
30° FRAGMENT BEAM
30 GRAIN FRAGMENTS
1.5 C/M RATIO
0
20
40
60
80
100
120
140
R.M.S. GUIDANCE ERROR, σg, FT.
0
.2
.4
.6
.8
1.0
KILL PROBABILITY, PA
SECRET
A-KILL PROBABILITY - 600-LB FRAGMENTATION WARHEAD & T-3010 FUZE

Figure 45

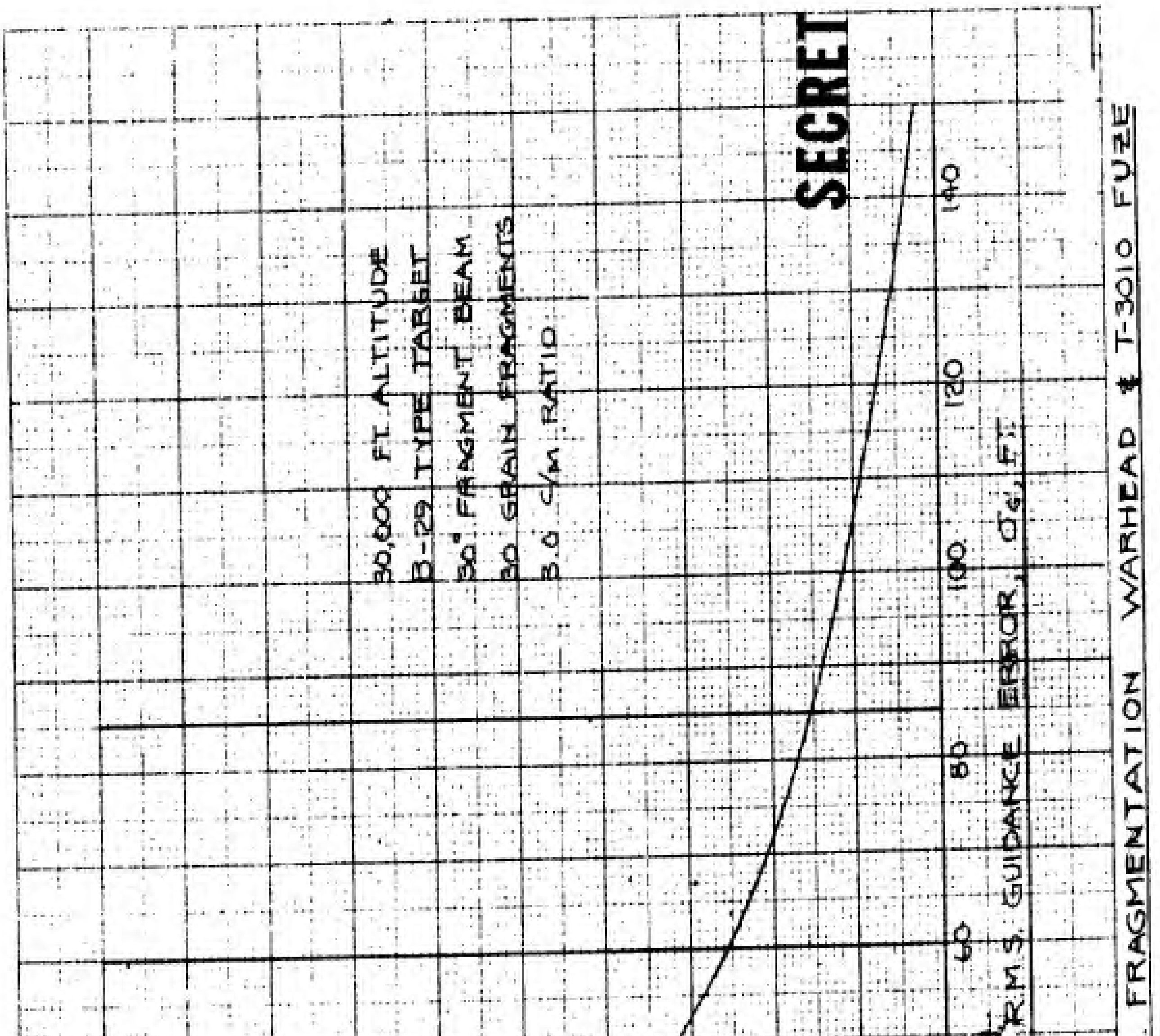
SECRET
30,000 FT. ALTITUDE
B-29 TYPE TARGET
30° FRAGMENT BEAM
30 GRAIN FRAGMENTS
3.0 C/M RATIO
KILL PROBABILITY, P_K
1.0
.8
.6
.4
.2
0
R.M.S. GUIDANCE ERROR, σ_G, FT.
0
20
40
60
80
100
120
140
A-KILL PROBABILITY - 300-LB. FRAGMENTATION WARHEAD & T-3010 FUZE
SECRET

Figure 46

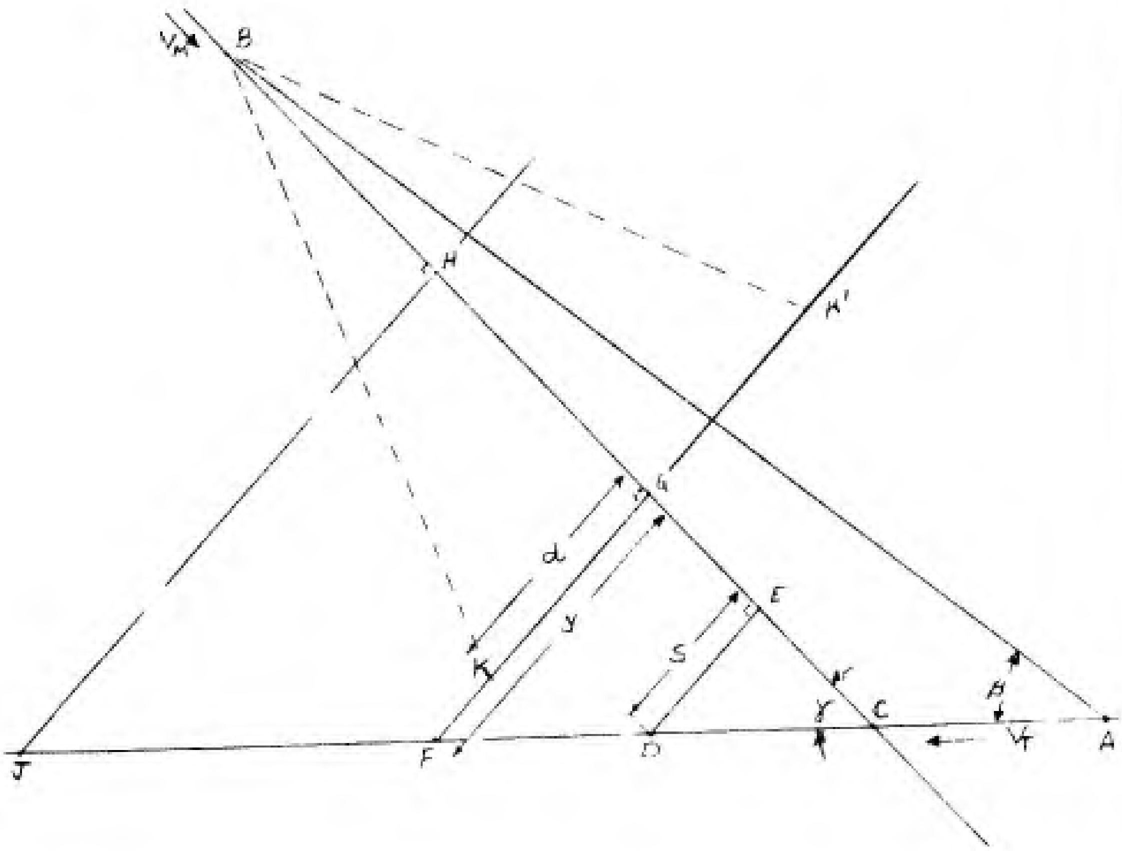

GENERAL ILLUSTRATION OF
TERMINAL ENCOUNTER - KINEMATICS

AGC 842-1

Figure 47

Aerojet-General

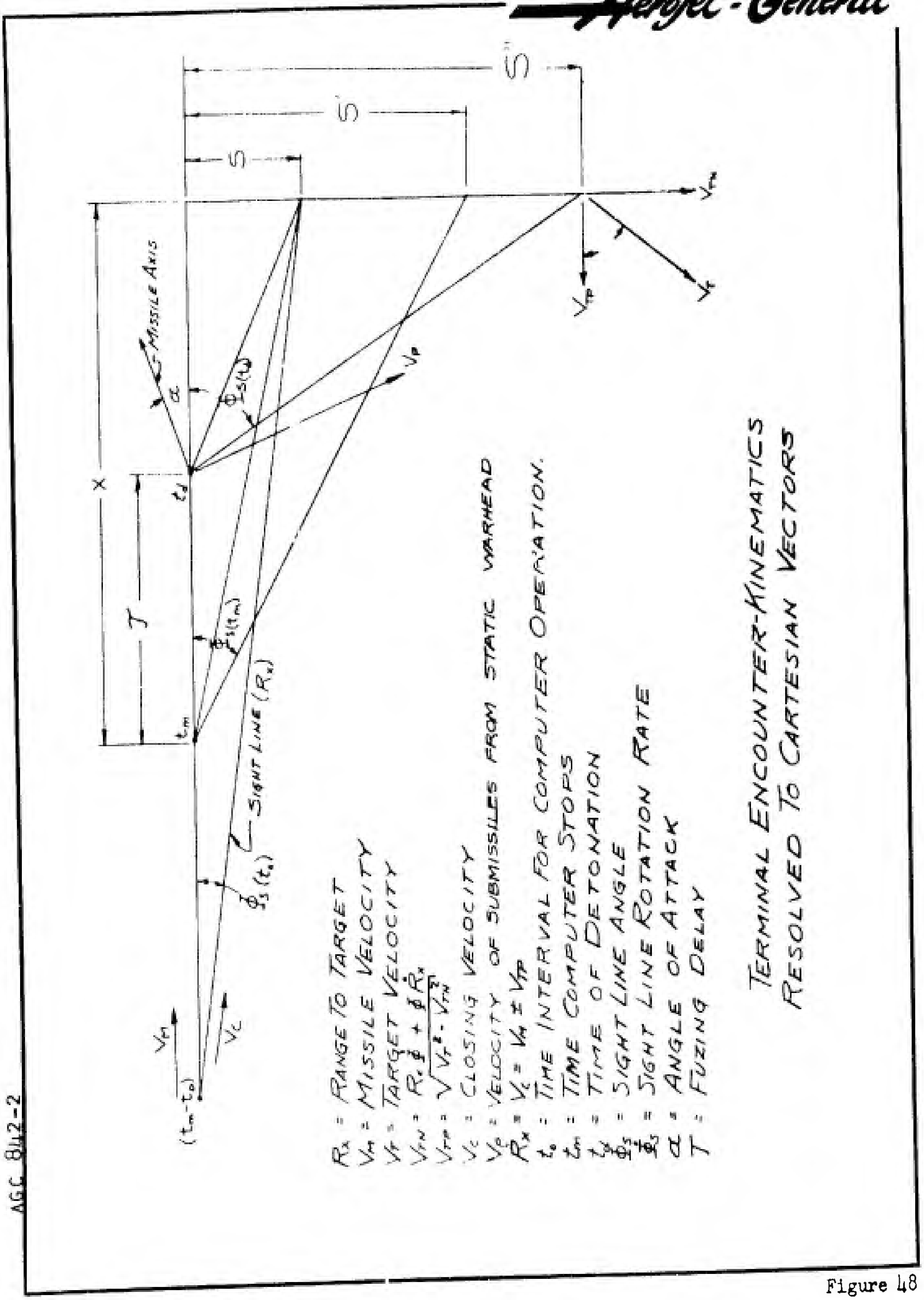

Figure 48

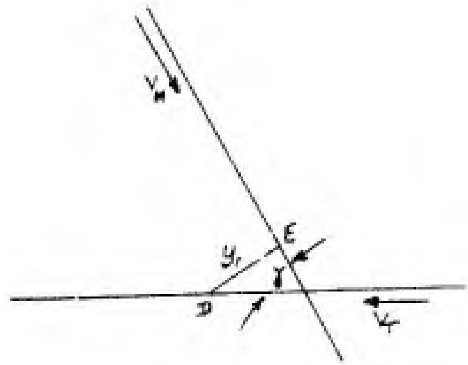

(a) HEAD-ON, MISS ABOVE, BEHIND

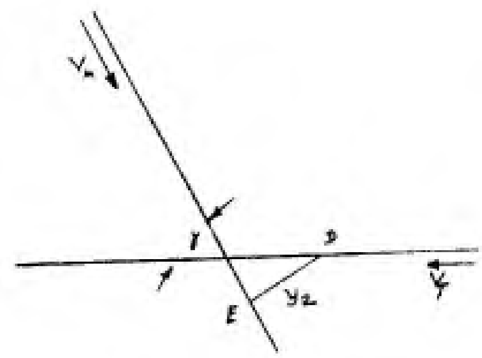

(b) HEAD-ON, MISS BELOW, AHEAD

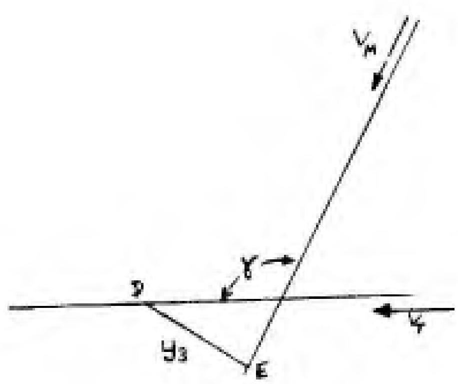

(c) HEAD-TO-TAIL, MISS BELOW, BEHIND

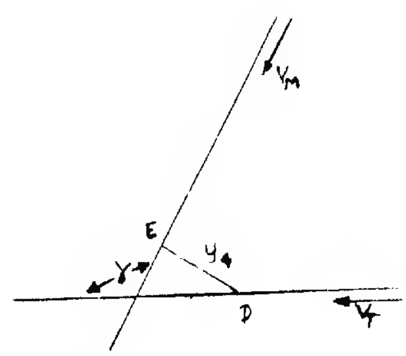

(d) HEAD-TO-TAIL, MISS ABOVE, BEHIND

FOUR APPROACH POSSIBILITIES FOR OVERHEAD ATTACK BY INTERCEPTOR

AGC 8442-2

Figure 49

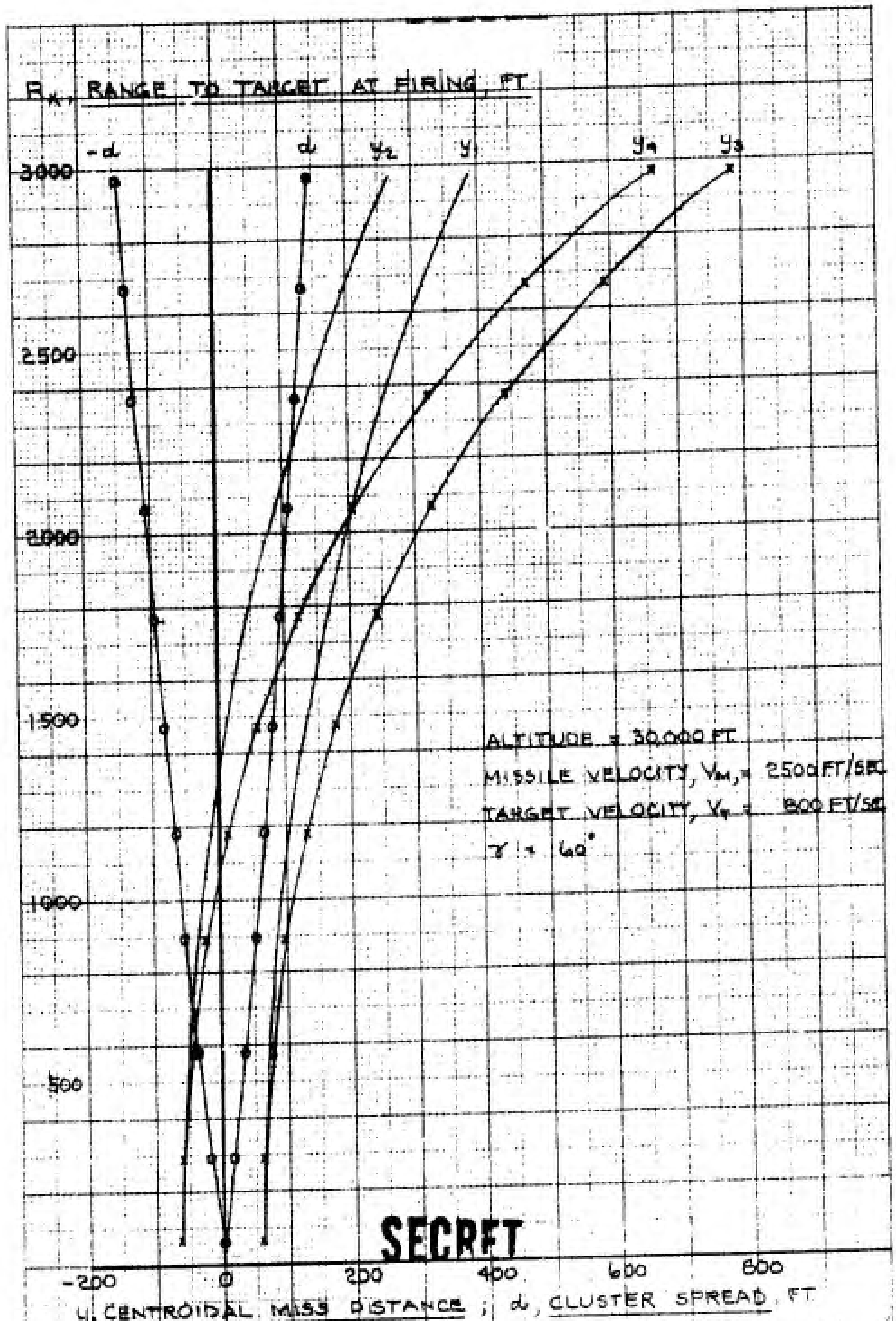

CENTROIDAL MISS DISTANCE, y, AND CLUSTER SPREAD, d, VS RANGE TO TARGET AT FIRING FOR CLUSTER WARHEAD

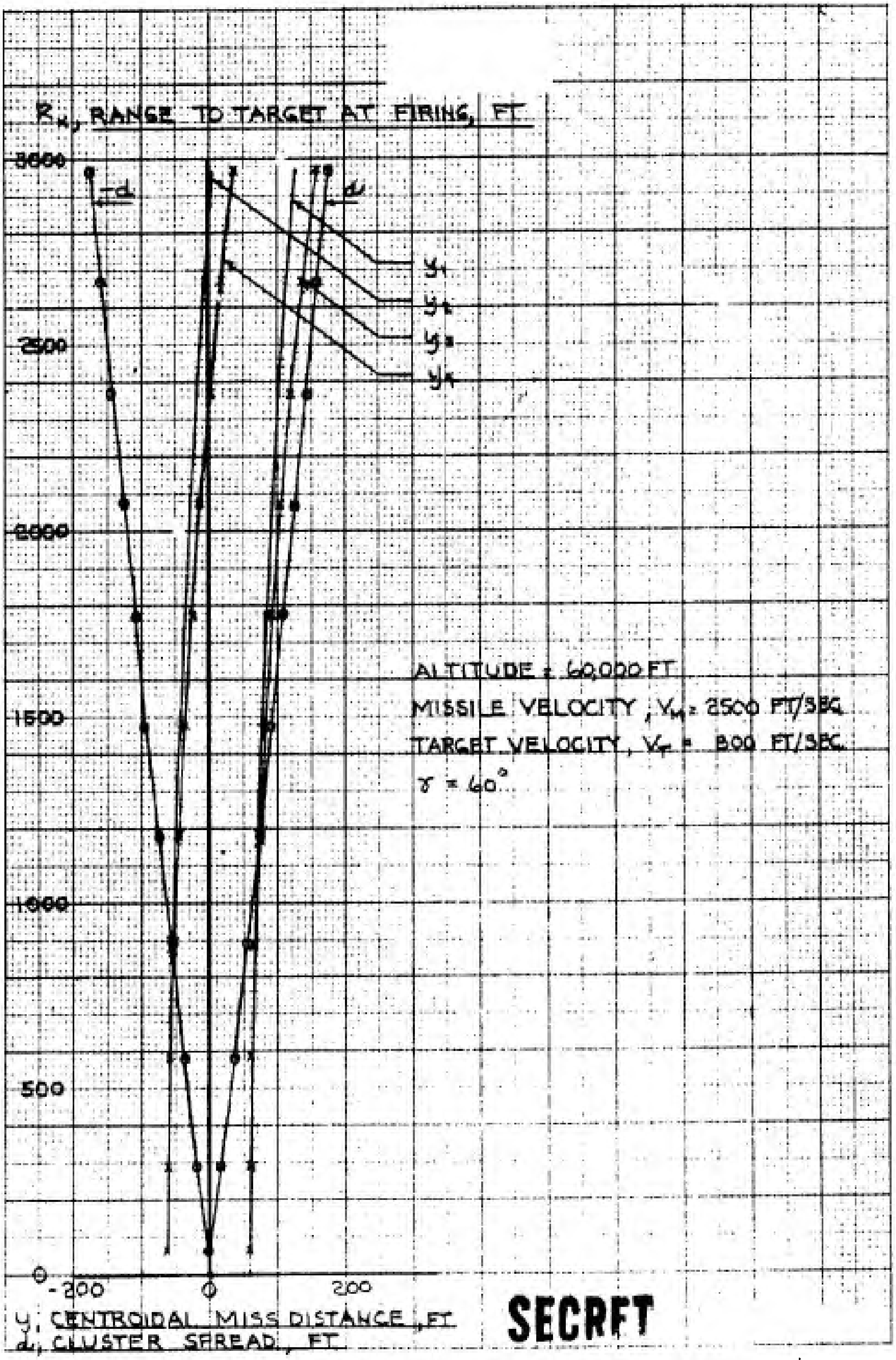

SECRET

CENTROIDAL MISS DISTANCE, y, AND CLUSTER SPREAD, d, VS. RANGE TO TARGET AT FIRING FOR CLUSTER WARHEAD

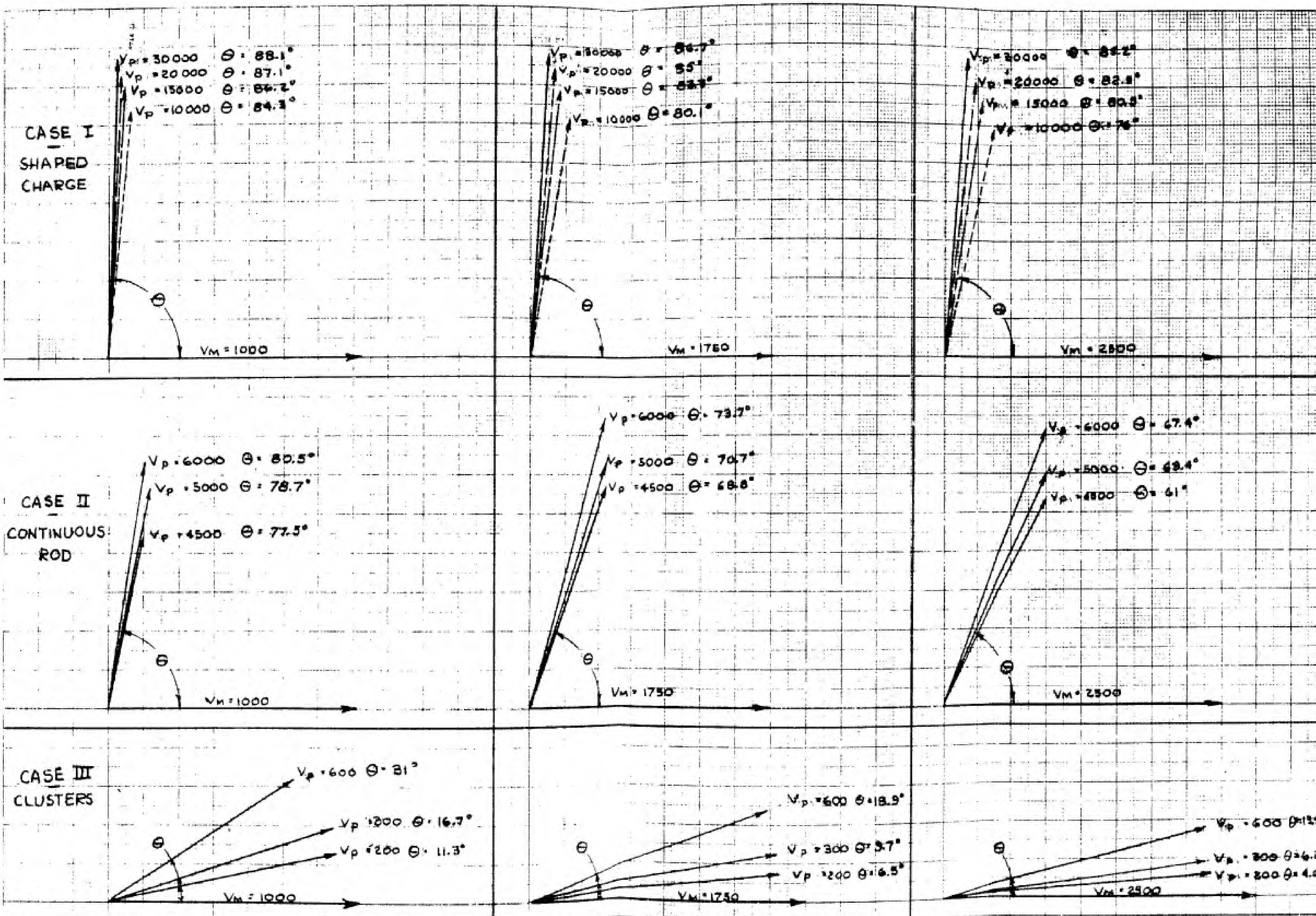

PLOTS OF ANGLE OF DEPARTURE (θ) AS FUNCTION OF MISSILE VELOCITY (V_M) AND SUBMISSILE RADIAL PROJECTION VELOCITY (V_P)

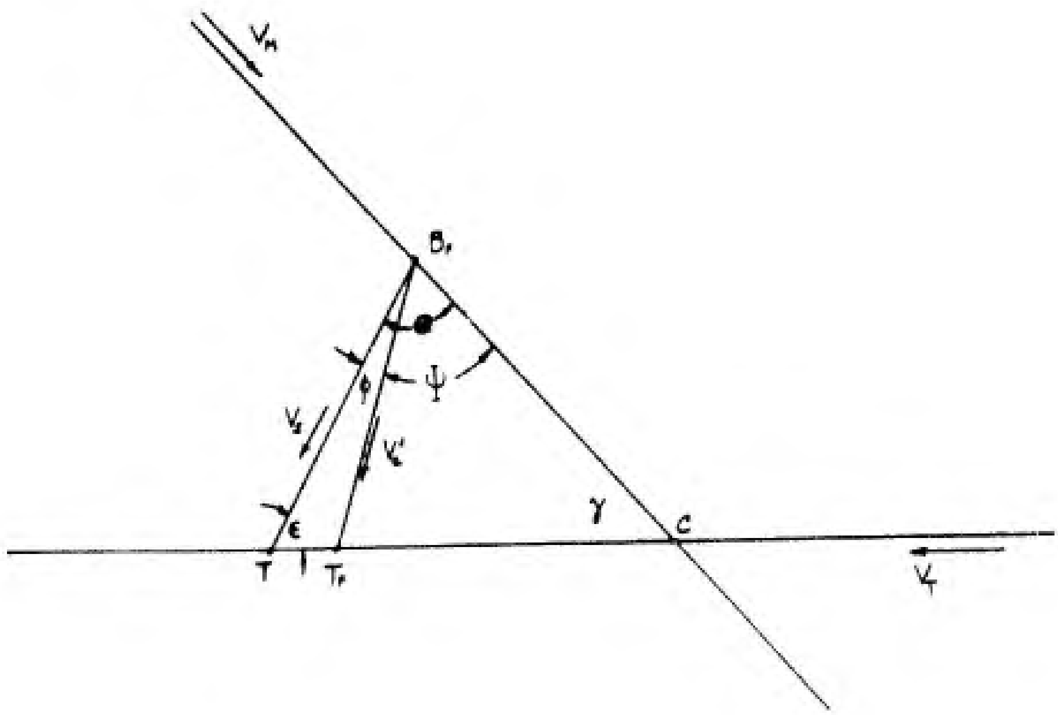

TERMINAL ENCOUNTER-KINEMATICS
FOR
HIGH VELOCITY SUB-MISSILE WARHEADS
CONICAL-SKIRT TYPE FUZE

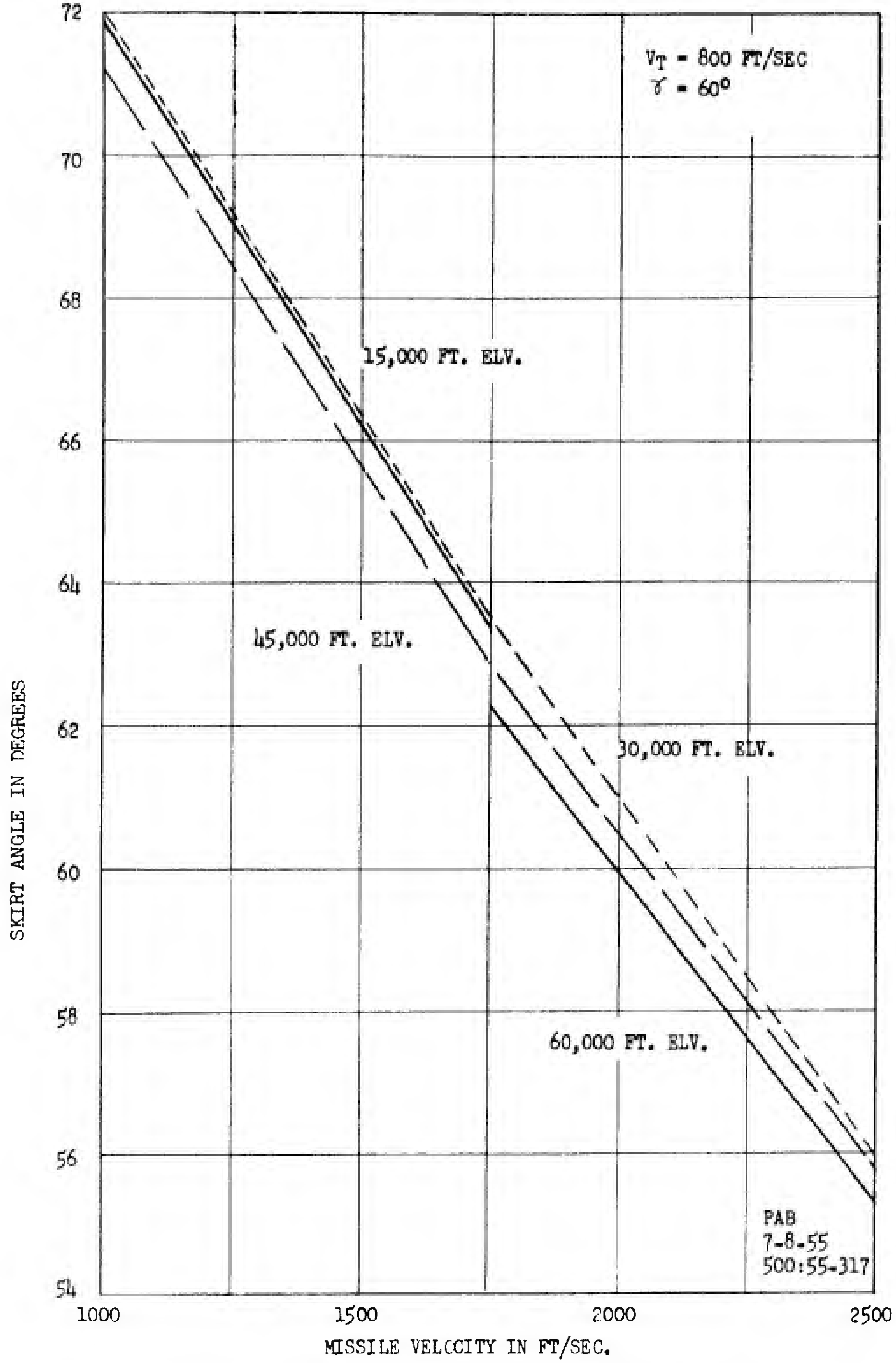

SKIRT ANGLE VS. MISSILE VELOCITY FOR HEAD ON ABOVE AND TAIL BELOW CONFIGURATIONS

Aerojet-General CORPORATION

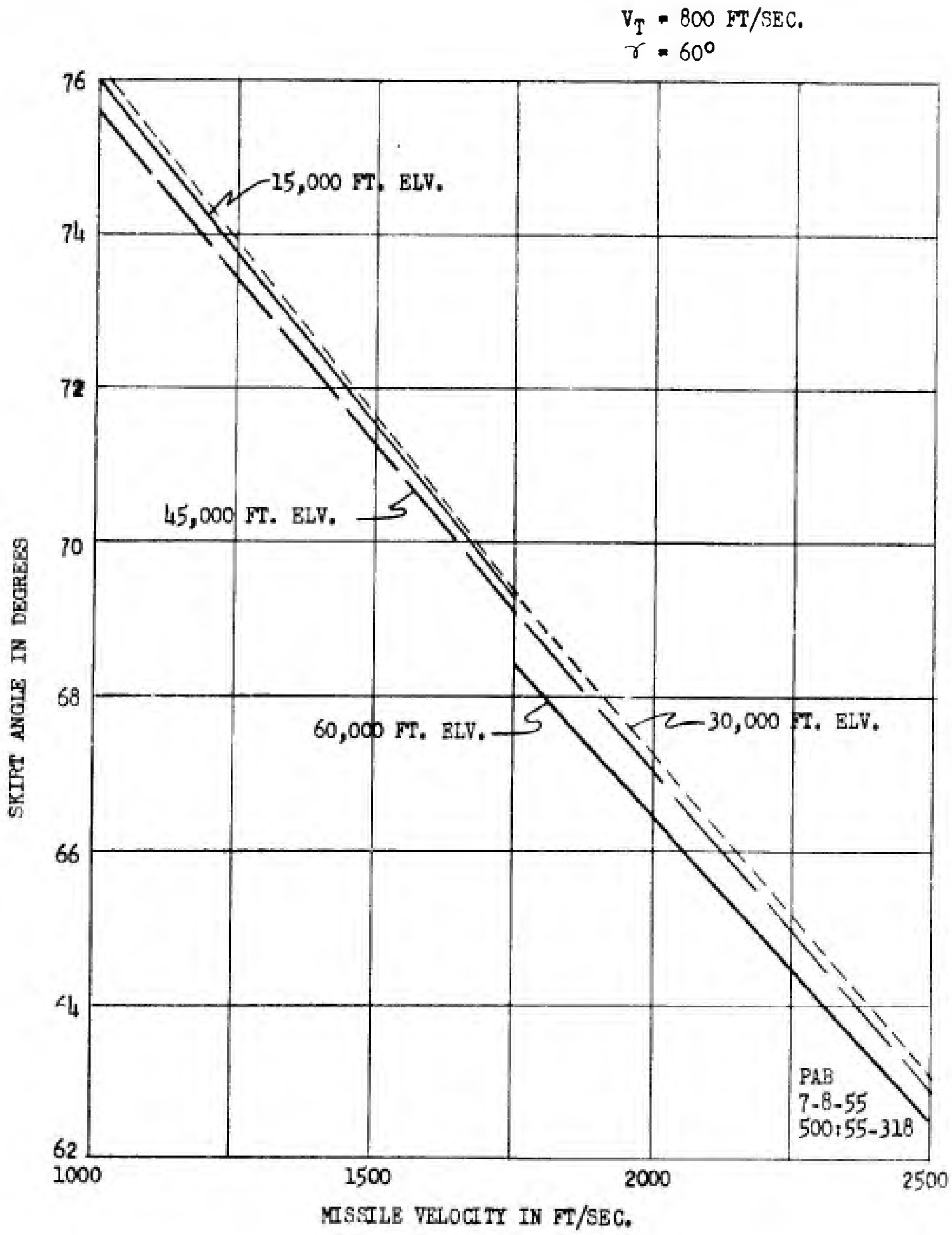

SKIRT ANGLE VS. MISSILE VELOCITY FOR
HEAD ON BELOW AND TAIL ABOVE CONFIGURATIONS

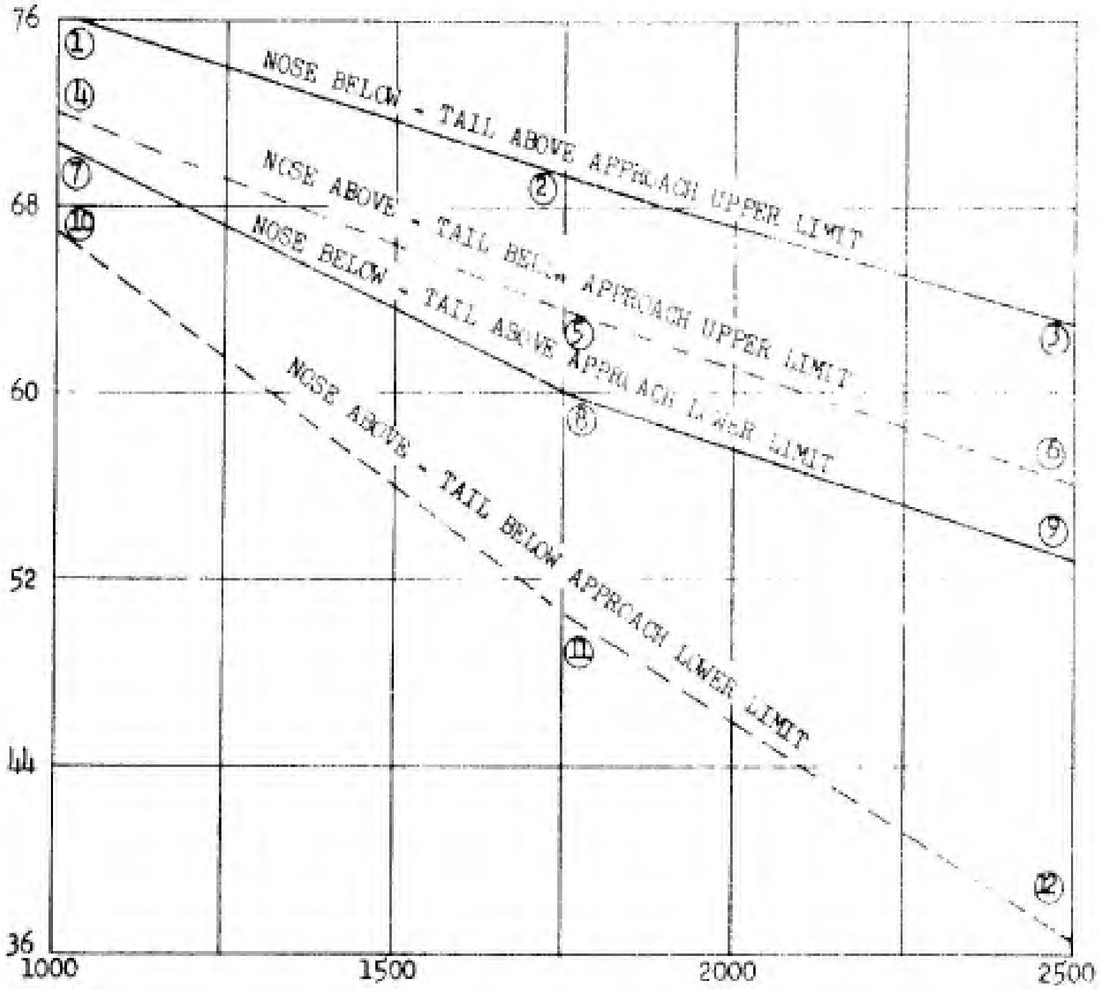

LIMITS:

VT; 800 - 2500 FT/SEC.
APPROACH ANGLE: 30° - 60° AND 120° - 150°
ALTITUDE: 15,000 FT - 60,000 FT.

VT VARIATIONS:

① → ② → ③	800 FT/SEC
④ → ⑤ → ⑥	800 FT/SEC
⑦ → ⑧	1000 → 1750 FT/SEC
⑧ → ⑨	1750 → 2500 FT/SEC
⑩ → ⑪	1000 → 1750 FT/SEC
⑪ → ⑫	1750 → 2500 FT/SEC

EXTREME VARIATIONS IN CONICAL SKIRT ANGLE
DUE TO VARIATIONS IN MISSILE VELOCITY, TARGET
VELOCITY AND APPROACH ANGLE

PAB
7-8-55
500:55-315

Aerojet-General
CORPORATION

Aerojet-General

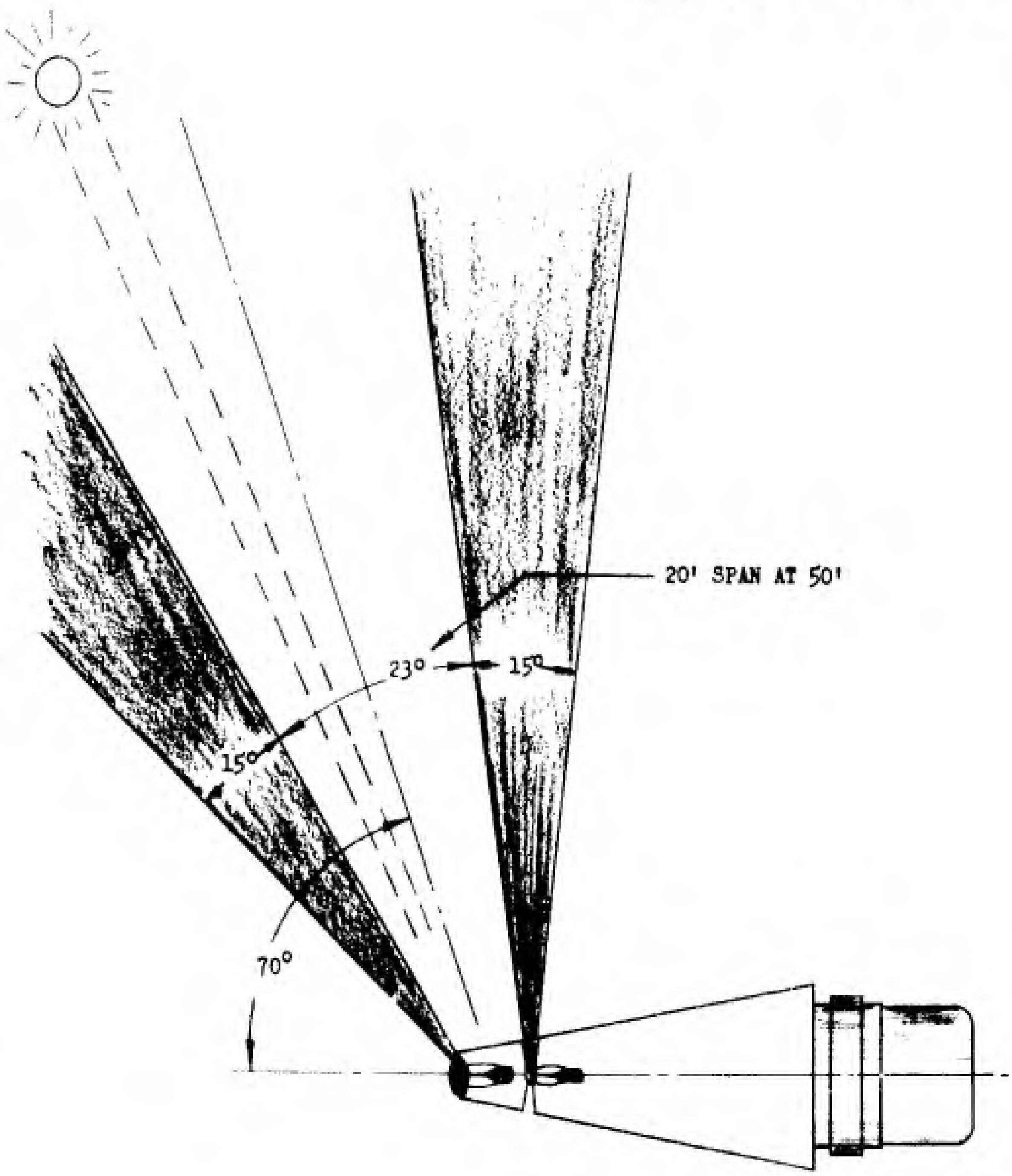

SCHEMATIC ARRANGEMENT DUPLEX CONE
ACTUATION SOLUTION - TWO CELLS

PAB
7-8-55
500:55-246

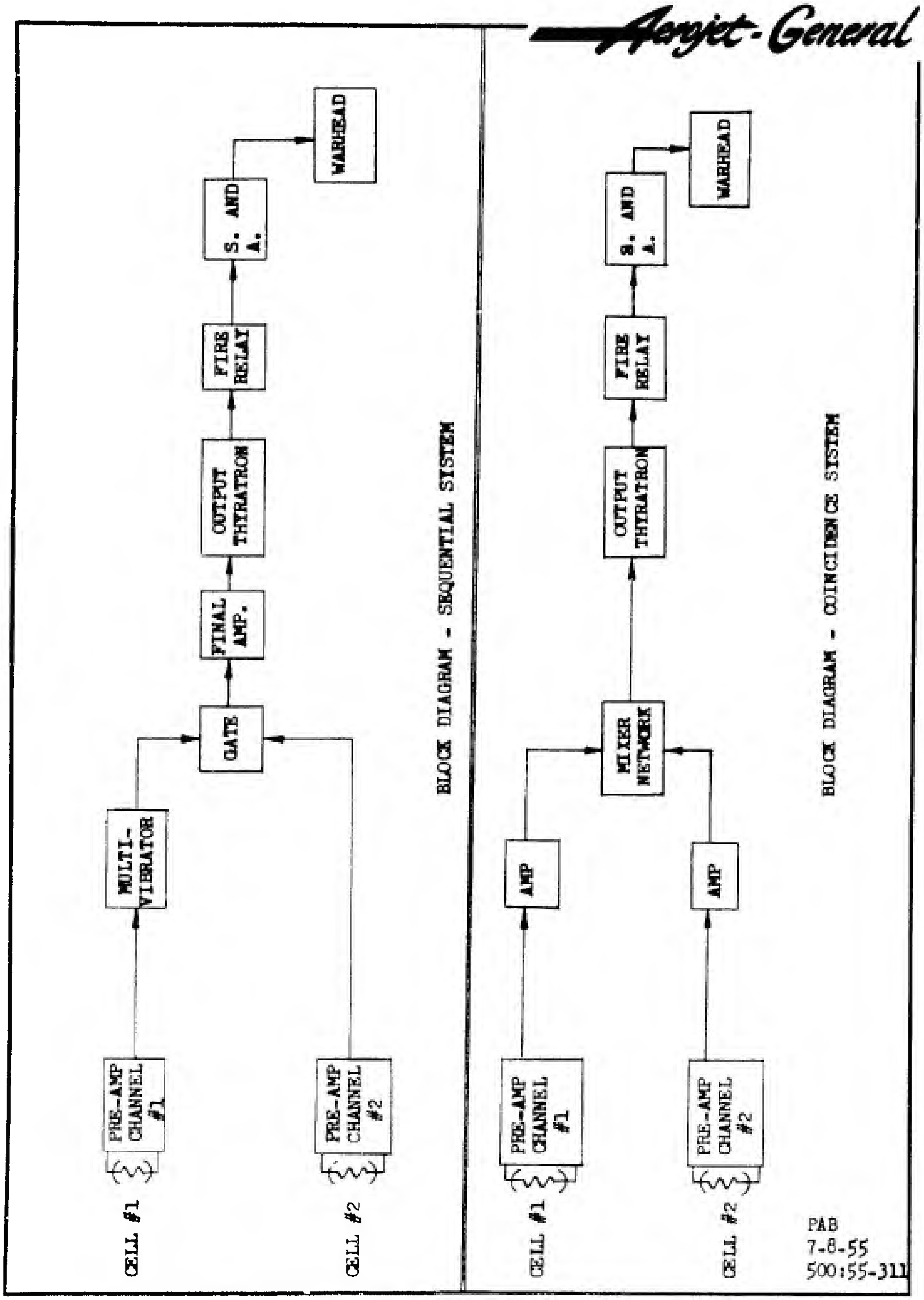
Aerojet-General
CELL #1
PRE-AMP CHANNEL #1
MULTI-VIBRATOR
CELL #2
PRE-AMP CHANNEL #2
GATE
FINAL AMP.
OUTPUT THYRATRON
FIRE RELAY
S. AND A.
WARHEAD
BLOCK DIAGRAM - SEQUENTIAL SYSTEM
CELL #1
PRE-AMP CHANNEL #1
AMP
CELL #2
PRE-AMP CHANNEL #2
AMP
MIXER NETWORK
OUTPUT THYRATRON
FIRE RELAY
S. AND A.
WARHEAD
BLOCK DIAGRAM - COINCIDENCE SYSTEM
PAB
7-8-55
500:55-311

Aerojet-General

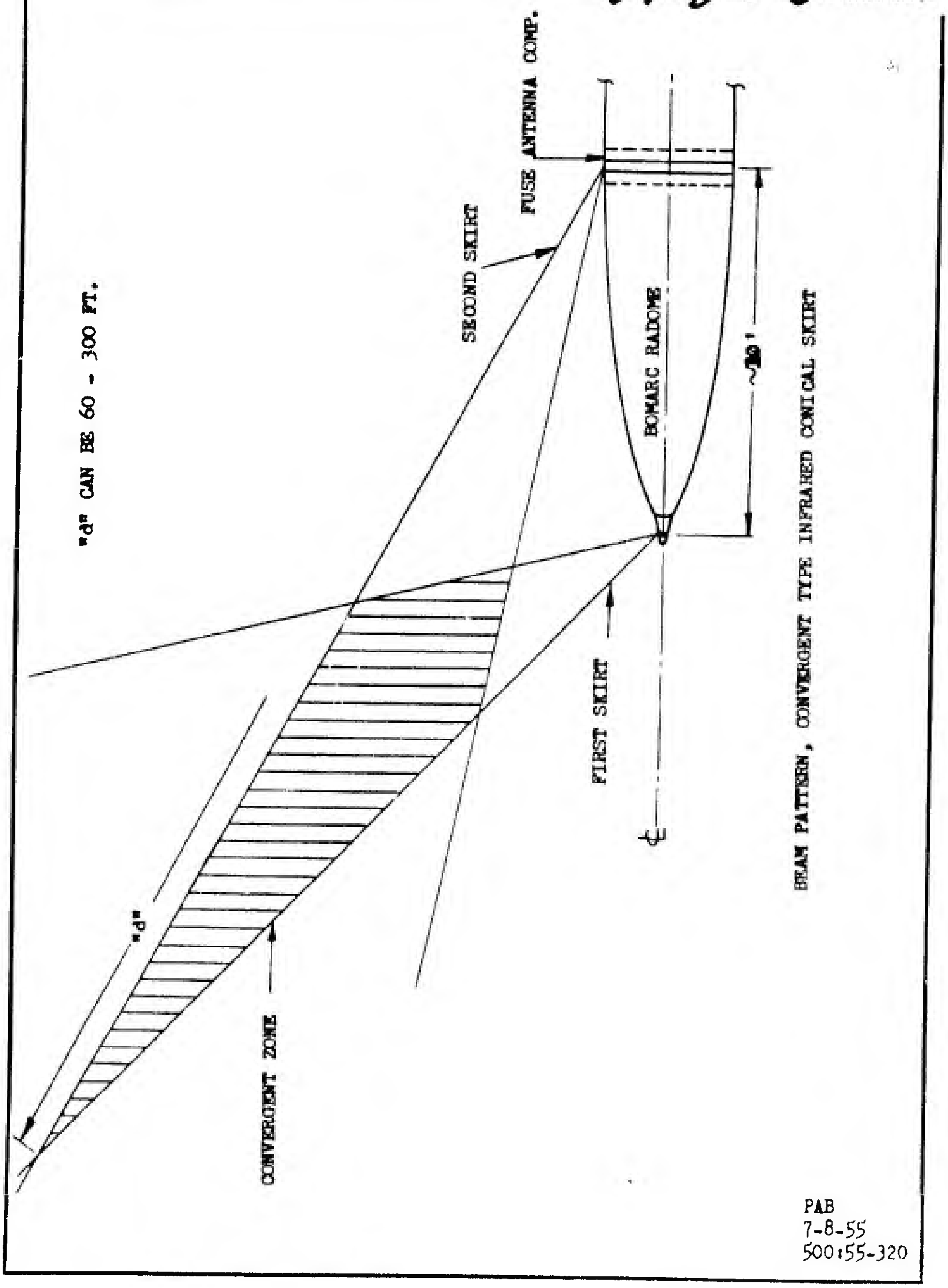

BEAM PATTERN, CONVERGENT TYPE INFRARED CONICAL SKIRT

PAB
7-8-55
500:55-320

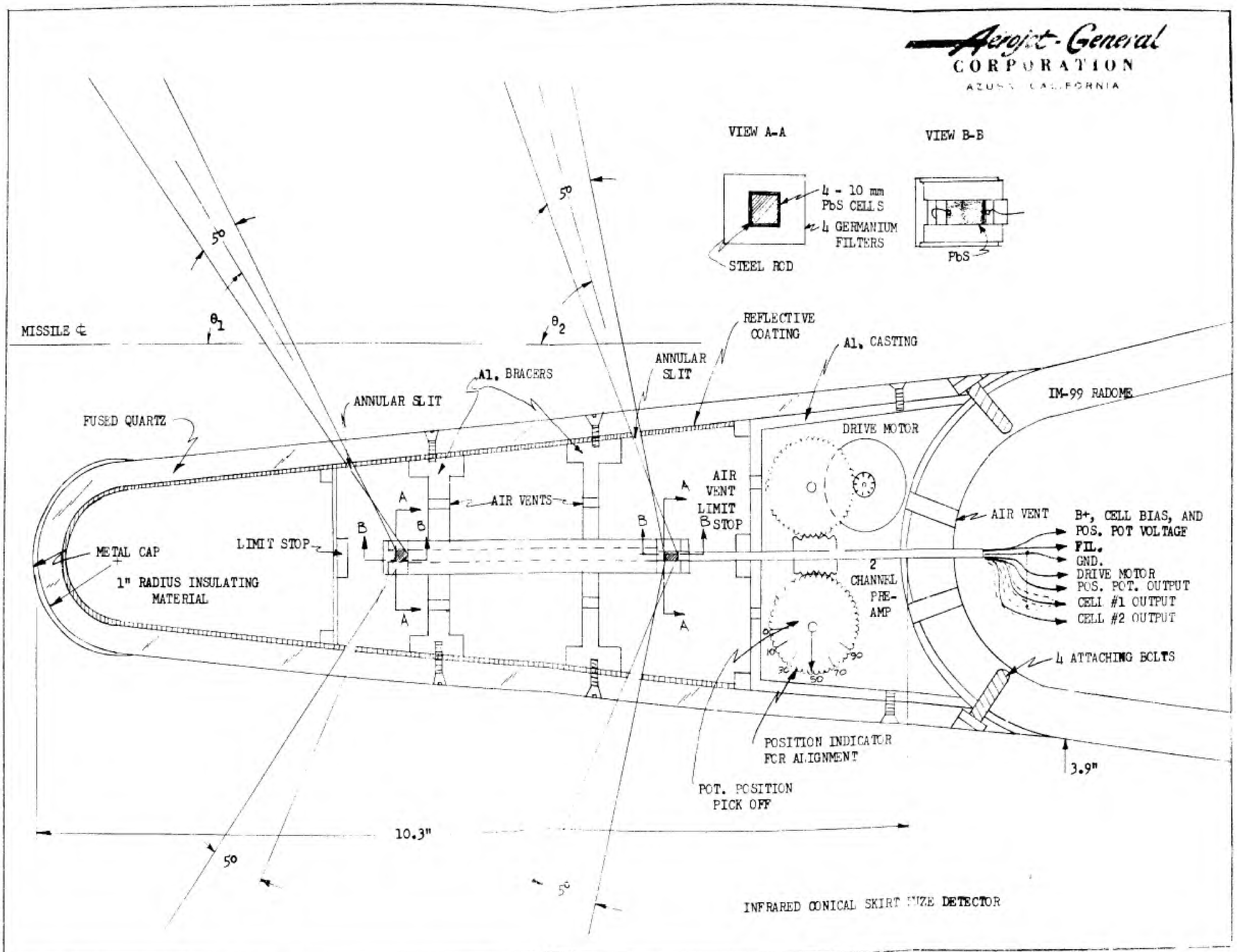
Aerojet-General
CORPORATION
AZUSA CALIFORNIA
VIEW A-A
VIEW B-B
4 - 10 mm
PbS CELLS
4 GERMANIUM
FILTERS
STEEL ROD
PbS
MISSILE ℄
θ1
θ2
5°
REFLECTIVE
COATING
Al. CASTING
ANNULAR
SLIT
Al. BRACERS
ANNULAR SLIT
IM-99 RADOME
FUSED QUARTZ
DRIVE MOTOR
AIR VENTS
AIR
VENT
LIMIT
STOP
AIR VENT
B+, CELL BIAS, AND
POS. POT VOLTAGE
FIL.
GND.
DRIVE MOTOR
POS. POT. OUTPUT
CELL #1 OUTPUT
CELL #2 OUTPUT
METAL CAP
LIMIT STOP
1" RADIUS INSULATING
MATERIAL
2
CHANNEL
PRE-
AMP
4 ATTACHING BOLTS
POSITION INDICATOR
FOR ALIGNMENT
3.9"
POT. POSITION
PICK OFF
10.3"
INFRARED CONICAL SKIRT FUZE DETECTOR

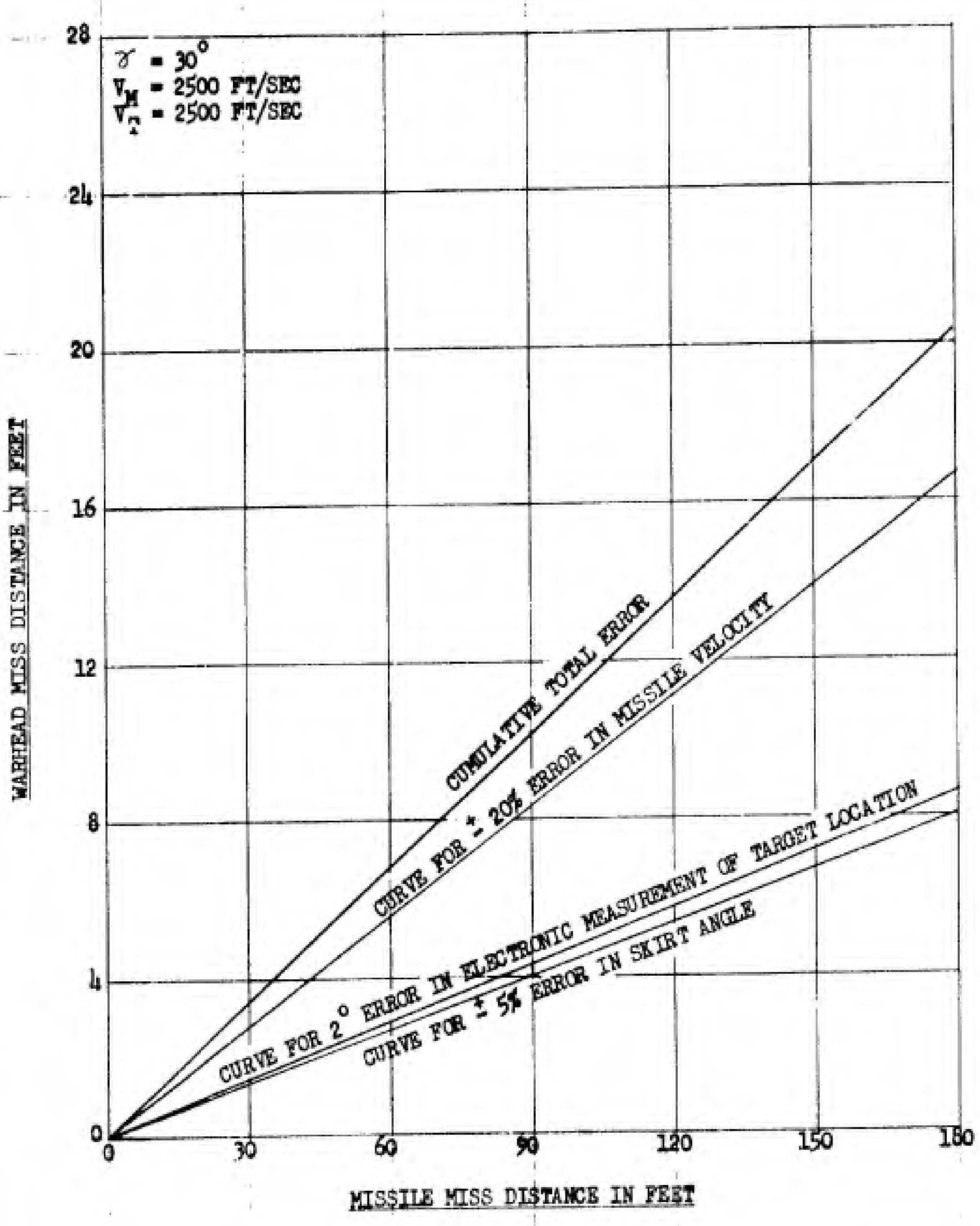

BREAKDOWN OF FUZING ERRORS FOR CONICAL SKIRT FUZING SYSTEM

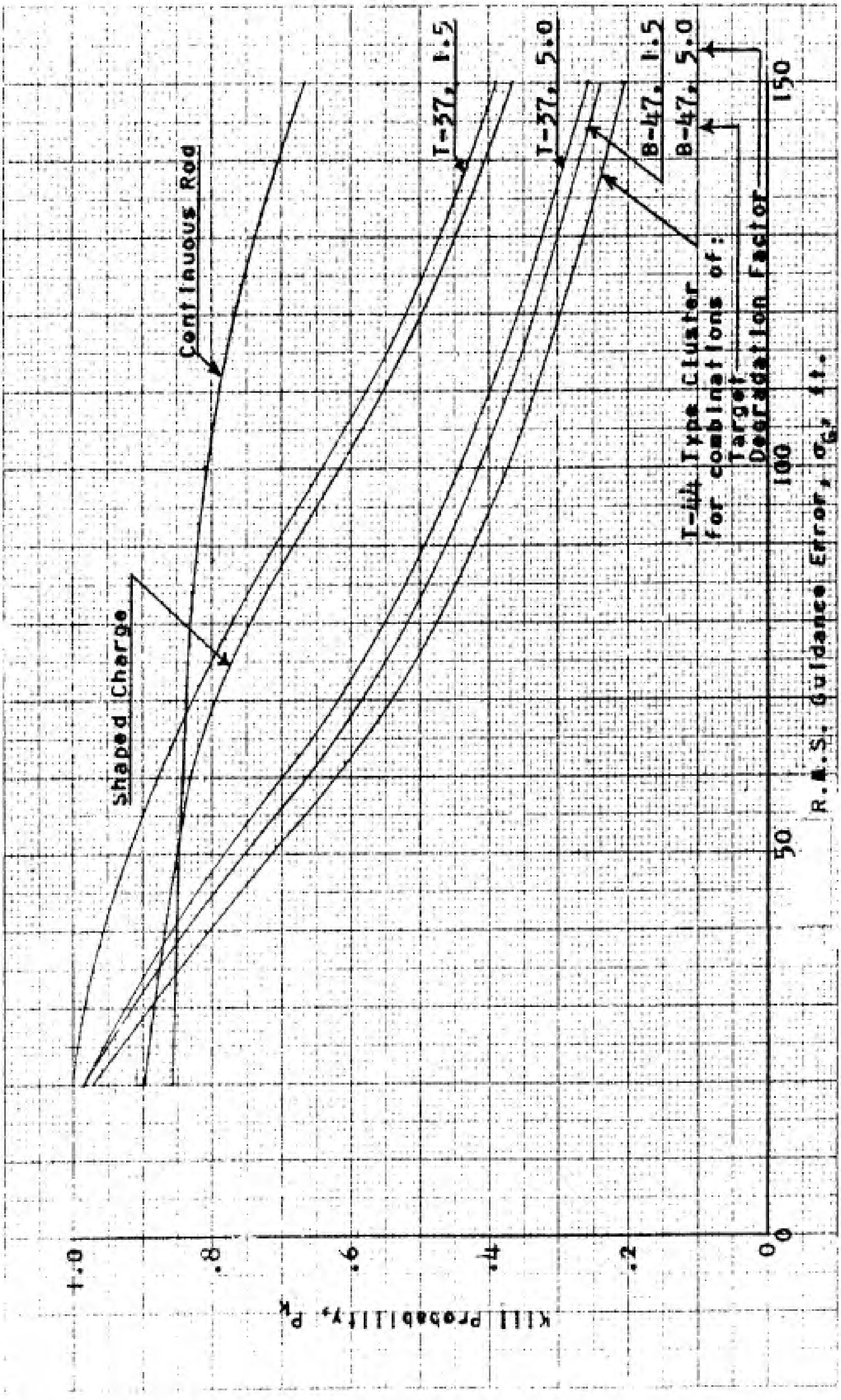

COMPARISON OF MAXIMUM ATTAINABLE KILL-PROBABILITY ESTIMATES - IM-99( ) WARHEAD

30,000 FT. ALTITUDE

Figure 62

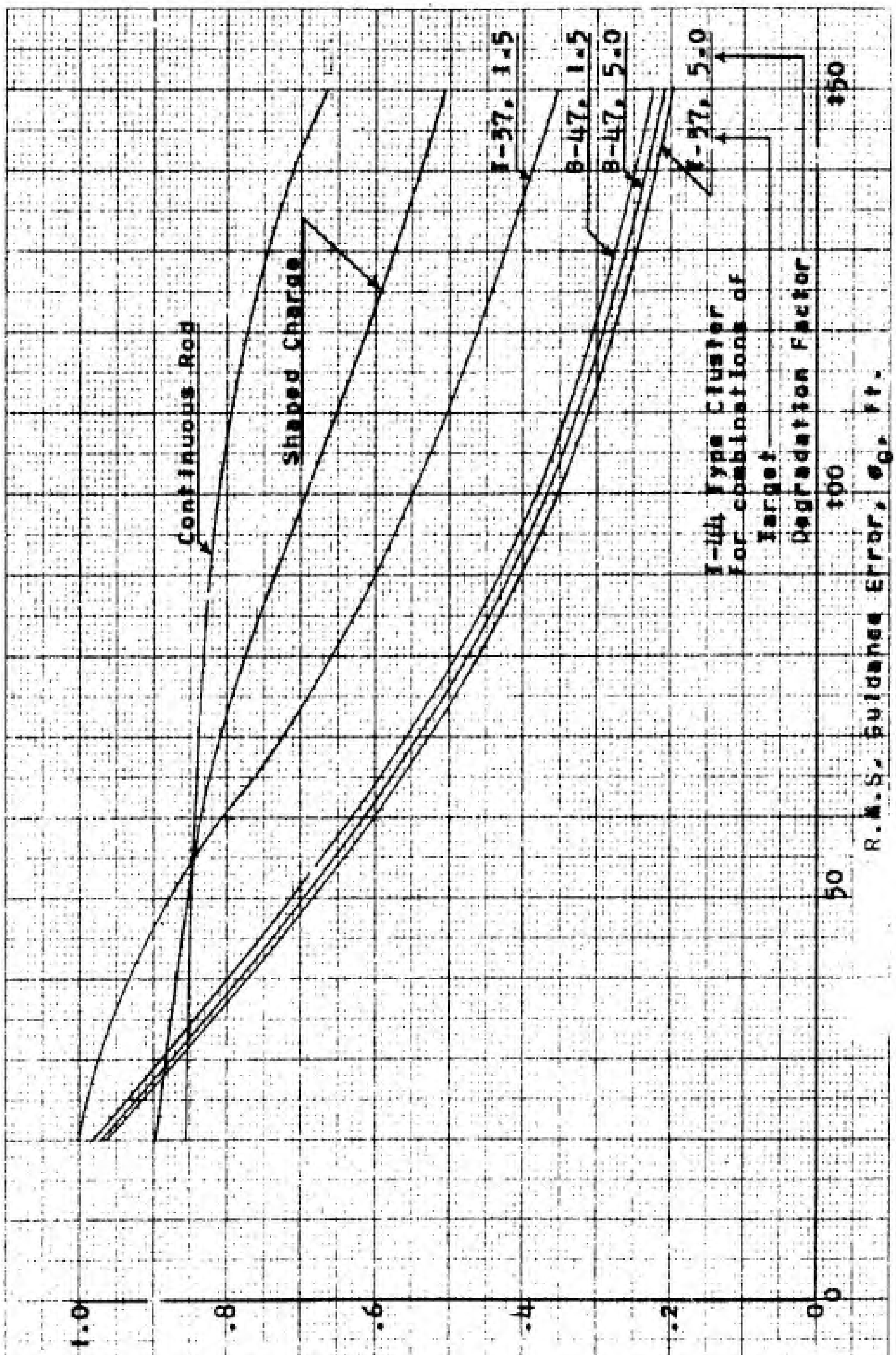

COMPARISON OF MAXIMUM ATTAINABLE KILL-PROBABILITY ESTIMATES - IM-99( ) WARHEAD

60,000 FT. ALTITUDE

Figure 63

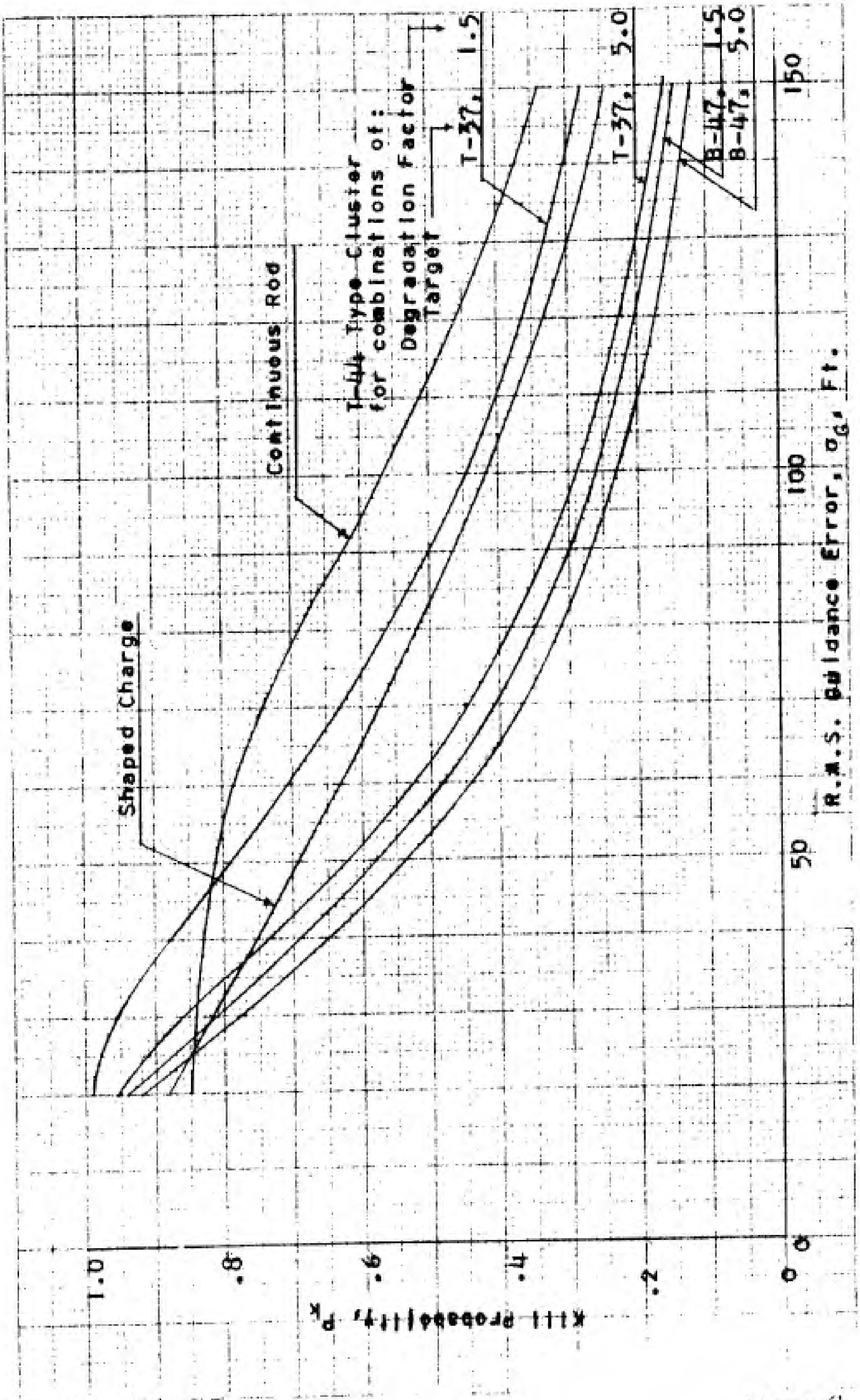

COMPARISON OF MAXIMUM ATTAINABLE KILL-PROBABILITY ESTIMATES - IM-99A WARHEAD
30,000 FT. ALTITUDE

Figure 64

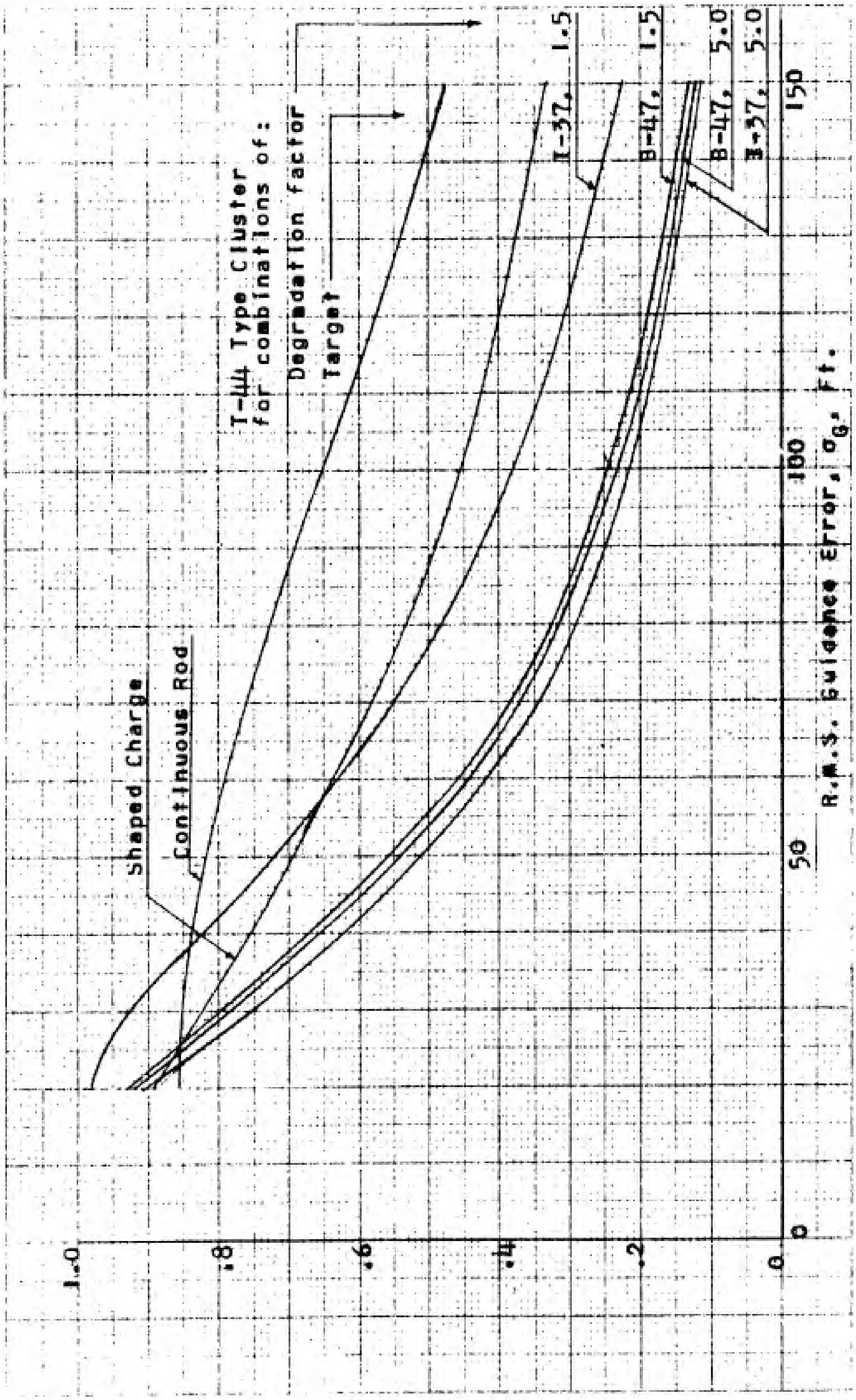

COMPARISON OF MAXIMUM ATTAINABLE KILL-PROBABILITY ESTIMATES - IM-99A WARHEAD
60,000 FT. ALTITUDE

Figure 65

TENTATIVE SCHEDULE FOR RECOMMENDED EXTENDED WORK

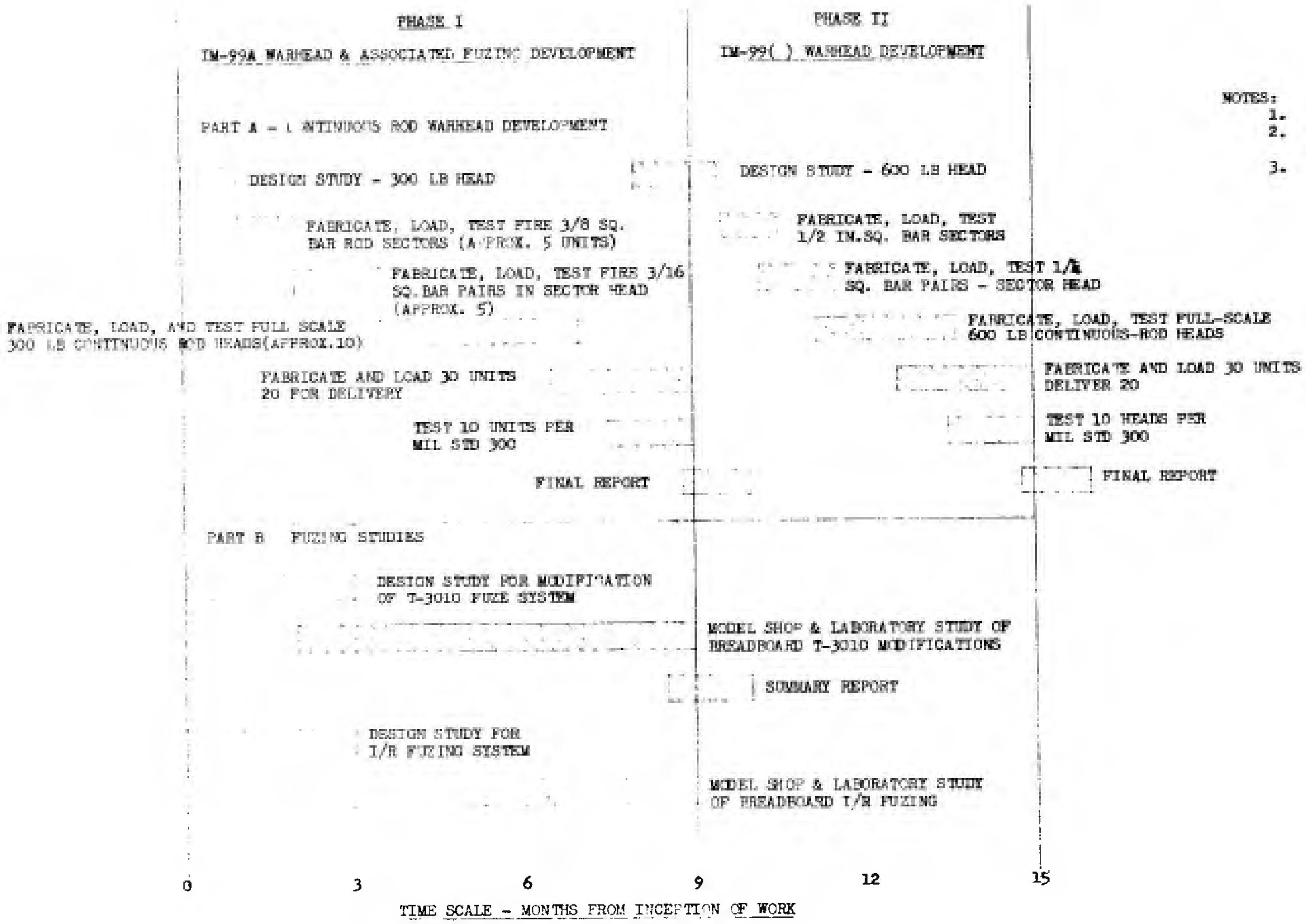

NOTES:
1. BASED ON COOPERATIVE EFFORT WITH NMIMT
2. PRELIMINARY TESTING AT AEROJET-GENERAL CHINO HILLS FACILITY WITH COMP.C-3 LOADING
3. FULL-SCALE HEADS TO BE H-6 LOADED AND TESTED AT AEROJET SACRAMENTO TEST FACILITY

Figure 66

APPENDIX

TABLE I

Calculated Results for Cluster Warhead Miss Distance

Sheet 1 of 10 Sheets

Altitude 15,000 feet
Missile Velocity (V_M) 1750 ft/sec

Note: See text for explanation and derivation

Target Velocity (V_T)	30° R_x	30° y_1	30° y_2	30° y_3	30° y_4	45° R_x	45° y_1	45° y_2	45° y_3	45° y_4	60° R_x	60° y_1	60° y_2	60° y_3	60° y_4	Cluster Radius (d)
800	60	60.0	-60.0	60	-60.	60	60.0	-60.0	60.0	-60.0	60	60.0	-60.0	60.0	-60.0	0
	245	61.5	-58.5	63.7	-56.3	232	62.2	57.8	64.6	-55.4	210	62.9	-57.1	64.9	-55.1	19.0
	489	65.9	-54.1	76.9	-43.1	466	68.8	-51.2	80.4	-39.6	437	71.8	-48.2	81.0	-39.0	36.4
	736	73.4	-46.6	104.3	-15.7	703	80.2	39.8	111.7	-8.3	663	87.2	-32.8	111.5	8.5	52.4
	983	84.1	-35.9	154.1	34.1	941	96.5	-23.5	165.1	45.1	887	109.5	-10.5	160.9	40.9	67.1
	1229	98.1	-21.9	243.5	123.5	1179	118.1	-1.9	252.3	132.3	1113	139.3	19.3	235.9	115.9	80.9
	1477	115.6	-4.4	409.	289.	1417	145.2	25.2	392.8	272.8	1338	177.1	57.1	345.9	225.9	93.7
	1724	136.7	16.7	759	639.	1655	178.1	58.1	626.8	506.8	1564	223.6	103.6	506.0	386.0	105.8
	1972	164.1	44.1	1765	1645.	1894	217.1	97.1	1044.	924.4	1790	279.3	159.3	740.6	620.6	117.2
	2219	190.0	70.0	14260	14140	2131	262.2	142.2	1897	1777	2015	344.6	224.6	1090	970.	127.9
	2467	222.3	102.6	-	-	2370	600.0	480.0	4304	4184	2241	420.5	300.5	1634	1514	138.1
1750	60	60.0	-60.0	60.0	-60.0	60	60.0	-60.0	60.0	-60.0	60	60.0	-60.0	60.0	-60.0	0
	328	62.3	-57.7	169.4	49.4	305	63.6	-56.1	89.8	-30.2	278	65.1	-54.9	77.8	-42.2	19.0
	663	69.3	-50.7			626	74.5	-45.5	260.5	140.5	579	80.5	-39.5	145.2	25.2	36.4
	1001	80.7	-39.3			949	92.5	-27.5	1538.	1418.	881	106.4	-13.6	300.7	180.7	52.4
	1338	96.5	-23.5			1260	117.6	-2.3			1184	143.0	23.0	637.4	517.4	67.1
	1676	116.7	-3.3			1595	149.9	29.9			1487	193.8	70.8	1454	1335.	80.9
	2014	141.1	21.1			1919	189.3	69.3			1789	258.7	138.7	4398	4278	93.7
	2351	169.8	49.8			2241	235.7	115.7			2093	320.1	200.1			105.8
	2690	202.5	82.5			2565	289.2	169.2			2395	402.1	282.1			117.2
	3027	239.0	119.0			2887	349.4	229.4			2699	495.6	375.6			127.9
	3366	279.5	159.5			3212	416.4	296.4			3001	601.0	481.0			138.1

TABLE I (Cont'd)

Calculated Results for Cluster Warhead Miss Distance

Sheet 2 of 10 Sheets

Altitude 15,000 feet
Missile Velocity (V_M) 1,000 ft/sec

Note: See text for explanation and derivation

Target Velocity (V_T)	APPROACH ANGLE (γ) 30°					45°					60°					Cluster Radius (d)
	R_x	y_1	y_2	y_3	y_4	R_x	y_1	y_2	y_3	y_4	R_x	y_1	y_2	y_3	y_4	
800	60	60.	-60	60.	-60.	60	60.	-60.	60.	-60.	60	60.	-60.	60.	-60.	0
	170	60.7	-59.3	64.5	-55.5	157	61.	-59.	64.2	-55.8	140	61.4	-58.6	63.6	-56.4	19.3
	339	62.7	-57.3	81.6	-38.4	318	64.6	-55.8	78.6	-41.4	291	65.7	-54.3	75.1	-44.9	37.7
	511	66.1	-53.9	123.0	3.0	482	69.4	-50.6	107.9	-12.1	445	73.0	-47.0	96.6	-23.4	55.0
	685	70.8	-49.2	218.8	98.8	648	76.7	-43.3	159.5	39.5	601	83.3	-36.7	130.5	10.5	71.6
	858	76.8	-43.2	486.0	366.0	814	86.1	-33.9	246.6	126.6	756	96.6	-23.4	180.2	60.2	87.4
	1031	84.2	-35.8	2318.7	2198.7	980	97.6	-22.4	397.4	277.4	912	113.0	-7.0	251.1	131.1	102.5
	1205	92.9	-27.1			1146	111.3	-8.7	681.1	561.1	1068	132.7	12.7	349.5	229.5	117.0
	1379	103.0	-17.0			1313	127.3	7.3	1297.6	1177.6	1224	155.6	35.6	488.3	368.3	130.8
	1552	114.4	-5.6			1479	145.3	25.3	3475.7	3355.7	1380	181.9	61.9	682.1	562.1	144.2
	1726	127.1	7.1			1645	165.7	45.7			1536	211.6	91.6	960.2	840.2	157.0
1,000	60	60.	-60.	60.	-60.	60	60.	-60.	60.	-60.	60	60.	-60.	60.	-60.	0
	187	60.8	-59.2	77.9	42.1	171	61.2	-58.8	68.4	-51.6	152	61.7	-58.3	65.5	-54.5	19.3
	375	63.0	-57.0	274.0	154.0	351	64.7	-55.3	101.1	-18.9	321	66.7	-53.3	83.7	-36.3	37.7
	567	66.8	-53.2			534	70.6	-49.4	182.9	62.9	492	75.0	-45.0	119.2	-.8	55.0
	759	72.1	-47.9			718	78.9	-41.1	385.9	265.9	665	86.8	-33.2	178.1	58.1	71.6
	953	78.8	-41.2			903	89.5	-30.5	1082.0	962.0	838	102.1	-17.9	271.1	151.1	87.4
	1145	86.9	-33.1			1087	102.3	-17.7	199697.	199577.	1010	120.8	.8	414.3	294.3	102.5
	1338	96.5	-23.5			1272	117.6	-2.4			1184	143.1	23.1	640.8	520.8	117.0
	1531	107.5	-12.5			1456	135.1	15.1			1356	169.0	49.0	1007.3	887.3	130.8
	1723	119.9	-.1			1641	155.1	35.1			1529	198.5	78.5	1656.2	1536.2	144.2
	1917	133.7	13.7			1825	177.3	57.3			1703	231.7	111.7	3000.2	2880.2	157.0

TABLE I (Cont'd)

Calculated Results For Cluster Warhead Miss Distance

Sheet 3 of 10 Sheets

Altitude 30,000 feet
Missile Velocity (V_M) 2500 ft/sec

Note: See text for explanation and derivation

Target Velocity (V_T)	APPROACH ANGLE (γ) 30° R_x	y_1	y_2	y_3	y_4	45° R_x	y_1	y_2	y_3	y_4	60° R_x	y_1	y_2	y_3	y_4	Cluster Radius (d)
800	60	60.	- 60.	60.	- 60.	60	60.0	- 60.0	60.0	- 60.0	60	60	- 60	60	- 60	0
	320	61.3	- 58.7	62.5	- 57.5	313	62.0	- 58.0	63.3	- 56.7	290	62.6	- 57.4	63.7	- 56.3	19.2
	639	65.5	- 54.5	70.9	- 49.1	615	68.2	- 51.8	74.2	- 45.3	585	70.7	- 49.3	75.7	- 44.3	36.9
	960	72.6	- 47.5	86.6	- 33.4	926	78.7	- 41.3	94.1	- 25.9	882	82.8	- 37.2	97.2	- 22.8	53.3
	1281	82.7	- 37.3	111.7	- 8.3	1237	93.8	- 27.2	125.5	5.5	1180	104.6	- 15.4	130.5	10.5	68.7
	1602	96.2	- 23.8	149.6	29.6	1549	114.1	- 5.9	171.7	51.7	1478	131.7	11.7	178.3	58.3	83.1
	1924	112.8	- 7.2	204.0	84.0	1861	139.3	19.3	235.8	115.8	1776	165.6	45.6	242.7	122.7	96.7
	2246	133.4	13.4	282.9	162.9	2172	170.6	50.6	325.7	205.7	2074	208.1	88.1	329.9	209.9	109.5
	2568	157.4	37.4	395.2	275.2	2484	207.4	87.4	447.4	327.4	2372	258.6	138.6	443.1	323.1	121.7
	2888	185.8	65.8	561.7	441.7	2796	251.1	131.1	617.1	497.1	2670	319.0	199.0	592.8	472.8	133.2
	3212	218.2	98.2	812.3	692.3	3107	301.2	181.2	851.5	731.5	2968	389.0	269.0	786.5	666.5	144.2
2500	60	60	- 60	60	- 60	60	60	- 60	60	- 60	60	60	- 60	60.	60.	0
	471	62.8	- 57.2	156.2	36.2	442	64.4	- 55.6	93.5	- 26.5	406	68.5	- 51.5	80.7	39.3	19.2
	952	71.3	- 48.7			903	77.6	- 42.4	261.3	141.3	838	84.9	- 35.1	157.5	37.5	36.9
	1435	85.1	- 34.9			1364	99.4	- 20.6	938	818	1270	116.0	- 4.0	320.8	200.8	53.3
	1917	104.4	- 15.6			1825	129.8	9.8	35395	35275	1703	160.1	40.1	636.9	516.9	68.7
	2400	129.2	9.2			2289	169.3	49.3			2135	217.9	97.9	1256.0	1136.0	83.1
	2883	158.7	38.7			2748	216.5	96.5			2568	287.9	167.9	2603.4	2483.4	96.7
	3367	193.9	73.9			3212	273.3	153.3			3001	372.8	252.8	6785.7	6665.7	109.5
	3848	233.7	113.7			3673	337.8	217.8			3434	471.4	350.4	93785.5	93625.5	121.7
	4332	279.0	159.0			4136	411.8	291.8			3868	583.5	463.5			133.2
	4817	328.8	206.8			4598	493.6	373.6			4299	709.9	589.9			144.2

TABLE I (Cont'd)

Calculated Results for Cluster Warhead Miss Distance

Sheet 4 of 10 Sheets

Altitude 30,000 feet
Missile Velocity (V_M) 1750 ft/sec

Note: See text for explanation and derivation

Target Velocity (V_T)	30° R_x	30° y_1	30° y_2	30° y_3	30° y_4	45° R_x	45° y_1	45° y_2	45° y_3	45° y_4	60° R_x	60° y_1	60° y_2	60° y_3	60° y_4	Cluster Radius (d)
	60	60	- 60	60	- 60	60	60	- 60	50	- 60	60	60	- 60	60	- 60	0
	245	60.9	- 59.1	62.1	- 57.9	232	61.3	- 58.7	62.6	- 57.4	210	61.7	- 58.3	62.9	- 57.1	19.4
	489	63.5	- 56.5	69.0	- 51.0	466	65.2	- 54.8	71.1	- 48.9	437	66.9	- 53.1	71.7	- 48.3	37.7
	736	67.8	- 52.2	82.0	- 38.0	703	71.8	- 48.2	86.6	- 33.4	663	75.7	- 44.3	87.5	- 32.5	55.0
	983	74.0	- 46.0	102.4	- 17.6	941	81.1	- 38.9	110.6	- 9.4	887	88.3	- 31.7	114.4	- 8.2	71.5
800	1229	82.0	- 38.0	132.6	12.6	1179	93.3	- 26.7	144.8	24.8	1113	104.7	- 15.3	144.6	24.6	87.2
	1477	91.9	- 28.1	175.6	55.6	1417	108.4	- 11.6	191.9	71.9	1338	115.3	5.3	188.9	68.9	102.2
	1724	103.8	- 16.2	246.4	116.4	1655	126.6	6.6	255.3	135.3	1564	150.2	30.2	246.3	126.3	116.5
	1972	117.7	- 2.3	322.1	202.1	1894	147.8	27.8	339.8	219.8	1790	179.6	59.6	319.5	199.5	130.3
	2219	133.6	13.6	444.6	324.6	2131	172.4	52.4	452.1	332.1	2015	213.8	93.8	411.9	291.9	143.5
	2467	151.6	31.6	625.2	505.2	2370	200.3	80.3	602.4	482.4	2241	252.8	132.8	527.7	407.7	156.2
	60	60	- 60	60.0	- 60.0	60	60	- 60	60	- 60	60	60	- 60	60.0	- 60.0	0
	328	61.4	- 58.6	93.0	- 27.0	305	62.1	- 57.9	75.0	- 45	278	63.0	- 57.0	69.8	- 57.2	19.4
	663	65.5	- 54.5	526.3	406.3	626	68.6	- 51.4	136.2	- 13.6	579	72.1	- 47.9	103.4	- 16.6	37.7
	1001	72.4	- 47.6			949	79.3	- 40.6	292.0	172.0	881	87.4	- 32.6	169.0	49.0	55.0
	1338	81.9	- 38.1			1260	94.3	- 25.7	700.6	580.6	1184	108.8	- 11.2	278.9	158.9	71.5
1750	1676	94.1	- 25.9			1595	113.5	- 6.5	2320.	2200.	1487	136.5	16.5	453.6	333.6	87.2
	2014	108.9	- 11.1			1919	136.9	16.9			1789	170.5	60.5	727.8	607.8	102.2
	2351	126.3	6.3			2241	164.6	44.6			2093	211.1	91.1	1169.	1049.	116.5
	2690	146.2	26.3			2565	196.5	76.5			2395	258.2	138.2	1918.	1798.	130.3
	3027	168.8	48.8			2887	230.0	110.0			2699	312.1	192.1	3334.	3214.	143.5
	3366	193.8	73.8			3212	273.1	153.1			3001	372.6	252.6	6703.	6583	156.2

TABLE I (Cont'd)

Calculated Results for Cluster Warhead Miss Distance

Sheet 5 of 10 Sheets

Altitude 30,000 feet
Missile Velocity (V_M) 1000 ft/sec

Note: See text for explanation and derivation

Target Velocity (V_T)	APPROACH ANGLE (γ) 30° R_x	30° y_1	30° y_2	30° y_3	30° y_4	45° R_x	45° y_1	45° y_2	45° y_3	45° y_4	60° R_x	60° y_1	60° y_2	60° y_3	60° y_4	Cluster Radius (d)
800	60	60	- 60	60	- 60	60	60	- 60	60	- 60	60	60	- 60	60	- 60	0
	170	60.4	- 59.6	62.5	- 57.5	157	60.6	- 59.4	62.4	- 57.6	140	60.9	- 59.1	62.1	- 57.9	19.4
	339	61.6	- 58.4	70.6	- 49.4	318	62.4	- 57.6	69.8	- 50.2	291	63.3	- 56.7	68.3	- 51.7	38.1
	511	63.6	- 56.4	87.5	- 32.5	482	65.5	- 54.5	84.2	- 35.8	445	67.7	- 52.3	79.9	- 40.1	56.3
	685	66.4	- 53.6	116.0	- 4.0	648	69.9	- 50.1	106.3	- 13.7	601	73.7	- 46.3	96.8	- 23.2	73.8
	858	70.1	- 49.9	163.0	43.0	814	75.5	- 44.5	138.8	+ 18.8	756	81.5	- 38.5	120.4	.4	90.9
	1031	74.4	- 45.6	238.4	118.4	980	82.2	- 37.8	183.3	63.3	912	90.9	- 29.1	150.6	30.6	107.5
	1205	79.6	- 40.4	368.2	248.2	1146	90.3	- 29.7	245.5	125.5	1068	102.3	- 17.7	189.8	69.8	123.6
	1379	85.6	- 34.4	609.5	489.5	1313	99.7	- 20.3	339.9	209.9	1224	115.5	- 4.5	238.7	118.7	139.3
	1552	92.4	- 27.6	1157.	1037.	1479	110.2	- 9.8	445.9	325.9	1380	130.5	10.5	298.9	178.9	154.5
	1726	99.9	- 20.1	3295.	3175.	1645	122.0	2.0	607.6	487.6	1536	147.3	27.[illegible]	372.6	252.6	169.4
1000	60	60	- 60	60	- 60	60	60	- 60	60	- 60	60	60	- 60	60	- 60	0
	187	60.5	- 59.5	68.5	- 51.5	171	60.7	- 59.3	64.6	- 55.4	152	61.0	- 59.0	63.2	- 56.8	19.4
	375	61.8	- 58.2	107.2	- 12.8	351	62.8	- 57.2	80.0	- 40.0	321	63.9	- 56.1	72.8	- 47.2	38.1
	567	64.1	- 55.9	258	137.8	534	66.3	- 53.7	112.1	- 7.9	492	68.9	- 51.1	90.9	- 29.1	56.3
	759	67.2	- 52.8	2117	1997.	718	71.2	- 48.8	167.6	47.6	665	75.8	- 44.2	118.6	- 1.4	73.8
	953	71.3	- 48.7			903	77.6	- 43.2	261.3	141.3	838	84.9	- 35.1	157.5	37.5	90.9
	1145	76.1	- 43.9			1087	85.2	- 34.8	417.5	277.5	1010	95.7	- 24.3	209.3	89.3	107.5
	1338	81.9	- 38.1			1272	94.3	- 25.7	702.4	582.4	1184	108.7	- 11.3	278.1	158.1	123.6
	1531	88.6	- 31.4			1456	104.8	- 15.2	1292	1172	1356	123.9	3.9	369.2	249.2	139.3
	1723	96.1	- 23.9			1641	116.6	- 3.4	2998	2878	1529	141.0	21.0	485.8	365.8	154.5
	1917	104.4	- 5.6			1825	129.8	9.8	33034	32914	1703	160.1	40.1	636.6	516.6	169.4

TABLE I (Cont'd)

Calculated Results for Cluster Warhead Miss Distance

Sheet 6 of 10 Sheets

Altitude 45,000 feet
Missile Velocity (V_M) 2500 ft/sec

Note: See text for explanation and derivation

Target Velocity (V_T)	APPROACH ANGLE (γ) 30°					45°					60°					Cluster Radius (d)
	R_x	y_1	y_2	y_3	y_4	R_x	y_1	y_2	y_3	y_4	R_x	y_1	y_2	y_3	y_4	
800	60	60	- 60	60	- 60	60	60	- 60	60	- 60	60	60	- 60	60	- 60	0
	320	60.7	- 59.3	61.3	- 58.7	313	61.0	- 59.0	61.7	- 58.3	290	61.3	- 58.7	61.9	- 58.1	19.4
	639	62.8	- 57.2	65.3	- 54.7	615	64.2	- 55.8	66.9	- 53.1	585	65.4	- 54.6	67.7	- 52.3	38.0
	960	66.4	- 53.6	72.2	- 47.8	926	69.4	- 50.6	76.0	- 44.0	882	72.3	- 47.7	77.7	- 42.3	55.9
	1281	71.4	- 48.6	82.6	- 37.4	1237	76.9	- 43.1	89.3	- 30.7	1180	82.0	- 38.0	92.4	- 27.6	73.1
	1602	77.8	- 42.2	96.7	- 23.3	1549	86.5	- 33.5	107.3	- 12.7	1478	94.7	- 25.3	111.9	- 8.1	89.7
	1924	85.9	- 34.1	115.2	- 4.8	1861	98.5	- 21.5	130.7	- 10.7	1776	110.5	- 9.5	137.1	17.1	105.7
	2246	95.6	- 24.4	138.8	18.8	2172	113.1	- 6.9	160.4	40.4	2074	129.8	9.8	168.7	48.7	121.1
	2568	106.9	- 13.1	167.9	47.9	2484	130.0	10.0	196.4	76.4	2372	152.2	32.2	206.6	86.6	136.0
	2888	119.9	- .1	203.8	83.8	2796	149.5	19.5	240.4	120.4	2670	178.3	58.3	252.2	132.2	150.5
	3212	134.6	14.6	247.6	127.6	3107	171.7	51.7	293.1	173.1	2968	208.1	88.1	306.2	186.2	164.5
2500	60	60	- 60	60	- 60	60	60	- 60	60	- 60	60	60	- 60	60	- 60	0
	471	61.5	- 58.5	89.7	- 30.3	442	62.3	- 57.7	75.3	- 44.7	406	63.2	- 52.8	70.2	- 49.8	19.4
	952	65.9	- 54.1	271.7	211.7	903	69.2	- 50.8	131.3	11.3	838	72.8	- 47.2	103.8	- 16.2	38.0
	1435	73.1	- 46.9	2350	2290	1364	80.5	- 39.5	251.9	131.9	1270	88.8	- 31.2	165.5	45.5	55.9
	1917	83.3	- 36.7			1825	96.3	- 23.7	487.4	367.4	1703	111.3	- 8.7	262.9	142.9	73.1
	2400	96.1	- 23.9			2289	116.4	- 3.6	957.4	837.4	2135	140.0	20.0	405.0	285.0	89.7
	2883	111.8	- 8.2			2748	141.1	21.1	2040	1920	2568	175.5	55.5	607.2	487.2	105.7
	3367	130.4	10.4			3212	170.5	50.5	5918	5798	3001	218.1	98.1	892.4	772.4	121.1
	3848	151.5	31.5			3673	204.0	84.0			3434	266.7	146.7	1286	1166	136.0
	4332	175.5	55.5			4136	242.1	122.1			3868	322.4	202.4	1845	1725	150.5
	4817	202.0	82.0			4598	284.7	164.7			4299	385.1	265.1	2655	2535	164.5

TABLE I (Cont'd)

Calculated Results for Cluster Warhead Miss Distance

Sheet 7 of 10 Sheets

Altitude 45,000 Feet
Missile Velocity V_M 1750 Ft/Sec

Note: See text for explanation and derivation

Target Velocity V_T	APPROACH ANGLE (γ) 30° R_x	30° y_1	30° y_2	30° y_3	30° y_4	45° R_x	45° y_1	45° y_2	45° y_3	45° y_4	60° R_x	60° y_1	60° y_2	60° y_3	60° y_4	Cluster Radius (d)
	60	60	- 60	60	-60	60	60	-60	60	-60	60	60	-60	60	-60	0
	245	60.5	- 59.5	61.1	-58.9	232	60.7	-59.3	61.4	-58.6	210	60.9	-59.1	61.4	-58.6	19.4
	489	61.7	-58.3	64.2	-55.8	466	62.6	-57.4	65.3	-54.7	437	63.4	-56.6	65.6	-54.4	38.3
	736	64.0	-54.0	70.2	-49.8	703	66.1	-53.9	72.7	-47.3	663	68.0	-52.0	73.4	-46.6	56.6
	983	67.1	-52.9	78.7	-41.3	941	70.7	-49.3	[illegible]	-36.9	887	74.2	-45.8	84.2	-35.8	74.4
800	1229	71.2	-48.8	90.4	-29.6	1179	76.8	-43.2	97.1	-22.9	1113	82.4	-37.6	98.6	-21.4	91.8
	1477	76.1	-43.9	105.5	-14.5	1417	84.3	-35.7	115.2	- 4.8	1338	92.4	-27.6	116.9	- 3.1	108.6
	1724	82.1	-37.9	124.8	4.8	1655	93.3	-26.7	137.9	17.9	1564	104.5	-15.5	139.7	19.7	125.0
	1972	88.9	-31.1	148.4	28.4	1894	103.6	-16.4	165.3	45.3	1790	118.4	- 1.6	166.8	46.8	141.1
	2219	96.7	-23.3	177.3	57.3	2131	115.5	- 4.5	198.2	78.2	2015	134.4	14.4	198.8	78.8	156.7
	2467	105.5	-14.5	212.0	92.0	2370	128.8	8.8	237.0	117.0	2241	152.5	32.5	236.1	116.1	172.0
	60	60	-60	60	-60	60	60	-60	60	-60	60	60	-60	60	-60	0
	328	60.7	-59.3	73.1	-46.9	305	61.1	-58.9	67.3	-52.7	278	61.6	-58.4	65.0	-55.0	19.4
	663	62.8	-57.2	128.5	8.5	626	64.3	-55.7	90.6	-29.4	579	66.1	-53.9	79.9	-40.1	38.3
	1001	66.5	-53.5	315.9	195.9	949	70.1	-49.9	139.8	17.8	881	74.2	-45.8	108.6	-11.4	56.6
	1338	71.4	-48.3	1189	1069	1260	77.8	-42.2	219.6	99.6	1184	85.0	-35.0	150.2	30.2	74.4
1750	1676	77.8	-42.2			1595	87.7	-32.2	348.3	228.3	1487	99.1	-20.9	208.7	88.7	91.8
	2014	85.5	-34.5			1919	99.8	-20.2	553.7	433.7	1789	116.4	- 3.6	286.7	166.7	108.6
	2351	94.7	-25.3			2241	114.3	- 5.7	890.9	770.9	2093	137.1	17.1	399.3	279.3	125.0
	2690	105.2	-14.8			2565	130.8	10.8	1478	1358	2395	160.8	40.8	519.1	399.1	141.1
	3027	117.1	- 2.9			2887	149.5	29.5	2665	2545	2699	187.7	67.7	684.3	564.3	156.7
	3366	130.3	10.3			3212	170.3	50.3	5856	5736	3001	217.8	97.8	891.6	771.6	172.0

TABLE I (Cont'd)

Calculated Results For Cluster Warhead Miss Distance

Sheet 8 of 10 Sheets

Altitude 45000 Ft.
Missile Velocity V_M 1000 Ft/Sec

Note: See text for explanation and derivation

Target Velocity (V_T)	APPROACH ANGLE (γ) 30° R_x	30° y_1	30° y_2	30° y_3	30° y_4	45° R_x	45° y_1	45° y_2	45° y_3	45° y_4	60° R_x	60° y_1	60° y_2	60° y_3	60° y_4	Cluster Radius (d)
800	60	60	-60	60	-60	60	60	-60	60	-60	60	60	-60	60	-60	0
	170	60.3	-59.7	61.5	-58.5	157	60.4	-59.6	61.5	-58.5	140	60.6	-59.4	61.3	-58.7	18.7
	339	60.8	-59.2	65.0	-55.0	318	61.3	-58.7	64.8	-55.2	291	61.7	-58.3	64.2	-55.8	37.1
	511	61.9	-58.1	72.3	-47.7	482	63.0	-57.0	71.7	-48.3	445	64.1	-55.9	70.0	-50.0	55.2
	685	63.3	-56.7	82.4	-37.6	648	65.1	-54.9	80.7	-39.3	601	67.0	-53.0	77.5	-42.5	73.0
	858	65.2	-54.8	97.7	-22.3	814	68.0	-52.0	94.0	-26.0	756	71.1	-48.9	88.2	-31.8	90.4
	1031	67.4	-52.6	117.0	- 3.0	980	71.4	-48.6	110.0	-10.0	912	75.7	-44.3	100.9	-19.1	107.7
	1205	70.1	-49.9	143.8	23.8	1146	75.6	-44.4	131.2	11.2	1068	81.6	-38.4	117.3	- 2.7	124.6
	1379	73.2	-46.8	177.7	57.7	1313	80.3	-39.7	156.5	36.5	1224	88.1	-31.9	136.3	16.3	141.3
	1552	76.8	-43.2	222.0	102.0	1479	85.8	-34.2	187.8	67.8	1380	95.8	-24.2	159.1	39.1	157.7
	1726	80.6	-39.4	277.4	157.4	1645	91.8	-28.2	224.0	104.0	1536	104.1	-15.9	184.7	64.7	173.9
1000	60	60	-60	60	-60	60	60	-60	60	-60	60	60	-60	60	-60	0
	187	60.3	-59.7	64.7	-55.3	171	60.5	-59.5	62.8	-57.2	152	60.6	-59.4	62.0	-58.0	18.7
	375	60.9	-59.1	77.2	-42.8	351	61.4	-58.6	69.3	-50.7	321	62.0	-58.0	66.3	-53.7	37.1
	567	62.2	-57.8	107.6	-12.4	534	63.4	-56.6	83.1	-36.9	492	64.7	-55.3	75.2	-44.8	55.2
	759	63.7	-56.3	161.5	41.5	718	65.8	-54.2	102.1	-17.9	665	68.1	-51.9	86.9	-33.1	73.0
	953	65.9	-54.1	270.0	150.0	903	69.1	-50.9	131.0	11.0	838	72.8	-47.2	103.7	-16.3	90.4
	1145	68.4	-51.6	493.8	373.8	1087	73.0	-47.0	168.1	48.1	1010	78.2	-41.8	123.9	3.9	107.7
	1338	71.4	-48.6	1171	1051	1272	77.8	-42.2	219.8	99.8	1184	85.0	-35.0	150.2	30.2	124.6
	1531	74.9	-45.1	12,935	12,815	1456	83.1	-36.9	286.2	166.2	1356	92.6	-27.4	181.2	61.2	141.3
	1723	78.8	-41.2			1641	89.4	-30.6	373.8	253.8	1529	101.5	-18.5	219.0	99.0	157.7
	1917	83.1	-36.9			1825	96.1	-23.9	485.3	365.3	1703	111.0	- 9.0	261.9	141.9	173.9

TABLE I (Cont'd)
Calculated Results For Cluster Warhead Miss Distance

Sheet 9 of 10 Sheets

Altitude 60,000 feet
Missile Velocity (V_M) 2500 ft/sec

Note: See text for explanation and derivation.

Target Velocity (V_T)	APPROACH ANGLE (γ) 30° R_x	30° y_1	30° y_2	30° y_3	30° y_4	45° R_x	45° y_1	45° y_2	45° y_3	45° y_4	60° R_x	60° y_1	60° y_2	60° y_3	60° y_4	Cluster Radius (d)
800	60	60.0	-60.0	60.0	-60.0	60	60.0	-60.0	60.0	-60.0	60	60.0	-60.0	60.0	-60.0	0
	320	60.3	-59.7	60.6	-59.6	313	60.5	-59.5	60.8	-59.2	290	60.6	-59.6	60.9	-59.1	19.2
	639	61.4	-58.6	62.5	-57.5	615	62.0	-58.0	63.2	-56.8	585	62.6	-57.4	63.6	-56.4	38.1
	960	63.0	-57.0	65.6	-54.3	926	64.5	-55.5	67.3	-52.7	882	65.7	-54.3	68.1	-51.9	56.5
	1281	65.5	-54.5	70.2	-49.8	1237	68.0	-52.0	73.3	-46.7	1180	70.3	-49.7	74.7	-45.2	74.6
	1602	68.5	-51.5	76.2	-43.8	1549	72.6	-47.4	81.2	-38.8	1478	76.2	-43.8	83.2	-36.8	92.3
	1924	71.3	-47.7	83.7	-36.3	1861	78.3	-41.7	90.9	-29.1	1776	83.5	-36.5	93.9	-26.1	109.7
	2246	76.8	-43.2	92.9	-27.1	2172	84.9	-35.1	102.9	-17.2	2074	92.1	-27.9	106.7	-13.3	126.8
	2568	82.1	-37.9	103.1	-16.9	2484	92.7	-27.3	116.8	- 3.2	2372	102.1	-17.9	121.9	1.9	143.5
	2888	88.1	-31.9	116.5	- 3.5	2796	101.6	-18.4	133.1	13.1	2670	113.6	- 6.4	139.4	19.4	160.0
	3212	94.8	-25.2	131.2	+11.2	3107	111.6	- 8.4	151.8	31.8	2968	126.6	+ 6.6	159.5	39.5	176.1
2500	60	60	- 60.0	60.	-60	60	60	-60	60	-60.	60	60	-60	60	-60	0
	471	60.7	- 59.3	72.0	-48.0	442	61.1	-58.9	67.0	-53.0	406	61.6	-58.4	64.9	-55.1	19.2
	552	62.9	- 57.1	117.1	- 2.9	903	64.5	-55.5	89.6	-30.4	838	66.2	-53.8	79.9	-40.1	38.1
	1435	66.4	- 53.6	221.3	101.3	1364	69.9	-50.1	130.9	+10.9	1270	73.9	-46.1	105.7	-14.3	56.5
	1917	71.4	- 48.6	424.4	334.4	1825	77.7	-42.3	196.8	76.8	1703	84.9	-35.1	144.7	24.7	74.6
	2400	77.8	- 42.2	1040.	919.7	2289	[illegible]	-32.4	292.4	172.4	2135	98.8	-21.2	196.4	76.4	92.3
	2883	85.6	- 34.4	3544.	3424.	2748	99.8	-20.2	423.0	303.0	2568	116.0	- 4.0	263.9	143.9	109.7
	3367	94.7	- 25.3			3212	114.0	- 6.0	613.0	493.0	3001	136.3	16.3	347.9	227.9	126.8
	3848	105.2	- 14.8			3673	130.5	+10.5	870.6	750.6	3434	159.7	19.7	451.2	331.2	143.5
	4332	110.7	- 9.3			4136	149.2	29.2	1229.	1109.	3868	186.3	66.3	576.1	456.1	160.0
	4817	130.4	10.4			4598	170.1	60.1	1733.	1613	4299	216.1	96.1	725.0	605.0	176.1

TABLE I (Cont'd)
Calculated Results For Cluster Warhead Miss Distance

Sheet 10 of 10 Sheets

Altitude 60,000 feet
Missile Velocity (V_M) 1750 ft/sec

Note: See text for explanation and derivation.

Target Velocity (V_T)	APPROACH ANGLE (γ) 30°					45°					60°					Cluster Radius (d)
	R_x	y_1	y_2	y_3	y_4	R_x	y_1	y_2	y_3	y_4	R_x	y_1	y_2	y_3	y_4	
800	60	60	-60.0	60.0	-60.0	60	60	-60.0	60.0	-60.0	60	60.0	-60.0	60.0	-60.0	0
	291	60.1	-59.9	60.3	-59.7	232	60.2	-59.8	60.3	-59.7	210	60.2	-59.8	60.4	-59.6	18.8
	489	60.9	-59.1	62.0	-58.0	466	61.3	-58.7	62.5	-57.5	437	61.7	-58.3	62.7	-57.3	37.3
	736	61.8	-58.2	64.4	-55.6	703	62.8	-57.2	65.6	-54.3	663	63.6	-56.4	65.9	-51.0	55.5
	983	63.5	-56.5	68.5	-51.5	941	65.2	-54.8	70.6	-49.4	887	66.8	-53.2	71.2	-48.8	73.5
	1229	65.3	-54.6	73.2	-46.8	1179	68.0	-52.0	76.5	-43.5	1113	70.5	-49.5	77.4	-42.6	91.2
	1477	67.8	-52.2	79.8	-40.2	1417	71.7	-48.3	84.5	-35.5	1338	75.5	-44.5	85.9	-34.1	108.6
	[illegible]	70.5	-49.5	87.1	-32.9	1655	75.2	-44.2	93.5	-26.5	1564	81.0	-39.0	95.3	-24.7	137.2
	1972	73.9	-46.1	96.4	-23.6	1894	80.8	-39.2	104.8	-15.2	1790	87.7	-32.3	106.9	-13.1	142.8
	2219	77.5	-42.5	106.7	-13.3	2131	86.3	-33.9	117.3	- 2.7	2015	95.0	-25.0	119.8	- .2	159.7
	2467	81.8	-38.2	119.0	- 1.0	2370	92.7	-27.3	132.2	12.2	2241	103.6	-16.4	125.1	15.1	176.1
1750	60	60.0	-60.0	60.0	-60.0	60	60.0	-60.0	60.0	-60.0	60	60.0	-60.0	60.0	-60.0	0
	328	60.2	-59.8	62.9	-57.1	305	60.3	-59.7	61.8	-58.2	278	60.4	-59.6	61.2	-58.8	18.8
	663	61.4	-58.6	84.5	-35.5	626	62.2	-57.8	73.7	-46.3	579	63.0	-57.0	69.4	-50.6	37.3
	1001	63.0	-57.0	120.7	+ .7	949	64.6	-55.4	90.9	-29.1	881	66.5	-53.5	80.7	-39.3	55.5
	1338	65.6	-54.4	193.9	73.9	1260	68.7	-51.3	120.8	+ .8	1184	72.1	-47.9	99.6	-20.4	73.5
	1676	68.6	-51.4	311.9	191.9	1595	73.3	-46.7	158.7	38.7	1487	78.7	-41.3	122.4	2.4	91.2
	2014	72.6	-47.4	532.3	412.3	1919	79.5	-40.5	213.1	93.1	1789	87.4	-32.5	153.8	33.8	108.6
	2351	76.9	-43.1	946.8	826.8	2241	86.3	-33.7	278.9	158.9	2093	97.3	-23.0	189.5	69.5	137.2
	2690	82.3	-37.7	2010.	1890.	2565	94.6	-25.4	367.3	247.3	2395	108.7	-11.3	234.9	114.9	142.8
	3027	88.0	-32.0	7162	7042	2887	103.6	-16.4	474.0	354.0	2699	121.4	1.4	286.1	166.1	159.7
	3366	94.7	-25.3			3212	114.0	- 6.0	613.0	493.0	3001	136.3	16.3	348.2	228.2	176.1

Sheet 1 of 10 Sheets

TABLE II

Calculated Results for Accelerated Cluster Warhead Miss Distance

Altitude 15,000 feet
Missile Velocity (V_M) 1750 ft/sec

Note: See text for explanation and derivation.

Target Velocity (V_T)	APPROACH ANGLE (γ) 30°					45°					60°					Cluster Radius (d)
	R_x	y_1	y_2	y_3	y_4	R_x	y_1	y_2	y_3	y_4	R_x	y_1	y_2	y_3	y_4	
800	60	60.0	-60.0	60.0	-60.0	60	60.0	-60.0	60.0	-60.0	60	60.0	-60.0	60.0	-60.0	0
	245	58.6	-61.4	57.9	-63.1	232	57.9	-62.1	56.1	-63.9	210	57.2	-62.8	55.7	-64.3	21.1
	489	54.2	-65.8	48.7	-71.3	466	51.5	-68.5	45.3	-74.7	437	48.9	-71.1	43.7	-76.3	44.6
	736	55.7	-64.3	50.9	-69.1	703	53.6	-66.4	48.4	-71.6	663	41.7	-68.3	47.3	-72.7	68.2
	983	61.1	-58.9	62.7	-57.3	941	61.7	-58.3	63.3	-56.7	887	62.2	-57.8	63.6	-57.4	89.3
	1229	70.8	-49.2	89.3	-30.7	1179	76.2	-43.8	95.8	-24.2	1113	81.6	-38.4	97.3	-22.7	105.3
	1477	85.4	-34.6	141.7	21.7	1417	98.3	-21.9	155.5	35.5	1338	111.2	- 8.8	145.8	25.8	125.7
	1724	104.3	-15.7	234.5	114.5	1655	127.3	7.3	254.5	134.5	1564	151.1	31.1	246.4	126.4	141.6
	1972	128.9	28.9	414.8	294.8	1894	165.3	45.3	423.5	303.5	1790	203.9	83.9	387.5	267.5	156.4
	2219	158.8	38.8	804.9	684.9	2131	211.8	91.8	718.6	598.6	2015	269.6	149.6	601.8	481.8	170.2
	2467	194.6	74.6	1981	1861	2370	268.1	148.1	1285.	1165.	2241	350.3	230.3	934.7	814.7	183.0
1750	60	60.0	-60.0	60	-60	60	60	-60.0	60.0	-60.0	60	60.0	-60.0	60.0	-60.0	0
	328	57.6	-62.4	30.3	-79.7	305	56.3	-63.7	43.2	-76.8	278	54.9	-65.1	46.4	-73.6	21.1
	663	50.2	-69.8	2.7	-117.3	626	45.1	-74.9	4.0	-116.0	579	39.4	-80.6	11.0	-109.0	44.6
	1001	52.9	-67.1	.9	-119.1	949	49.0	-71.0	9.9	-110.1	881	44.8	-75.2	19.7	-100.3	68.2
	1338	61.8	-58.2	63.1	- 56.9	1260	62.8	-57.2	74.7	- 45.3	1184	63.9	-56.1	72.3	- 47.7	89.3
	1676	77.2	-42.8			1595	86.8	-33.2	337.9	217.9	1487	97.8	-22.2	203.3	83.3	106.3
	2014	99.2	-20.8			1919	121.5	+ 1.5	2010.	1890	1789	147.8	27.8	494.5	374.5	125.7
	2351	127.2	7.2			2241	166.1	46.1			2093	213.0	93.0	1136.	1016	141.6
	2690	162.0	42.0			2565	222.0	106.2			2395	296.2	176.2	3015.	2895	156.4
	3027	202.7	82.7			2887	288.1	168.1			2699	396.2	276.2	20139	20019	170.2
	3366	249.7	129.7			3212	364.9	244.9			3001	514.6	394.6			183.0

Sheet 2 of 10 Sheets

TABLE II (Cont'd)

Calculated Results for Accelerated Cluster Warhead Miss Distance

Altitude 15,000 feet
Missile Velocity (V_M) 1,000 ft/sec

Note: See text for explanation and derivation.

Target Velocity (V_T)	APPROACH ANGLE (γ) 30°					45°					60°					Cluster Radius (d)
	R_x	y_1	y_2	y_3	y_4	R_x	y_1	y_2	y_3	y_4	R_x	y_1	y_2	y_3	y_4	
800	60	60.0	-60.0	60.0	-60.0	60	60.0	-60.0	60.0	-60.0	60	60.0	-60.0	60.0	-60.0	0
	170	59.3	-60.7	56.7	-63.3	157	59.0	-61.0	56.6	-63.4	140	58.6	-61.4	56.8	-63.2	20.5
	339	57.2	-62.8	48.4	-71.6	318	55.8	-64.2	47.3	-72.7	291	54.3	-65.7	48.0	-72.0	42.3
	511	58.8	-61.2	54.4	-65.6	482	58.2	-61.8	55.2	-65.8	445	57.6	-62.4	54.6	-65.0	63.3
	685	60.3	-59.7	61.5	-58.5	648	60.4	-59.6	61.5	-58.5	601	60.5	-59.5	61.3	-58.7	84.5
	858	64.2	-55.8	88.6	-31.4	814	66.4	-53.6	86.3	-33.7	756	68.8	-51.2	82.1	-37.9	103.8
	1031	70.1	-49.9	145.0	25.0	980	74.8	-45.2	130.1	10.1	912	80.6	-39.4	115.6	- 4.4	122.2
	1205	75.9	-44.1	255.0	135.0	1146	84.5	-35.5	195.5	75.5	1068	94.1	-25.9	159.8	39.8	140.2
	1379	85.6	-34.4	582.0	462.0	1313	99.7	-20.3	325.8	205.8	1224	115.5	- 4.5	237.4	117.4	156.1
	1552	96.0	-24.0	2239.	2119.	1479	116.0	- 4.0	537.3	417.3	1380	138.8	18.8	338.1	218.1	171.9
	1726	104.8	-11.9			1645	135.0	15.0	941.3	821.3	1536	166.0	46.0	479.2	359.2	187.0
1000	60	60.0	-60.0	60.0	-60	60	60.0	-60.0	60.0	-60.0	60	60.0	-60.0	60.0	-60.0	0
	187	59.2	-60.8	52.2	-67.8	171	58.8	-61.2	54.0	-66.0	152	58.3	-61.7	55.4	-64.6	20.5
	375	56.9	-63.1	35.6	-84.4	351	55.2	-64.8	38.7	-81.3	321	53.3	-66.7	32.6	-77.4	42.3
	567	58.7	-61.3	46.8	-73.2	534	58.0	-62.0	49.8	-70.2	492	57.2	-62.8	52.1	-67.9	63.3
	759	60.3	-60.3	64.4	55.6	718	60.5	-59.5	62.7	-57.3	665	60.6	-59.4	61.9	-58.1	84.5
	953	64.7	-55.3	193.3	73.3	903	67.3	-52.7	113.8	- 6.2	838	70.2	-49.8	94.1	-25.9	103.8
	1145	70.9	-49.1	4081	3961	1087	76.9	-43.1	223.3	103.3	1010	83.9	-36.1	148.3	28.3	122.2
	1338	87.8	-42.2			1272	87.8	-32.2	450.0	330.0	1184	99.4	-20.6	228.3	104.3	140.2
	1531	88.6	-31.4			1456	104.8	-15.2	1213	1093	1356	123.9	3.9	365.7	245.7	156.1
	1723	100.1	-19.9			1641	123.[illegible]	3.1	10030.	9910.	1529	150.4	30.4	568.5	448.5	171.9
	1917	113.3	- 6.7			1825	144.1	24.1			1703	181.2	61.2	890.5	760.5	187.0

TABLE II (Cont'd)

Calculated Results for Accelerated Cluster Warhead Miss Distance

Sheet 3 of 10 Sheets

Altitude 30,000 feet
Missile Velocity (V_M) 2500 ft/sec

Note: See text for explanation and derivation.

Target Velocity (V_T)	APPROACH ANGLE (γ) 30° R_x	30° y_1	30° y_2	30° y_3	30° y_4	45° R_x	45° y_1	45° y_2	45° y_3	45° y_4	60° R_x	60° y_1	60° y_2	60° y_3	60° y_4	Cluster Radius (d)
800	60	60.0	-60.0	60.0	-60.0	60	60.0	-60.0	60.0	-60.0	60	60.0	-60.0	60.0	-60.0	0
	320	58.7	-61.3	57.8	-62.2	313	58.1	-61.9	57.0	-63.0	290	57.5	-62.5	56.6	-63.4	20.9
	639	54.7	-65.3	51.5	-68.5	615	52.3	-67.7	48.6	-71.4	585	50.1	-69.9	47.0	-73.0	43.8
	960	56.1	-63.9	53.3	-66.7	926	54.2	-65.8	41.1	-68.9	882	52.5	-67.5	49.9	-70.1	66.7
	1281	60.8	-59.2	61.5	-58.5	1237	61.2	-58.8	61.9	-58.1	1180	61.6	-58.4	62.2	-58.8	87.6
	1602	69.4	-50.6	77.9	-42.1	1549	73.9	-46.1	83.4	-36.6	1478	78.1	-41.9	86.1	-33.9	106.8
	1924	82.1	-37.9	105.5	-14.5	1861	92.8	-27.2	118.7	- 1.3	1776	102.9	-17.1	124.4	4.4	124.5
	2246	99.1	-20.9	148.1	28.1	2172	118.3	- 1.7	171.8	51.8	2074	136.8	16.8	180.6	60.6	140.9
	2568	121.0	1.0	211.9	91.9	2484	151.3	31.3	249.1	129.1	2372	181.0	61.0	260.1	140.1	156.3
	2888	147.9	27.9	306.0	186.0	2796	192.2	72.2	358.8	238.8	2670	236.2	116.2	368.7	248.7	170.7
	3212	180.3	60.3	445.7	325.7	3107	241.6	121.6	513.9	393.9	2968	303.8	183.8	515.6	395.6	184.3
2500	60	60.0	-60.0	60.	-60.	60	60.0	-60.0	60.0	-60.0	60	60.0	-60.0	60.0	-60.0	0
	471	57.1	-62.9	34.7	-85.3	442	55.6	-64.4	39.1	-80.9	406	53.8	-66.2	43.4	-76.6	20.9
	952	48.2	-71.8	-15.3	-135.3	903	42.0	-78.0	-11.2	-131.2	838	35.2	-84.8	-0.9	-120.9	43.8
	1435	51.4	-68.6	-15.9	-135.9	1364	46.7	-73.3	- 2.6	-122.6	1270	41.6	-78.4	10.4	-109.6	66.7
	1917	61.7	-58.3	87.8	-32.2	1825	62.7	-57.3	76.5	-43.5	1703	63.7	56.3	71.5	-48.5	87.6
	2400	79.5	-40.5	1836.	1716.	2289	90.3	-29.7	331.	211.	2135	102.6	17.4	213.3	93.3	106.8
	2883	104.6	-15.4			2748	129.7	9.7	1210.	1090.	2568	158.9	38.9	490.4	370.4	124.5
	3367	136.8	16.8			3212	180.8	60.8	13,524.	13,404.	3001	233.0	113.0	1019.3	899.3	140.9
	3848	176.5	56.5			3673	244.1	124.1			3434	326.1	206.1	2110.	1990.	156.3
	4332	223.3	103.3			4136	319.3	199.3			3868	438.1	318.1	4855.	4735.	170.7
	4817	277.1	157.1			4598	406.6	286.6			4299	569.9	449.9	13,523.	18403.	184.3

TABLE II (Cont'd)

Calculated Results for Accelerated Cluster Warhead Miss Distance

Sheet 4 of 10 Sheets

Altitude 30,000 feet

Missile Velocity (V_M) 1750 ft/sec

Note: See text for explanation and derivation.

Target Velocity (V_T)	APPROACH ANGLE (γ) 30° R_x	y_1	y_2	y_3	y_4	45° R_x	y_1	y_2	y_3	y_4	60° R_x	y_1	y_2	y_3	y_4	Cluster Radius (d)
800	60	60.0	-60.0	60.0	-60.0	60	60.0	-60.0	60.0	-60.0	60	60.0	-60.0	60.0	-60.0	0
	245	59.2	-60.8	58.2	-61.8	232	58.8	-61.2	57.7	-62.3	210	58.4	-61.6	57.5	-62.5	20.5
	489	56.6	-63.4	53.0	-67.0	466	55.0	-65.0	50.9	-69.1	437	53.4	-66.6	50.1	-69.9	42.4
	736	57.5	-62.5	54.5	-65.5	703	56.3	-63.7	53.0	-67.0	663	55.1	-64.9	52.4	-67.6	64.3
	983	60.4	-59.6	60.9	-59.1	941	60.6	-59.4	61.1	-58.9	887	60.7	-59.3	61.2	-58.8	84.9
	1229	65.4	-54.6	73.5	-46.5	1179	68.1	-57.9	76.8	-43.2	1113	70.7	-49.3	77.8	-42.2	104.2
	1477	72.6	-47.4	94.1	-25.9	1417	78.9	-41.1	101.7	-18.3	1338	85.2	-34.8	103.4	-16.6	122.6
	1724	82.0	-38.0	124.2	4.2	1655	93.1	-26.9	137.2	17.2	1564	104.2	-15.8	139.1	19.1	139.9
	1972	93.7	-26.3	168.1	48.1	1894	111.0	- 9.0	187.3	67.3	1790	128.4	8.4	187.8	67.8	156.4
	2219	107.9	-12.1	230.4	110.4	2131	132.6	12.6	255.3	135.3	2015	157.9	37.9	251.6	131.6	172.1
	2467	118.8	- 1.2	295.8	175.8	2370	149.3	29.3	321.5	201.5	2241	181.0	61.0	309.6	189.6	190.2
1750	60	60.0	-60.0	60.0	-60.0	60	60.0	-60.0	60.0	-60.0	60	60.0	-60.0	60.0	-60.0	0
	328	58.7	-61.3	46.[illegible]	-73.3	305	57.9	-62.1	49.6	-70.4	278	57.1	-62.9	52.0	-68.0	20.5
	663	54.4	-65.6	16.9	-104.1	626	51.3	-68.7	22.2	-97.8	579	48.0	-72.0	28.9	-91.1	42.4
	1001	55.9	-64.1	19.2	-100.8	949	53.6	-66.4	22.2	-97.8	881	51.2	-68.8	35.5	-84.5	64.3
	1338	60.6	-59.4	69.2	- 50.8	1260	61.0	-59.0	65.7	-54.3	1184	61.3	-58.7	64.1	-55.9	84.9
	1676	68.7	-51.3	320.8	200.8	1595	73.5	-46.5	160.8	40.8	1487	79.0	-41.0	123.6	3.6	104.2
	2014	80.1	-39.9			1919	91.2	-28.8	377.5	257.5	1789	104.1	-15.9	226.2	106.2	122.6
	2351	94.6	-25.4			2241	114.0	- 6.0	864.7	744.7	2093	136.7	16.7	385.1	265.1	139.9
	2690	116.4	- 7.6			2565	142.2	12.2	2534.	2414.	2395	177.3	57.3	636.6	516.6	156.4
	3027	133.4	13.4			2887	175.5	55.5			2699	195.9	105.9	1032.[illegible]	912.[illegible]	172.1
	3366	148.9	28.9			3212	200.4	80.4			3001	262.7	142.7	1538.[illegible]	1418.[illegible]	190.2

TABLE II (Cont'd)

Calculated Results for Accelerated Cluster Warhead Miss Distance

Sheet 5 of 10 Sheets

Altitude 30,000 feet
Missile Velocity (V_M) 1000 ft/sec

Note: See text for explanation and derivation.

Target Velocity (V_T)	APPROACH ANGLE (γ)															Cluster Radius (d)
	30°					45°					60°					
	R_x	y_1	y_2	y_3	y_4	R_x	y_1	y_2	y_3	y_4	R_x	y_1	y_2	y_3	y_4	
800	60	60.0	-60.0	60.0	-60.0	60	60.0	-60.0	60.0	-60.0	60	60.0	-60.0	60.0	-60.0	0
	170	59.6	-60.4	58.0	-62.0	157	59.4	-60.6	58.0	-62.0	140	59.2	-60.8	58.1	-61.9	20.0
	339	58.3	-61.7	52.7	-67.7	318	57.5	-62.5	51.8	-68.2	291	56.6	-63.4	52.5	-67.5	40.8
	511	58.7	-61.3	53.6	-66.4	482	58.1	-61.9	53.4	-66.6	445	57.3	-62.1	54.0	-66.0	61.6
	685	60.1	-59.9	60.4	-59.6	648	60.1	-59.9	60.4	-59.6	601	60.1	-59.9	60.3	-59.7	81.6
	858	62.2	-57.8	73.7	-46.3	814	63.4	-56.6	73.1	-46.9	756	64.7	-55.3	71.3	-48.7	101.0
	1031	65.3	-54.7	96.9	-23.1	980	68.2	-51.8	93.8	-26.2	912	71.3	-48.7	88.4	-31.6	119.8
	1205	69.3	-50.7	133.1	13.1	1146	74.2	-45.8	123.3	3.3	1068	79.7	-40.3	111.5	- 8.5	137.9
	1379	74.1	-45.9	189.9	69.9	1313	81.7	-38.3	164.6	44.6	1224	90.0	-30.0	142.2	22.2	155.5
	1552	79.8	-40.2	279.3	159.3	1479	90.6	-29.4	221.1	101.1	1380	102.5	-17.5	181.4	61.4	172.6
	1726	86.4	-33.6	427.3	307.3	1645	100.9	-19.1	297.9	177.9	1536	117.0	- 3.0	230.8	110.8	189.2
1000	60	60.0	-60.0	60.0	-60.0	60	60.0	-60.0	60.0	-60.0	60	60.0	-60.0	60.0	-60.0	0
	187	59.6	-60.4	55.0	-65.0	171	59.3	-60.7	56.3	-63.7	152	59.9	-60.1	57.2	-62.8	20.0
	375	58.1	-61.9	42.2	-77.8	351	57.1	-62.9	45.8	-74.2	321	54.0	-64.0	48.9	-71.1	40.8
	567	58.6	-61.4	43.7	-76.3	534	57.8	-62.2	48.1	-71.9	492	56.9	-63.1	41.1	-68.9	61.6
	759	60.1	-59.9	61.1	-58.9	718	60.1	-59.9	60.7	-59.3	665	60.2	-59.8	60.5	-59.5	81.6
	953	62.5	-57.5	108.0	-12.0	903	63.9	-56.1	85.5	-34.5	838	65.4	-54.6	77.2	-42.8	101.0
	1145	66.0	-54.0	236.5	116.5	1087	73.2	-46.8	131.5	11.5	1010	73.1	-46.9	103.8	-16.2	119.8
	1338	70.4	-49.6	722.5	602.5	1272	76.2	-43.8	199.1	79.1	1184	82.8	-37.2	140.7	20.7	137.9
	1531	75.8	-44.2			1456	84.7	-35.3	310.8	190.8	1356	94.8	-25.2	191.1	71.1	155.5
	1723	82.2	-37.8			1641	94.7	-25.3	492.8	372.8	1529	109.1	-10.9	257.7	137.7	172.6
	1917	89.6	-30.4			1825	106.3	-13.7	808.8	688.8	1703	125.7	5.7	344.6	224.6	189.2

TABLE II (Cont'd)

Calculated Results for Accelerated Cluster Warhead Miss Distance

Sheet 6 of 10 Sheets

Altitude 45,000 feet
Missile Velocity (V_M) 2500 ft/sec

Note: See text for explanation and derivation.

Target Velocity (V_T)	Approach Angle (γ) 30° R_x	30° y_1	30° y_2	30° y_3	30° y_4	45° R_x	45° y_1	45° y_2	45° y_3	45° y_4	60° R_x	60° y_1	60° y_2	60° y_3	60° y_4	Cluster Radius (d)
800	60	60.0	-60.0	60.0	-60.0	60	60.	-60.0	60.	-60.0	60	60.0	-60.	60.	-60.0	0
	320	59.3	-60.7	58.8	-61.2	313	59.0	-61.0	58.5	-61.5	290	58.7	-61.3	58.2	-61.8	20.3
	639	57.4	-62.6	55.6	-64.4	615	56.1	-63.9	54.1	-65.9	585	55.0	-65.0	53.3	-66.7	41.5
	960	57.1	-62.1	56.5	-63.4	926	57.0	-63.0	55.3	-64.7	882	56.1	-63.9	54.7	-65.3	62.8
	1281	60.3	-59.7	60.4	-59.6	1237	60.4	-59.6	60.6	-59.4	1180	60.5	-59.5	60.7	-59.3	83.0
	1602	64.2	-55.8	67.6	-52.4	1549	66.2	-53.8	70.0	-50.0	1478	68.0	-52.0	71.2	-48.8	102.5
	1924	69.8	-50.2	78.4	-41.6	1861	74.4	-45.6	84.1	-35.9	1776	78.8	-41.2	86.8	-33.2	121.1
	2246	77.0	-43.0	93.2	-26.8	2172	85.2	-34.8	103.2	-16.8	2074	92.8	-27.2	107.8	-12.2	139.0
	2568	85.9	-34.1	112.4	- 7.6	2484	98.5	-21.5	127.8	7.8	2372	110.3	- 9.7	134.7	14.7	156.2
	2888	96.7	-23.3	137.1	17.1	2796	114.6	- 5.4	159.1	39.1	2670	131.5	11.5	168.4	48.4	172.8
	3212	109.6	-10.4	168.5	48.5	3107	133.9	13.9	198.4	78.4	2968	157.1	37.1	210.3	90.3	188.8
2500	60	60.0	-60.0	60.0	-60.0	60	60.0	-60.0	60.0	-60.0	60	60.0	-60.0	60.0	-60.0	0
	471	58.5	-61.5	44.4	-75.6	442	57.7	-62.3	48.3	-71.7	406	56.9	-63.1	51.1	-68.9	20.3
	952	54.2	-65.8	10.1	-109.9	903	51.1	-68.9	18.5	-101.5	838	47.7	-72.3	27.0	-93.0	41.5
	1435	55.6	-64.4	12.6	-107.4	1364	53.1	-66.9	24.4	-95.6	1270	50.5	-69.5	-33.0	-87.0	62.8
	1917	60.5	-59.5	67.7	-52.3	1825	60.8	-59.2	64.9	-55.1	1703	61.2	-58.8	63.5	-56.5	83.0
	2400	68.8	-51.2	253.2	133.2	2289	73.1	-46.3	153.7	33.7	2135	79.1	-40.9	121.7	1.7	102.5
	2883	80.3	-39.7	1007.4	887.4	2748	91.6	-28.4	318.7	198.7	2568	104.4	-15.6	214.3	94.3	121.1
	3367	95.0	-25.0			3212	114.6	- 5.4	615.7	495.7	3001	137.0	17.0	350.1	230.1	139.0
	3848	112.8	- 7.2			3673	142.4	22.4	1172.0	1052.0	3434	176.7	56.7	541.1	421.1	156.2
	4332	133.7	13.7			4136	175.4	55.4	2369.8	2249.0	3868	224.2	104.2	807.3	687.3	172.8
	4817	158.4	38.4			4598	214.4	94.4	6022.3	5902.5	4299	280.5	160.5	1181.4	1061.4	188.8

TABLE II (Cont'd)

Calculated Results for Accelerated Cluster Warhead Miss Distance

Sheet 7 of 10 Sheets

Altitude 45,000 feet
Missile Velocity (V_M) 1750 ft/sec

Note: See text for explanation and derivation.

Target Velocity (V_T)	APPROACH ANGLE (γ) 30°					45°					60°					Cluster Radius (d)
	R_x	y_1	y_2	y_3	y_4	R_x	y_1	y_2	y_3	y_4	R_x	y_1	y_2	y_3	y_4	
800	60	60.0	-60.0	60.0	-60.0	60	60.0	-60.0	60.0	-60.0	60	60.0	-60.0	60.0	-60.0	0
	245	59.5	-60.5	59.0	-61.0	232	59.3	-60.7	58.7	-61.3	210	59.1	-60.9	58.6	-61.4	20.0
	489	58.3	-61.7	56.2	-63.8	466	57.4	-62.6	55.2	-64.8	437	56.6	-63.4	54.8	-65.2	40.7
	736	58.7	-61.3	57.1	-62.9	703	58.1	-61.9	56.3	-63.7	663	57.5	-62.5	56.1	-63.9	61.4
	983	60.1	-59.9	60.3	-59.7	941	60.2	-59.8	60.4	-59.6	887	60.3	-59.7	60.4	-59.6	81.4
	1229	62.5	-57.5	66.0	-54.0	1179	63.8	-56.2	67.6	-52.4	1113	65.0	-55.0	68.1	-51.9	100.9
	1477	65.9	-54.1	74.6	-45.4	1417	68.8	-51.2	78.2	-41.8	1338	71.7	-48.3	79.3	-40.7	119.7
	1724	70.3	-49.7	86.3	-33.7	1655	75.4	-44.6	92.5	-27.5	1564	80.4	-39.6	94.2	-25.8	138.0
	1972	75.6	-44.4	101.5	-18.5	1894	83.5	-36.5	111.0	- 9.0	1790	91.2	-28.8	113.3	- 6.7	155.8
	2219	82.1	-37.9	120.9	.9	2131	93.2	-26.8	134.2	14.2	2015	104.2	-15.8	136.9	16.9	173.2
	2467	89.5	-30.5	144.7	24.7	2370	104.4	-15.6	162.4	42.4	2241	119.3	- .7	165.3	45.3	190.0
1750	60	60.0	-60.0	60.0	-60.0	60	60.0	-60.0	60.0	-60.0	60	60.0	-60.0	60.0	-60.0	0
	328	59.2	-60.8	51.2	-68.8	305	58.8	-61.2	53.7	-66.3	278	58.4	-61.6	55.3	-64.7	20.0
	663	57.1	-62.9	32.1	-87.9	626	55.6	-64.4	38.2	-81.8	579	53.9	-66.1	43.1	-76.9	40.7
	1001	57.9	-62.1	35.8	-84.2	949	56.7	-63.3	42.6	-87.4	881	55.5	-64.5	47.0	-73.0	61.4
	1338	60.2	-59.8	63.0	-57.0	1260	60.3	-59.7	61.9	-58.1	1184	60.5	-59.5	61.4	-58.6	81.4
	1676	64.1	-55.9	135.4	15.4	1595	66.3	-53.7	101.0	-19.0	1487	68.9	-51.1	87.9	-32.1	100.9
	2014	69.6	-50.4	312.9	192.9	1919	74.8	-45.2	166.9	46.9	1789	80.8	-39.2	128.6	8.6	119.7
	2351	76.5	-43.5	834.2	714.2	2241	85.6	-34.4	269.4	149.4	2093	96.0	-24.0	185.2	65.2	138.0
	2690	85.0	-35.0	5135	5015.0	2565	98.9	-21.1	476.1	306.1	2395	114.8	- 5.2	261.1	141.1	155.8
	3027	95.0	-25.0			2887	114.6	- 5.4	667.9	547.9	2699	137.2	17.2	359.9	239.9	173.2
	3366	106.6	-13.4			3212	132.7	12.7	1050	930.2	3001	163.0	43.0	486.3	366.3	190.0

TABLE II (Cont'd)

Calculated Results for Accelerated Cluster Warhead Miss Distance

Sheet 8 of 10 Sheets

Altitude 45,000 feet
Missile Velocity (V_M) 1000 ft/sec

Note: See text for explanation and derivation.

Target Velocity (V_T)	APPROACH ANGLE (γ) 30°					45°					60°					Cluster Radius (d)
	R_x	y_1	y_2	y_3	y_4	R_x	y_1	y_2	y_3	y_4	R_x	y_1	y_2	y_3	y_4	
800	60	60.0	-60.0	60.0	-60.0	60	60.0	-60.0	60.0	-60.0	60	60.0	-60.0	60.0	-60.0	0
	170	59.8	-60.2	59.1	-60.9	157	59.7	-60.3	59.1	-60.9	140	59.7	-60.3	59.2	-60.8	18.3
	339	59.1	-60.9	55.7	-64.3	318	58.7	-61.3	55.5	-64.5	291	58.2	-61.8	56.0	-64.0	37.1
	511	59.4	-60.6	56.7	-63.3	482	59.0	-61.0	56.6	-63.4	445	58.7	-61.3	57.0	-63.0	55.8
	685	60.0	-60.0	60.0	-60.0	648	60.0	-60.0	60.0	-60.0	601	60.0	-60.0	60.0	-60.0	74.2
	858	61.1	-58.9	66.2	-53.8	814	61.6	-58.4	66.1	-53.9	756	62.3	-57.7	65.4	-54.6	92.3
	1031	62.6	-57.4	75.9	-44.1	980	64.0	-56.0	75.4	-44.6	912	65.5	-54.5	73.3	-46.7	110.1
	1205	64.5	-55.5	89.3	-30.7	1146	67.0	-53.0	87.6	-32.4	1068	69.6	-50.4	83.6	-36.4	127.5
	1379	66.9	-53.1	107.4	-12.6	1313	70.6	-49.4	103.7	-16.3	1224	74.7	-45.3	96.8	-23.2	144.7
	1552	69.8	-50.2	133.3	11.3	1479	75.0	-45.0	123.9	3.9	1380	80.7	-39.3	113.1	- 6.9	161.6
	1726	73.0	-47.0	161.7	41.7	1645	79.8	-40.2	148.5	28.5	1536	87.6	-32.4	132.1	12.1	178.2
1000	60	60.0	-60.0	60.0	-60.0	60	60.0	-60.0	60.0	-60.0	60	60.0	-60.0	60.0	-60.0	0
	187	59.8	-60.2	57.7	-62.3	171	59.7	-60.3	58.4	-61.6	152	59.6	-60.4	58.8	-61.2	18.3
	375	59.0	-61.0	49.1	-70.9	351	58.5	-61.5	52.0	-68.0	321	57.9	-62.1	54.0	-66.0	37.1
	567	59.3	-60.7	51.1	-68.9	534	58.9	-61.1	53.9	-66.1	492	58.5	-61.5	55.5	-64.5	55.8
	759	60.0	-60.0	60.0	- 60.0	718	60.0	-60.0	60.0	-60.0	665	60.0	-60.0	60.0	-60.0	74.2
	953	61.2	-58.8	79.4	-40.6	903	61.9	-58.1	71.6	-48.4	838	62.6	-57.4	68.1	-51.9	92.3
	1145	63.0	-57.0	115.1	- 4.9	1087	64.6	-55.4	89.7	-30.3	1010	66.4	-53.6	80.2	-39.8	110.1
	1338	65.1	-54.9	174.8	54.8	1272	68.0	-52.0	114.8	- 5.2	1184	71.1	-48.9	96.1	-23.9	127.5
	1531	67.8	-52.2	286.6	166.6	1456	72.1	-47.9	149.1	29.1	1356	77.0	-43.0	116.7	- 3.3	144.7
	1723	71.0	-49.0	477.0	357.0	1641	77.1	-42.9	194.1	74.1	1529	84.0	-36.0	142.4	22.4	161.6
	1917	74.6	-54.4	920.0	800.0	1825	82.8	-37.2	253.0	133.0	1703	92.0	-28.0	172.8	52.8	178.2

TABLE II (Cont'd)

Calculated Results for Accelerated Cluster Warhead Miss Distance

Sheet 9 of 10 Sheets

Altitude 60,000 feet

Missile Velocity (V_M) 2500 ft/sec

Note: See text for explanation and derivation.

Target Velocity (V_T)	APPROACH ANGLE (γ)															Cluster Radius (d)
	30°					45°					60°					
	R_x	y_1	y_2	y_3	y_4	R_x	y_1	y_2	y_3	y_4	R_x	y_1	y_2	y_3	y_4	
800	60	60.0	-60.0	60.0	-60.0	60	60.0	-60.0	60.0	-60.0	60	60.0	-60.0	60.0	-60.0	0
	320	59.7	-60.3	59.4	-60.6	313	59.5	-60.5	59.2	-60.8	290	59.4	-60.6	59.1	-60.9	19.7
	639	58.7	-61.3	57.7	-62.3	615	58.0	-62.0	56.9	-63.1	585	57.4	-62.6	56.5	-63.5	39.8
	960	58.9	-61.1	58.1	-61.9	926	58.4	-61.6	57.6	-62.4	882	58.0	-62.0	57.2	-62.8	59.9
	1281	60.1	-59.9	60.1	-59.9	1237	60.1	-59.9	60.1	-59.9	1180	60.1	-59.9	60.2	-59.8	79.5
	1602	61.8	-58.2	63.2	-56.8	1549	62.6	-57.4	64.2	-55.8	1478	63.4	-56.6	64.8	-55.2	98.7
	1924	64.4	-55.6	67.9	-52.1	1861	66.5	-53.5	70.5	-49.5	1776	68.4	-51.6	71.8	-48.2	117.5
	2246	67.6	-52.4	74.0	-46.0	2172	71.2	-48.8	78.3	-41.7	2074	74.5	-45.5	80.5	-39.5	136.0
	2568	71.5	-48.5	81.6	-38.4	2484	77.0	-43.0	88.2	-31.8	2372	82.1	-37.9	91.5	-28.5	154.1
	2888	76.5	-43.5	91.3	-28.7	2796	84.3	-35.7	100.9	-19.1	2670	91.7	-28.3	105.5	-14.5	171.8
	3212	81.8	-38.2	102.2	-17.8	3107	92.6	-27.7	115.0	- 5.0	2968	102.1	-17.9	121.0	+ 1.0	189.2
2500	60	60.0	-60.0	60.0	-60.0	60	60.0	-60.0	60.0	-60.0	60	60.0	-60.0	60.0	-60.0	0
	471	59.3	-60.7	51.3	-68.7	442	58.9	-61.1	53.9	-66.1	406	58.5	-61.5	55.8	-64.2	19.7
	952	57.1	-62.9	18.8	-91.2	903	55.4	-64.5	36.7	-83.3	838	53.8	-66.2	42.3	-77.7	39.8
	1435	57.7	-62.3	32.2	-87.8	1364	56.5	-63.5	40.6	-79.4	1270	55.1	-64.9	45.7	-74.3	59.9
	1917	60.1	-59.9	61.9	-58.1	1825	60.2	-59.8	61.2	-58.8	1703	60.3	-59.7	60.9	-59.1	79.5
	2400	63.8	-56.2	123.6	+ 3.6	2289	65.9	-54.1	96.8	-13.2	2135	68.2	-51.8	85.4	-34.6	98.7
	2883	69.3	-50.7	251.	131.	2748	74.3	-45.7	156.4	+36.4	2568	80.1	-39.9	124.2	+ 4.2	117.5
	3367	75.9	-44.1	486.	366.	3212	84.7	-35.3	239.3	119.3	3001	94.6	-25.4	174.5	54.5	136.0
	3848	84.1	-35.9	982.	862.	3673	97.4	-22.6	355.0	235.0	3434	112.5	- 7.5	1858.	1738.	154.1
	4332	94.2	-25.8	2373.	2253.	4136	113.2	- 6.8	520.4	400.4	3968	134.8	+14.8	2718.	2598	171.8
	4817	105.1	-14.9	12198	12198.	4598	130.2	+10.2	731.7	611.7	4299	159.0	39.0	3709.	3589	189.2

TABLE II (Cont'd)

Calculated Results for Accelerated Cluster Warhead Miss Distance

Sheet 10 of 10 Sheets

Altitude 60,000 feet
Missile Velocity (V_M) 1750 ft/sec

Note: See text for explanation and derivation.

Target Velocity (V_T)	APPROACH ANGLE (γ) 30°					45°					60°					Cluster Radius (d)
800	60	60.0	-60.0	60.0	-60.0	60	60.0	-60.0	60.0	-60.0	60	•60.0	-60.0	60.0	-60	0
	291	59.7	-60.3	59.3	-60.7	232	59.5	-60.5	59.1	-60.9	210	59.4	-60.6	59.1	-60.9	19.1
	489	59.1	-60.9	58.1	-61.9	466	58.7	-61.3	57.5	-62.5	437	58.3	-61.7	-57.3	-62.7	38.4
	736	59.4	-60.6	58.6	-61.4	703	59.1	-60.9	58.2	-61.8	663	58.7	-61.2	58.1	-61.9	57.7
	983	60.1	-59.9	60.2	-59.8	941	60.1	-59.9	60.2	-59.8	887	60.1	-59.9	60.2	-59.8	76.8
	1229	61.2	-58.8	62.8	-57.2	1179	61.8	-58.2	63.6	-56.4	1113	62.4	-57.6	63.8	-56.2	95.5
	1477	62.8	-57.2	66.7	-53.3	1417	64.2	-55.8	68.4	-51.6	1338	65.6	-54.4	69.0	-51.0	114.0
	1724	64.7	-55.3	71.3	-48.7	1655	67.0	-53.0	74.1	-45.9	1564	69.2	-50.8	75.0	-45.0	132.3
	1972	67.2	-52.8	77.6	-42.4	1894	70.7	-49.3	82.0	-38.0	1790	74.2	-45.8	83.3	-36.7	150.2
	2219	70.1	-49.9	85.3	-34.7	2131	75.2	-44.8	91.5	-28.5	2015	80.1	-39.8	93.3	-26.7	167.9
	2467	73.6	-46.4	94.5	-25.5	2370	80.3	-39.7	102.7	-17.3	2241	87.0	-33.0	105.1	-14.9	185.4
1750	60	60.0	-60.0	60.0	-60.0	60	60.0	-60.0	60	-60	60	60	-60	60.0	-60	0
	328	59.5	-60.5	53.6	-66.4	305	59.2	-60.8	55.7	-64.3	278	58.9	-61.1	56.9	-63.1	19.1
	663	58.6	-61.4	43.6	-76.4	626	57.8	-62.2	48.2	-71.8	579	56.9	-63.1	-51.3	-68.7	38.4
	1001	59.0	-61.0	47.2	-72.8	949	58.4	-61.6	51.3	-68.7	881	57.8	-62.2	-53.6	-66.4	57.7
	1338	60.1	-59.9	61.5	-58.5	1260	60.2	-59.8	61.0	-59.0	1184	60.2	-59.8	60.7	-59.7	76.8
	1676	62.0	-58.0	91.0	-29.0	1595	63.1	-56.9	78.6	-41.4	1487	64.3	-55.7	73.1	-46.9	95.5
	2014	64.6	-55.4	141.7	-21.7	1919	67.1	-53.9	105.3	-14.7	1789	69.9	-50.1	91.0	-29.0	114.0
	2351	67.6	-52.4	217.3	97.3	2241	71.7	-48.3	138.7	+18.7	2093	76.4	-43.6	112.5	- 7.5	132.3
	2690	71.6	-48.4	346.4	226.4	2565	78.0	-42.0	187.3	67.3	2395	85.2	-34.8	142.6	22.6	150.2
	3027	76.4	-43.6	562.7	442.7	2887	85.4	-34.6	250.3	130.3	2699	95.6	-24.4	179.5	59.5	167.9
	3366	81.8	-38.2	941.8	821.8	3212	93.9	-26.1	329.6	209.6	3001	107.7	-12.3	223.8	103.8	185.4

TABLE III

Calculated Results for Continuous Rod Warhead Miss Distance

Sheet 1 of 10 Sheets

Altitude 15,000 feet
Missile Velocity (V_M) 1750 ft/sec

Note: See text for explanation and derivation.

Target Velocity (V_T)	APPROACH ANGLE (γ) 30°					45°					60°					Hoop Radius (d)
	R_x	y_1	y_2	y_3	y_4	R_x	y_1	y_2	y_3	y_4	R_x	y_1	y_2	y_3	y_4	
800	60.0	60.00	-60.00	60.00	-60.00	60.0	60.00	-60.0	60.0	-60.00	60.0	60.00	-60.00	60.0	-60.00	0
	61.09	60.02	-59.98	60.04	-59.96	59.0	60.03	-59.97	60.05	-59.95	57.3	60.04	-59.96	60.06	-59.94	49.6
	71.35	60.07	-59.93	60.17	-59.83	67.2	60.11	-59.89	60.22	-59.78	63.1	60.14	-59.86	60.23	-59.77	98.6
	87.61	60.16	-59.84	60.39	-59.61	81.7	60.24	-59.76	60.49	-59.51	75.5	60.32	-59.68	60.52	-59.48	147.1
	107.2	60.29	-59.71	60.71	-59.29	99.8	60.44	-59.56	60.89	-59.11	91.9	60.58	-59.42	60.94	-59.06	194.9
	128.6	60.46	-59.54	61.13	-58.87	120.1	60.68	-59.32	61.40	-58.60	110.5	60.91	-59.09	61.49	-58.51	242.1
	150.9	60.66	-59.34	61.64	-58.36	141.3	60.99	-59.01	62.04	-57.96	130.3	61.31	-58.69	62.16	-57.84	288.8
	174.0	60.90	-59.10	62.27	-57.73	163.3	61.34	-58.66	62.81	-57.19	151.0	61.78	-58.22	62.97	-57.03	335.0
	197.4	61.17	-58.83	63.00	-57.00	185.8	61.76	-58.24	63.72	-56.28	172.1	62.33	-57.67	63.91	-56.09	380.6
	221.2	61.48	-58.52	63.85	-56.15	208.6	62.22	-57.78	64.75	-55.25	193.5	62.95	-57.05	64.99	-55.01	425.7
	245.1	61.84	-58.16	64.84	-55.16	231.6	62.75	-57.25	65.95	-54.05	215.2	63.66	-56.34	66.23	-53.77	470.2
1750	60.0	60.00	-60.00	60.0	-60.0	60.0	60.0	-60.00	60.0	-60.0	60.0	60.00	-60.00	60.0	-60.0	0
	60.8	60.03	-59.97	60.5	-59.5	56.2	60.05	-59.95	60.3	-59.7	52.5	60.06	-59.94	60.2	-59.8	49.6
	77.9	60.12	-59.88	62.0	-58.0	69.4	60.19	-59.81	61.2	-58.8	60.3	60.26	-59.74	60.8	-59.2	98.6
	103.6	60.27	-59.73	65.0	-55.0	92.5	60.41	-59.59	62.7	-57.3	79.1	60.57	-59.43	61.8	-58.2	147.1
	133.0	60.47	-59.53	70.2	-49.8	120.0	60.73	-59.27	65.0	-55.0	103.0	61.03	-58.97	63.3	-57.7	194.9
	164.1	60.74	-59.26	78.5	-41.5	149.4	61.15	-58.85	68.2	-51.8	129.3	61.61	-58.39	65.3	-54.7	242.1
	196.1	61.06	-58.94	91.8	-28.2	179.8	61.65	-58.35	72.3	-47.7	156.6	62.31	-57.69	67.7	-52.3	288.8
	228.6	61.44	-58.56	112.9	- 7.1	210.8	62.24	-57.76	77.5	-42.5	184.6	63.15	-56.85	70.7	-49.3	335.0
	261.5	61.88	-58.12	149.8	+29.8	242.2	62.93	-57.07	84.0	-36.0	213.0	64.12	-55.88	74.2	-45.7	380.6
	295.1	62.38	-57.62	222.6	+102.6	273.8	63.70	-56.30	91.9	-28.1	241.7	65.20	-54.80	78.5	-41.5	425.7
	327.8	62.94	-57.06	419.1	+299.1	305.5	64.57	-55.43	101.8	-19.2	270.5	66.44	-53.56	83.3	-36.7	470.2

TABLE III (Cont'd)

Calculated Results For Continuous Rod Warhead Miss Distance

Sheet 2 of 10 Sheets

Altitude 15,000 feet

Missile Velocity (V_M) 1,000 ft/sec

Note: See text for explanation and derivation.

Target Velocity (V_T)	APPROACH ANGLE (γ) 30°					45°					60°					Hoop Radius (d)
	R_x	y_1	y_2	y_3	y_4	R_x	y_1	y_2	y_3	y_4	R_x	y_1	y_2	y_3	y_4	
800	60.0	60.	-60.	60.	-60.00	60.0	60.00	-60.	60.00	-60.00	60.0	60.00	-60.	60.00	-60.00	0
	58.5	60.01	-59.99	60.05	-59.95	56.5	60.02	-59.98	60.05	-59.95	54.9	60.02	-59.98	60.05	-59.95	49.5
	62.1	60.04	-59.96	60.20	-59.80	57.8	60.06	-59.94	60.20	-59.80	54.0	60.08	-59.92	60.18	-59.82	98.7
	69.9	60.08	-59.92	60.46	-59.54	63.7	60.12	-59.88	60.45	-59.55	57.5	60.17	-59.83	60.40	-59.60	147.5
	80.8	60.14	-59.86	60.83	-59.17	72.9	60.21	-59.79	60.81	-59.19	64.6	60.29	-59.71	60.70	-59.30	196.0
	93.6	60.21	-59.79	61.31	-58.69	84.5	60.33	-59.67	61.26	-58.74	74.4	60.45	-59.55	61.09	-58.97	244.2
	107.8	60.31	-59.69	61.92	-58.08	97.5	60.47	-59.53	61.83	-58.17	86.0	60.65	-59.35	61.58	-58.42	292.0
	122.7	60.42	-59.58	62.07	-57.33	111.5	60.72	-59.28	62.82	-57.18	98.7	60.88	-59.12	62.16	-57.84	339.5
	138.3	60.55	-59.45	63.56	-56.44	126.1	60.84	-59.16	63.34	-56.66	112.1	61.15	-58.85	62.84	-57.16	386.7
	154.2	60.69	-59.31	64.62	-55.38	141.2	61.06	-58.94	64.30	-55.70	126.0	61.46	-58.54	63.64	-56.36	433.5
	170.5	60.85	-59.15	65.83	-54.17	156.6	61.31	-58.69	65.37	-54.63	140.3	61.80	-58.20	64.52	-55.48	480.0
1,000	60.0	60.00	-60.00	60.00	-60.00	60.0	60.00	-60.00	60.00	-60.00	60.0	60.00	-60.00	60.00	-60.00	0
	58.1	60.01	-59.99	60.16	-59.84	55.7	60.02	-59.98	60.10	-59.90	53.5	60.02	-59.98	60.07	-59.93	49.5
	62.4	60.04	-59.96	60.63	-59.37	57.1	60.06	-59.94	60.38	-59.62	52.2	60.09	-59.91	60.27	-59.73	98.7
	71.8	60.09	-59.91	61.47	-58.53	64.2	60.14	-59.86	60.86	-59.14	56.4	60.19	-59.81	60.60	-59.40	147.5
	84.7	60.16	-59.84	62.76	-57.24	75.3	60.24	-59.76	61.55	-58.45	65.1	60.34	-59.66	61.06	-58.94	196.0
	99.6	60.24	-59.76	64.54	-55.46	88.8	60.38	-59.62	62.45	-57.55	76.8	60.53	-59.47	61.66	-58.34	244.2
	115.9	60.35	-59.65	66.98	-53.02	103.9	60.54	-59.46	63.59	-56.41	90.4	60.75	-59.25	62.40	-57.60	292.0
	133.0	60.47	-59.53	70.25	-49.75	120.0	60.73	-59.27	65.00	-55.00	105.0	61.03	-58.97	63.30	-56.70	339.5
	150.6	60.62	-59.38	74.29	-45.71	136.7	60.96	-59.04	66.67	-53.33	120.4	61.34	-58.66	64.35	-55.65	386.7
	168.6	60.78	-59.22	79.86	-40.14	153.7	61.21	-58.79	68.68	-51.32	136.2	61.70	-58.30	65.59	-54.41	433.5
	186.9	60.96	-59.04	87.03	-32.97	171.0	61.49	-58.51	70.98	-49.02	152.3	62.10	-57.90	66.97	-53.03	480.0

TABLE III (Cont'd)

Calculated Results For Continuous Rod Warhead Miss Distance

Sheet 3 of 10 Sheets

Altitude 30,000 feet
Missile Velocity (V_M) 2500 ft/sec

Note: See text for explanation and derivation.

Target Velocity (V_T)	APPROACH ANGLE (γ) 30° R_x	30° y_1	30° y_2	30° y_3	30° y_4	45° R_x	45° y_1	45° y_2	45° y_3	45° y_4	60° R_x	60° y_1	60° y_2	60° y_3	60° y_4	Hoop Radius (d)
800	60.0	60.00	-60.00	60.00	-60.00	60.0	60.00	-60.00	60.00	-60.00	60.0	60.00	-60.00	60.00	-60.00	0
	64.5	60.01	-59.99	60.02	-59.98	62.4	60.02	-59.98	60.03	-59.97	60.5	60.02	-59.98	60.03	-59.97	49.7
	82.4	60.06	-59.94	60.11	-59.89	78.3	60.09	-59.91	60.15	-59.85	74.1	60.12	-59.88	60.17	-59.83	98.8
	107.2	60.12	-59.88	60.28	-59.72	101.5	60.22	-59.78	60.37	-59.63	95.4	60.29	-59.71	60.41	-59.59	147.6
	135.1	60.27	-59.73	60.49	-59.51	128.2	60.40	-59.60	60.65	-59.35	120.4	60.52	-59.48	60.73	-59.27	195.5
	164.6	60.43	-59.57	60.79	-59.21	156.6	60.64	-59.36	61.04	-58.96	148.6	60.83	-59.17	61.16	-58.83	243.0
	195.0	60.62	-59.38	61.14	-58.86	185.8	60.91	-59.09	61.50	-58.50	175.0	61.18	-58.83	61.68	-58.32	290.1
	225.8	60.85	-59.15	61.58	-58.42	215.6	61.26	-58.74	62.07	-57.93	203.3	61.63	-58.37	62.32	-57.68	336.7
	257.0	61.11	-58.89	62.08	-57.92	245.7	61.64	-58.36	62.72	-57.38	232.0	62.14	-57.86	63.04	-56.96	382.8
	288.3	61.41	-58.59	62.65	-57.35	276.1	62.08	-57.92	63.46	-56.54	261.0	62.70	-57.30	63.84	-56.14	428.5
	319.8	61.75	-58.25	63.30	-56.70	306.6	62.58	-57.42	64.33	-55.67	290.1	63.36	-56.64	64.82	-55.18	473.7
2500	60.0	60.00	-60.00	60.0	-60.0	60.0	60.00	-60.00	60.00	-60.00	60.0	60.00	-60.00	60.00	-60.00	0
	66.6	60.03	-59.97	60.4	-59.6	60.1	60.04	-59.96	60.25	-59.75	53.6	60.06	-59.94	60.18	-59.82	49.7
	99.7	60.14	-59.86	62.2	-57.8	88.8	60.21	-59.79	61.30	-58.70	76.8	60.29	-59.71	60.91	-59.09	98.8
	141.7	60.33	-59.67	65.9	-54.1	128.2	60.51	-59.49	63.26	-56.74	112.6	60.71	-59.29	62.22	-57.78	147.6
	186.8	60.58	-59.42	71.5	-48.5	171.1	60.89	-59.11	65.94	-54.06	152.3	61.25	-58.75	63.98	-56.02	195.5
	233.2	60.91	-59.09	80.4	-39.6	215.3	61.41	-58.59	69.74	-50.26	193.8	61.98	-58.02	66.40	-53.60	243.0
	280.4	61.30	-58.70	93.4	-26.6	260.1	62.02	-57.98	74.50	-45.50	235.6	62.83	-57.17	69.33	-50.67	290.1
	327.6	61.79	-58.21	113.3	- 6.7	305.5	62.77	-59.23	80.69	-39.31	278.0	63.89	-56.11	73.01	-46.99	336.7
	375.4	62.33	-57.67	143.0	23.0	351.0	63.62	-56.38	88.11	-31.89	320.7	65.08	-54.92	77.28	-42.72	382.8
	423.0	62.93	-57.07	190.0	70.0	396.7	64.55	-55.44	97.00	-23.00	363.5	66.41	-53.59	82.18	-37.82	428.5
	471.1	63.63	-56.37	273.3	153.3	442.4	65.65	-54.35	107.95	-12.05	406.3	67.94	-52.06	87.99	-32.01	473.7

TABLE III (Cont'd)
Calculated Results For Continuous Rod Warhead Miss Distance

Sheet 4 of 10 Sheets

Altitude 30,000 feet
Missile Velocity (V_M) 1750 ft/sec

Note: See text for explanation and derivation.

Target Velocity (V_T)	APPROACH ANGLE (γ) 30° R_x	30° Y_1	30° Y_2	30° Y_3	30° Y_4	45° R_x	45° Y_1	45° Y_2	45° Y_3	45° Y_4	60° R_x	60° Y_1	60° Y_2	60° Y_3	60° Y_4	Hoop Radius (d)
800	60.0	60.00	-60.00	60.00	-60.00	60.0	60.00	-60.00	60.00	-60.00	60.0	60.00	-60.00	60.00	-60.00	0
	61.1	60.02	-59.98	60.04	-59.96	59.0	60.02	-59.98	60.05	-59.95	57.3	60.03	-59.97	60.05	-59.95	49.7
	71.3	60.05	-59.95	60.17	-59.83	67.2	60.07	-59.93	60.15	-59.85	63.1	60.10	-59.90	60.16	-59.83	99.1
	87.6	60.10	-59.90	60.24	-59.76	81.7	60.15	-59.85	60.30	-59.70	75.5	60.20	-59.80	60.32	-59.68	148.3
	107.2	60.17	-59.83	60.40	-59.60	99.8	60.25	-59.75	60.50	-59.50	91.9	60.33	-59.67	60.53	-59.47	197.1
	128.6	60.27	-59.73	60.65	-59.35	120.1	60.40	-59.60	60.81	-59.19	110.5	60.55	-59.47	60.86	-59.14	245.4
	150.9	60.41	-59.59	60.98	-59.02	141.3	60.61	-59.39	61.23	-58.77	130.3	60.88	-59.20	61.31	-58.69	293.1
	174.0	60.55	-59.45	61.33	-58.67	163.3	60.81	-59.19	61.66	-58.34	151.0	61.08	-58.92	61.76	-58.24	340.9
	197.4	60.70	-59.30	61.72	-58.28	185.8	61.05	-58.95	62.15	-57.85	172.1	61.39	-58.61	62.28	-57.72	388.3
	221.2	60.89	-59.11	62.21	-57.79	208.6	61.34	-58.66	62.76	-57.24	193.5	61.77	-58.23	62.92	-57.08	435.1
	245.1	61.11	-58.89	62.76	-57.38	231.6	61.66	-58.34	63.43	-56.57	215.2	62.19	-57.81	63.63	-56.37	481.7
17500	60.0	60.00	-60.00	60.00	-60.00	60.0	60.00	-60.00	60.00	-60.00	60.0	60.00	-60.00	60.00	-60.00	0
	60.8	60.03	-59.97	60.40	-59.60	56.2	60.04	-59.96	60.25	-59.75	52.5	60.06	-59.94	60.18	-59.82	49.7
	77.9	60.08	-59.92	61.27	-58.73	69.4	60.13	-59.87	60.76	-59.24	60.3	60.18	-59.82	60.54	-59.46	99.1
	103.6	60.16	-59.84	62.71	-57.29	92.5	60.25	-59.75	61.57	-58.43	79.1	60.35	-59.65	61.09	-58.91	148.3
	133.0	60.27	-59.73	64.83	-55.17	120.0	60.42	-59.58	62.69	-57.31	103.0	60.59	-59.41	61.84	-58.16	197.1
	164.1	60.44	-59.56	68.33	-51.67	149.4	60.68	-59.32	64.43	-55.57	129.3	60.95	-59.05	63.00	-57.00	245.1
	196.1	60.66	-59.34	73.55	-46.45	179.8	61.02	-58.98	66.84	-53.16	156.6	61.43	-58.57	64.57	-55.43	293.1
	228.6	60.88	-59.12	79.72	-41.28	210.8	61.37	-58.63	69.41	-50.59	184.6	61.91	-58.09	66.19	-53.81	340.9
	261.5	61.13	-58.87	87.51	-32.49	242.2	61.75	-58.25	72.40	-47.60	213.0	62.46	-57.54	67.47	-51.94	388.3
	295.1	61.44	-58.56	98.89	-21.11	273.8	62.24	-57.76	76.25	-43.75	241.7	63.14	-56.84	70.40	-49.60	435.1
	327.8	61.79	-58.21	113.33	- 6.67	305.5	62.77	-57.23	80.62	-39.38	270.5	63.89	-56.11	73.00	-47.00	481.7

TABLE III (Cont'd)

Calculated Results For Continuous Rod Warhead Miss Distance

Sheet 5 of 10 Sheets

Altitude 30,000 feet
Missile Velocity(V_M) 1,000 ft/sec

Note: See text for explanation and derivation.

Target Velocity (V_T)	APPROACH ANGLE (γ) 30°					45°					60°					Hoop Radius (d)
	R_x	y_1	y_2	y_3	y_4	R_x	y_1	y_2	y_3	y_4	R_x	y_1	y_2	y_3	y_4	
800	60.0	60.00	-60.00	60.00	-60.00	60.0	60.00	-60.00	60.00	-60.00	60.0	60.00	-60.00	60.00	-60.00	0
	58.5	60.00	-60.00	60.03	-59.97	56.5	60.01	-59.99	60.03	-59.97	54.9	60.01	-59.99	60.02	-59.98	49.1
	62.1	60.02	-59.98	60.11	-59.89	57.8	60.03	-59.97	60.11	-59.89	54.0	60.04	-59.96	60.09	-59.91	98.1
	69.9	60.05	-59.95	60.29	-59.71	63.7	60.08	-59.92	60.28	-59.72	57.5	60.10	-59.90	60.25	-59.75	146.7
	80.8	60.08	-59.92	60.48	-59.52	72.9	60.13	-59.87	60.47	-59.53	64.6	60.18	-59.82	60.42	-59.58	195.2
	93.6	60.13	-59.87	60.76	-59.24	84.5	60.20	-59.80	60.74	-59.26	74.4	60.27	-59.73	60.65	-59.35	243.5
	107.8	60.18	-59.82	61.10	-58.90	97.5	60.28	-59.72	61.07	-58.93	86.0	60.39	-59.61	60.93	-59.07	291.6
	122.7	60.25	-59.75	61.52	-58.48	[illegible]11.5	60.39	-59.61	61.47	-58.53	98.7	60.[illegible]3	-59.47	61.28	-58.72	339.5
	138.3	60.33	-59.67	62.02	-57.9[illegible]	126.1	60.51	-59.49	61.95	-58.05	112.1	60.70	-59.30	61.69	-58.31	387.1
	154.2	60.42	-59.58	62.59	-57.41	[illegible].2	60.64	-59.36	62.49	-57.51	126.0	60.89	-59.11	62.15	-57.85	434.6
	170.5	60.52	-59.48	[illegible]3.22	-56.78	156.6	60.79	-59.21	63.08	-56.92	140.3	61.09	-58.91	62.65	-57.35	481.9
1000	60.0	60.00	-60.00	60.00	-60.00	60.0	60.00	-60.00	60.00	-60.00	60.0	50.[illegible]	-60.00	60.00	-60.00	0
	58.1	60.01	-59.99	60.08	-59.92	55.7	60.01	-59.99	60.05	-59.95	53.5	60.01	-59.99	60.03	-59.97	49.1
	62.4	60.02	-59.98	60.32	-59.68	57.1	60.03	-59.97	60.20	-59.80	52.2	60.05	-59.95	60.14	-59.86	98.1
	71.8	60.06	-59.94	60.87	-59.13	64.2	60.09	-59.91	60.53	-59.47	56.4	60.12	-59.88	60.37	-59.63	146.7
	84.7	60.09	-59.91	61.50	-58.50	75.3	60.15	-59.85	60.90	-59.10	65.1	60.20	-59.80	60.63	-59.37	195.2
	99.6	60.15	-59.85	62.40	-57.60	88.8	60.23	-59.77	61.41	-58.59	76.8	60.32	-59.68	60.98	-59.02	243.5
	115.9	60.21	-59.79	63.56	-56.44	103.9	60.32	-59.68	62.04	-57.96	90.4	60.45	-59.55	61.41	-58.59	291.6
	133.0	60.29	-59.71	65.06	-54.94	120.0	60.44	-59.56	62.83	-57.17	105.0	60.62	-59.38	61.91	-58.06	339.5
	150.6	60.38	-59.62	66.93	-53.07	136.7	60.58	-59.42	63.78	-56.22	120.4	60.82	-59.18	62.57	-57.43	387.1
	168.6	60.48	-59.52	69.13	-50.87	153.7	60.74	-59.26	64.84	-55.16	136.[illegible]	61.03	-58.97	63.27	-56.73	434.6
	186.9	60.58	-59.42	71.69	-48.31	171.0	60.90	-59.10	66.02	-53.92	152.3	61.27	-58.73	64.04	-55.96	481.9

TABLE III (Cont'd)

Calculated Results for Continuous Rod Warhead Miss Distance

Sheet 6 of 10 Sheets

Altitude 45,000 feet

(V_M) Missile Velocity 2500 ft/sec

Target Velocity (V_T)	APPROACH ANGLE (γ) 30°					45°					60°					Hoop Radius (d)
	R_x	y_1	y_2	y_3	y_4	R_x	y_1	y_2	y_3	y_4	R_x	y_1	y_2	y_3	y_4	
800	60.0	60.00	-60.00	60.00	-60.00	60.0	60.00	-60.00	60.00	-60.00	60.0	60.00	-60.00	60.00	-60.00	0
	64.5	60.01	-59.99	60.02	-59.98	62.4	60.01	-59.99	60.02	-59.98	60.5	60.02	-59.98	60.02	-59.98	49.5
	82.4	60.03	-59.97	60.06	-59.94	78.3	60.05	-59.95	60.08	-59.92	74.1	60.06	-59.94	60.08	-59.92	98.7
	107.2	60.08	-59.92	60.14	-59.86	101.5	60.12	-59.88	60.19	-59.81	95.4	60.15	-59.85	60.18	-59.82	147.7
	135.1	60.14	-59.86	60.25	-59.75	128.2	60.21	-59.79	60.33	-59.67	120.4	60.27	-59.73	60.33	-59.67	196.3
	164.6	60.22	-59.78	60.40	-59.60	156.6	60.33	-59.67	60.53	-59.47	148.6	60.42	-59.58	60.52	-59.48	244.8
	195.0	60.32	-59.68	60.58	-59.42	185.6	60.47	-59.53	60.76	-59.24	175.0	60.61	-59.39	60.74	-59.26	292.9
	225.8	60.44	-59.56	60.79	-59.21	215.6	60.64	-59.36	61.04	-58.96	203.3	60.84	-59.16	61.02	-58.98	340.8
	257.0	60.57	-59.43	61.04	-58.96	245.7	60.84	-59.16	61.36	-58.64	232.0	61.09	-58.91	61.33	-58.67	388.4
	288.3	60.72	-59.28	61.32	-58.68	276.1	61.07	-58.93	61.73	-58.27	261.0	61.38	-58.62	61.69	-58.31	435.7
	319.8	60.89	-59.11	61.63	-58.37	306.6	61.32	-58.68	62.14	-57.86	290.1	61.71	-58.29	62.09	-57.91	482.9
2500	60.0	60.00	-60.00	60.00	-60.00	60.0	60.00	-60.00	60.00	-60.00	60.0	60.00	-60.00	60.00	-60.00	0
	66.6	60.02	-59.98	60.27	-59.73	60.1	60.03	-59.97	60.17	-59.83	53.6	60.04	-59.96	60.12	-59.88	49.5
	99.7	60.07	-59.93	61.10	-58.90	88.8	60.11	-59.89	60.68	-59.32	76.8	60.16	-59.84	60.48	-59.52	98.7
	141.7	60.17	-59.83	62.69	-57.31	128.2	60.26	-59.74	61.61	-58.39	112.6	60.37	-59.63	61.13	-58.87	147.7
	186.8	60.30	-59.70	64.97	-55.03	171.1	60.47	-59.53	62.90	-57.10	152.3	60.65	-59.35	62.01	-57.99	196.3
	233.2	60.47	-59.53	68.16	-51.84	215.3	60.73	-59.27	64.62	-55.3[illegible]	193.8	61.02	-58.98	63.17	-56.83	244.8
	280.4	60.68	-59.32	72.35	-47.65	260.1	61.05	-58.95	66.78	-53.22	235.6	61.47	-58.53	64.62	-55.38	292.9
	327.6	60.92	-59.08	77.75	-42.25	305.5	61.43	-58.57	69.41	-50.59	278.0	62.00	-58.00	66.35	-53.65	340.8
	375.4	61.21	-58.79	84.50	-35.50	351.0	61.87	-58.03	72.50	-47.50	320.7	62.61	-57.39	68.34	-51.66	388.4
	423.0	61.52	-58.48	92.82	-27.18	396.7	62.36	-57.64	76.11	-43.89	363.5	63.31	-56.69	70.65	-49.35	435.7
	471.1	61.88	-58.12	102.99	-17.01	442.4	62.91	-57.09	80.24	-39.76	406.3	64.08	-55.92	73.25	-46.75	482.9

TABLE III (Cont'd)

Calculated Results For Continuous Rod Warhead Miss Distance

Sheet 7 of 10 Sheets

Altitude 45,000 feet
Missile Velocity (V_M) 1,750 ft/sec

Note: See text for explanation and derivation.

Target Velocity (V_T)	APPROACH ANGLE (γ) 30° R_x	30° y_1	30° y_2	30° y_3	30° y_4	45° R_x	45° y_1	45° y_2	45° y_3	45° y_4	60° R_x	60° y_1	60° y_2	60° y_3	60° y_4	Hoop Radius (d)
800	60.0	60.00	-60.00	60.00	-60.00	60.0	60.00	-60.00	60.00	-60.00	60.0	60.00	-60.00	60.00	-60.00	0
	61.1	60.01	-59.99	60.01	-59.99	59.0	60.01	-59.99	60.01	-59.99	57.3	60.01	-59.99	60.02	-59.98	49.2
	71.3	60.02	-59.98	60.05	-59.95	67.2	60.03	-59.97	60.07	-59.93	63.1	60.04	-59.96	60.07	-59.93	98.3
	87.6	60.05	-59.95	60.12	-59.88	81.7	60.08	-59.92	60.15	-59.85	75.5	60.10	-59.90	60.16	-59.84	147.1
	107.2	60.09	-59.91	60.21	-59.79	99.8	60.14	-59.86	60.27	-59.73	91.9	60.18	-59.82	60.29	-59.71	195.8
	128.6	60.14	-59.86	60.33	-59.67	120.1	60.21	-59.79	60.42	-59.58	110.5	60.28	-59.72	60.45	-59.55	244.2
	150.9	60.21	-59.79	60.48	-59.52	141.3	60.31	-59.69	60.61	-59.39	130.3	60.40	-59.60	60.73	-59.27	292.5
	174.0	60.28	-59.72	60.66	-59.34	163.3	60.42	-59.58	60.83	-59.17	151.0	60.55	-59.45	60.89	-59.11	340.6
	197.4	60.36	-59.64	60.87	-59.13	185.8	60.54	-59.46	61.09	-58.91	172.1	60.72	-59.28	61.16	-58.84	388.5
	221.2	60.46	-59.54	61.10	-58.90	208.6	60.69	-59.31	61.38	-58.62	193.5	60.91	-59.09	61.47	-58.53	436.2
	245.1	60.57	-59.43	61.37	-58.63	231.6	60.85	-59.15	61.71	-58.29	215.2	61.13	-59.87	61.83	-58.17	483.8
1750	60.0	60.00	-60.00	60.00	-60.00	60.0	60.00	-60.00	60.00	-60.00	60.0	60.00	-60.00	60.00	-60.00	0
	60.8	60.01	-59.99	60.12	-59.88	56.2	60.01	-59.99	60.07	-59.93	52.5	60.02	-59.98	60.05	-59.95	49.2
	77.9	60.04	-59.96	60.56	-59.44	69.4	60.06	-59.94	60.35	-59.65	60.3	60.08	-59.92	60.25	-59.75	98.3
	103.6	60.08	-59.92	61.27	-58.73	92.5	60.13	-59.87	60.78	-59.22	79.1	60.18	-59.82	60.55	-59.45	147.1
	133.0	60.15	-59.85	62.32	-57.68	120.0	60.23	-59.77	61.40	-58.60	103.0	60.32	-59.68	60.98	-59.02	195.8
	164.1	60.23	-59.77	63.72	-56.28	149.4	60.36	-59.64	62.19	-57.81	129.3	60.50	-59.50	61.53	-58.47	244.2
	196.1	60.33	-59.67	65.58	-54.42	179.8	60.52	-59.48	63.22	-56.78	156.6	60.72	-59.28	62.24	-57.76	292.5
	228.6	60.45	-59.55	67.86	-52.14	210.8	60.70	-59.30	64.44	-55.56	184.6	60.98	-59.02	63.06	-56.94	340.6
	261.5	60.59	-59.41	70.61	-49.39	242.2	60.92	-59.08	65.86	-54.14	213.0	61.28	-58.72	64.01	-55.99	388.5
	295.1	60.75	-59.25	73.86	-46.14	273.8	61.16	-58.84	67.50	-52.50	241.7	61.62	-58.38	65.10	-54.90	436.2
	327.8	60.93	-59.07	77.82	-42.18	305.5	61.43	-58.57	69.40	-50.60	270.5	62.00	-58.00	66.35	-53.65	383.8

TABLE III (Cont'd)

Calculated Results for Continuous Rod Warhead Miss Distance

Sheet 8 of 10 Sheets

Altitude 60,000 feet
Missile Velocity (V_M) 2,500 ft/sec

Note: See text for explanation and derivation.

Target Velocity (V_T)	APPROACH ANGLE (γ) 30° R_x	y_1	y_2	y_3	y_4	45° R_x	y_1	y_2	y_3	y_4	60° R_x	y_1	y_2	y_3	y_4	Hoop Radius (d)
800	60.0	60.00	-60.00	60.00	-60.00	60.0	60.	-60.00	60.00	-60.00	60.0	60.00	-60.00	60.00	-60.00	0
	64.5	60.01	-59.99	60.01	-59.99	62.4	60.07	-59.993	60.01	-59.99	60.5	60.01	-59.99	60.01	-59.987	48.5
	82.4	60.02	-59.98	60.03	-59.97	78.3	60.025	-59.975	60.04	-59.96	74.1	60.03	-59.97	60.04	-59.955	97.0
	107.1	60.04	-59.96	60.07	-59.93	101.5	60.058	-59.942	60.09	-59.91	95.4	60.07	-59.93	60.10	-59.897	145.2
	135.1	60.07	-59.93	60.12	-59.88	148.6	60.101	-59.899	60.16	-59.84	120.4	60.13	-59.87	60.180	-59.820	193.4
	164.6	60.11	-59.89	60.19	-59.81	156.5	60.159	-59.841	60.25	-59.75	148.6	60.21	-59.79	60.28	-59.215	241.4
	194.9	60.16	-59.84	60.28	-59.72	185.8	60.230	-59.770	60.37	-59.63	175.0	60.30	-59.70	60.41	-59.586	289.3
	225.8	60.21	-59.79	60.38	-59.62	215.6	60.313	-59.687	60.50	-59.50	203.3	60.41	-59.59	60.56	-59.436	337.1
	257.0	60.28	-59.72	60.50	-59.50	245.7	60.410	-59.590	60.66	-59.34	232.0	60.53	-59.47	60.74	-59.261	384.7
	288.3	60.35	-59.65	60.63	-59.37	276.1	60.516	-59.484	60.83	-59.17	261.0	60.67	-59.33	60.93	-59.069	432.2
	319.9	60.43	-59.57	60.78	-59.22	306.6	60.638	-59.362	61.03	-58.97	290.1	60.83	-59.17	61.15	-58.85	479.6
2500	60.0	60.00	-60.00	60.00	-60.00	60.0	60.00	-60.00	60.00	-60.00	60.0	60.00	-60.00	60.00	-60.00	0
	66.6	60.01	-59.99	60.14	-59.86	60.1	60.02	-59.98	60.09	-59.91	53.6	60.02	-59.98	60.07	-59.93	48.5
	99.7	60.04	-59.96	60.53	-59.47	88.8	60.06	-59.94	60.33	-59.67	76.8	60.08	-59.92	60.24	-59.76	97.0
	141.7	60.08	-59.92	61.23	-58.77	128.2	60.12	-59.87	60.77	-59.23	112.6	60.18	-59.82	60.55	-59.45	145.2
	186.8	60.15	-59.85	62.19	-57.81	171.1	60.23	-59.77	61.35	-58.65	152.3	60.31	-59.69	60.96	-59.04	193.4
	233.2	60.23	-59.77	63.53	-56.47	215.3	60.36	-59.64	62.15	-57.85	193.8	60.50	-59.50	61.51	-58.49	241.4
	280.4	60.33	-59.67	65.23	-54.77	260.1	60.51	-59.49	63.15	-56.85	235.6	60.72	-59.28	62.20	-58.80	289.3
	327.6	60.45	-59.55	67.27	-52.73	305.5	60.70	-59.30	64.32	-55.68	278.0	60.98	-59.02	63.01	-56.99	337.1
	375.4	60.59	-59.41	69.73	-50.27	351.0	60.91	-59.09	65.69	-54.31	320.7	61.28	-58.72	63.95	-56.05	384.7
	423.0	60.74	-59.26	72.50	-47.50	396.7	61.15	-58.85	67.22	-52.78	363.5	61.61	-58.39	64.99	-55.01	432.2
	471.1	60.92	-59.08	75.82	-44.18	442.4	61.42	-58.58	68.99	-51.01	406.3	61.99	-58.01	66.19	-53.81	479.6

TABLE III (Cont'd)

Calculated Results For Continuous Rod Warhead Miss Distance

Sheet 9 of 10 Sheets

Altitude 45,000 feet
Missile Velocity (V_M) 1,000 ft/sec

Note: See text for explanation and derivation.

Target Velocity (V_T)	APPROACH ANGLE (γ)															Hoop Radius (d)
	30°					45°					60°					
	R_x	y_1	y_2	y_3	y_4	R_x	y_1	y_2	y_3	y_4	R_x	y_1	y_2	y_3	y_4	
800	60.0	60.00	-60.00	60.00	-60.00	60.0	60.00	-60.00	60.00	-60.00	60.0	60.00	-60.00	60.00	-60.00	0
	58.5	60.00	-60.00	60.01	-59.99	56.5	60.00	-60.00	60.01	-59.99	54.9	60.01	-59.99	60.01	-59.99	47.2
	62.1	60.01	-59.99	60.06	-59.94	57.8	60.02	-59.98	60.06	-59.94	54.0	60.02	-59.98	60.05	-59.95	94.2
	69.9	60.02	-59.98	60.13	-59.87	63.7	60.04	-59.96	60.13	-59.87	57.5	60.05	-59.95	60.12	-59.88	141.1
	80.8	60.04	-59.96	60.24	-59.76	72.9	60.07	-59.93	60.24	-59.76	64.6	60.09	-59.91	60.21	-59.79	188.0
	93.6	60.07	-59.93	60.38	-59.62	84.5	60.10	-59.90	60.38	-59.62	74.4	60.14	-59.86	60.33	-59.67	234.7
	107.8	60.10	-59.90	60.55	-59.45	97.5	60.15	-59.85	60.54	-59.46	86.0	60.20	-59.80	60.48	-59.52	281.3
	122.7	60.13	-59.87	60.76	-59.24	111.5	60.20	-59.80	60.74	-59.26	98.7	60.28	-59.72	60.65	-59.35	327.8
	138.3	60.17	-59.83	60.99	-59.01	126.1	60.26	-59.74	60.98	-59.02	112.1	60.36	-59.64	60.86	-59.14	374.2
	154.2	60.21	-59.79	61.26	-58.74	141.2	60.33	-59.67	61.23	-58.77	126.0	60.45	-59.55	61.08	-58.92	420.6
	170.5	60.27	-59.73	61.57	-58.43	156.6	60.41	-59.59	61.53	-58.47	140.3	60.56	-59.44	61.34	-58.66	466.8
1000	60.0	60.00	-60.00	60.00	-60.00	60.0	60.00	-60.00	60.00	-60.00	60.0	60.00	-60.00	60.00	-60.00	0
	58.1	60.00	-60.00	60.04	-59.96	55.7	60.01	-59.99	60.03	-59.97	53.5	60.01	-59.99	60.02	-59.98	47.2
	62.4	60.01	-59.99	60.18	-59.82	57.1	60.02	-59.98	60.12	-59.88	52.2	60.03	-59.97	60.08	-59.92	94.2
	71.8	60.03	-59.97	60.39	-59.61	64.2	60.04	-59.96	60.25	-59.75	56.4	60.06	-59.94	60.17	-59.83	141.1
	84.7	60.05	-59.95	60.72	-59.28	75.3	60.07	-59.93	60.45	-59.55	65.1	60.10	-59.90	60.32	-59.68	188.0
	99.5	60.08	-59.92	61.15	-58.85	88.8	60.12	-59.88	60.71	-59.29	76.8	60.17	-59.83	60.50	-59.50	234.7
	115.9	60.11	-59.91	61.67	-58.33	103.9	60.17	-59.83	61.01	-58.99	90.4	60.24	-59.76	60.72	-59.28	281.3
	133.0	60.15	-59.85	62.32	-57.68	120.0	60.22	-59.77	61.40	-58.60	105.0	60.32	-59.68	60.98	-59.02	327.8
	150.6	60.20	-59.80	63.10	-56.90	136.7	60.30	-59.70	61.85	-58.15	120.4	60.42	-59.58	61.29	-58.71	374.2
	168.6	60.24	-59.76	63.96	-56.04	153.7	60.38	-59.62	62.34	-57.66	136.2	60.53	-59.47	61.63	-58.37	420.6
	186.9	60.30	-59.70	64.99	-55.01	171.0	60.47	-59.53	62.91	-57.09	152.3	60.65	-59.35	62.02	-57.98	466.8

TABLE III (Cont'd)

Calculated Results for Continuous Rod Warhead Miss Distance

Sheet 10 of 10 Sheets

Altitude 60,000 feet
Missile Velocity (V_M) 1750 ft/sec

Target Velocity (V_T)	APPROACH ANGLE (γ) 30° R_x	30° γ_1	30° γ_2	30° γ_3	30° γ_4	45° R_x	45° γ_1	45° γ_2	45° γ_3	45° γ_4	60° R_x	60° γ_1	60° γ_2	60° γ_3	60° γ_4	Hoop Radius (d)
800	60	60	- 60	60	- 60	60	60	- 60	60	- 60	60	60	- 60	60	- 60	0
	61.1	60	- 60	60.01	- 59.99	59.0	60.01	- 59.99	60.01	- 59.99	57.3	60.01	- 59.99	60.01	- 59.99	47.2
	71.3	60.01	- 59.99	60.03	- 59.97	67.2	60.02	- 59.98	60.03	- 59.97	63.1	60.02	- 59.98	60.04	- 59.96	94.4
	87.6	60.03	- 59.97	60.06	- 59.94	81.7	60.04	- 59.96	60.08	- 59.92	75.5	60.05	- 59.95	60.08	- 59.92	141.4
	107.2	60.04	- 59.96	60.10	- 59.90	99.8	60.07	- 59.93	60.13	- 59.87	91.9	60.09	- 59.91	60.14	- 59.86	188.4
	128.6	60.07	- 59.93	60.16	- 59.84	120.1	60.10	- 59.90	60.20	- 59.80	110.5	60.14	- 59.86	60.22	- 59.78	235.2
	150.9	60.10	- 59.90	60.24	- 59.76	141.3	60.15	- 59.85	60.30	- 59.70	130.3	60.20	- 59.80	60.32	- 59.68	282.0
	174.0	60.14	- 59.86	60.32	- 59.68	163.3	60.20	- 59.80	60.40	- 59.60	151.0	60.27	- 59.73	60.43	- 59.57	328.7
	197.4	60.18	- 59.82	60.42	- 59.58	185.8	60.26	- 59.74	60.52	- 59.48	172.1	60.35	- 59.65	60.56	- 59.44	375.3
	221.2	60.22	- 59.78	60.53	- 59.47	208.6	60.33	- 59.67	60.66	- 59.34	193.5	60.44	- 59.56	60.71	- 59.29	421.8
	245.1	60.28	- 59.72	60.65	- 59.35	231.6	60.41	- 59.59	60.82	- 59.18	215.2	60.55	- 59.45	60.88	- 59.12	468.3
1750	60	60	- 60	60	- 60	60	60	- 60	60	- 60	60	60	- 60	60	- 60	0
	60.8	60.01	- 59.99	60.08	- 59.92	56.2	60.01	- 59.99	60.05	- 59.95	52.5	60.01	- 59.99	60.04	- 59.96	47.2
	77.9	60.02	- 59.98	60.26	- 59.74	69.4	60.03	- 59.97	60.16	- 59.84	60.3	60.04	- 59.96	60.12	- 59.88	94.4
	103.6	60.04	- 59.96	60.63	- 59.37	92.5	60.07	- 59.93	60.39	- 59.61	79.1	60.09	- 59.91	60.28	- 59.72	141.4
	133.0	60.07	- 59.93	61.07	- 58.93	120.0	60.11	- 59.89	60.67	- 59.33	103.0	60.16	- 59.84	60.47	- 59.53	188.4
	164.1	60.12	- 59.88	61.70	- 58.30	149.4	60.17	- 59.83	61.05	- 58.95	129.3	60.24	- 59.76	60.74	- 59.26	235.2
	196.1	60.17	- 59.83	62.50	- 57.50	179.8	60.25	- 59.75	61.53	- 58.47	156.6	60.35	- 59.65	61.08	- 58.92	282.0
	228.6	60.23	- 59.77	63.40	- 56.60	210.8	60.34	- 59.66	62.07	- 57.93	184.6	60.48	- 59.52	61.46	- 58.54	328.7
	261.5	60.30	- 59.70	64.52	- 55.48	242.2	60.45	- 59.55	62.72	- 57.28	213.0	60.62	- 59.38	61.91	- 58.09	375.3
	295.1	60.38	- 59.62	65.79	- 54.21	273.8	60.57	- 59.43	63.46	- 56.54	241.7	60.79	- 59.21	62.42	- 57.58	421.8
	327.8	60.47	- 59.53	67.27	- 52.73	305.5	60.70	- 59.30	64.30	- 55.70	270.5	60.98	- 59.02	63.01	- 56.99	468.3

REPORT NO. ______ DATE ______ PAGE ______

Sheet 1 of 2 Sheets

TABLE IV

Aerojet-General

FUZING ANGLE (ψ) AS A FUNCTION OF ENCOUNTER PARAMETERS

Continuous Rod
V_p = 5000 Ft/Sec

Altitude			15000		30000		45000		60000	
V_M	V_T	γ	ψ	$ψ_L$	ψ	$ψ_L$	ψ	$ψ_L$	ψ	$ψ_L$
1000	800	30	69°38'	72°27'	69°48'	72°36'	69°8'	72°1'		
		45	70°23'	74°9'	70°34'	74°18'	69°52'	73°44'		
		60	71°49'	76°3'	72°0'	76°12'	71°13'	75°38'		
	1000	30	67°19'	71°7'	67°21'	71°16'	66°49'	70°42'		
		45	68°9'	73°13'	68°20'	73°21'	67°37'	72°48'		
		60	69°53'	75°31'	70°4'	75°40'	69°19'	75°7'		
1750	800	30	62°0'	65°38'	62°1'	65°39'	61°47'	65°27'	60°0'	64°45'
		45	62°24'	67°23'	62°25'	67°24'	62°10'	67°12'	61°23'	66°31'
		60	63°26'	69°17'	63°28'	69°18'	63°13'	69°6'	62°21'	68°25'
	1750	30	51°36'	60°55'	51°37'	60°55'	51°24'	60°45'	50°40'	60°8'
		45	51°31'	64°23'	51°33'	64°24'	51°18'	64°13'	50°29'	63°38'
		60	52°59'	68°2'	53°0'	68°3'	52°44'	67°52'	50°50'	67°17'
2500	800	30			55°14'	59°24'	55°4'	59°15'	54°36'	58°50'
		45			55°21'	61°9'	55°10'	61°0'	54°40'	60°35'
		60			56°3'	63°0'	55°52'	62°51'	55°21'	62°26'
	2500	30			38°48'	53°16'	38°39'	53°9'	38°15'	52°48'
		45			37°8'	57°46'	36°59'	57°39'	36°32'	57°19'
		60			37°5'	62°22'	36°54'	62°15'	36°24'	61°55'

REPORT NO

DATE

PAGE

Sheet 2 of 2 Sheets

TABLE IV

Aerojet-General

FUZING ANGLE (ψ) AS A FUNCTION OF ENCOUNTER PARAMETERS

Multiple Shaped Charge

V_p = 15000 ft/sec

Altitude			All Altitudes	
V_M	V_T	γ	ψ	$ψ_1$
1000	800	30	83°23'	83°42'
		45	83°48'	84°5'
		60	84°25'	84°54'
	1000	30	82°40'	83°8'
		45	83'11'	83°48'
		60	83°56'	84°36'
1750	800	30	80°30'	80°59'
		45	80°53'	81°30'
		60	81°27'	82°12'
	1750	30	76°59'	78°23'
		45	77°45'	79°35'
		60	78°59'	80°58'
2500	800	30	77°40'	78°17'
		45	78°0'	78°51'
		60	78°32'	79°32'
	2500	30	71°15'	73°59'
		45	72°7'	75°43'
		60	73°43'	77°40'